Intracellular RNA signalling in RNAi and its role in antiviral defence

By

Pengcheng Zhang

A dissertation submitted to the University of Worcester in fulfillment

of the requirements for the degree of

Doctor of Philosophy

in Plant Biology

School of Science and the Environment

The University of Worcester

November 2023

Acknowledgements

First of all, I am very grateful to my supervisors, Prof Mahmut Tör and Prof Yiguo Hong. I would like to thank them for their help and advice during my PhD studies, as well as for their unfailing care in my life. Their knowledge, scientific rigour, international outlook, enthusiasm and dedication to research have inspired me. This thesis was completed under the careful guidance of the two professors, and every aspect of the thesis has been devoted to the wisdom and efforts of my supervisors, without whose knowledge and experience I could not have completed this thesis. Here I would like to express my deepest respect and sincere gratitude to my supervisors.

Secondly, I would like to thank Dr Rob Herbert, Dr David Storey, Joanna Jervis, Dr Charlotte Taylor and Dr Fleur Visser at the University of Worcester; Prof Nongnong Shi, Prof Huizhong Wang, Dr Tongfei Lai and Dr Zhiming Yu at Hangzhou Normal University; Prof Yule Liu at Tsinghua University; Prof José-Antonio Daròs from CSIC-Universitat Politècnica de València, Spain; and all the teachers who were involved in my PhD and provided me with a lot of generous help.

Once again, I would also like to thank Catherine Jimenez Quiros, Christopher Norman, Zhenhui Jin from the University of Worcester, Chengyong He and Zhen Liu from China Agricultural University, and Leizhen Wang from Hangzhou Normal University and to all my fellow PhD students, thank you for all your help.

Last but not least, I would like to express my special thanks to my parents and wife for their continued silent support and understanding of my studies and for being my strongest support, allowing me to devote myself to my studies.

Table of contents

List of Figures

List of Tables

List of abbreviations

Abbreviation	Full name
AGO	Argonaute protein
bp	Base pair
CARS	Cell-autonomous RNA silencing
CCR	Central conserved region
cDNA	Complementary dexyribouncleic acid
CP	Coat protein
csRNA	Chloroplastic small RNA
cvd-siRNA	Chloroplastic viroid siRNA
	Chlororibulose-1, 5-bisphosphate carboxylase/oxygenase
RbCL	*large subunit*
CsPP2	Cucumber phloem protein 2
dpi	Day(s) post inoculation
DNA	Deoxyribonucleic acid
DCL	Dicer-like
DBP	DNA binding protein
dsRNA	Double-stranded RNA
GFP	Green fluorescent protein
HP	Harpin
HC-Pro	Helper component proteinase
HTS	High Throughput Sequencing
HEN1	HUA Enhancer 1
HGP	Human Genome Project
H_2O_2	Hydrogen peroxide
ICTV	International Committee on Taxonomy of Viruses
IR	Inverse repeats
L-siRNA	Local siRNA

LB	Lysogeny broth
mRNA	Messenger RNA
miRNA	MicroRNA
MP	Movement protein
nat-siRNAs	Natural-antisense-transcripts small interfering RNAs
NGS	Next generation sequencing
Non-CARS	Non-cell autonomous RNA silencing
NEP	Nuclear-encoded RNA polymerase
nt	Nucleotide
PCR	Polymerase chain reaction
PD	Plasmodesmata
PTGS	Post transcriptional gene silencing
phasiRNA	Phased secondary short interfering RNA
piRNA	PIWI-interacting RNA
ra-siRNAs	Repeat-associated siRNAs
RdRP	RNA-dependent RNA polymerase
RdDM	RNA-directed DNA methylation
RISC	RNA induced silencing complex
RNA	Ribonucleic acid
RNAi	RNA interference
RNA pol II	RNA polymerase II
rpm	Revolutions per minute
RT-PCR	Reverse transcription-polymerase chain reaction
rRNA	Ribosomal RNA
RSS	RNA silencing suppressor
SDE	RNA helicase-like protein
SGS3	Suppressor of Gene Silencing3
sir VIGS	SiRNA-mediated virus-induced gene silencing
SMD	Silencing movement-deficient

ssRNA	Single-stranded RNA
siRNA	Small interfering RNA
sRNA	Small RNA
ta-siRNAs	Transacting small interfering RNAs
TGS	Transcriptional gene silence
tRNA	Transfer RNA
µg	Microgram
µL	Microliter
VSR	Viral suppressor of RNA silencing
vd-sRNAs	Viroid-derived sRNAs
VirP1	Viroid-binding protein 1
vasiRNAs	Virus-activated siRNAs
VIGS	Virus-induced gene silencing
vs-sRNAs	Virus-derived sRNAs
vsiRNA	Virus-derived siRNAs
VSR	Viral suppressor of RNA silencing

Abbreviation	**Latin name**
At	*Arabidopsis thaliana*
ASSVd	*Apple scar skin viroid*
ASBVd	*Avocado sunblotch viroid*
C. elegans	*Caenorhabditis elegans*
CSVd	*Chrysanthemum stunt viroid*
CEVd	*Citrus exocortis viroid*
CCCVd	*Coconut cadang-cadang viroid*
CMV	*Cucumber mosaic virus*
ELVd	*Eggplant latent viroid*
HSVd	*Hop stunt viroid*
Nb	*Nicotiana benthamiana*
PVX	*Potato virus X*

PSTVd	*Potato spindle tuber viroid*
SCMV	*Sugarcane mosaic virus*
TBSV	*Tomato bushy stunt virus*
TSWV	*Tomato spotted wilt virus*
TYLCCNV	*Tomato yellow leaf curl China virus*
TCV	*Turnip crinkle virus*
TuMV	*Turnip mosaic virus*

Abstract

RNA silencing (also known as RNA interference, RNAi) is a conserved and common cellular regulatory and defence mechanism in plants, animals, fungi and other eukaryotes. It plays an important role in regulating growth and development and maintaining genomic stability in response to biotic and abiotic stresses. RNA silencing operares in two forms, transcriptional gene silencing (TGS) and post-transcriptional gene silencing (PTGS). It is an important mechanism in a variety of antiviral defence mechanisms in plants. RNAi is involved in mobile RNA signalling and various genetic factors. Although studies on how RNAi is transported from cells to systems are controversial, there are some indications that intracellular RNAi and RNA are transported between organelles. For example, there have been clear reports that intracellular RNA transport between the cytoplasm and chloroplasts may occur. However, how RNAi spreads from the cytoplasm to chloroplasts, mitochondria, and other organelles in plant cells and its biological relevance to plant antiviral defence remains to be investigated. On the other hand, intracellular RNA signalling in RNAi and the spread of RNAi within plant cells may be a new mode of gene regulation and defence mechanism that regulates the expression of organelle genes through small RNAs derived from nuclear genes. In plants, the combined function of DCL2 and DCL3 is essential for their concerted defence, while DCL4 is required for the nucleus replication of viral infectors. However, how RNA silencing targets and counteracts chloroplast replicating viruses remains largely unknown.

In this project, we transformed infectious RNA clones of ELVd into binary plasmids using *Eggplant latent viroid* (ELVd), a chloroplast replication viroid and a set of transgenic *Nicotiana benthamiana* (*N. benthamiana*) RNAi lines RDR6i and DCLi and initiated ELVd replication in wild-type and transgenic *N. benthamiana* plants using Agrobacterium infiltration. *N. benthamiana* knocking out various DCLs or RDR6 in infiltrated leaves, combined with high-throughput small RNA sequence analysis, I examined the effect of ELVd infection on microRNA and sRNA biogenesis of chloroplast-derived small RNAs in *N. benthamiana* leaves and the effect of RNA silencing on ELVd siRNA. The role of *DCLs* and *RDR6* on the dynamic RNA silencing-mediated response to ELVd infection is revealed and extensive experimental data are reported. *DCL1i*, *DCL2i*, *DCL3i* and *DCL4i* enhanced ELVd RNA levels, but *RDR6i* had little effect on ELVd RNA accumulation in the early and late infection stages. *DCL2* had little effect on the generation of 22nt ELVd siRNA. *DCL3* is functionally redundant with

DCL2 and targets ELVd RNA for 24nt chloroplast virus siRNA (cvd-siRNA) biogenesis. *DCL4* is involved in the production of the less abundant 21nt cvd-siRNA. *DCL1* and *RDR6* did not contribute to the biogenesis of cvd-siRNA. However, ELVd infection reduced the microRNA processed by *DCL1* in both wild-type and RNAi plants, suggesting that DCL1 may be indirectly involved in protecting plants from ELVd attack. These results also demonstrate that different processing processes may be responsible for the production of chloroplast small RNAs (csRNAs) in chloroplasts. csRNAs dynamics during ELVd infection suggest that csRNAs may be biologically relevant to chloroplast virus-host plant interactions.

Keywords: RNA silencing; *Eggplant latent viroid* (ELVd); Dicer-like (DCL); Chloroplastic viroid siRNA (cvd-siRNA); Chloroplastic small RNA (csRNA); Signal transduction.

Chapter 1 General Introduction

1.1 Overview of RNA silencing

1.1.1 RNA silencing discovery

RNA silencing or gene silencing (also known as RNA interference, RNAi) is an evolutionarily highly conserved defence mechanism that exists in plants, animals, fungi and other eukaryotes to maintain genomic stability and to regulate their own growth and development. It is also an effective means of regulating virus and pathogen resistance and stress tolerance in response to biotic and abiotic stresses (Baulcombe et al., 2004; Fusaro et al., 2006; Kalantidis et al., 2008; Sarkies and Miska., 2014; Zhang et al., 2019; Wu et al., 2023).

In 1990, when Napoli et al. investigated the effect of chalcone synthase (CHS) on the rate of anthocyanin synthesis in *Petunia hybrida Vilm.* When they overexpressed *CHS*, a gene that forms the red color of flowers, to obtain deeper-colored petunias, they accidentally obtained white and white-purple petunias. They hypothesized that the exogenously transferred gene encoding *CHS* simultaneously repressed the expression of the endogenous *CHS* in the flower and discovered for the first time the phenomenon of RNA silencing, which was then called "co-repression", an early approach to the concept of RNA silencing (Napoli et al., 1990). In 1995, Guo et al found that injections of both sense RNA and antisense RNA could effectively and specifically suppress the expression of the *par-1* gene in *Caenorhabditis elegans* and discovered the phenomenon of RNA interference (Guo et al, 1995). It was not until 1998 that Fire et al. found that the behaviour of *C. elegans* did not change significantly when the mRNA and antisense mRNA encoding muscle proteins were injected separately into the nematode, and that when the sense and antisense mRNAs were injected simultaneously into the nematode the nematode showed peculiar twitching movements. This indicates that sense or antisense ssRNA inhibits weakly, whereas highly purified dsRNA can efficiently and specifically inhibit gene expression. The discovery that the inhibition of homologous gene expression is triggered by the contamination of trace amounts of dsRNA in RNA prepared by in vitro transcription is the first evidence that double-stranded RNA (dsRNAs) induces RNA silencing. The concept of RNAi was formally introduced when it was called RNA interference (Fire et al., 1998).

In biological evolution, RNA silencing is a widespread phenomenon in eukaryotes (plants, animals, fungi), which refers to RNA-mediated sequence-specific interactions induced by dsRNA, causing efficient and specific degradation of homologous mRNAs and suppression of gene expression (Voinnet et al., 2005). This phenomenon of dsRNA-mediated RNAi has been found in many eukaryotes with different expressions. RNAi has different manifestations, from RNAi interference in animals (Fire et al., 1998) to post-transcriptional gene silence (PTGS) (Brodersen and Voinnet., 2006; Xu et al., 2006) or cosuppression in plants (Napoli et al., 1990; Palauqui et al., 1997), and in fungi, it is called quelling (Romano et al., 1992).

1.1.2 RNA silencing mechanism

With the development of the state of the art in molecular and biochemical analysis, the molecular mechanisms of RNA silencing are slowly being revealed. In planta, RNA silencing uses RNA-dependent RNA polymerase (RdRP) for synthesis of dsRNA. Then dsRNA is under the cleaving action of the dsRNA-specific RNA endonuclease DICER (an RNase III family endonuclease) or DICER-Like (DCL) to generate small interfering RNA (siRNA) of 21-24 nucleotides (nt) in length. These siRNAs bind to ARGONAUTEs (AGO1/2/4) proteins to form the "RNA induced silencing complex" (RISC). RISC then specifically recognizes its target RNA or RNA-directed DNA methylation (RdDM) through small RNA base complementary pairing, resulting in target RNA cleavage, translational repression or target DNA methylation, thereby regulating eukaryotic gene expression at the post-transcriptional or translational level (Post-transcriptional gene silencing (PTGS) or (Transcriptional gene silencing (TGS) (Bernstein et al., 2001; Hamilton et al., 2002; Meister et al., 2004; Jones et al., 2006； Chen et al., 2009; Ding et al., 2009; Ding et al., 2010; Sarkies and Miska. 2014; Zhang et al., 2019; Navarro et al., 2021a; 2021b; Ramesh et al., 2021).

RNA silencing is an important antiviral mechanism that occurs in plants and animals when they are attacked by viruses. First, viral infection of host cells activates the RNA silencing defense mechanism, virus-induced gene silencing (VIGS), which results in the cleavage of viral RNA or the methylation of viral DNA, and this inhibits viral replication and thus reduces the pathogenicity of the virus. The pathway by which the virus activates RNA silencing is well studied (Figure 1.1). During RNA silencing, DCL cleaves dsRNA into primary siRNA, RDR reconstitutes the siRNA into dsRNA and then cleaves the newly synthesized dsRNA into more secondary siRNA. thus, RNA-

dependent RNA polymerase (RdRP) is involved in the generation of additional secondary siRNAs, which act as signal amplifiers in RNA silencing, and these siRNAs in turn trigger the systematic silencing of target RNAs (Tang et al., 2001; Voinnet et al., 2008; Cuperus, et al., 2010; Garcia-Ruiz et al., 2010).

Figure 1.1 Viral infection-activated plant RNAi pathway

In plants, single-stranded RNA (ssRNA) can form double-stranded (ds) structures via intramolecular base-paring or convert into dsRNA by RNA-dependent RNA polymerase (RdRP). Dicer-like (DCL) endonucleases slice dsRNA into small interfering RNA (siRNA). Subsequently, the guide-strand of siRNA and Argonautes (AGOs), along with other cellular factors form the RNA-induced silencing complex (RISC), which targets specific RNA for cleavage or homologous DNA for RNA-dependent DNA methylation, leading to post-transcriptional (PTGS) or transcriptional gene silencing (TGS), respectively **(Adapted from Wang et al., 2022).**

RNA silencing in plants can be divided into two categories according to the target: RNA as the target, which is degraded or protein translation is inhibited, called post-transcriptional gene silencing (PTGS); chromatin as the target, through chromatin heterochromatinization or DNA methylation modification, to inhibit RNA transcription

initiation, called transcriptional gene silencing (TGS). Both PTGS and TGS can occur autonomously in a single cell, known as cell-autonomous RNA silencing (CARS); they can also spread between cells, tissues, and within individual organisms, resulting in "non-cell-autonomous RNA silencing" (Non-CARS) (Ryabov et al., 2004; Jones et al., 2006; Melnyk et al., 2011). Non-CARS is one of the main features of RNAi. Non-CARS is RNAi that occurs in cells or tissues that do not introduce or express dsRNA. In multicellular organisms, non-CARS can also be followed by CARS. Non-CARS includes both intercellular and systemic long-distance RNAi. CARS include both intercellular and systemic long-distance silent transport modes, often referred to as intercellular non-CARSs and systemic non-CARS. Both PTGS and TGS have non-CARS properties. Therefore, non-CARS research is of great fundamental theoretical value and provides technical support for the development of RNA-mediated disease resistance strategies for food and cash crops.

Endogenous small RNAs (sRNAs) are small non-coding RNAs with regulatory effects that are widely found in plants, animals and fungi. SRNAs can bind to proteins such as AGO in eukaryotes to interfere with RNA and thereby inhibit the expression of mRNAs from other genes. These include microRNAs (miRNAs), small interfering RNAs (siRNAs), transacting small interfering RNAs (ta-siRNAs), natural-antisense RNAs (nat-siRNAs), repeat-associated siRNAs (ra-siRNAs), viral siRNAs (vsiRNAs), virus-activated siRNAs (vasiRNAs) and piwi-interacting RNAs (piRNAs) among others (Valli et al., 2016), where miRNAs and siRNAs are the main components of sRNAs, and more than 80% of sRNAs in plant cells are siRNAs (Klevebring et el; 2009). Different types of sRNAs play essential roles in plant development, stress response, heterochromatin silencing, viral infection, and host-pathogen interactions, respectively (Bologna and Voinnet., 2014). miRNA and siRNA are 21-24 nt in size, miRNA is a small molecule of RNA encoded by a gene, while siRNA is cleavaged by Dicer completely complementary long dsRNAs are cleavaged by Dicer. siRNA can be endogenous or exogenous and is mainly involved in the RNAi phenomenon; it is also an important mechanism of antiviral action, which regulates gene expression in a specific way. The molecules of miRNAs, on the other hand, are endogenous molecules derived from RNA precursors capable of forming hairpin structures and are processed by Dicer enzymes. The molecules of piRNAs, which are 29-30 nt in length, are generated through the transcriptional process of gene sequences rather than by Dicer cleavage, and are mainly found in animal germ cells and stem cells, where they regulate gene silencing by binding to piwi subfamily proteins.

The key core factors in the RNA silencing pathway include Dicer-like nucleases (DCLs), double-stranded DNA binding proteins (DBPs), RNA-dependent RNA polymerases (RdRPs), and Argonaute proteins (AGOs). The model plant *Arabidopsis* encodes four DCLs (DCL1, DCL2, DCL3, DCL4) (Bologna and Voinnet., 2014), five DRBs (HYL1/DRB1, DRB2, DRB3, DRB4, and DRB5) (Hiraguri et al., 2005), six RDRs (RDR1, RDR2, RDR3a, RDR3b, RDR3c and RDR6) (Wassenegger and Krczal., 2006) and ten AGOs (AGO1, AGO2, AGO3, AGO4, AGO5, AGO6, AGO7, AGO8, AGO9, AGO10) (Li et al., 2002; Brodersen and Voinnet., 2006; Mallory and Vaucheret., 2010). These proteins interact with each other to evolve different RNA silencing pathways that play a role in plant growth, development and antiviral resistance, among others. Three of these DCLs and seven AGOs were found to be involved in antiviral RNAi in plants, while RDR1, RDR2, and RDR6 all mediate the amplification of viral siRNAs (vsiRNAs) (Liu et al., 2022).

1.1.3 RNA silencing applications

Plants have involved and developed a variety of sophisticated defence mechanisms against viruses, the most effective and important of which is RNA silencing. Virus-induced gene silencing (VIGS) is a technique based on RNA-mediated defence mechanisms in plants. It is currently a common research and analysis tool for the screening and identification of functional plant genes and the functional study and analysis of plant genes (Barciszewska-Pacak et al., 2016; Mohamed et al., 2022).

RNA silencing plays an important role in a variety of biological processes such as cellular immune resistance, growth and development (Li et al., 2017; Deng et al., 2018; Ortola et al., 2021). During this process, mobile primary and secondary small RNAs are produced, which are silencing signals for intercellular and systemic RNAs (Chen et al., 2010; Cognat et al., 2017; Chen et al., 2018; Zhang et al., 2019). In plant-fungus interactions, it is even possible to exchange small RNA molecules between plant and fungal cells to induce RNA silencing in the corresponding fungal and plant recipient cells (Weiberg et al., 2013). In 1995, Kumagai et al. constructed the first VIGS vector (TMV-PDS) to be used to silence the octaheydro lycopene dehydrogenase gene (PDS), resulting in a distinct photobleaching phenotype on the leaves in *Nicotia*na *benthamiana* (Nb) (Kumagai et al., 1995). Since then, a variety of plant viruses have been modified into VIGS and based on VIGS vectors, a variety of genes have been reported to regulate disease resistance (Downward et al. 2003), symbiosis (Ekengren

et al., 2003), plant growth and development (Dong et al., 2007), and so on. A variety of RNAi pathways have been developed in organisms to regulate their own growth and development and to respond to the effects of changing external environments on the plant itself (Baulcombe et al., 2004).

RNA silencing plays an important role in plant resistance to abiotic adversity and crop quality improvement. Zhang et al. (2011) showed that the expression of the ascorbate peroxidase (APX) gene in tomato fruit mitochondria was suppressed by RNAi technology, and the viability of APX in RNAi plants was reduced by 40%-80% compared to wild-type plants, while the content of vitamin C in fruits was increased by more than 1.4-fold (Zhang et al., 2011). Kadomura-Ishikawa et al. (2015) disrupted the *FaMYB1* gene in strawberries (*Fragaria ananassa*) and found that the pigment accumulation and anthocyanin content in the fruits of *FaMYB*-RNAi plants were higher than those of wild-type and overexpression plants (Kadomura-Ishikawa et al., 2015). Plants showed improved salt and drought tolerance, with several genes associated with stress tolerance significantly up regulated under both normal and stress conditions (Hu et al., 2017). A study of three *Solanum tuberosum* viruses, PVX, PVY, and PVS, revealed that the nucleic acid sequences of the three interspersed capsid proteins were relatively conserved and based on this, RNAi vectors were constructed, and the transgenic potato plants obtained did not exhibit a susceptible phenotype after inoculation with these viruses (Hameed et al., 2017). There is also resistance to insects (Fofana et al., 2004) in terms of nutrient uptake and stress (Fu et al., 2006), and abiotic stress effects (Gabrie et al., 2007).

In plants, RNA silencing also plays an important role in antiviral defence (Moissiard et al., 2007; Aliyari et al., 2009; Csorba, et al., 2015; Liu et al., 2022). Virus-induced gene silencing (VIGS) is one of the most studied and well-understood mechanisms of plant resistance to viruses. The VIGS technique involves the cloning and insertion of a gene fragment from the plant to be silenced into a viral vector and then transferring the VIGS vector into the plant by mechanical inoculation of in vitro transcripts, or into a vector using *Agrobacterium*-mediated transformation or by gene gun bombardment (DNA viral vector) to induce degradation or histone modification of the pathogen dsRNA and mRNA of the homologous virus, making it impossible for the virus to accumulate in the plant. This can be achieved by inducing degradation or histone modification of the pathogenic dsRNA and homologous viral mRNA, preventing virus accumulation in the plant (Moissiard et al., 2006; Baumberger et al., 2007; Pantaleo et al., 2007). Plants can use PTGS and TGS to resist virus infection, and DCL is used to process plant viral

RNAs after virus infection to produce virus-derived small interfering RNAs (vsiRNAs) that mediate the degradation of viral RNAs or inhibit the transcription of viral genes. It was found that if DCL4 and the 21nt vsiRNA form the first frontline of defence against viruses in plant cells, then DCL2 and the 22nt vsiRNA build the second barrier of defence against viruses in plant cells. DCL2 and 22nt siRNA are primarily involved in intercellular silencing and systemic silencing, they play a key role in *N. benthamiana* and also coordinates defence against local viral infection (Qin et al., 2017). DCL3 and 24-nt vsiRNAs, as well as DCL1 and microRNA, play important roles in the fight against DNA viruses (Blevins et al., 2006). Recently, multiple RNAi-associated factors were reported to play an important role in RNA silencing in antiviral defence, using *Arabidopsis*-virus as the pathogenic system (e.g. Figure 1.2).

Figure 1.2 Schematic representation of RNAi-based antiviral defenses in plants

Plant virus infection can produce dsRNAs. DCL recognises viral dsRNAs and generates 21-24 nt siRNAs, which then bind to AGOs to form complex RISCs that inhibit viral infection through transcriptional gene silencing (TGS) and post-transcriptional gene silencing (PTGS). TGS is induced viral DNA methylation through the AGO4 24 nt siRNAs-dependent RdDM pathway. PTGS is induced to cleave viral RNA or inhibits translation of viral RNA through RISC, a complex of 21 or 22 nt siRNAs composed of multiple AGOs (AGO1/2/3/5/7/10). Viral RNA can be recruited by RDR

and SGS3 to synthesise dsRNA, generate secondary siRNAs and amplify silencing signals. Reported RNAi regulators include AVI2, ALA1/2, ENOR3, ROD5, and VIRl. BAM1 and BAM2 are receptor-like kinases that are required for intercellular movement of RNAi.

Abbreviations: ALA, aminophospholipid transporting ATPase; AVI2, antiviral RNAi-defective 2; BAM1/2, barely any meristem 1/2; DRM2, domains rearranged methylase 2; DRB, double-RNA binding protein; ENOR3, enhancer of RDR6 3; Pol V, RNA polymerase V; RdDM, RNA-directed DNA methylation; RDO5, reduced dormancy 5; RDR, RNA-dependent RNA polymerase; SGS3, suppressor of gene silencing 3; VIR1, antiviral RNAi regulator 1 **(Adapted from Li et al., 2022).**

1.2 Non-cell-autonomous RNA silencing

1.2.1 Non-cell-autonomous RNA silencing in animals

In 1998, Fire A. and Mello C. found that dsRNA added as a control showed a stronger inhibitory effect than either sense or antisense RNA in RNA-mediated suppression experiments in *Caenorhabditis elegans*. It is hypothesized that there is an amplification effect, and an enzymatic activity involved in the dsRNA-directed repression process. The induction of RNA silencing by dsRNAs was first demonstrated and the phenomenon was named RNA interference (Fire et al., 1998).

Studies have shown that in *C. elegans*, the genes *Sid-1* (systemic interference defective), *Rsd-2* (RNAi spreading defective), *Rsd-3,* and *Rsd-6* control systemic RNA silencing. These mutated genes cause the nematode to fail to undergo systematic RNA silencing (Winston WM et al., 2002; Timmons et al., 2003; Feinberg and Hunter, 2003; Tijsterman et al., 2004). In *C. elegans*, RNAi is also transmissible and can spread between cells, a phenomenon known as systemic RNAi (Winston et al., 2002; Jae-Yean et al., 2005). In 2002, Novina et al. used RNAi to suppress the HIV-1 virus (Novina et al., 2002) and in 2004, Morris et al. used RNAi to suppress human genes (Morris et al., 2004).

1.2.2 Non-cell-autonomous RNA silencing in plants

1.2.2.1 Discovery of non-cell-autonomous RNAi phenomena in plants

The phenomenon of plant non-cell-autonomous RNAi was first discovered in *N.*

benthamiana in 1997. Voinnet *et al*. infiltrated a suspension of *Agrobacterium* tumefaciens with a green fluorescent protein GFP-tagged reporter gene into *N. benthamiana* leaves transgenic for GFP. At first GFP expression was silenced only in the injected area, and after 18 d it was found that GFP expression in the upper leaves was also fully silenced (Voinnet et al., 1997). Non-CARS can also be induced by gene gun bombardment of dsRNA or siRNA into leaves (Klahre et al., 2002; Dunoyer et al., 2010). In addition, grafting experiments on *N. benthamiana* (Paluqui et al., 1996), *Cucumis sativus L.* (Yoo et al., 2004), and *Solanum lycopersicum L.* (Shaharuddin et al., 2006) plants have also revealed non-CARS spreading, but not inheritance (Kalantidis et al., 2008).

1.2.2.2 Non-cell-autonomous RNAi spread

In plants, different types of RNA silencing signals can move from cell to cell either through the plasmodesmata (PD) (Voinnet et al., 1998) or through the siliques for systemic long-distance vascular system transport, thus regulating plant growth and development, nutrient allocation and other physiological processes (Palauqui et al., 1997, 1999; Ueki et al., 2001; Yoo et al., 2004; Baulcombe, 2004; Jones et al., 2006; Tournier et al., 2006). The non-cell-autonomous nature of RNA allows it to act in individual cells (unicellular). The non-cellular autonomy of RNA allows it to act in a single cell (unicellular RNA silencing) or to spread between adjacent cells (intercellular/local RNA silencing), the latter being divided into RNAi for intercellular transport and RNAi for long-distance transport (Long-distance RNAi or systemic RNA silencing). Intercellular RNAi spread consists of two sequential processes: local silencing spread and extensive silencing spread.

1.2.2.2.1 Local silencing spread

Local silencing spread is limited to intercellular PD spread from a silenced cell to the neighbouring cells, usually around 10-15 cells. RNA-dependent RNA polymerase (RdRP) is not required for local silent spread. DRB4 and DCL4 together participate in dsRNA cleaving to produce 21nt siRNA, and the 21nt siRNA silencing signal then spreads between cells via intercellular PD (Himber et al., 2003; Parizotto et al., 2004; Yang et al., 2006). It was shown that in *Arabidopsis*, 21-nt siRNAs generated by DCL4 cleavage can spread between cells and that translocation is accompanied by the involvement of at least three genes related to *Arabidopsis SMD1*, *SMD2* and *SMD3* (silencing movement-deficient), of which *SMD1* and *SMD2* encode *Arabidopsis* RDR2

and NRPD1a (RNA polymerase IVa), respectively. It is suggested that 21-nt small interfering RNA (siRNA) may be the intercellular RNA silencing signal (Dunoyer et al., 2005, Dunoyer et al., 2007; Dunoyer et al., 2010). In addition, *Arabidopsis* NRPD1a, RDR2, DCL3 (DICER-like 3), and AGO4 (ARGONAUTE 4) have also been associated with long-distance RNA silencing translocation (Brosnan et al., 2007). In most plants, intercellular PD is the intercellular transport channel for silencing factors, but in *Arabidopsis*, mature guard cells were also found to transport silencing factors, suggesting that other intercellular transport pathways may exist in plants (Lucas et al., 2004; Oparka et al., 2004; Kim et al., 2005; Maule et al., 2008).

1.2.2.2.2 Systemic silencing spread

Systemic silencing spread differs from local silencing spread in the mechanism of RNA silencing, which generally refers to intercellular RNA silencing beyond 15 cells. Both extensive silencing spread and systemic RNA silencing transit in plants require siRNA as the silencing signal molecule and rely on the involvement of RDR6 and RNA helicase-like protein SDE3 (RNA helicase) (Dalmay et al., 2000). There is an amplification of RNA silencing during long-distance silencing spread. Firstly, DCL cleaves the dsRNA into primary siRNA, secondly, RDR assembles and reconstitutes the siRNA into dsRNA, and finally, the newly synthesized dsRNA is then cut by DCL4 to produce more secondary siRNA, which does not overlap with the primary siRNA, thus producing more siRNA for spread. (Himber et al., 2003; Dunoyer et al., 2007).

1.2.2.3 Intercellular spread

In plants, intercellular plasmodesmata are important channels for the transport of substances and information transfer between two neighboring plant cells and and they are the unique protoplasmic connections of both cells. The intercellular plasmodesmata is also a highly dynamic structure during plant growth and development. It controls the spread of small molecules and metabolites between cells through its size exclusion limit (SEL) and also facilitates and regulates the intercellular transport of large molecules such as transcription factors and hormones (Lee et al., 2009; Wu et al., 2024). It has been found that some mobile RNA molecules can move through intercellular plasmodesmata, such as sRNAs (both miRNAs and siRNAs), miR165/166, miR390 and SUC1 mRNA (Lucas et al., 2013; Saplaoura et al., 2016; Kehr et al., 2018; Xia et al., 2020; Wu et al., 2024).

The main source of intercellular silencing is the local silencing assay via *Agrobacterium* permeabilis, and systemic non-cell-autonomous RNA silencing in plants must have intercellular non-cell-autonomous RNA silencing involved in its occurrence, but intercellular non-cell-autonomous RNA silencing does not necessarily lead to systemic non-cell-autonomous RNA silencing (Ryabov et al., 2004). In *Arabidopsis*, experiments have shown that amplification of siRNA silencing signals is required for the transmission of intercellular RNA silencing. Intercellular non-CARS PTGS requires the involvement of DCL4 and 21nt siRNAs (Dunoyer et al., 2005; Liang et al., 2012); overexpression of DCL2 in the dcl4 *Arabidopsis* mutant produces a large number of 22nt siRNAs, while DCL4 promotes 21nt siRNA production via the RDR6/DCL4 pathway, thereby enhancing intercellular transport of PTGS; however, this contradicts the loss of function of DCL4 in the dcl4 mutant (Parent et al., 2015). In addition, enhanced intercellular transport of PTGS was also observed in different *Arabidopsis* dcl4 mutants, suggesting that DCL4 may play an inhibitory role in intercellular PTGS (Parent et al., 2015). Therefore, whether intercellular non-CARS requires DCL4 and the 21nt siRNA formed by DCL4 processing is subject to further study (Berg et al., 2016). It has also been found that cytokines such as SNF2, THO, and JMJ14 have been implicated in intercellular Non-CARS in *Arabidopsis*, with the SNF2 structural domain (containing the CLASSY1 protein) able to act in concert with RDR2 and NRPD1a to influence the transmission of RNA silencing (Smith et al., 2007).JMJ14 acts as a histone H3 JMJ14, a histone H3K4 (H3K4) trimethyl demethylase, can affect RNA silencing by down-regulating the expression of RDR2 and AGO4 (Jones et al., 2006; Searle et al., 2007; Smith et al., 2007; Searle et al., 2010; Yelina et al., 2010).

Researchers have also discovered through grafting experiments that mRNA can move between different plants such as *Arabidopsis*, rice, tomato, potato cucumber, and grape (Mahajan et al., 2012; Yang et al., 2015; Zhang et al., 2016; Xia et al., 2020)

1.2.2.4 Spread of virus-induced gene/RNA silencing (VIGS) between different cells

In *N. benthamiana* transgenic for GFP, a recombinant *Turnips crinkle virus* (TCV/GFPΔCP) lacking the viral coat protein (CP) can induce GFP gene silencing in single-leaf epidermal cells and transfer to nearby epidermal and mesophyll cells in a three-dimensional manner (Zhou et al., 2008; Shi et al., 2009). RDR6 and TCV movement proteins p8 and p9 have involved in TCV/GFPΔCP-induced intercellular

VIGS (Zhou et al., 2008; Qin et al., 2012). Notably, it has also been shown that *Tobacco mosaic virus* (TMV) 30K movement protein enhances non-CARS (Vogler et al., 2008); in addition, Rosas-Diaz *et al.* showed that a geminiviral protein interacts with plant competent kinases to prevent the latter from accelerating intercellular transport of RNA silencing (Rosas-Diaz et al., 2018). Our recent studies suggest that *DCL4* plays an important role in intracellular viral siRNA biosynthesis in cell-autonomous VIGS but inhibits intercellular transport in non-cell-autonomous VIGS. In contrast, DCL2 may bind to RNA signaling (22nt siRNA) to promote intercellular VIGS. Also, we found that DCL4 negatively regulates intercellular non-CARS transport by down-regulating DCL2 expression (Qin et al., 2017).

1.2.2.5 Long-distance transport of RNA silencing

The vascular system of plants consists mainly of the phloem, the formative layer, and the xylem, which transports water, minerals, and organic nutrients for the growth and development of distal tissues and organs, etc. In 2006, the use of in vivo phloem tracers and the classical 'leaf-shading/removal' experiment confirmed that the long-distance delivery channel for RNAi silencing is the phloem rather than the xylem (Tournier et al., 2006). The long-distance transmission of cellular non-autonomous RNA silencing is also known as Systematic Non-CARS. Silencing in local tissues can be transferred to distal tissues via the phloem transport channel or systemic non-cell autonomous RNA silencing can also be induced from rootstock to scion by grafting connections (Jones et al., 2006; Sarkies and Miska. 2014). Plant small RNA molecules can act as functional molecules for signaling, that is, they are transported to adjacent cells via intercellular plasmodesmata and then to distant tissues via the phloem, the RNA long-distance transport channel is mainly done through the phloem, which is therefore also known as the highway for transmitting mobile signals in plants (Oys et al., 2001; Lucas et al., 2013; Saplaoura et al., 2016).

In competent cells, DCL2 mediates the formation of 22nt siRNAs and DCL4 mediates the formation of 21nt siRNAs leading to systemic PTGS. for example, RDR2 and DCL3 are involved in the regulation of systemic. Non-CARS and RDR6 are involved in silencing signals in the *N. benthamiana* reception system (Schwach et al., 2005), but in *Arabidopsis*, AGO4 is involved in PTGS signal reception, however, DCL2, DCL4, and RDR6 are not involved in the generation of the *Arabidopsis* silencing signal nor in the long-distance transmission of the silencing signal (Brosnan et al., 2007). This contradicts Taochy et al. (2017) who found that *Arabidopsis* DCL2 plays an important

role in the RDR6-dependent transport of PTGS from roots to new shoots (Taochy et al., 2017).

Recent studies have shown that DCL2 is required for RNAi propagation and has a very important role in the systemic Non-CARS of *N. benthamiana* (Chen et al., 2018). In addition, DCL2 is also involved in the formation of silent movement signals that affect the response of recipient cells to non-CARS PTGS signals (Taochy et al., 2017; Chen et al., 2018). Furthermore, Liang et al. proposed that endogenous H_2O_2 and reactive oxygen species (ROS) production is regulated by peroxidase to alter local cell wall structure and thus the permeability of intercellular plasmodesmata, which in turn regulates non-cell-autonomous RNA silencing (Liang et al., 2012).

Studies have shown that feeding transgenic RNAi plants to fungi and insects can effectively silence homologous complementary genes in both fungi and insects, suggesting that transgene-induced RNA silencing can be transmitted between plants and host plants (Mao et al., 2007; Melnyk et al., 2011). Alternatively, fungi can encode some sRNAs that can be transmitted through the cell wall and disrupt the RNA silencing defense pathway in plants (Weiberg et al., 2013). Thus, cellular non-autonomous RNA silencing signals can be transmitted not only between cell-to-cell and over long distances, but also outside the plant body, e.g. between plants and host plants.

In plants, the viral RNA silencing pathway interacts with functionally diverse interactions and motor pathways of various RDR, DCL, and AGO proteins (e.g. Figures. 1.3 and 1.4).

Figure 1.3 PTGS of viral RNA and Mobile sRNAs

PTGS of viral RNAs is mediated by 21 or 22 nt sRNAs and AGOs that cause cleavage or translational repression of the target viral RNA. The 22-nt sRNA of DCL2 triggers the production of SGS3 secondary sRNA, thereby amplifying the silencing signal compared to the 21-nt sRNA. 22-nt sRNA 3′ nucleotide protrudes from the AGO, permitting binding of SGS3, resulting in ribosomal arrest. dsRNA is synthesized by the RDR after binding by SGS3 and is cleaved by the DCL to form secondary sRNA. Meanwhile, sRNA can move short distances through the plasma membrane and, if they enter the phloem, they can be transported over long distances, triggering RNA silencing. sRNAs are also free to move, but they are depleted from mobile sRNAs when their 5′ nucleotides are bound by the AGO, and 5′-U and 5′-A sRNAs are the carriers of AGO1 and AGO2, respectively **(Adapted from Lopez-Gomollon and Baulcombe., 2022).**

Figure 1.4 TGS of viral DNA

TGS of viral DNA is mediated by 24 nt sRNAs produced from Pol IV transcribed RNA, which is converted to dsRNA by RDR2 and catabolised by DCL3. These 24 nt sRNAs form a complex with AGO4 that targets and binds Pol V transcripts, thereby causing DNA methylation by binding to DRM1/2. Other sRNA sources pathways include dsRNAs, 21 or 22 nt sRNAs associated with AGO1, and other sRNAs **(Adapted from Lopez-Gomollon and Baulcombe., 2022).**

1.2.3 Mobile RNA signalling in non-cell-autonomous RNA silencing in plants

1.2.3.1 RNA signaling

The systematic non-cell autonomous propagation properties of RNA silencing suggest that there are mobile signaling molecules in the RNA silencing pathway. Molecules of mRNA, miRNA, siRNA, siRNA, rRNA, tRNA, and various other plant RNAs are found outside the cell in most plants, indicating that RNA is mobile in plants. Intercellular and systemic RNA silencing signals may be DNA or RNA molecules such as mRNAs, miRNAs, siRNAs, viral DNA or RNAs, dsRNAs, long stranded ssRNAs, RNA transcription products or derivatives of silenced genes, dsRNA molecules initiating RNA silencing, and complexes formed by RNA and protein. In plants, single-cell, intercellular, and systemic RNA silencing are induced, all of which can be transported over long distances via intercellular plasmodesmata for transport between cells and then through the phloem (Nodine et al., 2000; Braunstein et al., 2002; Klahre et al., 2002; Garcia-Perez et al., 2004; Melnyk et al., 2011; Drusin et al., 2016; Cognat et al., 2017; Reagan et al., 2018; Bélanger et al., 2023). From the studies that have been reported, it appears that in animals this silent mobile signal is dsRNA (Jose et al., 2011; Chen et al., 2018). In *Cryptobacterium showyeri*, systemic RNAi involves the intertissue transfer of the dsRNA selective importer SOD-1 and the entry of gene-specific dsRNAs into the cytoplasm (Feinberg and Hunter., 2003). However, in plants, silencing signals have been a hotspot of debate and research among researchers, and currently siRNAs are the mobile RNA silencing signal molecules that most scientists can accept in plants.

The research demonstrated that RNA molecules (including RNA viruses, endogenous plant mRNAs and non-coding small RNAs) were shown to be non-cell autonomous. Detection of RNA molecules in phloem sap using high-throughput sequencing techniques has detected many major endogenous RNA molecules, including mRNAs and non-coding small RNAs such as siRNAs, miRNAs and rRNAs (Kehr et al., 2018).

They are present in plant phloem molecules and can be transported over long distances, and these short 21-24nt RNAs are involved in plant growth and development, and gene regulation in response to stresses of adversity through movement between cells. Non-cell autonomous miRNAs play a motor signalling role in the regulation of plant growth and development (Skopelitis et al., 2017). In 2018, mobile miRNAs were found to act as local positional signals during plant growth and development and coordinate the stress response of the whole plant (Skopelitis et al., 2018). In addition, other RNAs have been found to be transportable, such as rRNAs and tRNAs found in sap in the phloem by high-throughput sequencing. sequencing results showed that rRNAs (including 5S, 5.8S, 18S and 25S) were detected in rape and pumpkin phloem (Zhang et al., 2009; Ostendorp et al., 2017); in the pumpkin phloem RNA library, a large number of tRNAs were detected (Zhang et al., 2009).

In most plants, there are four DCL proteins, of which DCL1 mainly cleaves miRNA precursors, resulting in 21-nt sRNAs, which are mainly involved in the production of synthesis in the microRNA (miRNA) pathway that regulates plant growth and development (Kurihara and Watanabe., 2004); DCL2 predominantly cleaves dsRNAs of viral origin, resulting in the production of 22-nt sRNAs that act as resistance to viral infection. The cleavage product of DCL3 is a 24-nt sRNA and DCL3 recognizes and cleaves highly repetitive sequences. The sRNAs produced by DCL3 are involved in DNA methylation and chromosome modification (Baulcombe et al., 2004). DCL4 is involved in the production of 21nt siRNAs (Mukherjee et al., 2013; Chen et al., 2018).

In plants, DCL1, DCL2, DCL3, and DCL4 are all involved in the biosynthesis of different si RNAs and regulate gene expression. In *Arabidopsis*, mutants' dcl1-7, dcl1-8, dcl1-9, and dcl1-15 of the DCL1 gene affect significantly lower miRNA accumulation in vivo (Kurihara et al., 2004; Kurihara et al., 2006; Willmann et al., 2011). DCL2 gene function has been shown to play an important role in the synthesis of 22-nt siRNAs in plant resistance to viral infection (Xie et al., 2004; Akbergenov et al., 2006). These 24-nt siRNAs are mainly involved in DNA methylation and chromatin modification (Zilberman et al., 2003; Akbergenov et al., 2006; Wierzbicki et al., 2009). The dcl3-mediated formation of 24nt siRNA can be transported over long distances, leading to systemic TGS, which causes RNA-mediated DNA methylation (RdDM) in the recipient cell (Lewsey et al., 2016; Melnyk et al., 2011). DCL4 is able to cleave reverse repeats inserted in transgenic plants to form 21-nt siRNAs (Dunoyer et al., 2005). DCL4 also plays an important role in antiviral processes by cleaving a variety of DNA and RNA

viruses to form 21-nt siRNAs (Blevins et al., 2006; Deleris et al., 2006; Fusaro et al., 2006; Diaz-Pendon et al., 2007). The dcl4-mediated formation of 21nt siRNA in *Arabidopsis* acts as a PTGS movement signal that can move from leaf companion cells to adjacent cells (Dunoyer et al., 2005). Non-CARS has also been reported to occur in the absence of si RNA (Brosnan et al., 2007). Therefore, how RNA signalling in plant non-cell-autonomous RNA silencing is propagated remains to be investigated (Jose et al., 2011; Devanapally et al., 2015).

In higher plants, it is common for many different families of genes to functionally overlap, resulting in functional redundancy of DCLs. In the absence of the DCL3 function, DCL2 and DCL4 are able to produce RDR2-dependent siRNAs (Blevins et al., 2006; Deleris et al., 2006; Diaz-Pendon et al., 2007). In the absence of DCL4 function, DCL2 and DCL3 are able to produce 22- and 24-nt virus-induced siRNAs, and DCL2 and DCL3 are able to produce RDR6-dependent siRNAs that would otherwise be produced by DCL4 (Gasciolli et al., 2005). In addition to the functional overlap between DCLs and proteins, there is also for example, DCL1 can inhibit the function of DCL4 (Qu et al., 2008).

1.2.3.2 Mobile siRNA

The function of the mobile RNAi signalling molecule siRNA replication and motility has been a hot topic of frontier scientific research. siRNAs are formed from single-stranded RNAs that are transformed into dsRNAs by RNA-dependent RNA polymerases (RdRPs) and further cleaved by Dicer-like (DCL) enzymes. In *Arabidopsis*, these dsRNAs are mainly cleaved by DCL2, DCL3 and DCL4 to produce 22, 24 and 21nt siRNAs, respectively. SiRNAs are then produced to form RISC complexes with different AGO proteins (AGO1, AGO2, AGO3, AGO4, AGO6 and AGO9), which in turn regulate gene expression. 2020. Voinnet's lab discovered that the amount of AGO proteins in the cell determines siRNA transport and that siRNAs can shuttle between cells and move in a double-stranded fashion (Devers et al., 2020).

In *Arabidopsis* thaliana, using micrografting and deep sequencing, sequencing results showed that accumulation of small RNAs tended towards the right-hand strand, perhaps predicting that single-stranded siRNAs are mobile, providing the first evidence that endogenous 22-, 23- and 24-nt siRNAs can all be delivered intercellularly and systemically over long distances (Molna et al., 2010). In *N. benthamiana*, Chen et al.

(2018) induced local siRNA production (L-siRNA) by hairpin-type dsRNA in DCLs by PTGS. High-throughput sequencing of small RNAs resulted in the detection of a large number of 21-24-nt L-siRNAs in systemic leaves, with 22-nt L-siRNAs being the most abundant, followed by a large number of 21-nt L-siRNAs and the fewest 24-nt L-siRNAs. These findings differ from the siRNA results of the *Arabidopsis* and tobacco systemic movement (Taochy et al., 2017; Chen et al., 2018). However, L-siRNAs did not have any amplification effect in distal recipient cells, suggesting that 21-24-nt L-siRNAs can spread between cells via intercellular linkages and can spread over long distances. No mRNA-induced local silencing was detected in young leaves, implying that long ssRNAs are not the motor signal that causes non-CARS. In contrast, a large number of 22-nt L-siRNAs were detected in systemic tissues, suggesting that mobile 22-nt L-siRNAs may be the locomotor signal for non-CARS. Furthermore, inhibition of DCL3 or DCL4 expression enhanced systemic silencing, so the associated 21 or 24nt L-siRNAs are unlikely to be motor silencing signals (Chen et al., 2018). These results suggest that DCL2 is essential for non-CARS in plants and that the 22-nt L-siRNA should be a movement signal for *N. benthamiana* non-autonomous PTGS, are there other signalling molecules involved? The DCL2-mediated formation of 22nt L-siRNA is involved in non-CARS-PTGS transport, which is also consistent with the reported function of DCL2 in siRNA synthesis (Chen et al., 2010).

Studies have shown that DCL2 and its cleavage of virus-derived dsRNAs, generating 22-nt siRNAs, can influence plant development, and play an important role in virus infection. New evidence for the movement of 22-nt siRNAs as a non-cell-autonomous silencing mobile signal in *A.* thaliana and *N. benthamiana*, provides a discussion of siRNA mobility studies opening up a new way of understanding genetic components and small RNA signaling molecules (Yu et al., 2017). At present, the RNA silencing mobile signal still requires further investigations.

1.2.3.3 RNA silencing suppressors

In order to cope with the RNAi mechanism in host plants for efficient replication and infection in hosts, viruses have evolved a series of proteins that inhibit specific RNA silencing functions, called viral suppressors of RNA silencing (VSR) (Lakatos et al., 2006). Different VSRs can act on different components of the host RNA silencing pathway, effectively inhibiting the host's antiviral defense response and driving the immune escape of the virus.

Plants can use PTGS and TGS to resist viral infection. Viruses infesting plants produce a large number of virus-derived small interfering RNAs (vsiRNAs) that mediate the degradation of viral RNAs or repress the transcription of viral genes, and during long-term co-evolution with plants, viruses encode one or more viral suppressors of RNA silencing (VSRs) to suppress gene silencing in plants, thereby escaping this plant defense response. More than 70 VSRs have been reported (Csorba et al., 2015), and most plant viruses encode RNA silencing suppressors, including single-stranded (positive and negative) RNA viruses, double-stranded RNA viruses, and DNA viruses. Their main modes of action are as follows.

1) Inhibition of siRNA production: the production of secondary siRNAs is inhibited by preventing siRNA from binding to RNA (Csorba et al., 2015). Studies have reported that the p19 protein of (*Tomato bushy stunt virus*, TBSV) interferes with host plant gene silencing by binding 21nt siRNA to block siRNA and mediates the down regulation of miRNA expression, incorporating into AGO1 to form the RISC complex (Burgyan et al., 2011; Schott et al., 2012). In addition to P19, P21 of Beet yellows virus, HC-Pro of Potyviral, P15 of PCV virus, and P38 of TCV all function to bind specific small RNAs (Merai et al., 2006; Lakatos et al., 2006). The V2 protein of CaMV is able to directly interact with CaMV's V2 protein is able to interact directly with SGS3, preventing the synthesis of SGS3-associated secondary siRNAs (Glick et al., 2008). The V2 protein in PVX P25 or TYLCV can bind SGS3, reduce SGS3 activity and inhibit secondary sRNA synthesis (Chiu et al., 2010; Rajamaki et al., 2014) HC-Pro of sugarcane mosaic virus (SCMV) interferes with miRNA and siRNA accumulation and inhibits RISC formation. (Glick et al., 2008).

2) Interference with the function of the RISC complex: most VSRs resist RNAi by affecting RISC assembly. For instance, PVX P25 degrades AGO1, AGO2, and AGO4 proteins leading to blocked RISC assembly (Brosseau et al., 2015); the 2b protein of *Cucumber mosaic virus* (CMV) blunts AGO1 activity and inhibits RISC assembly (Fang et al., 2016; Zhang et al., 2017). The TBSV P19 induces miRNA168 expression by binding siRNA to prevent its integration into RISC to achieve viral infection, and the inhibition of RNA silencing by P19 is associated with protein accumulation (Varallyay et al., 2014; Yang et al., 2014; Yang et al., 2016; Yang et al., 2018). In CMV-infected *Arabidopsis*, CMV 2b interacts with AGO1 to reduce RISC activity, which in turn inhibits RISC cleavage of the target (Zhang et al., 2006); the dsRNA-binding activity of the 2b protein plays an important role in CMV pathogenicity, and the 2b-AGO-binding complex

can inhibit host RDR1 - and RDR6-dependent disease resistance silencing (Zhang et al., 2017). Also, 2b proteins inhibit RNA-mediated DNA methylation (RdDM) effects (Brigneti et al., 1998; Duan et al., 2012, Hamera et al., 2016). The vast majority of VSRs can bind RNAi silencing components and resist host disease resistance. For example, the NSs protein of *tomato spotted wilt virus* (TSWV) binds dsRNA, resulting in reduced sRNA biosynthesis and blocked RNA silencing (Ocampo et al., 2016); the twin viruses *Tomato yellow leaf curl China virus* (TYLCCNV), a satellite DNA virus encoding the RNA silencing repressor βC1, binds to RDR6 and induces inhibition of RDR6 expression, which in turn reduces the methylation level of the viral genome and inhibits gene silencing (Yang et al., 2011; Xu et al., 2020).

3) Binding of dsRNA: Inhibiting dsRNA recognition and siRNA production inhibits the function of DCL, one is that the repressor binds preferentially to dsRNAs derived from hairpin structures and inverted repeats, preventing them from being cleaved into sRNAs by DCL, e.g. in vitro, P14 of PoLV and p38 of *Turnip crinkle virus* (TCV) specifically bind long double-stranded RNAs, preventing them from being cleaved into sRNAs by DCL. The p38 protein of PoLV and *Turnip crinkle virus* (TCV) specifically binds long double-stranded RNAs and prevents their cleavage into sRNAs by DCL (Merai et al., 2005; Merai et al., 2006); the P6 protein of CaMV inhibits the function of DCL4 by directly interacting with the double-stranded RNA-binding protein DRB4 (Haas et al., 2008). The other is that the repressor binds to sRNAs or hides them, thus preventing the formation of the silencing complex, as in the case of *Tomato bushy stunt virus* (TBSV) P19.

4) Silencing suppressors modify the host to interact with AGO1 or AGO2 or degrade AGO proteins to affect RISC assembly. The *Cucumber mosaic virus* (CMV) 2b protein and the *Potato Virus X* (PVX) P25 protein inhibit silencing by interacting with AGO, and the PVX P25 protein inhibits systemic silencing in the host mainly by blocking the expression of *Arabidopsis* AGO1, AGO2, AGO3 and AGO4 in *N. benthamiana*. The P25 protein of PVX suppresses systemic silencing in the host by blocking the expression of AGO1, AGO2, AGO3, and AGO4 in *N. benthamiana* (Chiu et al., 2010). Affects CAMTA3-mediated transcriptional activation of RDR6 by disrupting CaM-CAMTA3 interactions and regulates plant immunity to suppress RNAi (Wang et al., 2021; Wang et al., 2022).

Figure 1.5 Functional mechanism of different RNA silencing suppressors
RNA silencing suppressors (pink) has several ways of interfering with RNA silencing (from top to bottom of the figure). 1. by binding to dsRNAs to block the entry of DCL proteins. 2. by binding to sRNAs and sequestering them from the AGO. 3. by mediating degradation of the proteins in the RNA-silencing pathway or interfering with their function. double-stranded RNA-binding protein 4 (DRB4); helper component protease (HC-Pro); flower enhancer 1 (Hen1); nucleotide (nt); RNA polymerase V (Pol V); RNA-dependent RNA polymerase 6 (RDR6) **(Adapted from Lopez-Gomollon and Baulcombe., 2022).**

In recent years, there has been an increasing number of studies on the mechanism of action of viral gene silencing suppressors. By investigating the interaction of silencing suppressors with RNA or key protein molecules in the plant gene silencing pathway, we can explore the mechanism of interaction and suppress plant resistance to viruses to help us better understand the molecular mechanism between plants and viruses, and thus provide new strategic ideas for plant virus control (Figure 1.5) (Lopez-Gomollon and Baulcombe., 2022).

1.3 Viroid overview

Viroids are a class of naked, non-coding, single-stranded loop-closed RNA molecules with the ability to self-replicate, with a genome size of 246-434 nt, and do not encode any proteins (Diener et al., 1999; Flores et al., 2004; Ding et al., 2009; Di Serio et al., 2014; Serra et al., 2014; Zhang et al., 2014b; Ma et al., 2023). Viroids are the smallest

known pathogenic agents and are only found in higher plants (monocotyledons and dicotyledons), causing significant damage and serious economic losses to crop yield and quality (Flores et al., 2005; Ding et al., 2009; Ding et al., 2010; Flores et al., 2011; Navarro et al., 2012b; Cordero et al., 2017; Savary et al., 2019; Wu et al., 2023; Jones et al., 2024).

1.3.1 Discovery of viroids

In 1967, Theodor O. Diener studying the causal agent of potato spindle tuber disease, discovered that a completely different pathogenic agent had been isolated from the affected plants than had been thought to characterize plant viruses, and called it *Potato spindle tuber viroid* (PSTVd) (Diener and Raymer., 1967; Diener et al., 1971; Diener et al., 2003). In 1971, the American plant pathologist Diener named the new pathogen *Potato spindle tuber viroid* (PSTV), the first viroid to be identified. Later, researchers discovered *Citrus exocortis diseas* (CEVd), *Chrysanthemum stunt viroid* (CSVd), *Apple scar skin viroid* (ASSVd) (Hashimoto et al., 1987), *Hop latent viroid* (HLVd), *Coconut cadang-cadang viroid*, CCCVd (Haseloff et al., 1982), *Avocado sunblotch viroid*, ASBVd, *Eggplant latent viroid* (ELVd) (Semancik et al.,1972, 1973; Diener and Lawson., 1973; Hollings and Stone., 1973). The International Committee on Taxonomy of Viruses (ICTV) also formally included viroid species in its classification (Flores et al., 1998) and described them as a new plant pathogen. Since then, viroid organisms have become known as a class of naked, single-stranded, covalently closed, ring-like small RNA molecules.

1.3.2 Classification of viroids

Taxonomic units for viroid species include families, genera, and species, with the highest taxonomic level being family. According to the November 2022 ICTV classification report, there are currently more than 30 identified viroid families (Table 1.1)

The class of viroids is divided into two families based on the presence or absence of conserved region modules in their RNA structure: the potato spindle tuber-like viroids (*Pospiviroidae*) and the avocado day spot-like viroids (Avsunviroidae) (Flores et al., 1997; Flores et al., 2008; Flores et al., 1998; Flores et al., 2008; Flores et al., 2005b; Molina et al., 2007; Gustavo et al., 2012; Jose et al., 2016). The family of Potato spindle tuber viroids is divided into five genera inclduing more than 30 species, the typical

species being *Potato spindle tuber viroids* (PSTVd), members of which are mostly rod-shaped or quasi-rod-shaped, contain a characteristic CCR (central conserved region) in the middle of the molecule and undergo asymmetric rolling loop replication in the nucleus. Because they are found in the nucleus of plant cells and undergo physiological processes such as replication in the nucleus, they are also known as cytosolic viruses by their subcellular localization in plants (Gómez et al., 2010; Jose et al., 2016; Jose et al., 2018).

The family Avocado sunblotch viroids are divided into three genera consisting of five species, the typical species being *Avocado sunblotch viroid*, which are branched and do not have a CCR in their structure. The viroid has a branched structure without a central conserved region, and both its negative and negative strands have nuclease activity, allowing for hammerhead-mediated self-cleavage and symmetric loop replication in chloroplasts (Parisi et al., 2010; Di Serio et al., 2019; Sano et al., 2021). Because they are found in the chloroplasts of plants, where physiological processes such as replication takes place, they are also referred to as chloroplast-like viroids by plant subcellular localization (Jose et al., 2016; Jose et al., 2018).

Table 1.1 Classification of viroids in ICTV

Family	Genus	Species	Abbreviation
Avsunviroidae	*Avsunviroid*	***Avocado sunblotch viroid***	**ASBVd**
Avsunviroidae	*Elaviroid*	***Eggplant latent viroid***	**ELVd**
Avsunviroidae	*Pelamoviroid*	*Apple hammerhead viroid*	AHVd
Avsunviroidae	*Pelamoviroid*	*Chrysanthemum chlorotic mottle viroid*	CChMVd
Avsunviroidae	*Pelamoviroid*	***Peach latent mosaic viroid***	**PLMVd**
Pospiviroidae	*Apscaviroid*	*Apple dimple fruit viroid*	ADFVd
Pospiviroidae	*Apscaviroid*	***Apple scar skin viroid***	**ASSVd**
Pospiviroidae	*Apscaviroid*	*Apscaviroid aclsvd*	ACFSVd
Pospiviroidae	*Apscaviroid*	*Apscaviroid cvd-VII*	CVd-VII
Pospiviroidae	*Apscaviroid*	*Apscaviroid dvd*	DVd
Pospiviroidae	*Apscaviroid*	*Apscaviroid glvd*	GLVd
Pospiviroidae	*Apscaviroid*	*Apscaviroid lvd*	LVd
Pospiviroidae	*Apscaviroid*	*Apscaviroid plvd-I*	PlVd-I
Pospiviroidae	*Apscaviroid*	*Apscaviroid pvd*	PVd
Pospiviroidae	*Apscaviroid*	*Apscaviroid pvd-2*	PVd-2
Pospiviroidae	*Apscaviroid*	*Australian grapevine viroid*	AGVd
Pospiviroidae	*Apscaviroid*	*Citrus bent leaf viroid*	CBLVd
Pospiviroidae	*Apscaviroid*	*Citrus dwarfing viroid*	CDVd
Pospiviroidae	*Apscaviroid*	*Citrus viroid V*	CVd V
Pospiviroidae	*Apscaviroid*	*Citrus viroid VI*	CVd VI

Pospiviroidae	*Apscaviroid*	*Grapevine yellow speckle viroid 1*	GYSVd 1
Pospiviroidae	*Apscaviroid*	*Grapevine yellow speckle viroid 2*	GYSVd 2
Pospiviroidae	*Apscaviroid*	*Pear blister canker viroid*	PBCVd
Pospiviroidae	*Cocadviroid*	*Citrus bark cracking viroid*	CBCVd
Pospiviroidae	*Cocadviroid*	***Coconut cadang-cadang viroid***	**CCCVd**
Pospiviroidae	*Cocadviroid*	*Coconut tinangaja viroid*	CTiVd
Pospiviroidae	*Cocadviroid*	*Hop latent viroid*	HLVd
Pospiviroidae	*Coleviroid*	***Coleus blumei viroid 1***	**CbVd-1**
Pospiviroidae	*Coleviroid*	*Coleus blumei viroid 2*	CbVd-2
Pospiviroidae	*Coleviroid*	*Coleus blumei viroid 3*	CbVd-3
Pospiviroidae	*Coleviroid*	*Coleviroid cbvd-5*	CbVd-5
Pospiviroidae	*Coleviroid*	*Coleviroid cbvd-6*	CbVd-6
Pospiviroidae	*Hostuviroid*	*Dahlia latent viroid*	DLVd
Pospiviroidae	*Hostuviroid*	***Hop stunt viroid***	**HSVd**
Pospiviroidae	*Pospiviroid*	*Chrysanthemum stunt viroid*	CSVd
Pospiviroidae	*Pospiviroid*	*Citrus exocortis viroid*	CEVd
Pospiviroidae	*Pospiviroid*	*Columnea latent viroid*	CLVd
Pospiviroidae	*Pospiviroid*	*Iresine viroid 1*	IVd 1
Pospiviroidae	*Pospiviroid*	*Pepper chat fruit viroid*	PCFVd
Pospiviroidae	*Pospiviroid*	*Pospiviroid plvd*	PoLVd
Pospiviroidae	*Pospiviroid*	***Potato spindle tuber viroid***	**PSTVd**
Pospiviroidae	*Pospiviroid*	*Tomato apical stunt viroid*	TASVd
Pospiviroidae	*Pospiviroid*	*Tomato chlorotic dwarf viroid*	TCDVd
Pospiviroidae	*Pospiviroid*	*Tomato planta macho viroid*	TPMVd

Blod font: Bloded font is representative of species in this genus (https://ictv.global/msl, Accessed October 29, 2022). **(Source: Pengcheng Zhang, 2024)**

1.3.3 Secondary structure of viroid

1.3.3.1 *Pospiviroidae*

Members of the family *Pospiviroidae* have a rod-like or quasi-rod-like secondary structure at their minimum free energy, and the genome structure generally contains a CCR and a terminal conserved region (TCR) or terminal conserved hairpin (TCH). This hairpin structure has an important role in replication because the TCR and TCH occur at relatively the same location in different members of the family Pospiviroidae, so they may have some specific unknown function, e.g., some members can infest monocotyledonous plants, whereas others can only infect dicotyledonous plants. Members of the family undergo asymmetrical rolling loop replication in the nucleus. At present, the family *Pospiviroidae* contains genera *Pospiviroid*, *Cocadviroid*,

Hostuviroid, *Coleviroid,* and *Apscaviroid* (Moreno et al., 2019). (Figure 1.6).

Figure 1.6 The circular structure model and phylogenetic tree of viroids

The central conserved region (CCR), terminal conserved region (TCR), and terminal conserved hairpin structure (TCH) are shown. Sequence-specific TCH and TCR elements do not appear at the same time in the same viroid species. Megax software Maximum-likelihood analysis method was used to construct a phylogenetic tree based on the viroid nucleotide sequence **(photos was quoted from Di Serio et al., 2021).**

1.3.3.2 *Avsunviroidae*

Members of the family *Avsunviroidae* generally have a rod-like or branched conformational structure, and both the positive and negative strands have

hammerhead nuclease structures and undergo symmetric loop replication in the chloroplast. The members of the family *Avamoviroideae* lack CCR typical of the *Pospiviroidae* members, but contain the typical hammerhead nuclease, and other features such as GC content, solubility in 2M LiCl solution. Currently, three genera, *Avsunviroid*, *Elaviroid,* and *Pelamoviroid*, are included (Di Serio et al., 2018). In vitro, they can exhibit rod-like, quasi-rod-like, or branched structures, and they form a similar conformation in vivo (Figure 1.7). In addition, the genomic (+) strand, the most abundant (+) and (-) strand in vivo, both form active hammerhead nucleases involved in the replication process (Figure 1.8 and Figure 1.9) (Dadami et al., 2017; Di Serio et al., 2021).

Figure 1.7 Secondary structure of representative members of Avsunviroidae Conserved nucleotides in the hammerhead catalytic core have filled and open shadows representing ribozymes formed in the positive and negative strands of the viroids, respectively **(photo was quoted from Di Serio et al., 2018).**

Figure 1.8 Hammerhead structure formed by positive strands of two viroids
The catalytic core (black fill), self-cleavage sites (arrows) and helical structures (I, II, III) are shown **(images cited from Di Serio et al., 2018).**

Figure 1.9 Predicted the secondary structure of ELVd (AJ536613) folded at minimum free energy
(Figure was quoted from Daròs et al., 2016)
The domains of the + and - hammerhead ribozymes are highlighted on yellow and orange backgrounds, respectively. The ribozyme self-cleavage sites are indicated by black arrowheads.

1.3.4 Biological features of viroid

Viroid is a class of single-stranded, ring-shaped, covalently closed, naked, low-molecular-weight RNAs that do not encode any proteins but have an important role in host infection, replication, transport, and pathogenesis (Adkar-Purushothama and Perreault., 2020; Ma et al., 2023). Viroid nucleotide sequences are highly complementary, and the genome consists of a dsRNA forming the most stable

secondary structure, flanked by loops and bumps that can form a rod-like or multi-branched conformation (Figure 1.10). Researchers have predicted secondary conformation for viroids with cellular nucleus replication based on electron microscopy, in silico prediction, and biophysics. Later, folding into substable hairpin diagrams were obtained based on three-dimensional atomic force micrograph, possibly showing concave loops or bumps in the molecular conformation, and also showing consistency with the predicted secondary conformation (Figure. 1.10). The spatial conformation of viroid RNAs may be closely related to their biological properties (Moreno et al., 2019; Navarro et al., 2021).

Figure 1.10 Secondary structure and biological features of viroids

(a) Viroids of the family Pospiviroidae replicate in the nucleus in a rod-like secondary structure. They contain specific CCRs and TCH or TCR. Red arrows indicate inverted repeat sequences that fold with the CCR into hairpin I (lower left). Three-dimensional image of an atomic force micrograph of PSTVd RNA (lower right). (b) Viroids of the family Avsunviroidae replicate in chloroplasts with rod-like or branched secondary structures. Three-dimensional image of an atomic force micrograph of PLMVd RNA (lower right) **(Adapted from Navarro et al., 2021).**

1.3.5 Replication and trafficking of viroids

1.3.5.1 viroid replication

Viroid genome contains only a single circular RNA and does not encode any proteins, so they are highly dependent on their host proteins or other factors for replication and reproduced by RNA-mediated loop replication (Flores et al., 2008). However, their replication processes are not identical. Members of the family *Pospiviroidae* replicate in the nucleus of their hosts by the asymmetric pathway of the rolling-circle mechanism, whereas members of the family *Avsunviroidae* replicate in the chloroplasts of their hosts by the symmetric pathway of the rolling-circle mechanism. This difference is mainly due to differences in their genome structure. Because the genome of the family *Avsunviroidae* can form a nuclease structure during folding, which mediates the self-cleavage process, the family *Pospiviroidae* do not possess nuclease activity and therefore must rely on host enzymes for cleaving during replication.

Nuclear replicating viroids first have to enter the host's nucleus in order to replicate (Figure 1.11) (Navarro et al., 2021). Nuclear replicating viroids replicate by asymmetric rolling loop replication (Gago-Zachert et al., 2016). Firstly, RNA polymerase II (RNA pol II) uses the abundant positive strand (+) as a template to translate into a multiplexed negative strand (-) RNA that is complementary to it. Secondly, the multiplexed negative strand RNA is not directly cleaved but is used as a template for the synthesis of multiplexed positive-strand RNA by DdRP II. The synthesized multiplexed positive-stranded RNA is cleaved by RNAase III into multiple viral-like monomeric lengths of stranded RNA. Finally, the RNA ligase activity of DNA ligase I cyclize the stranded viroid monomers into mature viruses and releases them from the nucleus (Nohales et al., 2012a; Kovalskaya and Hammond., 2014; Gago-Zachert et al., 2016; Delgado et al., 2019; Prasad et al., 2023).

Chloroplast-replicating viroids replicate within the host chloroplast (Figure 1.11). Chloroplast replication viroids enter the chloroplast via the endogenous RNA import pathway. Firstly, the genomic circular positive-stranded RNA of the virus-like species is used as a template for transcription to form stranded negative-stranded RNA under the action of nuclear encoded RNA polymerase (NEP). Members of the chloroplast-replicating viroids family have both positive and negative strands with hammerhead structures that are capable of self-cleavage. Secondly, the unit-length molecules are cyclized by tRNA ligase. Then, NEP uses the cyclized unit-length negative-stranded RNA as a template to synthesize positive-stranded RNA, which is subsequently self-cleavage into unit-length positive-stranded RNA and cyclized by tRNA ligase to form a mature viroid. Finally, it is released from the chloroplast into the cytoplasm. (Ding et al.,

2005; Ding et al., 2009; Flores et al., 2009; Gago-Zachert et al., 2016; Marquez-Molins et al., 2021).

During viroid replication, RNApol II and NEP are involved in the transcription of nucleus-replicating viroids and chloroplast-replicating viroids, respectively. (Warrilow et al., 1999; Navarro et al., 2000; Rodio et al., 2007) (Figure 1.11). Both proteases function in the host to transcribe DNA into mRNA and are diverged to transcribe RNA templates in viroid replication (Gago et al., 2009; López-Carrasco et al., 2017). Interestingly, some mammalian and bacterial DNA-dependent RNA polymerases can also use RNA templates to transcribe shorter cellular regulatory RNA molecules (Wassarman et al., 2006; Wagner et al., 2013).

Although a number of transcription factors that assist RNA pol II in mediating HDV replication have been identified (Lucifora et al., 2020), but only limited information of the host-protein involvement on the viroid replication. In contrast, the PSTVd RNA is used as a template to transcribe the negative polarity strand of PSTVd, which is initiated at a specific nucleotide site (Kolonko et al., 2006; Mudiyanselage et al., 2020). It is therefore hypothesized that there is also a specific but unknown initiation site for transcription of the positive polarity strand of cytosolic replication viroids. On the other hand, the NEP-mediated transcriptional start site has been identified in both polar chains of most chloroplast replication viroids. It consists of an AU-rich terminal loop in ASBVd and a short double-strand RNA (dsRNA) stem loop containing a hammerhead self-cleavage site in PLMVd (Flores et al., 2009). In contrast, the transcription start sites of the two polar strands of ELVd are localized to different sequence/structural motifs (López-Carrasco et al., 2016). The cleavage sites of the positive-strand RNA oligomers of representative members of the *Pospiviroidae* (CEVd, HSVd, and ASSVd) are in equivalent positions in their respective hairpin I (HP I) structures (Gas et al., 2007) (Figure 1.11). Although the cleavage enzyme has not been identified, it is assumed that an RNase III-like enzyme is involved. In the proposed cleavage model, two consecutive monomers of HP I may interact to produce a transient dsRNA structural domain suitable for RNase III-like enzyme-mediated cleavage. Importantly, CEVd RNA in vivo contains a 5'-phosphate mono-ribonucleotide and a 3'-hydroxyl terminus with terminal features compatible with RNases III enzyme-mediated cleavage termini (Gas et al., 2008).

In contrast to nuclear-replicating viroids, the self-cleavage of positive and negative-

stranded poly RNA in chloroplast-replicating viroids is an autocatalytic process mediated by cis-acting hammerhead ribozymes (HRzs) (Daròs et al., 1994). Although ribozyme activity is protein-independent, host factors may be involved in facilitating the formation of active hammerhead conformations in vivo, such as the chloroplast protein PARBP33, which binds ASBVd in vivo and promotes viroids self-cleavage in vitro (Daròs et al., 2002). After cleavage into monomers, oligomeric RNA molecules complete the replication cycle by cyclizing the monomeric RNA through the catalytic activity of ligases. The chloroplast isoform of tRNA ligase was found to be involved in the cyclization of chloroplast replication viroids (Nohales et al., 2012b). The substrates of this enzyme are 5-hydroxy and 2, 3-phosphodiester terminated, corresponding to those produced by hammerhead-mediated self-cleavage of oligomeric viral RNAs. Interestingly, ELVd can only be cyclized by tRNA ligase when the end is opened from the self-cleavage site, suggesting that specific viroid structural motifs play a key role in the ligation process (Nohales et al., 2012a; Teresa et al., 2018). Based on these findings, it was demonstrated that the HRz structural domain of ELVd is involved in the in vivo cyclization of this class of viroids, based on the analysis of mutations in *E. coli* that heterologously express chloroplast tRNA ligases (Cordero et al., 2018). Surprisingly, it was shown that the enzyme involved in the monomer ligation of PSTVd, as well as other nuclear replication-like viruses, is cytosolic DNA ligase 1 (Nohales et al., 2012b), which provides a paradigm for the forced replacement of DNA-based host enzymes with RNA by viroids. Further studies are therefore required to fully resolve the host factors involved in viroid replication, including the identification of enzymes involved in the cleavage and their functional details on replication of cytosolic viroids, as well as host factors that may interact with structural motifs associated with viroid RNA replication (Ma et al., 2022) (Figure 1.11).

Figure 1.11 Replication and transport mechanisms of viroids

Red arrows indicate viroid transport pathways. Black arrows indicate host proteins and Rz is involved in the replication cycle of viroid. Grey arrows indicate viroid as triggers and targets of RNA silencing mechanisms. Blue arrows indicate other possible pathogenic pathways. Abbreviations: AGO: Argonaute; CsPP2: cucumber phloem protein 2; DCL: Dicer-like protein; ETI: effector-triggered immunity; MAPK: mitogen-activated protein kinase; mRNA: messenger RNA; NEP: nuclear-encoded RNA polymerase; PAMP: pathogen-associated molecular pattern; PD: plasmodesmata; PTI: pathogen-associated molecular pattern–triggered immunity; RDR: RNA-dependent RNA polymerase; RNApol II: RNA polymerase II; ROS: reactive oxygen species; rRNA: ribosomal RNA; Rz: ribozyme; tRNA: transfer RNA; vd-sRNAs: viroid-derived small RNA **(photo was quoted from Navarro et al., 2021).**

1.3.5.2 Viroid movement

It has been previously reported that viroid as non-coding RNA can move not only intracellularly, intercellularly between cells but also systematically within the host tissues, providing a good system for studying RNA transport mechanisms in plants

(Wang et al., 2010; Kitagawa et al., 2015). Once a viroid enters a cell, it can specifically enter the nucleus or chloroplast for replication. After being released into the cytoplasm, the cyclized mature RNA is transferred via intercellular plasmodesmata to neighboring cells and reaches the distal end of the plant via the phloem (Ding et al., 1997; Qi et al., 2003; Mathieu et al., 2003; Gómez et al., 2003; Zhu et al., 2001; Otero et al., 2016; Ma et al., 2022; Ma et al., 2023) (Figure 1.12).

Viroid inoculation or mechanical transmission occurs mainly by rub inoculation. The cycle of viroid infection is divided into five main steps: a) entry of the viroids into the susceptible host cell; b) entry through the cytoplasm into the nucleus or chloroplast, c) self-replication and newly synthesized viroid enters the cytoplasm from the organelle and enters adjacent cells via intercellular plasmodesmata; d) enters the vascular system for long-distance transport via the phloem; e) it reaches the leaves and other non-inoculated leaves such as roots via the phloem, completing the systemic infection of the plant. (Figure 1.12) (Ding et al., 2009; Ding and Wang., 2009; Takeda and Ding., 2009).

In terms of viroid entry from the cytoplasm into the nucleus, Woo et al. inoculated treated *N. benthamiana* cells with fluorescently labeled PSTVd. The results showed that the entry of PSTVd from cytoplasm into nucleus was a cytoskeleton-free process that was mediated by a sequence or structure-specific receptor. The same size mRNA and two other chloroplast-replication viroids did not occur similarly in the control group. (Woo et al., 2010; Prasad et al., 2023).

In terms of intercellular transport, microinjection of fluorescently labeled PSTVd-infected clones with in vitro transcription products revealed that PSTVd moves between cells via intercellular plasmodesmata, and that this movement is likely to be mediated by specific sequences or structural units (Ding et al., 1997; Wu et al., 2024). Qi et al. found that some variants of PSTVd that exist in nature do not cross specific cell boundaries, and they identified a motif that effectively facilitates the transport of PSTVd from vimentin sheaths into chloroplasts, but not in reverse (Qi et al., 2004).

Although no role has been identified for host factors in the transport of viroid organisms between host cells, the systemic movement of viroid organisms in plants is regulated by host factors. Viroid binding protein 1 (VirP1) in tomatoes is able to bind to the right terminal region of PSTVd, thereby affecting the systemic movement of the viroid

organisms in the plant (Maniataki et al., 2003). The phloem protein 2 (PP2) in cucumber binds to HSVd and facilitates its long-distance transport in cucumber (Gómez and Pallás., 2001; Owens et al.,2001; Gómez and Pallás., 2004).

Only chloroplast replication viroids are known to cross host bilayer plastid membranes, whereas this has not been reported for other host RNA, so it has been speculated whether host RNA would also enter or leave the chloroplast via the same pathway as the viroid. Notably, exogenous mRNAs fused to ELVd or CChMVd RNAs are able to enter the chloroplast, suggesting that the aforementioned viroid RNA molecules contain specific chloroplast localization signals (Gómez et al., 2010; Baek et al., 2017). Cucumber phloem protein 2 (CsPP2), one of the most abundant proteins in the cucumber phloem, may interact with HSVd in vitro and in vivo through a dsRNA binding domain (Gómez et al., 2001; Owens et al., 2001; Gómez et al., 2004;). Interspecific grafting experiments have shown that the ribonucleoprotein complex of HSVd/CsPP2 can be translocated from the rootstock to the scion, suggesting that CsPP2 is involved in the systemic movement of HSVd, in addition to the possible involvement of CsPP2 in cellular RNA movement. Finally, Solovyev et al. reported that the *N. benthamiana* 4/1 protein (*N. benthamiana* 4/1, Nt-4/1) may play an important role in the long-distance movement of PSTVd (Solovyev et al., 2013).

Figure 1.12 Pathways for systemic trafficking of viroids

A. Spread of viroids from the inoculated leaf to the upper leaves and roots. B. Intercellular spread from infected epidermal cells to phloem cells. The various cell types in the mesophyll, xylem, and phloem are not depicted. C. Spread of viroid from

phloem cells to non-vascular cells in systemically infected leaves. D. Intercellular spread of intercellular symplastic transport (SPT) through the plasmodesmata. The plasma membrane (PM) allows specific molecules to be exchanged across the cell wall via apoplastic transport (APT). ER=endoplasmic reticulum) ; CS=cytoplasmic sleeve **(Adapted from Takeda and Ding., 2009).**

1.3.6 Viroid disease

As they do not encode any protein, they need to replicate and complete their systemic infection with the help of the host system (Ding et al., 2009; Flores et al., 2016; Prasad et al., 2023). Viroid infection of most angiosperms (both herbaceous and woody) causes diseases such as leaf curl and blotch, bark splitting, necrosis, plant dwarfing, vein discoloration, flower, and fruit deformities and, in a few cases, outright plant death, causing economic losses to crops (Flores et al., 2005; Kovalskaya and Hammond., 2014; Savary et al., 2019; Ortola and Daros., 2023) (Figure 1.13). These symptoms are similar to viruses, suggesting that viroid pathways may share similar signaling pathways with viruses in the pathogenic process (Flores et al., 2016). Recent studies have suggested that viroid pathogens may cause disease through three pathways: 1) an interaction pathway with host proteins; 2) a hormone-mediated signaling pathway; and 3) an RNA silencing pathway (Navarro et al., 2012b).

Viroid pathogenesis is long-lasting and has a wide range of effects, from devastating to symptomless diseases. For example, in Japan, hops (*Humulus lupulus*) dwarf disease has caused significant economic losses to the country's hops industry (Sano et al., 2013). In the Philippines, diseases caused by coconut death-like viroids have killed hundreds of thousands of coconut trees (Vadamarai et al., 2017). PSTVd mutant strains show strong symptoms in tomatoes while being virtually symptomless in *N. benthamiana* (Wu et al., 2013). The eggplant latent class of viroids has also been reported to have no significant effect on plants (Fadda et al., 2003).

Figure 1.13 Symptoms of different types of viroid infection in various crops
(A) Potato was infected by PSTVd. (B) Eggplant was infected by ELVd. (C) Peach was infected by PLMVd. (D) Chrysanthemum was infected by CSVd. (E) Citrus was co-infested by CBLVd and CDVd (left). Citrus was co-infected by CEVd and CBCVd (middle), and citrus was infected by CBCVd (right) **(Adapted from Ortola, B and Daros, JA., 2023).**

1.3.7 Viroid Defence Mechanisms

Plants have evolved multiple defense mechanisms over time in response to different pathogen infections. The main defence mechanisms in plants against viroids include 1) RNA silencing of viroid RNAs, 2) degradation of viroid RNAs by nucleases and 3) modification of viroid RNAs (Ding et al., 2009). The most studied and important of these three pathways is the RNA silencing pathway (Gómez et al., 2012b).

1.3.7.1 RNA silencing defense against viroids

The RNA silencing pathway functions in two ways: RNA silencing can regulate the

expression of host genes to facilitate their infection and pathogenicity; similarly, RNA silencing can be used by host plants to inhibit the infection of viroids (Flores et al., 2015; Navarro et al., 2012b). RDR is important in the defense mechanism of plants against viroid infection and constitutes the first line of defense against viroids (Kalantidis et al., 2008). It is suggested that other proteins are also involved in this process, uncovering the role of the genes encoding these proteins in plant defense against viroid infections remains a current hot topic in viroid research (Lopez-Gomollon and Baulcombe., 2022).

1.3.7.1.1 DCLs involved in defense viroids

DCL genes are central components of the RNA silencing pathway and play an important role in the biosynthesis of microRNA (miRNA) and small interfering RNA (siRNA) (Emily et al., 2001; Ding et al., 2009). Most plants encode four DCLs, DCL1 is involved in the production of 21 nt or 22 nt miRNAs; DCL2 is involved in the production of 22 nt siRNAs in plants or pathogens (Bouche et al., 2006); DCL3 is involved in the production of endogenous 24 nt siRNAs that mediate DNA methylation in heterochromatin regions and maintain genomic stability (Qi et al., 2005). DCL4 is involved in the production of 21 nt siRNAs, mediating the cleavage of target mRNAs and their degradation (Watanabe et al., 2004; Xie et al., 2004; Qi et al., 2005; Xie et al., 2005; Mossiard et al., 2007; Salcador et al., 2016; Wang et al., 2018).

DCLs play important roles in plant defense against virus infection. The roles of DCLs in virus resistance were revealed using single or double mutants of DCLs. Potato virus X (PVX) accumulation was low in the root systems of the dcl2 or dcl3 mutants of *N. benthamiana*, while virus accumulation was high in the roots of the dcl4 mutant. This suggests that DCL4 is able to inhibit PVX replication in *N. benthamiana* roots (Andika et al., 2015). In the *Arabidopsis* dcl2/dcl4 mutant, the accumulation of cucumber mosaic virus (CMV) and turnip mosaic virus (TuMV) was increased (Diaz-Pendon et al., 2007; Garcia-Ruiz et al., 2010). In addition, the accumulation of potato virus Y (PVY) was increased in the tomato dcl2/dcl4 mutant (Kwon et al., 2020), suggesting that DCL2 and DCL4 are the main components of resistance to virus infection. In addition, in the absence of DCL4 gene function, it is mainly DCL2 that mediates plant resistance to viruses (Llave et al., 2010). For example, in the case of down-regulated expression or loss of function of the DCL4 gene, DCL2 produces a 22 nt-siRNA with resistance to turnip crinkle virus (TCV) (Deleris et al., 2006).

Changes in DCL expression levels can affect plant resistance to viroid agents. In *N. benthamiana*, down-regulation of expression of the DCL4 gene, or simultaneous down-regulation of DCL4 in combination with DCL1, DCL2, and DCL3, using RNA interference techniques, retards viroid infection (Dadami et al., 2013; Katsarou et al., 2016). However, if both DCL2 and DCL3 are down-regulated, viroid infectious is enhanced (Katsarou et al., 2016). In tomatoes, simultaneous down-regulation of expression of DCL2 and DCL4 using RNAi technology facilitated the initial infection of PSTVd (Suzuki et al., 2019). Taken together, DCLs have important functions in plant resistance to viroids.

1.3.7.1.2 AGOs involved in defense viroids

Argonaute (AGOs) proteins are the core components of RISC, there are multiple Argonaute family proteins in different species, in *Arabidopsis*, there are 10 AGO proteins AGO1-10, of which AGO1, AGO2, AGO4, AGO5, AGO7, AGO10 have antiviral properties. AGO enzymes generally possess a PAZ and A PIWI structural domain (Hammond et al., 2000), which generally affects the efficiency of RNA and protein-virus interactions (Dalmadia et al., 2019), AGO is a major player in the formation of miRNA-induced gene silencing complex (miRISC) and is responsible for the accumulation of siRNA with gene methylation modification (Yang et al., 2006) and tasi RNA formation (Qu et al., 2008) and even AGOs are the catalytic part of the RNA-induced silencing complex (RISC), and in addition to their function in cleaving target mRNAs, AGOs can inhibit mRNA translation and mediate DNA methylation (Bortolamiol et al., 2007; Csorba et al., 2010; Fusaro et al., 2012; Derrien et al., 2012). AGO1 and AGO2 in *Arabidopsis* are major components of RNAi-mediated resistance to RNA viruses (Yang et al., 2006; Baumerger et al., 2007).

Different AGO proteins bind to sRNAs to form RISCs, which play a silencing role in the PTGS and TGS pathways (Mallory and Vaucheret., 2010). In addition to binding siRNAs, AGOs also catalyze the specific cleavage of target RNAs by RISC.

In *Arabidopsis*, there are 10 AGO proteins, of which AGO1, AGO2, and AGO7 normally bind to 21 or 22 nt siRNAs; AGO4, AGO6, and AGO9 bind to 24 nt-siRNAs and mediate TGS occurrence; and although AGO5 also binds to 24 nt-siRNAs, AGO1, AGO2, and AGO5 mediate PTGS (Qi et al., 2006; Yang et al., 2006; Takeda et al., 2008; Bologna

and Voinnet., 2014). It has been shown that AGO binds to viral sRNA to form RISC, deactivating RNAs that are complementary to it (Ho et al., 2010).

In contrast, in *N. benthamiana*, AGO1, AGO2, and AGO3 bind primarily to 21 and 22 nt of PSTVd-sRNA, whereas AGO4, AGO5, and AGO9 bind to 24 nt of PSTVd-sRNA. The accumulation of PSTVd was delayed when AGO1, AGO2, AGO4, and AGO5 were overexpressed, suggesting that AGO not only binds viroid sRNAs but also functions as an antagonist against them (Minoia et al., 2014).

1.3.7.1.3 RDRs involved in defense viroids

Expression of RDRs in plants is regulated by a variety of endogenous signaling molecules and biological stresses. RDR-mediated RNA silencing signaling has an important role in antagonizing viroid resistance, mainly because RDR-mediated secondary siRNAs amplify the RNA silencing signal and participate in disease resistance and are involved in plant-virus interactions through multiple pathways (Naoi et al., 2020).

There are six RDRs in most plants, of which both RDR1 and RDR6 are involved in viroid processes. Li et al. demonstrated that RDR6 is involved in a pathway of virus-crop interactions, whereby the viral RDR alters the distribution of the regulatory HSP20 protein, thereby influencing plant defense. (Li et al., 2015; Kumar et al., 2015).

For example, an infection of cucumber with different variants of HSVd (HSVd-g54 and HSVd-h) both significantly induced the expression of the host RDR1 gene (Xia et al., 2017; Schiebel et al., 1998). In addition, the accumulation levels of PSTVd, as well as PSTVd-sRNA, were increased by VIGS down-regulated expression of RDR6 in *N. benthamiana* (Adkar-Purushothama and Perreault., 2019). Another study found that in transgenic *N. benthamiana* overexpressing RDR1 delayed the accumulation of the viroid organisms (Li et al., 2021). In *N. benthamiana*, silencing RDR6 by RNAi was able to accumulate the viroid in the SAM of the plant and the accumulation was high (Di Serio et al., 2010a; Di Serio et al., 2010b).

1.3.7.2 Ribonuclease degradation

In a study of host nuclease degradation of viroid organisms, Matoušek et al. found that pollen nucleases play an important role in the degradation of HLVd (hop latent viroid, HLVd) (Matoušek et al., 1995; Matoušek et al., 1999; Matoušek and Patzak., 2000). HLVd proliferates in the mononuclear pollen of hops but disappears after the first mitotic phase during pollen vesiculation and maturation, which is associated with the expression of pollen nucleases and other specific nucleases. The pollen nuclease HBN1 (Hop bifunctional nuclease 1), for example, reaches its highest activity during the vesiculation phase and then decreases in mature pollen. The selective degradation of HLVd during pollen maturation may also be related to the 7SL RNA (signal recognition particle RNA) of hops, which is similar in size and secondary structure to viroid RNA and which is more stable during pollen maturation, but the degradation of hops latent viroid (HLVd) is selective, and this the degradation was not the result of RNA silencing, as the 100-230 nt RNA produced by degradation was not the Hops latent virus (HLVd)-specific 21-24 nt sRNA that is characteristic of RNA silencing (Matoušek et al., 1995; Matoušek et al., 1999; Matoušek and Patzak., 2000; Matoušek et al., 2008; Ding et al., 2009).

1.3.7.3 Viroid RNA processing modifications

One potential possible mechanism for host inhibition of the infection of the viroid species is by modifying the genome of the viroid RNA to inactivate the interaction of the RNA with the host factor and inhibit its binding, thus achieving restriction of the viroid infection (Ding et al., 2007). ME1, a type I ribosome-inactivating protein (RIP), is reported to be an enzyme that deletes adenine (A) specific to the sarcin/ricin loop or rRNA E loop of hypoxanthine. In vitro, treatment of PSTVd transcript products with ME1 was found to partially denature and incapacitate the host. However, the possibility of depurination or otherwise modifying the viroid organism in the host for defense against the virus requires further investigation (Park et al., 2004; Ding et al., 2009).

1.4 High Throughput Sequencing

As an important experimental technique in molecular biology, DNA sequencing has also greatly advanced research and development in life sciences due to its rapid DNA sequencing methods. The first-generation sequencing technologies, represented by the Sanger strand termination method and the Maxam and Gilbert chemical degradation method in 1977, were used in the Human Genome Project (HGP), which

also directly contributed to the development of Next-Generation Sequencing (NGS). NGS was born and has grown significantly. Next-generation sequencing technologies, also known as Deep Sequencing or High Throughput Sequencing (HTS), are represented by the Roche 454 pyrophosphate sequencer, the Illumina Solexa polymerase synthesis sequencer, and the ABI SOLiD ligase sequencer. Compared to the first generation of testing technologies, high-throughput sequencing can read millions of sequences at a time, resulting in a comprehensive analysis of the genome and transcriptome of a species, and has become a mainstream testing method that is now widely used due to its high accuracy, large data volume, speed, and low cost. With the development and refinement of the technology, the HeliScope platform of the Genetic Analysis System by Helicos HeliscopeTM (2008), the Single Molecule Real Time (SMRT) by Pacific Biosciences (2009), and the Genetic Analysis System by Helicos HeliscopeTM (2009), Nanopore sequencing from Oxford Nanopore (2012), DNA nanoball sequence from BGI -Tech (2015) and represent the third generation of sequencing technologies. Illumina HiSeq combines the advantages of high throughput, high accuracy, low cost, and sequencing read lengths are being extended. According to incomplete statistics, Illumina currently has the highest market share of sequencers. BGI -Tech has independently developed into a new desktop-based sequencing system, DNBSEQ, and its market acceptance is skyrocketing. Nanopore single-molecule technology is expected to be the least expensive single-molecule sequencing method (Barba et al., 2014; Heather and Chain., 2016)

1.4.1 Types of RNA Sequencing

1.4.1.1 Transcriptome sequencing

Transcriptome sequencing, also known as RNA sequencing (RNA-seq), is the sum of all the RNAs that can be transcribed from a given cell in a given functional state, including mainly mRNA and non-coding RNAs. The sequencing results are analyzed. The process of transcriptome sequencing includes sample preparation, library construction, DNA cluster amplification, high-throughput sequencing, and data analysis. Transcriptome sequencing can be divided into sequencing with a reference genome and sequencing without a reference genome.

Transcriptome sequencing with a reference genome involves the comparison of RNA-seq results with a reference genome in species where genome sequencing has been completed, analysis of mRNA sequence information, and analysis of gene structure and new transcripts generated, leading to analysis of gene expression differences,

gene structural variation, variable cleave sites and screening of molecular markers. For transcriptome sequencing without a reference genome, de novo transcriptome sequencing is performed, and the sequenced reads are de novo assembled to obtain a single gene sequence set (unigenes), which is used as the reference sequence for subsequent analysis.

1.4.1.2 Small RNA sequencing

Small RNA deep sequencing technology is a method for sequencing small interfering RNAs (siRNAs) produced by a viral invasion of plants, Small RNA is a class of non-coding RNA molecules about 20-30 nt long, which is a large and diverse group of molecules that play an important role in the regulation of gene expression, biological growth and development, metabolism and disease development, and other physiological processes.

The process of small RNA sequencing is to first isolate small RNA in the range of 18-30 nt from total RNA, add specific junctions at each end, and then reverse transcribe it in vitro to make cDNA before further processing, and then use a sequencer to directly sequence the DNA fragments at the one-way ends. The flow chart for small RNA deep sequencing technology is as follows (Figure 1.14).

High-throughput sequencing technology based on sRNA can analyze and quantify miRNAs, siRNAs, and piRNAs in the transcriptome and genome of a species' cells or tissues, identify known sRNAs, predict new sRNAs and predict the target genes of sRNAs, providing powerful tool to study the functions and regulatory mechanisms of sRNAs. Most of the current sRNA sequencing is based on the detection of miRNAs, from which a genome-wide miRNA map of the species can be obtained, enabling scientific applications including the mining of new miRNA molecules, the prediction, and identification of their target genes, differential expression analysis between samples, clustering of miRNAs and expression profiling.

Figure 1.14 Flow chart of small RNA deep sequencing technology (Adapted from BGI-Tech, China)

1.4.1.3 Degradome sequencing

Degradome sequencing focuses on the sequencing of miRNA-mediated cleave degradation fragments, screening miRNA-acting target genes from experiments, and combining the advantages of bioinformatics analysis to determine the precise pairing information between degraded fragments and miRNAs.

The vast majority of miRNAs in plants use cleaving to regulate the expression of target genes, and cleaving often occurs at the tenth nucleotide in the region complementary to the miRNA and mRNA. The target gene is cleaved to produce two fragments, a 5' fragment, and a 3' fragment. The 3' fragment, which contains a free 5' monophosphate and 3' polyA tail, can be ligated by RNA ligase and the ligated product can be used for downstream high-throughput sequencing, while the intact gene containing a 5' cap structure, a 5 ' fragments or other RNAs lacking a 5' monophosphate group cannot be ligated by RNA ligases and therefore cannot be used in downstream sequencing experiments; in-depth comparative analysis of the sequencing data reveals visually that there is a peak at a site in the mRNA sequence that is a candidate miRNA cut site This is where the candidate miRNA cut site is located. The use of degradome

sequencing allows for the identification of miRNA target genes from experiments without the limitations of bioinformatic prediction.

1.4.2 Application of high-throughput sequencing in plant virology research

High-throughput sequencing technologies have been used in all aspects of biological research, and the discovery and identification of new viruses and viroids is increasingly being reported, together with their mechanisms of plant-virus/viroid interactions. These technologies will play important roles for scientific and technological research in the next 10-30 years.

1.4.2.1 Detection and identification of plant viruses and viroids

High-throughput technology has been an effective method for the detection, discovery, and identification of plant viruses. The technology does not require knowledge of virus sequences and pathogenic genome sequences and allows the genome or transcriptome of a sample to be determined in a short time and at a low cost. A large number of plant virus or viroid genomes have been discovered and identified using high-throughput sequencing and bioinformatics analysis, and many new viruses have been discovered and identified, these include RNA viruses (Ai Rwahnih et al., 2009; Donaire et al., 2009; Wu et al., 2023) and viroids (Ai Rwahnih et al., 2009; Lee et al., 2022). In recent years, hundreds of new plant viruses have been reported (Hadidi et al., 2016). However, only a few new classes of viroids have been reported, such as grapevine hammerhead viroid (GHVd) (Wu et al., 2012), persimmon viroid 2 (PVd 2) (Ito et al., 2013), grapevine latent viroid (GLVd) (Zhang et al., 2014b), apple hammerhead viroid (AHVd) (Zhang et al., 2014b; Serra et al., 2018) and Lychee viroid (LVd) (Jiang et al., 2017), among others.

When using NGS technology to detect and identify plant viruses or viroids, the detection process includes sample preparation, library construction, high-throughput sequencing, data analysis, and validation of results. Plant viruses and viroids can also be detected indirectly by NGS in the form of siRNAs. NGS can detect the virus or viroid-derived siRNAs (virus or viroid-derived siRNAs) in plants that overlap in sequence and can be assembled to obtain genomic fragments of viruses or viroids, and as the siRNAs are the length of 21-24 nt, they can also be used directly as primers for PCR or RT-PCR to amplify viral or viroid genomic fragments, depending on their sequence (Al Rwahnih et al., 2009; Barba et al., 2014).

1.4.2.2 Unravelling the mechanisms of plant-virus or viroid interactions

High-throughput sequencing techniques also have a wide range of applications in the study of plant-virus or viroid interaction mechanisms. For example, the role of RNA silencing in plant-viroid interaction studies has been investigated by high-throughput sequencing of viroid-derived small RNA (vd-sRNA) (Di Serio et al., 2009; Navarro et al., 2009). Vd-sRNA and virus-derived small RNA (vsRNA) are the most important components of the host plant's response to foreign replicons through silencing mechanisms. High-throughput sequencing of vd-sRNA or vsRNA also allows for the study of various aspects of viroid and virus characteristics, accumulation, phylomotor activity, pathogenicity, biosynthesis and host-host interaction (Hadidi et al., 2009). Interactions with the host (Hadidi et al., 2016; Wu et al., 2023).

It was reported that the PSTVd/tomato system was used to analyze the mechanism of plant-viroid interactions by transcriptome sequencing (Zheng et al., 2017), and it was found that variable cleaving of most genes occurred after PSTVd infection of tomato, host miRNA-mediated cleaving activity was enhanced, and phased secondary short interfering RNA (phasiRNA). Kappagantu et al. analyzed changes in gene expression in HSVd-infected hops by transcriptome sequencing and found changes in the expression of defense-related genes, suggesting that HSVd infection altered host metabolism, physiology and plant These results suggest that HSVd infection alters host metabolism, physiology, and plant defense responses (Kappagantu et al., 2017).

1.5 Purpose and significance of the research

1.5.1 Identification of a Research Gap

A great deal of work has been done on intercellular and systemic RNAi as opposed to intercellular and systemic RNAi. RNA silencing can be used by plants to resist viral infections. RNAi involves mobile RNA signalling and various genetic factors. Although studies on how RNAi is transported from cells to systems are controversial, we know little about the propagation of RNAi between organelles within cells. However, intracellular RNAi can target organelle-specific pathogenic RNA. It has been reported that non-coding siRNA has been found to be associated with the chloroplast genome. In addition, certain types of pathogenic RNA, such as ELVd RNA can specifically enter chloroplasts. For example, it has been clearly reported that intracellular RNA transport

between the cytoplasm and the chloroplast may occur (Gómez et al., 2012b). These sporadic hints imply that intracellular RNAi and RNA signalling may occur between organelles in plant cells for transport. However, intracellular RNA signalling in RNAi and the role of RNAi in intracellular propagation in plants are areas of research that have long been neglected. Therefore, we present this project based on 'some hints' of research. How RNAi propagates from the cytoplasm to chloroplasts, mitochondria and other organelles in plant cells remains to be investigated. On the other hand, the intracellular spread of RNAi may be a new mode of regulation, whereby small RNAs derived from nuclear genes regulate the expression of organelle genes. In this project, we will use a chloroplast-localised viroid, *Eggplant latent viroid* (ELVd), as a tool, and our newly established series of unique DCL-RNAi transgenic lines as a study to investigate how intracellular RNAi propagates from the cytoplasm to the chloroplast and to explore how RNA signalling and associated genetic networks on the mechanisms regulating PTGS during intracellular inter-organelle transport, and its biological relevance to plant antiviral defence (Fadda et al., 2003; Gómez et al., 2012b; Daròs et al., 2016). These are very interesting and challenging research questions, and in order to study these areas we may reveal new regulatory and defence mechanisms. The successful outcome of these innovative efforts will not only be of fundamental scientific interest but will also provide insights into how new strategies for disease control in food and cash crops can be developed. The project-specific technology roadmap is as follows (Figure 1.15).

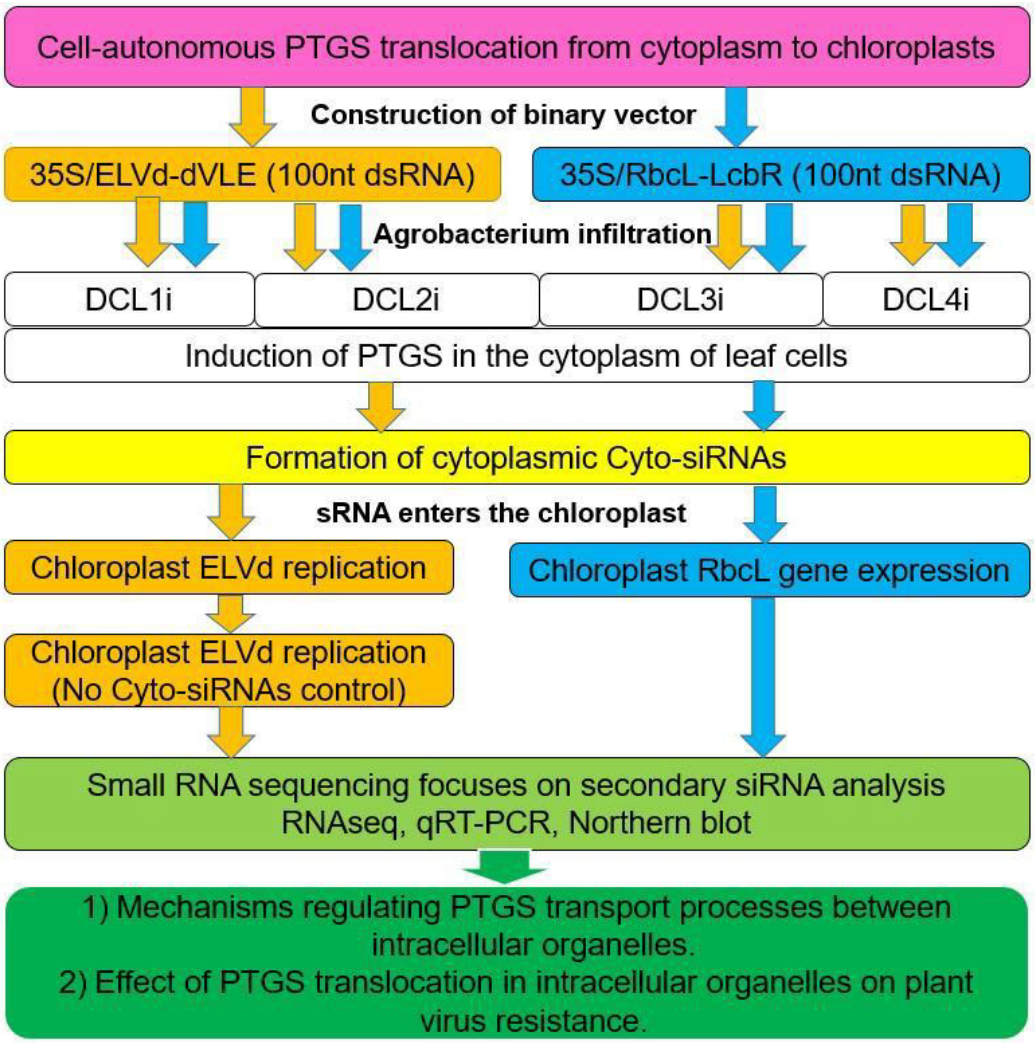

Figure 1.15 Technology roadmap of the project

(Source: Pengcheng Zhang, 2024)

1.5.2 Research questions

1) Is intracellular signaling of RNAi among organelles genetically programmed?
2) Does intracellular spread of RNAi involve small RNA signals?
3) What is the role of spread of RNAi among organelles in cellular defence against pathogen infection?

1.5.3 Research Aims and Objectives

Overall aim of the project is to reveal, 1) the genetic mechanism and molecular signals involved in intracellular signaling for RNAi within plant cells; and 2) the role of intracellular spread of RNAi in plant defence.

The specific aims and objectives of the project include:

1) Investigating the involvement of intracellular RNAi in plant cellular defense against ELVd infection.

2) Identifying genetic requirements and siRNA signals for plant intracellular RNAi-mediated defense.

3) Determining the role of intracellular spread of RNAi in plant defense.

1.5.4 Methodology/critical framework for the research

1. Intracellular spread of RNAi from cytoplasm to chloroplast

1) Establishment of intracellular RNAi that targets genes encoded by chloroplast genome – A series of hairpin-RNAi constructs were generated. These RNAi constructs will be used to generate siRNAs that are specific to short range of approximately 200nt portions of selected chloroplast genes in cytoplasm. Chloroplast samples will then be collected for RNA extraction. Small RNA libraries will be constructed and sequenced by Illumina siRNA sequencing. Length and distribution of siRNAs across chloroplast genome will be profiled. These experiments will establish whether cytoplasmic siRNA will be able to trigger RNAi-mediated degradation of chloroplast mRNAs within plant cells.

2) A similar set of experiments will be performed in transgenic DCL-RNAi lines in order to reveal which type of DCLs and which type of siRNAs are required for cytoplasm-originated siRNA to trigger RNAi in chloroplasts.

3) Induce PTGS to produce siRNA targeting chloroplast gene (*RbcL*, ribulose-1,5-biphosphate carboxylase/oxygenase large subunit gene) in the cytoplasm of *N. benthamiana* and transgenic DCL-RNAi (DCL1i, DCL2i, DCL3i, DCL4i) by hairpin dsRNA.

4) Construct binary vectors for potential chloroplast ribonuclease genes.

5) Establish chloroplast isolation and chloroplast sRNA sequencing methods to analyze whether siRNA could be transported from cytoplasm to chloroplast.

6) Analyze the regulation mechanism of cytoplasmic siRNA on *RbcL* gene expression by qRT-PCR or Northern blot.

7) Analyze the effect of DCLs on the chloroplast gene siRNA formation.

8) Carry out deep sequencing and bioinformatics analysis of siRNAs.

2. Intracellular RNAi in plant cellular defence against ELVd infection and RNAi-based defence again ELVd infection will be investigated in wilt-type and transgenic DCL-RNAi lines. After agro-infiltration of plant leaves, ELVd-infected tissues will be collected and

used:

1) To study the impact of DCLs on ELVd infection using Northern blot and qRT-PCR detection of the chloroplast-localized viroid RNA.
2) To profile the effect of cytoplasmic siRNA on ELVd replication in chloroplasts.
3) To investigate how DCLs affect ELVd siRNA biogenesis.
4) To perform deep sequencing and bioinformatics analysis of siRNA.
5) To write the PhD thesis.

1.5.5 Research Significance

The intracellular spread of RNAi, including “cytoplasm - to - chloroplasts”, has not been investigated in detail. Currently, it is unknown whether RNAi is involved in the regulation of gene expression in chloroplasts, whether small RNAs could move from cytoplasm to chloroplasts, and how these processes are controlled. Thus, the outcomes of this Ph.D. project will generate novel knowledge in these fields. The successful outcomes of these innovative efforts will not only be of fundamental scientific interest but will also provide insights into how new strategies for disease control in food and cash crops can be developed.

1.5.6 Ethical Consideration

There is no issue here as the joint PhD project does not use humans or animals.

Chapter 2 Materials and Methods

2.1 Experimental materials and instruments

2.1.1 Plant materials and growth conditions

The seeds of wild-type *N. benthamiana* (*Nb*) and transgenic RNAi *N. benthamiana* lines including DCL1-1i, DCL1-2i, DCL2-6i, DCL2-8i, DCL3-1i, DCL3-6i, DCL4-4i DCL4-10i, RDR6i, and Nb were obtained from the Plant RNA Signaling Research Centre, Hangzhou Normal University (from previous research in our laboratory). They were abbreviated as DCL1A, DCL1B, DCL2A, DCL2B, DCL3A, DCL3B, DCL4A, DCL4B and RDR6i, respectively.

All wild-type *N. benthamiana* and transgenic plants were grown and maintained in the plant growth rooms. The optimal growth conditions for plants were set by manual simulation, such as temperature 25°C, light intensity 6000 Lumilux, humidity 60%, and photoperiod 16h light and 8h dark periods.

2.1.2 Plasmid and vector materials

2.1.2.1 Bacterial strains

Agrobacterium tumefaciens (*A. tumefaciens*) competent cells GV3101 were provided by our laboratory and stored at -80°C. *Escherichia coli* (*E. coli*) Trans1-T1 competent cells were purchased from TransGen Biotech.

2.1.2.2 Plasmid vectors

The original ELVd infectious clone p53ELVd was presented by José-Antonio Daròs laboratory.

pCAMBIA1300-35S and pRNAi-LIC were provided by our laboratory.

2.1.2.3 Primers

The primers used in this project were as follows.

Table 2.1 Primers sequences for PCR and Detection

Primer name	sequence (5′ to 3′)
1300-35S ELVd ter F	aaaaaa**GGTACC**GATTCCATTGCCCAGCTATC

1300-35S ELVd ter R	aaaaaa**CTGCAG**CTGGATTTTGGTTTTAGGAA
1300-SEQ-F	CGCAATTAATGTGAGTTAGCTCAC
1300-SEQ-R	ATCGGTGCGGGCCTCTTCGC
ELVd-2F	TTAAGCTTCTGTATATTCTGCCCAAATTTG
ELVd-2R	TTCAAACTAAAGAAAATTTAATGAAACCAG
ELVd-3F	AAAGGTCGAAATGGGGTTTCGCCATGGGTCGGGAC
ELVd-3R	AGAGGTACACCCACCCTCCTAGGGAACACATCCTT
Pdk intron F	CGCAAATACGCATACTGTTATCTG
Pdk intron R	TATATCCCAATGGCATCGTAAA
PP271 F	CGG CTA CCA CAT CCA AGG AAG G
PP272 R	GAG CTG GAA TTA CCG CGG CTG
NbRbCL RNAi-F	CGACGACAAGACCCTtaggtaacgtatttgggttca
NbRbCL RNAi-R	GAGGAGAAGCCCTtcatctttagtaaaatca

Blod font: GGTACC is a *KpnI* cleavage site and CTGCAG is a *PstI* cleavage site. **(Source: Pengcheng Zhang, 2024)**

2.1.3 Reagents and instruments

2.1.3.1 Molecular biological reagent

The restriction endonuclease KpnI-HF, PstI, Nco I-HF, Nde I-HF, Sall-HF, Spe I-HF and RNA polymerase T7 RNA Polymerase, T3 RNA Polymerase and SP6 RNA Polymerase were all purchased from New England Biolabs.

Other enzyme T4 DNA Ligase, Primer STAR HS DNA Polymerase and DNA marker were purchased from TAKARA, PCR kit 2×Taq Master Mix; and 2×UltraSYBR mixture were purchased from CWBIO.

2.1.3.2 Experimental kits

The kits for molecular biolgy were purchased from Tiengen, Roche and Qiagen. They included RNAprep Pure Plant Kit and FastQuant RT Kit with gDNase (TIENGEN); HP PCR Product Purification Kit; DIG-High Prime DNA Labeling and Detection Starter Kit II and DIG RNA Labeling Kit, (ROCHE); QIAprep Spin Miniprep Kit and QIAquick Gel Extraction Kit (QIAGEN).

2.1.3.3 Preparation of medium

The chemicals such as Yeast extract; Tryptone (OXOID); Sodium chloride; Kan; Amp (SANGON); Agar (SIGMA) used to prepare the medium were purchased from Oxoid, Sangon and Sigma.

2.1.3.4 Other Chemical reagent

Other chemical reagents were purchased Biotech, Biowest, and Invitrogen, including 2-Hydroxy-1-ethanethiol (BIOTECH); Agarose (BIOWEST); Ethanol absolute; propane-2-ol, (SINOPHARM); Trizol (INVITROGEN); Hybond-N+ membranes (Amersham Biosciences).

2.1.3.5 General experimental instruments

The general experimental instruments in this project was used as follows: Research plus, Multipette plus, Centrifuge 5424R, Centrifuge 5430R, ThermoStat plus, Concentrator plus, Concentrator plus, (Eppendorf); ChemiDoc XRS+ imaging System, Gene Pulser Xcell Total System, SmartSpec Plus, CFX96 Touch Real-Time PCR Detection System, PowerPac Basic Power Supply, PowerPac Universal Power Supply, PowerPac HC Power Supply, PROTEAN IEF Cell, Mini-Sub Cell GT Cell, S1000 Thermal Cycler (BioRad); Laser Scanning Confocal Microscope A1Si, Fluorescence Microscope SMZ1500/Ni-U/Ti, Free Zone Plus 2.5 Liter Cascade Freeze Dry Systems (Labconco), Digital Camera D7000 (Nikon); Biological Safety Cabinet, Forma 1300, MAXQ4000 Cryogenic freezer, Nanodrop 2000, (Thermo Scientific); Mili-Q Integral 5 (MILLIPORE), UVP* CX-2000 crosslinker (Fisher Scientific); Stuart CR302, Jenway 3520pH, Stuart SI30H, (Bibby); Hirayama HV 50 (Hirayama); Tissue Ruptor System (Jingxin); UVP* CX-2000 crosslinker (Fisher Scientific); Stuart CR302, Jenway 3520pH, Stuart SI30H, (Bibby); Hirayama HV 50 (Hirayama).

2.2 Basic experimental methods

2.2.1 Polymerase Chain Reaction (PCR)

To amplify the target genes, PrimerSTAR HS DNA polymerase were used to amplify the sequence. The PCR reaction system is 20 μL A: (5×Primer STAR Buffer, 4 μL; 10 mM dNTP Mixture, 2 μL; Template DNA, 1 μL; 10 μM Forward-Primer/Reverse-Primer, 0.5 μL each; 2.5 U/μL PrimerSTAR HS DNA polymerase, 0.2 μL; ddH_2O, 12.8 μL) or B: (2× Taq Master Mix, 10 μL; Template DNA, 1 μL; 10 μM Forward-Primer/Reverse-

Primer, 0.5 μL each; ddH_2O, 8 μL). The PCR reaction procedure was performed by pre-denaturation at 95 °C for 5 min; 30 cycles of denaturation at 95 °C for 30 s, annealing at 58 °C for 30 s, extension at 72 °C for 30 s; final extension at 72 °C for 10 min, and holding at 16 °C for 1 h. The PCR amplification products were stored at 4 °C. The quality of the PCR products was determined by 1.0 % agarose gel electrophoresis: 1× TAE electrophoresis buffer, 180 V, 15 min. 180 V for 15 min.

2.2.2 PCR product purification

The PCR product purification kit from Roche was used as follows: Firstly, the purified gel was placed in a 1.5ml centrifuge tube, followed by the addition of 500μL of Binding Buffer solution (volume of Binding Buffer: volume of PCR product = 5:1). The mixture was allowed to stand at 60°C for 5-10 minutes until completely melted, vortexed to mix thoroughly, transferred the mixture to the adsorption column and centrifuged at 10000 rpm for 1min at room temperature, the filtrate was discarded. Secondly, 600 μl of Washing Buffer to a centrifuge tube were slowly added and centrifuged at 10,000 rpm for 1 min at room temperature, the filtrate was discarded. The above steps were repeated once. Thirdly, the mixture was centrifuged at 10,000 rpm at room temperature for 1 min (in vacuo), followed by retransfer of the purification column into new 1.5 mL EP Tubes. Finally, 50 μl of ddH_2O was added to the purification column and left to stand at room temperature for 5 min, which was followed by centrifugation at 10,000 rpm for 1 min at room temperature. The concentration of the purified product was measured by NanoDrop; the purified product was stored in a freezer at -20°C until use.

2.2.3 Enzyme digestion

The enzymatic cleavage products need to be purified and recovered in the same way as the PCR product purification (Section 2.2.2). The digestion temperature depends on the enzyme was used; generally, 3h for PCR products and 8h for plasmids. The enzyme digestion system was 30 μL (10×CutSmart buffer, 3 μL; restriction endonuclease 1, 1 μL; restriction endonuclease 2, 1 μL; PCR products/plasmids, 1 μL; ddH_2O, Top up to 30 μL). CutSmart buffer, ddH_2O, restriction endonuclease 1, restriction endonuclease 2, and PCR products/plasmids were added together in a new 1.5 mL EP Tubes, mixed well, then incubated at 37 °C in a water bath for 3-5 h.

2.2.4 Ligation

The enzymatic purification products were ligated into the vector. The ligation reaction

system was 10 μL (Enzymatic purification products, 7 μL; 10×T4 DNA ligation buffer, 1 μL; Empty vector, 1 μL; T4 DNA ligase, 1 μL) and the above mixture were ligated at 4 °C overnight or 16 °C for 2 h.

2.2.5 Transformation of *E. coli* competent cells

The ligation product recombinant plasmid was transformed into *E. coli* competent cells and propagated. Then, sequence comparison was performed for verification and finally, stored at -80 °C. The protocol was as follows: Firstly, 2 μl of the sample was added to 50 μl of competent cells Trans1-T1, mixed well, and placed on ice for 30 min. Secondly, the mixture was heated at 42 °C for 1 min, and cooled in ice for 5 min. Thirdly, 500 μl of anti-liquid-free LB medium was added and incubated at 37 °C for 60 min on a 200-rpm shaker. Then, the mixture tube was centrifuged at 8000 rpm for 2 min at room temperature. 300 μl of supernatant was discarded and the bacterial solution was resuspended. Finally, 150 μl of the resuspended bacterial solution was taken out, and all of it was spreaded on LB solid medium with Kan and placed in an incubator at 37 °C for 12 h to observe the growth of colonies.

2.2.6 Plasmid Extraction

The QIAGEN kit extraction method (QIAprep Spin Miniprep Kit) was used for the experiment. Briefly, 10 ml of the overnight bacterial solution was removed, centrifuged at 5000 rpm for 8 min, and the supernatant was discarded. Then, 250 μl P1 Buffer was added, vortexed, and transferred to a new 1.5 ml EP centrifuge tube. 250 μl P2 Buffer was added and mixed well. Then, 350 μl N3 Buffer was added and mixed well. Then, the EP tube was centrifuged at 13000 rpm for 10 min, transferred the supernatant to a collection tube, centrifuged at 10000 rpm for 2 min at room temperature and the waste solution was discarded. Then, 500 μl Buffer PE was added, centrifuged at 13000 rpm for 1 min at room temperature and the waste solution was discarded. The above steps were repeated once. The EP tube was centrifuged at 13000 rpm for 2 min at room temperature and the supernatant was aspirated. Then, the adsorbent column was transferred to a new 1.5 ml centrifuge tube and left at room temperature for 10 min. Finaly, 30 μl of sterilized double-distilled water pre-warmed was added at 50 °C to the column, which was allowed to stand at room temperature for 2 min, centrifuged at 13000 rpm for 2 min, and the adsorbent column was discard. After, the plasmid concentration was measured using NanoDrop 2000 and stored it at -20 °C.

2.2.7 Transformation of *Agrobacterium* by electroporation

Firstly, the competent cells were removed from the -80 °C freezer, placed them immediately on ice, 5 μl of the ligation product was added to the competent state, and gently blew and mixed to avoid damaging the cells. The mixture transferred to a pre-cooled cuvette and inserted it into the ice until ready to use. Secondly, the electroporator was started and inserted the cuvette into the electroshock tank for 240 V electroshock. After the shock was completed, the cuvette was inserted into ice and transferred the mixture to a new 1.5 ml centrifuge tube. Thirdly, 500μl of anti-LB-free liquid medium was added and incubated at 28 °C, 200 rpm, with shaking for about 3 h. Finaly, 250 μl of supernatant were aspirated, blew and aspirated the remaining bacterial solution evenly. then the solution was spreaded on LB solid medium with corresponding resistance, incubatored at 28 °C and incubated upside down.

2.2.8 Single-colony PCR assay for transformants

To verify the bacterial transformation of the cloned vector, colony PCR was performed using Taq enzymes. Firstly, 2 μL of bacterial liquid was taken and positive single colonies were identified using the colony PCR method. The PCR system was 20 μL (2×Taq Master Mix, 10 μL; 10 μM F, 0.5 μL; 10 μM R, 0.5 μL; bacterial broth, 2 μL; ddH_2O, 7 μL), and the procedure was as before (Section 2.2.1 B). 1.0% agarose gel electrophoresis was used to check the quality of the PCR products. Based on the PCR results, the positive colony was selected and added to 10ml of liquid medium containing antibiotics resistance and incubated.

2.2.9 Positive plasmid sequencing

The plasmids were selected for PCR screening and enzyme digestion to verify that they were positive recombinant plasmids and sent to the company for sequencing. For sequencing, only primers 1300-SEQ-R were used because ELVd was a circular RNA molecule, and the F-terminus was attached to the 35S promoter. Sequence matching was then performed to identify the pCAMBIA1300-35S-ELVd recombinant plasmid vector with the correct sequence. Finally, the correct recombinant plasmid vector pCAMBIA1300-35S-ELVd was transformed into *Agrobacterium* GV3101 to obtain *Agrobacterium* pCAMBIA1300-35S-ELVd recombinant and stored at -80°C in a freezer for further *N. benthamiana* infection.

2.2.10 DNA extraction (TPS method)

To isolate DNA from plant tissues, the TPS method was employed. The protocol was as follows: Firstly, appropriate amount of plant leaves was taken into a 1.5ml EP

centrifuge tube, added 200μl of TPS extract and 2 steel balls, and grinded with a grinder (55Hz, 2min). Secondly, the minture was centrifuged at 13000rpm, room temperature for 10min, transferred supernatant to a new 1.5ml centrifuge tube, added an equal amount of isopropanol and mixed upside down. And the tube was centrifuged at 13000rpm for 5min at room temperature and the supernatant was discarded. Thirdly, 500μl of 75% ethanol was added, vortexed for 30 seconds, centrifuged at 13,000rpm for 5min at room temperature, and the supernatant was discarded. the previous step was repeated. Fourthly, the tube was centrifuged at 13000 rpm for 2 min at room temperature and the liquid from the tube was aspirated. Fifthly, the tube was inverted for 10 min, 50 μl pre-warmed ddH_2O at 50°C was added and left it to dissolve completely. Finaly, to measure the DNA concentration of the sample was measured using NanoDrop 2000 and stored it at -20°C.

2.2.11 DNA purification

The DNA purification protocol was as follows: 1) 100 μl of phenol/chloroform in equal volume was added, vortexed for 10 s, centrifuged at 13000 rpm for 3 min, and the supernatant was transferred to a new 1.5 ml EP tube. 2) The previous step was repeated. 3) the supernatant was transferred to a new 1.5 ml EP tube, two points five times the volume (250 μl) of 100% ethanol and 1/10th of the volume of 10 μl sodium acetate (pH=5.2) aspirate were added and mixed well. 4) to the mixture were precipitated at -80 °C for 1h. 5) The mixture wascentrifuged at 13000 rpm, 4 °C, for 10 min and the supernatant was discarded. 6) 100μl of 70% ethanol was added, aspirated, and mixed well. 7) The mixture was centrifuged at 13000rpm, 4 °C for 5min, supernatant was discarded. 8) The mixture was centrifuged at 13,000rpm, 4 °C, 2min in vacuo, supernatant was discarded. 9) At room temperature, the EP tube was inverted for 10min, and dissolved by adding 50μl of sterilised ddH_2O. 10) DNA concentration was measured with NanoDrop 2000.

2.2.12 RNA Extraction

To isolate DNA from plant tissues, the RNAprep Pure Plant Kit from TIANGEN was employed. All procedures were carried out in accordance with the instructions as follows: 1) Appropriate amount of plant leaves were taken in a 1.5ml RNase-Free EP centrifuge tube, 2 steel beads were added, quickly frozen in liquid nitrogen, and placed in a grinder to quickly grind to a powder, 450 μl RL Buffer was added, vortexed and mixed well. 2) All the solution were transferred to a filter column CS, centrifuged at 13,000 rpm for 5 min, and carefully aspirated the supernatant (approximately 400 μl)

from the collection tube into a new 1.5 ml RNase-Free EP centrifuge tube. 3) 0.5 times the volume of anhydrous ethanol (200 μl) was added and mixed well adsorbent was transferred column CR3, centrifuged at 13000 rpm for 2 min, and the waste solution was discarded. 4) 350 μl RW1 Buffer was added, centrifuged at 13000 rpm for 2 min, and the waste solution was discarded. 5) 80 μl DNaseI working solution was added and left for 15 min or incubated at 30°C for 15 min. 6) Step 4 was repeated. 7) 500 μl of RW Buffer was added, left for 2 min, centrifuged at 13,000 rpm for 1 min, and the waste solution was discarded. 8) Step 7 was repeated. 9) the CR3 column was centrifuged at 13000 rpm for 3 min, placed the column in a new RNase-Free centrifuge tube and left for 10 min. 10) 50 μl of RNase-Free ddH_2O pre-warmed at 50°C was added, standed for 5 min, and centrifuged at 13000 rpm for 2 min to obtain the resulting RNA solution. 11) RNA concentration was measured by NanoDrop 2000 and electrophoresised to detect RNA quality.

2.2.13 RNA reverse transcription

The FastQuant RT Kit with gDNase was developed using the TIANGEN kit as follows: 5 x gDNA Buffer, FQ-RT Primer Mix, 10 x Fast RT Buffer, RNase-free ddH_2O and template RNA were thawed on ice Standby. The Genomic DNA (gDNA) Removal Mix were prepared (5×gDNA Buffer, 2 μL; Total RNA, 1 μg; RNase-free ddH_2O, add to 10 μL), mixed well and incubated for 3 min in a 42 °C metal incubator, then placed on ice. The reverse transcription mix 10×Fast RT Buffer, 2 μL; RT Enzyme Mix, 1 μL; FQ-RT Primer Mix, 2 μL; RNase-free ddH_2O were added to 10 μL, and then the reverse transcription mix was added to the gDNA removal mix and mixed thoroughly. It was placed in a metal incubator at 42 °C and incubated for 15 min. It was placed in a metal incubator at 95 °C and incubated for 4 min, then placed on ice, cooled rapidly and the resulting was stored cDNA at -20 °C.

2.2.14 Northern blot

The specific steps of the Northern blot were as follows: 1) Gel was prepared by operation in a fume hood. A 1.5% agarose gel containing 0.66 M or 1.1% formaldehyde (0.7 g agarose, 6 mL 10 x MOPS, 54 mL RNA free ddH_2O for a total of 60 ml) using 1 x MOPS buffer was prepared, dissolved by heating in a microwave oven, cooled to about 60°C, Subsequenctly, 4 μL GelRed (Biotium) and 3 mL formaldehyde were added, gently shaken and poured into a gel-making cast. 2) Sample was prepared. The loading buffer was mixed with an equal volume of the appropriate amount of RNA sample (1-2 μg of total RNA), denatured at 68 °C for 15 min, and immediately inserted

on ice for 15 min. 3) Preparation of electrophoresis buffer. 10 x MOPS was diluted to 1 x MOPS and used as electrophoresis buffer. 4) Electrophoresis. Electrophoresis at 120 V for about 15 min at constant pressure was stopped when the bromophenol blue reaches the middle of the gel. 5) Film washing. The gel was rinsed in 3 times of distilled water for 15 min each, followed by 10*SSC with EthBr for 15 min (if necessary); The gel was rinsed in 10*SSC for 15 min and taken the pic. 6) Transfer film. The gel was transferred directly to vacuum blotter as described for Southern. The films were transferred for 30-60 min at 5 atmospheres by using a vacuum transfer machine (BIO-RAD). 7) Fixation. At the end of the transfer, the membrane was placed on filter paper and on the front of the membrane, the order of the dotted samples was marked with a pencil, and the nucleic acids were immobilized on the cellulose membrane by UV crosslinking for 45 s under 100 μJ/cm2 UV light using a UV crosslinker (CL-1000 Ultraviolet Crosslinker, UVP) and crosslinked 2 times. 8) Pre-hybridization. The membrane was put into the hybridization vial with the back side against the wall, and 8 mL/vial of hybridization solution was added (the amount of hybridization solution could be increased according to the size of the membrane) to wet the membrane, drive out any air bubbles between the wall of the vial and the membrane, tighten the lid, fix the vial into the hybridization oven and pre-hybridize at 68°C for at least 1 h. 9) Probe denaturation. 1-5 μl of probe (PCR product) was diluted into 30 μl water and denatured in a PCR tube at 99˚C for 5 minutes and then quickly cooled down on wet ice. The probe was immediately added to the 10 ml hybridization mixture in the tube with the blot. Ensure that the probe was well diluted before touching the blot. 10) Hybridization. After pre-hybridization, 1 μL of probes was added to each vial of hybridization solution and hybridized overnight at 68°C (at least 6 h of hybridization).

Once hybridization was completed, membrane washing for imaging can be started as follows. 1) The membrane was washed twice at room temperature for 5 min each time with 30 mL/bottle of 2 x SSC solution. 2) The solution in the hybridization vial was poured out, and 30 mL/vial of a solution containing 0.1× SSC and 0.1% SDS preheated at 68°C was added, and the membrane was washed twice at 68°C for 15 min each time. 3) The solution in the hybridization vials was poured out, and 15 mL/vial of closure solution (0.15 g of closure agent heated and dissolved in 15 mL of maleic acid) was added and closed for 0.5-3 h at room temperature. 4) The blocking solution was poured out, and 15 mL/vial of antibody solution was added (1 μL of antibody in 15 mL of blocking solution), and the reaction was carried out for 30-40 min at room temperature. 5) The antibody solution was poured out and 30 mL/vial of washing solution (90 μL of

Tween 20 added to 30 mL of maleic acid solution) was added, and the membrane was washed twice at room temperature for 15 min each time. 6) The assay solution was prepared at 30 mL/bottle, a sufficient amount of assay solution was aspirated to dilute the CSPD (10 drops of CSPD into 1 mL of assay solution), and the remaining assay solution was added to the hybridization bottle and reacted for 3-5 min at room temperature. 7) The membrane was removed from the hybridization tube and placed face up in the hybridization bag. and diluted CSPD solution was added to the membrane, and 1 mL of CSPD solution should be added to 100 cm^2 of membrane. The hybridization bag was sealed, placed flat, and nudged repeatedly with a soft paper towel to make the CSPD solution uniformly and fully bonded to the film, and left for 5 min at room temperature. 8) One corner of the hybridisation bag was cut open and excess solution and air bubbles were squeezed out and then resealed. 9) Exposure Imaging was performed with the ChemiDoc XRS Imaging System (BIO-RAD).

2.2.15 *Agrobacterium* infiltration (Agroinfiltration)

Agrobacterium verified positive according to the above experiment was incubated in a rotation incubator of 200 rpm at 28°C, and stopped when OD595 reached 1.0-1.5, the culture was centrifuged at 8000 rpm for 8-10 minutes and then resuspended in sterile distilled water to bring the final OD595 to 1.0, infiltrated and inoculated for use.

Wearing latex gloves, six true leaves of a good, uniform size of *N. benthamiana* plant were selected and two spreading systemic young leaves at the upper end of each plant were selected as inoculated leaves. First, the needle of a 1 ml syringe was used to gently poke two holes on the back of the leaf blade to be inoculated (the holes were selected on both sidesof the leaf veins), and then 1 ml of the inoculated *Agrobacterium* suspension was sucked up by the syringe and slowly infiltrated the holes so that the bacterial solution infiltrates the whole inoculated leaf; (Figure 2.1), 1 ml of *Agrobacterium* suspension per *N. benthamiana* plant for 2 leaves.

After inoculation, the *N. benthamiana*, lightly sprayed with water, was incubated in a dark room for one day and then in a growth chamber at about 25 °C with 60% to 80% humidity, 16 hours of light, and 8 hours of darkness. On 4 days (4 dpi) of virus inoculation with ELVd, some leaves of the inoculated leaves were collected and tested for DCL1 heterozygosity and ELVd virus infection. Two inoculated leaves and two apical neonatal leaves were collected at day 6 (6 dpi) and day 14 (14 dpi) post-inoculation (Figures 2.2 and 2.3), and the collected leaf tissue was rapidly frozen in

liquid nitrogen and then stored in a -80°C freezer for storage.

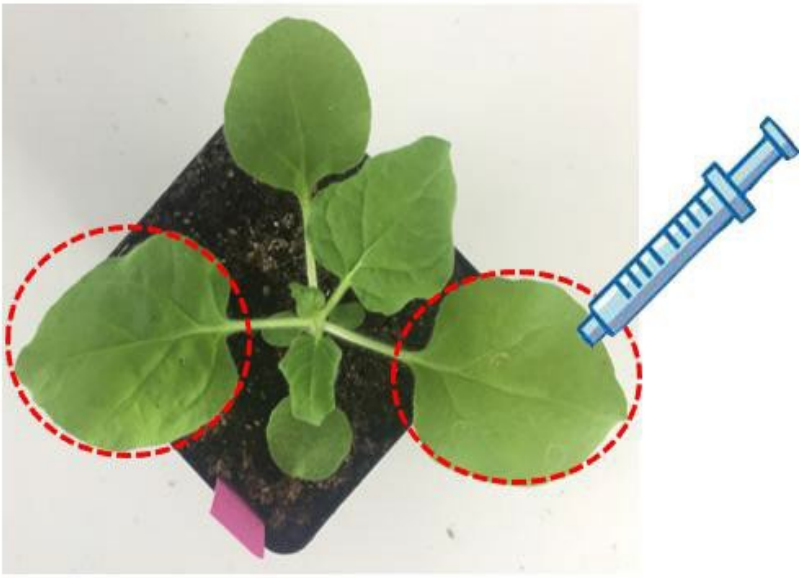

Figure 2.1 Agroinfiltration of *N. benthamiana* leaves

Inoculated leaves were marked with red circles and inoculated with a 1 ml syringe without needle. Each plant was inoculated with 1 ml of infection solution and two leaves were inoculated twice each. **(Source: Pengcheng Zhang, 2024)**

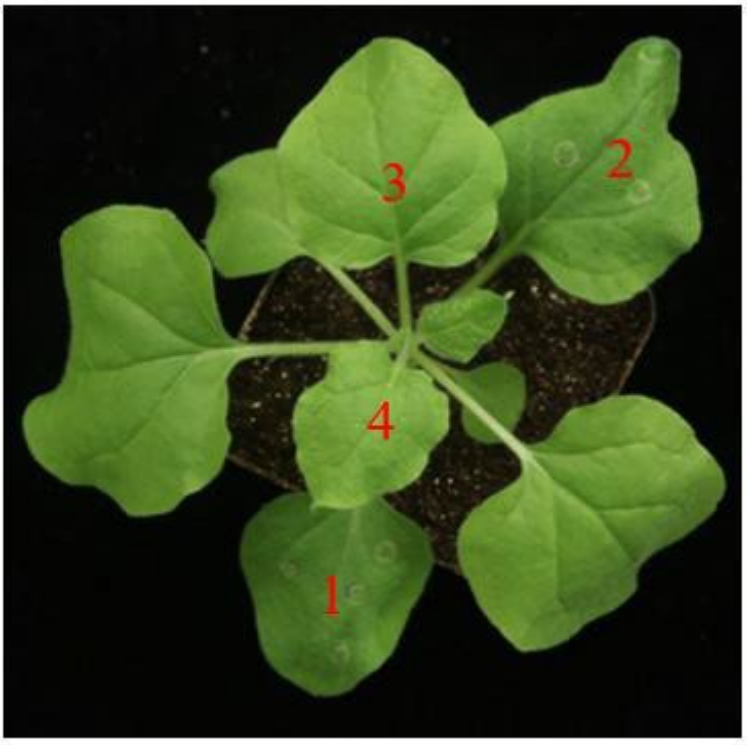

Figure 2.2 Agroinfiltration of *N. benthamiana* plant at 6dpi

Note: Each plant was inoculated with 1 ml of infection solution and two leaves were

inoculated twice each. At 6 days post inoculation (6dpi), numbers 1 and 2 indicates inoculated leaves and numbers 3 and 4 indicates young new leaves. **(Source: Pengcheng Zhang, 2024)**

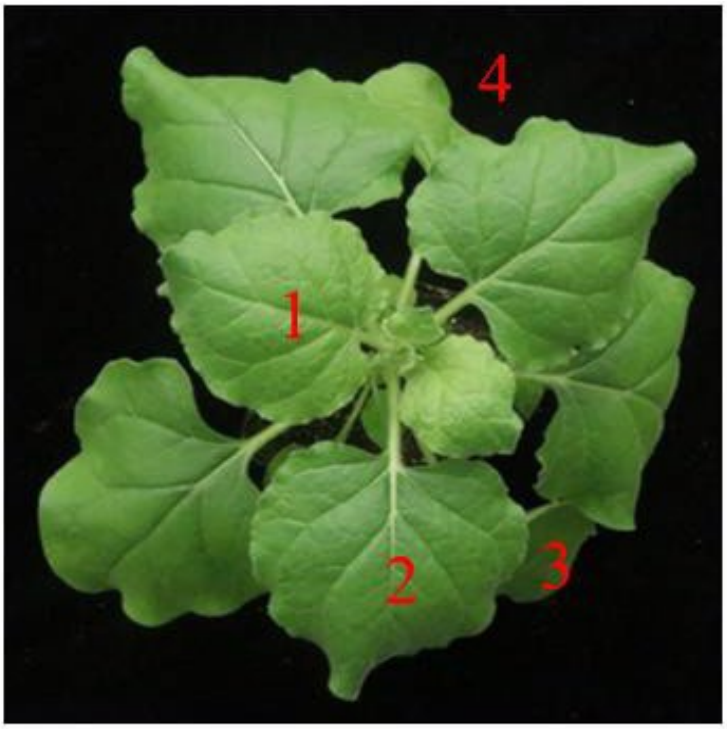

Figure 2.3 Agroinfiltration of *N. benthamiana* plant at 14dpi

Note: Each plant was inoculated with 1 ml of infection solution and two leaves were inoculated twice each. At 14 days post inoculation (14dpi), numbers 1 and 2 indicates young new leaves and numbers 3 and 4 indicates inoculated leaves. **(Source: Pengcheng Zhang, 2024)**

2.2.16 DNA Probe Preparation

PCR reaction system was 50 μL (10×Ex Taq Buffer, 5 μL; **10x DIG dNTP**, 1 μL; p53ELVd (10ng/μl), 1 μL; 10 μM ELVd-2F, 1 μL; 10 μM ELVd-2R, 1 μL; LA Taq, 0.2 μL; ddH_2O, 40.8 μL). The PCR reaction procedure was performed by pre-denaturation at 95 °C for 5 min; 35 cycles of denaturation at 95 °C for 30 s, annealing at 58 °C for 30 s, extension at 72 °C for 1 min 45 s; final extension at 72 °C for 10 min, and holding at 16 °C for 0.5 h. The PCR amplification products were stored at 4 °C. The quality of the PCR products was determined by 1.0 % agarose gel electrophoresis: 1× TAE electrophoresis buffer, 180 V, 15 min. 180 V for 15 min.

2.2.17 Southern blot

For Southern blot method, see section 4.2.7 Northern blot. Here, DNA was used

instead of RNA and other conditions were left as the same.

2.2.18 Inoculated leaf internal reference gene 18s rRNA PCR

PCR reaction system of 18s rRNA was 20 μL (2× Taq Master Mix, 10 μL; cDNA, 1 μL; 10 μM PP271 F, 0.5 μL; 10 μM PP272 R, 0.5 μL; ddH_2O, 8 μL). The PCR reaction procedure was performed by pre-denaturation at 95 °C for 5 min; 25 cycles of denaturation at 95 °C for 30 s, annealing at 58 °C for 30 s, extension at 72 °C for 30 s; final extension at 72 °C for 10 min, and holding at 16 °C for 0.5 h. The PCR amplification products were stored at 4 °C. The quality of the PCR products was determined by 1.0 % agarose gel electrophoresis: 1× TAE electrophoresis buffer, 180 V, 15 min. 180 V for 15 min.

2.2.19 Construction of small RNA libraries for small RNA sequencing

Firstly, Small RNA was enriched: 1 μg of Total RNA sample was extracted and RNA was recovered by 15% urea denaturing polyacrylamide (PAGE) gel electrophoresis to cut and recover small RNA between 18-30 nt; then adaptor ligation: reverse transcription (RT) was performed after ligation of 5' and 3' end cleavages; The PCR products were then recovered from the RT-PCR amplification gels and libraries were constructed; the constructed libraries were tested for quality and yield, and the final ligated PCR products were sequenced on the machine. The sRNA cDNA sequencing for this study was done by Illumina HisEquation 2000 from BGI-Shenzhen, China. The small RNA sample library construction workflow was as follows (Figure 2.4).

Figure 2.4 Small RNA sample library construction

(Image cited from BGI-Tech, China)

Adaptor ligation: Firstly, the ligation system for the 3' adaptor was formulated at 70 °C for 2 min and then 25 °C for 2 h. Secondly, reverse transcription primers were then added at 65 °C for 15 min of ramp to 4 °C at a rate of 0.3 °C/sec. Thirdly, the the ligation system for 5' adaptor was added and prepared at 70 °C for 2 min and then 25 °C for 1h.

Reverse transcription-PCR amplification. The reverse transcription system was configured at 42 °C for 1 h and then 70 °C for 15 min. The PCR amplification system was configured, then 95 °C for 3 min, 15-18 cycles of (98 °C for 20 s, 56 °C for 15 s, 72 °C for 15 s); 72 °C for 10 min; 4 °C hold.

Purify PCR products. The PCR products were purified with PAGE gels, and the target bands were recovered by electrophoresis and stored in Buffer EB.

2.2.20 Bioinformatics analysis of small RNA sequences

Illumina HighSEquation 2000 sequencing generated a large number of reads, with 28 million reads per sRNA library. Reads were cropped to remove adapter sequences and compared to reference sequences using Bowtie2 (Source: http://bowtie-bio.sourceforge.net/index.shtml). The reference sequences included the ELVd RNA genome (GenBank number NC_039241.1, same as AJ536613.1), *RbCL* (GenBank

number J01450.1), *DCL1* (GenBank number FM986780), *DCL2* (GenBank number FM986781), *DCL3* (GenBank number FM986782), *DCL4* (GenBank number FM986783). Samtools pileup was used to produce siRNA and miRNA overlay profiles (Li et al., 2009). Comparison of normalized cvd-siRNA, microRNA or csRNA reads to total sRNA reads (per 10 million sRNA reads) resulted in the same number of cvd-siRNA, microRNA, or csRNA reads as the direct comparison.

Chapter 3 Construction of ELVd infectious clones

3.1 Introduction

Infectious clones are viral DNA or cDNA with the ability to infect, as well as in vitro transcription products with infection potency. Infectious cloning techniques are fundamental to the study of viral functional genomics, replication, and expression of viral proteins, and host-virus interactions, and have driven the rapid development of research fields related to molecular virology.

Nowadays, there are two methods of infectious clone construction, one is to clone the viral genome into a plasmid vector, add promoters for prokaryotic expression such as T7, SP6, T3, etc. to the front end of the sequence (Zheng et al., 2016), and then obtain a large amount of viral full-length RNA by in vitro transcription, and then inoculate the host plant by friction inoculation, thus realizing the infection of RNA viruses (Junqueira et al., 2014).The first infectious clone was successfully constructed by friction inoculation on TGMV in 1982. This method has since been successful on a variety of RNA viruses, such as PVX, TRV, and TMV viruses (Chapman, 2008; Ryabov, 2008; Wang et al., 2014). However, in vitro transcription of RNA through T7 promoter and T7 polymerase (Yoon et al., 2002; Kamboj et al., 2015; Zheng et al., 2016; Zhang et al., 2021) to obtain a large amount of viral RNA is costlier and cumbersome steps.

The second strategy of infectious clone construction is to transcribe the exogenous gene through the 35S promoter of *Cauliflower mosaic virus* (CaMV) on a plant binary expression vector (Chen et al., 2012; Orilio et al., 2014), and then inoculate the plant by *Agrobacterium* infiltration to realize the viral infectious (Kang et al., 2015; Zheng et al., 2015; Shakir et al., 2023), which is characterized by a simple and fast operation process, high infectious efficiency and good reproducibility.

Another important use of plant infectious clones is the construction of virus-induced gene silencing expression vectors. By appropriately modifying plant expression vectors containing infectious clones to form VIGS vectors, target gene fragments of unknown function in plants are inserted into the VIGS vectors, and viruses carrying the target genes will induce silencing of the endogenous genes when they infect the plants, which may lead to phenotypic changes (Wang et al., 2016; Shakir et al., 2023). This technical approach has become a very effective tool for studying plant gene function at present; for example, Holzberg et al. successfully established the VIGS system on

barley for the first time: partial sequences of barley PDS were inserted into the γ-chain of the modified barley streak mosaic virus BMSV, and gene silencing of endogenous PDS in barley was successfully induced by friction inoculation of barley leaves (Holzberg et al., 2002).

To study the distribution of siRNAs in plants after ELVd infection and plant antiviral virulence, an infectious cloning vector of pCAMBIA1300-35S-ELVd was constructed. Sequences of ELVd infection clones were shown in appendix 1. The ELVd genome was first amplified using the p53ELVd plasmid as a template, the primer pair 1300-35S ELVd ter F/R and PrimeStar HS DNA polymerase, then double cleaved with restriction enzymes *Kpn* I and *Pst* I, then ligated and the ELVd molecule was cloned into the pCAMBIA1300 vector to generate pCAMBIA1300-35S-ELVd, then transferred into *E. coli* Trans1-T1 competent strain that were spread on LB+Kan agar medium for resistance screening. The vector primer pair 1300-SEQ-F/R was used for PCR and sequencing of positive clones, and after sequence alignment, the correct sequence of the pCAMBIA1300-35S/ELVd recombinant plasmid vector was identified. The correct recombinant plasmid vector was then transformed into *Agrobacterium* GV3101. The vector is kanamycin (Kan^+) resistant, as detailed in Chapter 2.2.1-2.2.9.

3.2 Experimental results

3.2.1 ELVd cDNA PCR

The p53ELVd plasmid (see section appendix 1) was used as the template and 1300-35S ELVd ter F/R was used as the primer to PCR amplify the ELVd cDNA fragment, electrophoresis was performed to detect the amplification, and the target gene band was obtained at 1584bp as shown in Figure 3.1. The correct target gene band was cut and recovered to purify the PCR product, and then subsequent experiments were performed.

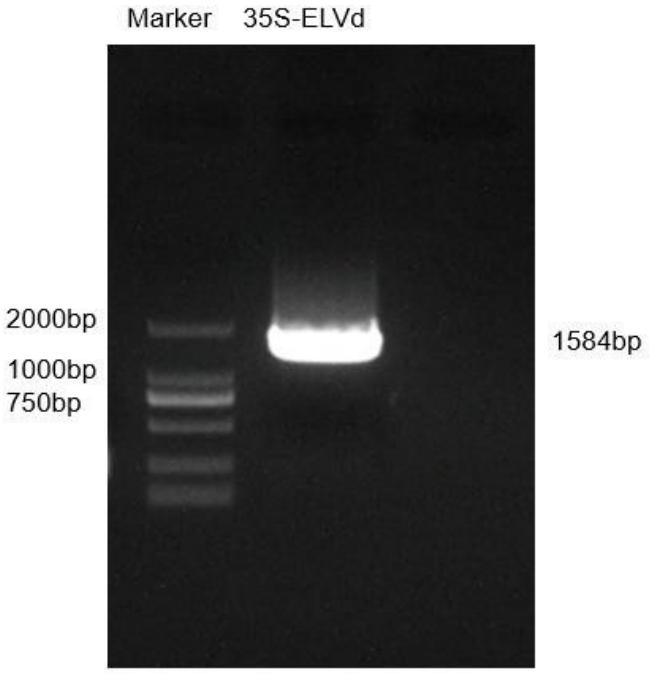

Figure 3.1 Gel electrophoresis analysis of the target gene fragment

35S-ELVd target gene fragment was electrophoresed in 1.0% agarose gel and stained in ethidium bromide. Sizes (1584bp) of 35S-ELVd target gene fragment is indicated. The top three bands of the marker 2000bp DNA ladder are indicated. **(Source: Pengcheng Zhang, 2024)**

3.2.2 Target PCR product and vector digestion

The ELVd fragment obtained after PCR amplification was subjected to double digestion using the restriction endonucleases *Kpn*I-HF and *Pst*I (left in Figure 3.2). CutSmart buffer, ddH_2O, *Kpn*I-HF, *Pst*I, and PCR products/plasmids were added together in a new 1.5 mL EP Tubes, mixed well, then incubated at 37 °C in a water bath for 3-5 h. The pCAMBIA1300 vector was also subjected to the same double RE digestion (Figure 3.2), followed by cut-gel recovery and purification in preparation for subsequent ligation.

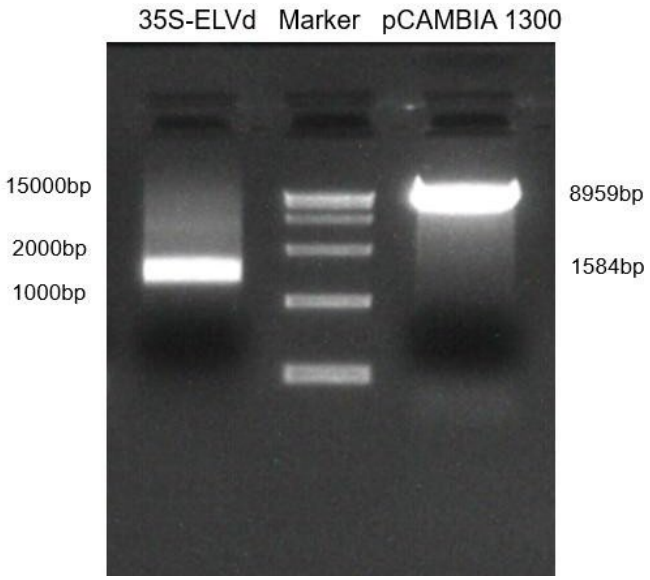

Figure 3.2 Double enzyme digestion gel electrophoresis analysis of the target gene fragment and vector

35S-ELVd and pCAMBIA1300 vector fragments were electrophoresed in 1.0% agarose gel and stained in ethidium bromide. The gel on the left shows 35S-ELVd and the one on the right shows the pCAMBIA1300 vector. Sizes of 35S-ELVd (1,584 bp) and pCAMBIA1300 vector (8,959 bp) fragments are indicated. The marker sizes of 15,000 bp DNA ladders are indicated on the left of the gel. **(Source: Pengcheng Zhang, 2024)**

3.2.3 Ligation, transformation and bacterial colony PCR

The ELVd cDNA and the pCAMBIA1300 vector were ligated overnight at 4°C using T4 DNA ligase. The ligation product was transformed into *E. coli* by heat excitation and propagation. After transformation, the plates were scribed and cultured to obtain single clones, and the PCR of the solution (Figure 3.3) was used for preliminary validation. 1300-35S-ELVd bacterial colony PCR size should be around 1584 bp, and of the eight selected single clones, only No. 2 and No. 6 showed incorrect size bands for the empty vector bands of 200-300 bp, while the others were all correct. Positive clones No.3 and No.4 hourboring the right insert were randomly selected, and bacteria were cultured respectively for extraction of recombinant plasmids.

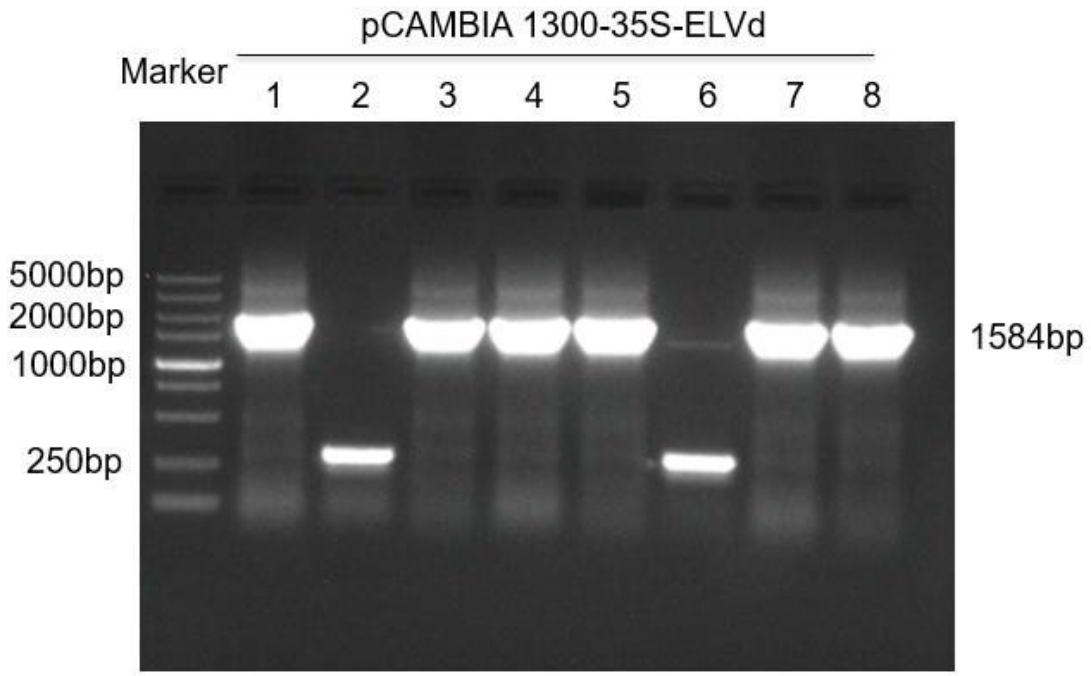

Figure 3.3 Agarose gel electrophoresis analysis of colony PCR screening

Lanes 1 to 8 are gel electrophoresis of eight bacterial colony PCR products on 1.0% agarose gel and stained in ethidium bromide. Sizes of the 35S-ELVd fragment (1584 bp) cloned in the pCAMBIA 1300-35S-ELVd vector are indicated. Sizes of DNA ladder 5000bp (Marker) are indicated on the left of the gel. Except clones 2 (lane 2) and 6 (lane 6), the remaining clones were tested positive. **(Source: Pengcheng Zhang, 2024)**

3.2.4 Recombinant plasmid digestion and sequencing assay

The plasmid DNA was extracted from the positive clones No. 3 and 4 (as shown in lanes 3 and 4 were randomly selected from Figure 3.3), the insertions were verified by restriction digestion (Figure 3.4), and their fidelities were further verified by DNA sequencing. The sequencing results were compared with the sequence of our vector and the results were consistent.

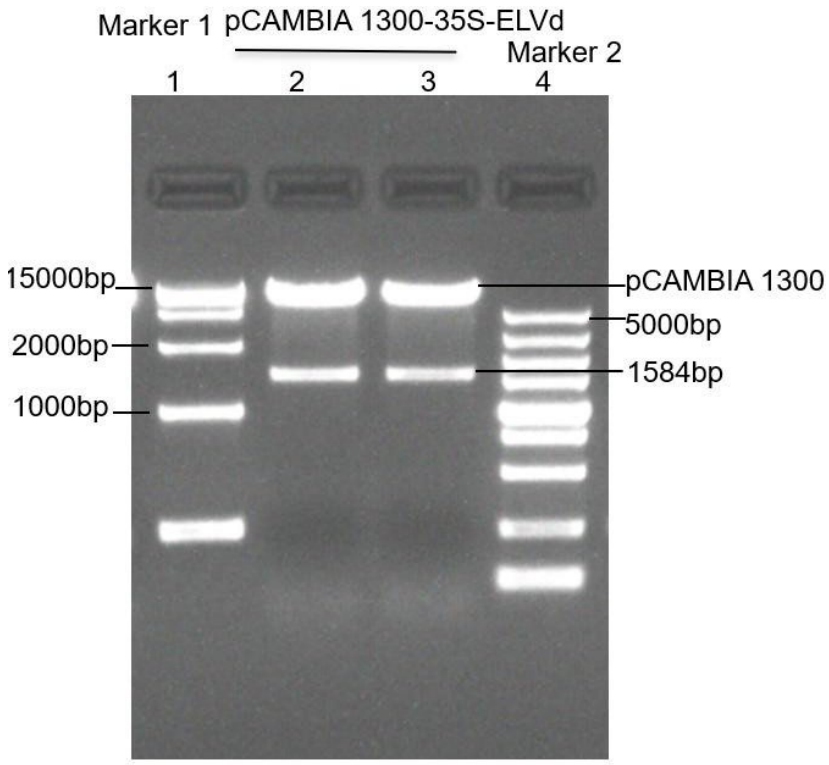

Figure 3.4 Agarose gel electrophoresis of the inserts in the double-digested recombinant plasmids

The digested pCAMBIA 1300-35S-ELVd were electrophoresed in 1.0% agarose gel and stained in ethidium bromide. Lane 1 is marker 15000bp. Lane 4 is marker 5000bp. Lanes 2 and 3 are the double-enzyme digestion of the recombinant contructs. Positions and sizes of the pCAMBIA 1300 vecter and 35S-ELVd are indicated. **(Source: Pengcheng Zhang, 2024)**

3.2.5 Transformation of *Agrobacterium* and colony PCR

The correct recombinant plasmid vector pCAMBIA1300-35S-ELVd was transformed into *Agrobacterium* GV3101, and five single-colonies were selected and verified by PCR screening (Figure 3.5). *Agrobacterium* harbouring pCAMBIA1300-35S-ELVd was then mixed with 80% glycerol and stored in a freezer at -80°C.

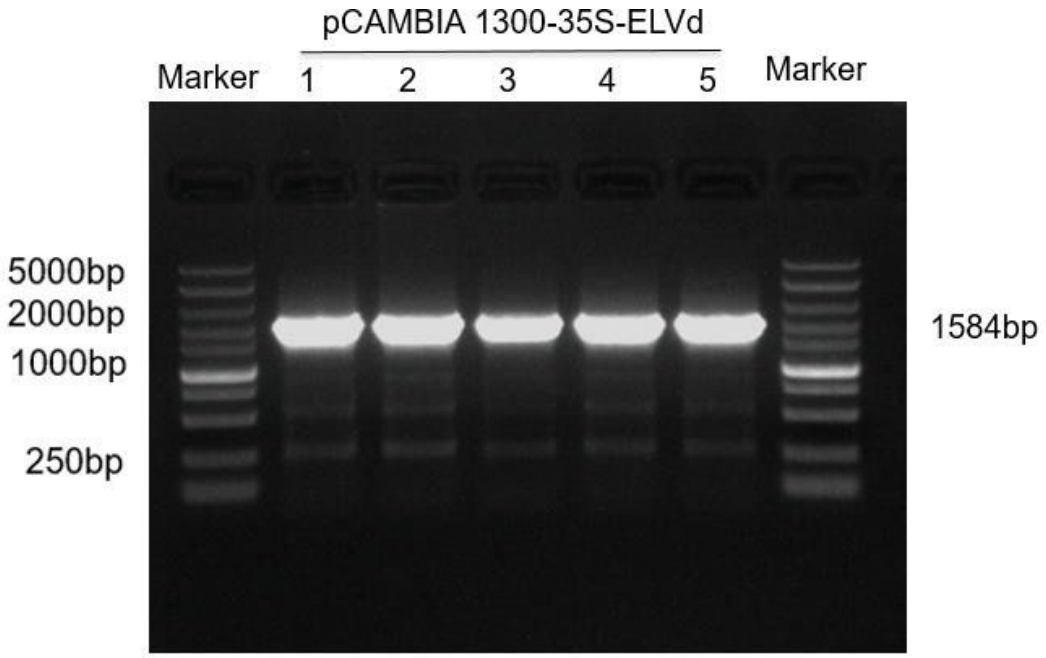

Figure 3.5 Agarose gel electrophoresis of colony PCR screening

The amplified PCR products using a specific pair of primers were electrophoresed in 1.0% agarose gel and stained in ethidium bromide. Sizes (1584 bp) of the 35S-ELVd fragments in the pCAMBIA 1300-35S-ELVd are indicated. Lanes 1 to 5 represent five randomly selected positive clones confirmed by colony PCR screening. Sizes and positions of the marker DNA ladder-5000bp are indicated**. (Source: Pengcheng Zhang, 2024)**

3.3 Discussion

The propagation, purification and maintenance of virus activity are essential for the study of virus genome function and pathogenicity. However, the replication ability of wild-type virus is not stable, and they are prone to homologous recombination and mutation in the natural environment. The construction of infectious clones of virus can effectively solve these problems (Orilio et al., 2014; Zheng et al., 2015; Wang et al., 2022; Shakir et al., 2023).

In order to study the distribution of siRNAs in plants after ELVd infection and plant antiviral, an infectious cloning vector of pCAMBIA1300-35S-ELVd was constructed in this section. The details of the constructed plasmid pCAMBIA1300-35S-ELVd are shown in Figure 3.6. In the experiments in this chapter, we first, obtained the ELVd CDS sequence by PCR amplification using the p53ELVd plasmid as a template (see section appendix 1) (Figure 3.1), the PCR product was purified and recovered, and the ELVd CDS molecule was cloned by T4 DNA ligase ligation under the double digestion

of restriction endonucleases (*Kpn* I and *Pst* I) (Figure 3.2) into the pCAMBIA1300 vector, and the recombinant DNA was transformed into *E. coli* for amplification and propagation using the heat shock method. The recombinant DNA was then subjected to bacterial liquids PCR (Figure 3.3). It was found that 6 out of 8 randomly picked bacterial clonies screened by colony PCR were positive. Two false positives may be related to antibiotic concentration, incubation time, viability of the bacterial culture, recombination or ligation. However, 75% positive monoclones were obtained in our laboratory higher than some of the already reported literature (Yoon et al., 2002; Kamboj et al., 2015; Zheng et al., 2016; Li et al., 2020; Wang et al., 2022; Likhith et al., 2024). Then, the recombinant plasmid was verified by enzymatic digestion (Figure 3.4) and other preliminary tests, and the obtained positive clones (Figure 3.5) were verified by Sanger sequencing, which were completely consistent by sequence comparison. Thus, the vector of pCAMBIA1300-35S-ELVd (Figure 3.6) was obtained for the next infection experiment. The details of the constructed plasmid pCAMBIA1300-35S-ELVd are shown in Figure 3.6.

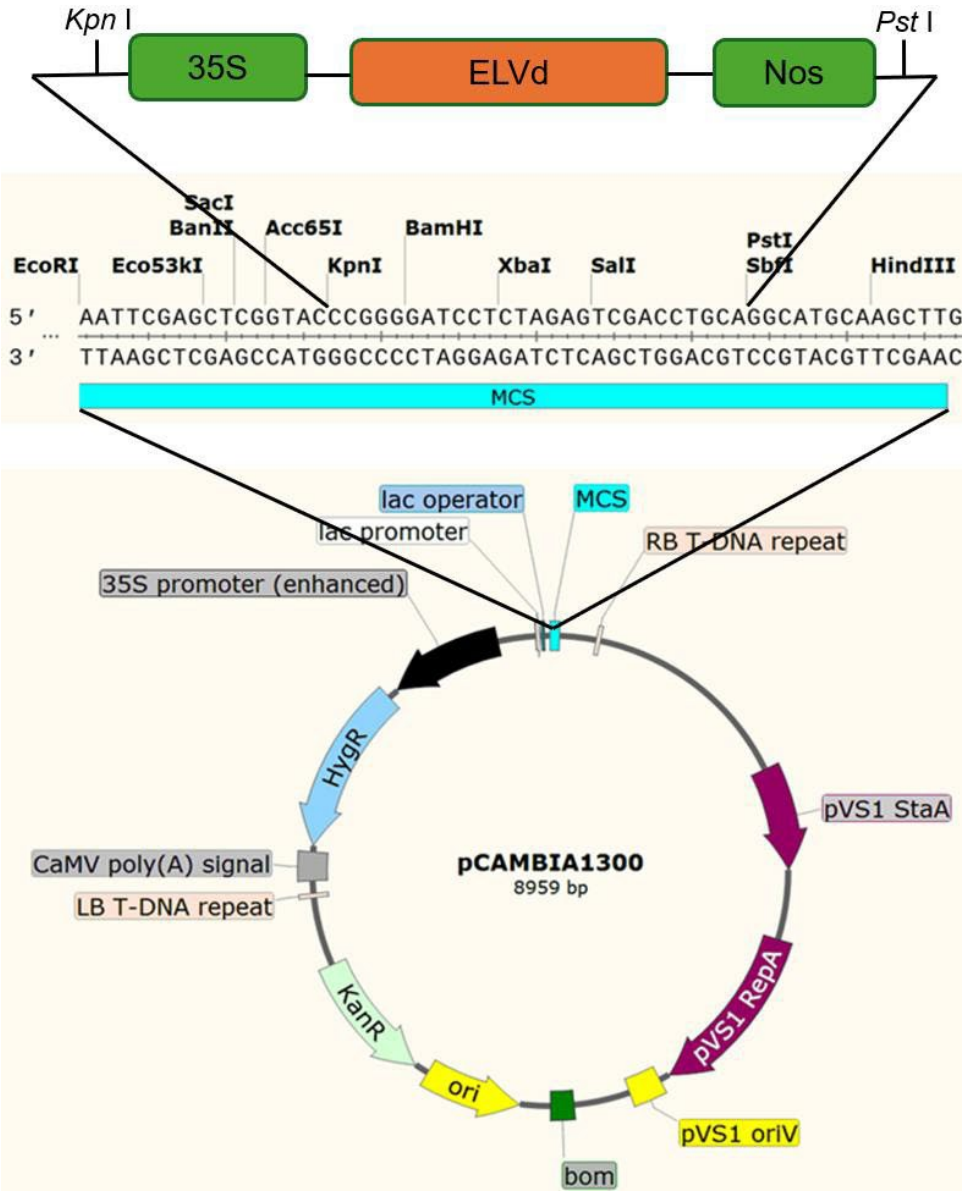

Figure 3.6 pCAMBIA1300 structure diagram

Agrobacterium binary vector pCAMBIA1300 for plant infection transformation contains hygromycin- and kanamycin-resistance genes. *Kpn I*-HF and *Pst* I are restriction endonucleases used for our vector construction. MCS, pUC18/19 multiple cloning sites. 35S promoter (enhanced), the cauliflower mosaic virus 35S promoter with a duplicated enhancer region. Lac promoter, promoter for the *E. coli* lac operon. Lac operator, the lac repressor binds to the lac operator to inhibit transcription in *E. coli*. This inhibition can be relieved by adding lactose or isopropyl-beta-D-thiogalactopyranoside (IPTG). RB T-DNA repeat, right border repeat from nopaline C58 T-DNA. pVS1 StaA, stability protein from the Pseudomonas plasmid pVS1. pVS1 RepA, replication protein from the Pseudomonas plasmid pVS1. pVS1 oriV, origin of replication for the Pseudomonas plasmid pVS1. Bom, basis of mobility region from pBR322. Ori, high-copy-number ColE1/pMB1/pBR322/pUC origin of replication. KanR, aminoglycoside

phosphotransferase. LB T-DNA repeat left border repeat from nopaline C58 T-DNA. CaMV poly(A) signal, cauliflower mosaic virus polyadenylation signal. HygR, aminoglycoside phosphotransferase from *E. coli*. **(Source: Pengcheng Zhang, 2024)**

In this section, we used a reverse genetics systematic approach to construct an infectious clone vector by cloning the ELVd genome into a binary vector under the control of the 35S promoter. The whole procedure is simple and fast, with low cost, high fidelity and good reproducibility, which is obviously superior to the more costly and cumbersome step-by-step characteristics of transcribing RNA in vitro through promoters such as T7, SP6, and T3 in order to obtain a large amount of viral RNA (Yoon et al., 2002; Kamboj et al., 2015; Zheng et al., 2016; Shakir et al., 2023). Infectious cDNA clone, which is the infectious cDNA or the infectious in vitro transcription product of cDNA of RNA viruses, is the basis for the study of RNA viruses through reverse genetic systems. The successful construction of infectious cDNA clones can effectively carry out RNA virus research at the DNA level (Tenllado et al., 2003；Wu et al., 2010; Shi et al., 2016; Wang et al., 2016; Li et al., 2020; Tu et al., 2021; Zhang et al., 2021; Leastro et al., 2024). Infectious clone technology is the basis for studying viral functional genomics, replication and expression of viral proteins, and host-virus interactions, and has driven the rapid development of related research fields in molecular virology (Tenllado et al., 2003；Wu et al., 2010; Shi et al., 2016; Wang et al., 2016; Li et al., 2020; Tu et al., 2021; Zhang et al., 2021; Leastro et al., 2024).

Chapter 4 Effects of *DCLi* and *RDR6i* on ELVd infection of plants

4.1 Introduction

In plants, RNA silencing represents an effective cellular defense against pathogens, including viruses and viroids (Shi et al., 2008; Csorba et al., 2015). Indeed, this cellular defense uses DCLs to process plant viral RNAs into virus-derived siRNAs (vsiRNAs). For example, DCL4 and its homologous-processed 21 nt vsiRNAs are essential in the first antiviral frontier of intracellular RNA silencing, while DCL2 may be associated with DCL2 processing of 22 nt vsiRNAs which are primarily involved in defensive intercellular silencing (Qin et al., 2017). DCL3 and 24 nt vsiRNAs, as well as DCL1 and microRNAs, are essential in, and also play an important role against DNA viruses in plants (Blevins et al., 2006; Aregger et al., 2012). The RNA silencing on viruses is a complex process and better understanding was achieved on the nuclear replicating viruses, although both nucleus and chloroplast-replicating viruses can be targets of RNA silencing (Wang et al., 2004; Dalakouras et al., 2015; Katsarou et al., 2016). As research continues, siRNAs specific to chloroplast replicating viruses (vd-siRNA) have also been analyzed to be closely related to RNA silencing (Di Serio et al., 2009; Zhang et al., 2014; Jiang et al., 2019). However, the mechanism of RNA silencing on chloroplast-like viruses and viroids remains largely unknown (Di Serio et al., 2009).

To address this issue, we utilized *Eggplant latent viroid* (ELVd) and a set of transgenic *RDR6*- and *DCL*-RNAi *N. benthamiana* lines in the current study (Chen et al., 2018). ELVd is the only species of the genus *Elaviroid* in the Avsunviroidae family and includes a 332-335 nt cyclic non-coding ssRNA genome (Molina-Serrano et al. 2007; Martínez et al. 2009; Nohales et al. 2012a), ELVd also contains hammerhead nucleases in both the + and - RNA strands (Fadda et al., 2003). It has a very narrow host range and can be transmitted mechanically and by seed. ELVd infects its natural host, aubergine (*Solanum melongena L.*), systemically and latently (Daròs., 2016). However, ELVd can also establish local infection in *N. benthamiana*, which represents an excellent model for studying intracellular RNA trafficking between the cytoplasm and chloroplasts (Gómez and Pallas, 2010; 2012; Nohales et al., 2012a). Based on these findings on ELVd together with the transgenic lines generated in our laboratory, that lack cellular RNA silencing, we investigated how DCLs and RDR6 affect chloroplast vd-siRNA biogenesis in plants.

We constructed an ELVd-infectious plasmid p1300/35S-ELVd as described in Chapter 3 and validated it by Sanger sequencing. We then transformed the plasmid p1300/35S-ELVd into *A. tumefaciens* GV3101, cultured Agrobacterium tumefaciens carrying p1300/35S-ELVd, and then performed *Agrobacterium tumefaciens* infection experiments on *N. benthamiana*, transgenic RNAi and RDR6i plants at the 6-leaf stage of tobacco to investigate the effect of DCLi and RDR6i on ELVd infection of plants.

4.2 Experimental Results

4.2.1 DCL1i heterozygote detection

According to the results of previous research in Hong's lab, NbDCL1i grows normally in T1 generation of heterozygotes, while the homozygotes do not bear seeds, which indicates that after DCL1 gene interference, NbDCL1i homozygotes are easy to die and highly sterile, and it is difficult to obtain homozygotes transgenic plants. In this experiment, we used the obtained heterozygous positive transgenic plants, so when using NbDCL1i strains for experiments, we have to use primers (intron F/intron R) to detect the positive transgenic plants. However, NbDCL2i, NbDCL3I, and NbDCL4i are homozygotes transgenic plants obtained from hybrid and do not require positive detection.

Nb DCL1i leaves were collected 4 dpi (days post incolcuation) for heterozygote detection by extracting DCL1i leaf genomic DNA followed by PCR amplification using Pdk intron F / Pdk intron R primers. PCR reaction system refers to 2.2.1. The PCR: Taq Mix , 25 cycles. Final agarose gel analysis showed that all plants tested in the DCL1-1i line were DCL1-RNAi, Plants (Numbers 3-6, 9, 13-14, 17-23, 25-29) of the DCL1-2i line are DCL1-RNAi. No transgenes were detected in these plants (No. 1, 2, 7, 8, 10-12, 15-16, 24, 30) (Figure 4.1). Plants with no detectable transgenes were discarded.

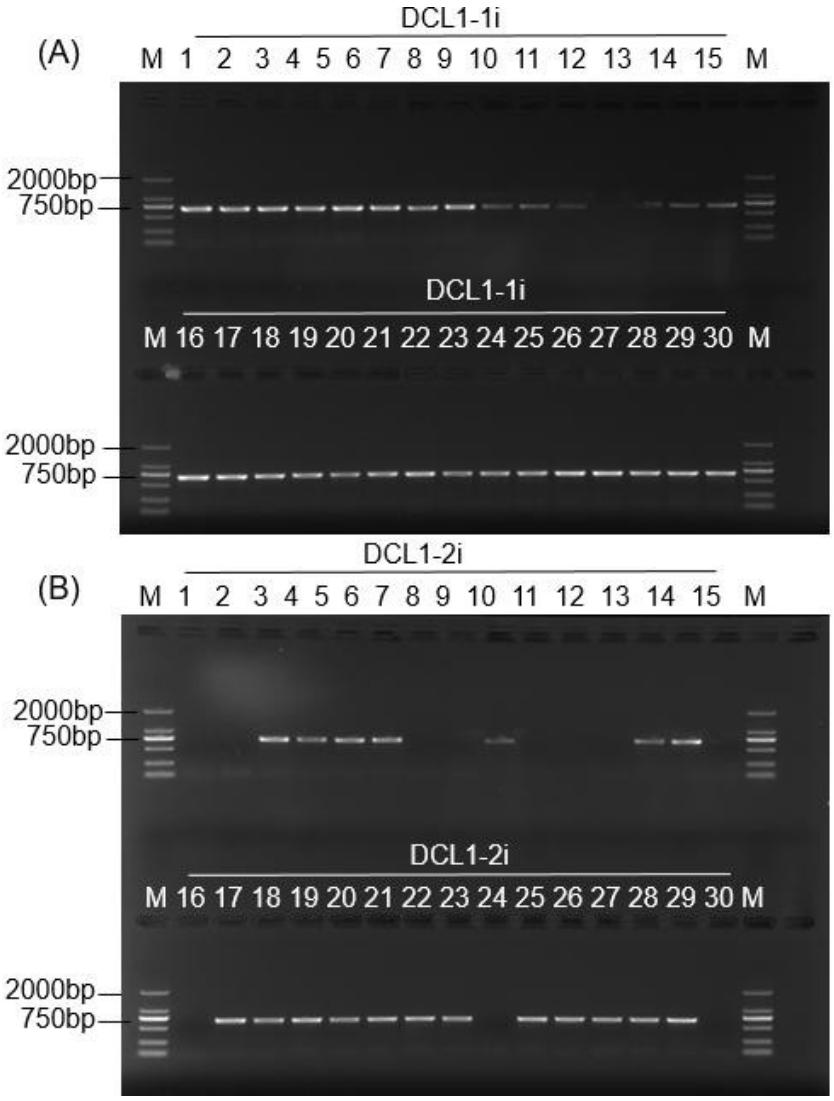

Figure 4.1 DCL1 genomic DNA-PCR

(A) DCL1-1i genomic DNA-PCR ; (B) DCL1-2i genomic DNA-PCR. The transgenic plant NbDCL1-1i is a multicopy gene, whereas NbDCL1-2i is a single-copy gene. Lanes 1 to 30 (A) indicated 30 different plants of the DCL1-1i line. Lanes 1 to 30 (B) indicated 30 different plants of the DCL1-2i line. The DCL1 genomic DNA-PCR (A and B) were electrophoresed in 1.0% agarose gel and stained in ethidium bromide. Sizes of the DCL1 genomic DNA-PCR were indicated. M: DNA ladder 2000bp. **(Source: Pengcheng Zhang, 2024)**

4.2.2 ELVd RNA inoculation

On day 4 (4 dpi) after ELVd infiltration inoculation, all inoculated Nb portion leaves were collected and used to detect the molecular infection of ELVd virus in the plants. The results of the gel electrophoresis analysis (Figure 4.2) showed that all plants had been successfully inoculated with ELVd, which was a good basis for the subsequent

experiments.

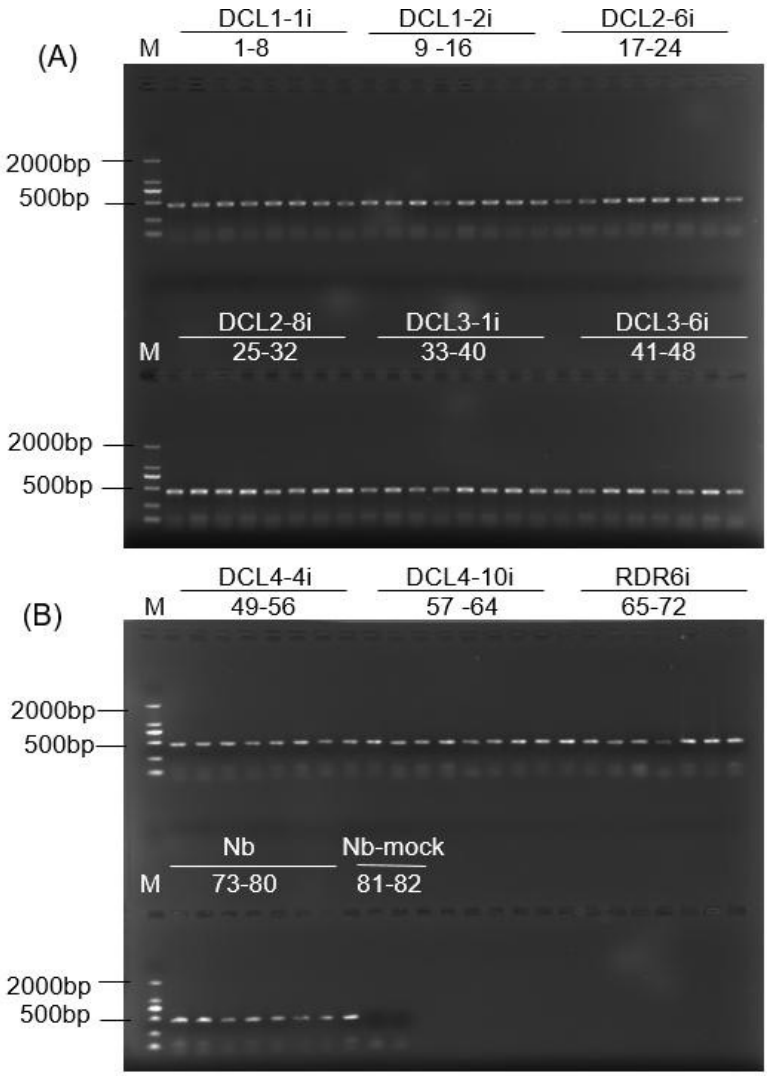

Figure 4.2 ELVd RNA infection detection

The ELVd RNA (A and B) were electrophoresed in 1.0% agarose gel and stained in ethidium bromide. (A) RT-PCR detection of ELVd RNA in DCL1i, DCL2i, and DCL3i plants. (B) RT-PCR detection of ELVd RNA in DCL4i, RDR6i, Nb and Nb-mock plants. Lanes 1 to 8 (A) indicated 8 different palnts of the DCL1-1i line. Lanes 9 to 16 (A) indicated 8 different plants of the DCL1-2i line. Lanes 17 to 24 (A) indicated 8 different plants of the DCL2-6i line. Lanes 25 to 32 (A) indicated 8 different plants of the DCL2-8i line. Lanes 33 to 40 (A) indicated 8 different plants of the DCL3-1i line. Lanes 41 to 48 (A) indicated 8 different plants of the DCL3-6i line. Lanes 49 to 56 (B) indicated from 8 different plants of the DCL4-4i line. Lanes 57 to 64 (B) indicated 8 different plants of the DCL4-10i line. Lanes 65 to 72 (B) indicated 8 different plants of the RDR6i line. Lanes 73 to 80 (B) indicated 8 different wild-type *N. benthamiana* (Nb) plants. Lanes 81 to 82 (B) indicated 2 different Nb-mock plants. Sizes and/or positions of the

ELVd-specific RT-PCR products and the marker DNA ladder-2000bp (M) are indicated. **(Source: Pengcheng Zhang, 2024)**

4.2.3 RT-PCR detection of ELVd RNA and Southern blot analysis

The ELVd DNA probe was successfully obtained by PCR amplification as described in Section 2.2.16, with DIG containing dNTP replacement and a normal dNTP mixture used as a control (Figure 4.3). Hence, 6dpi and 14dpi inoculated leaf Southern blot were performed and the results showed that the ELVd DNA probe was fine and the whole set of Southern blot process system was fine (Figure 4.4 and Figure 4.5).

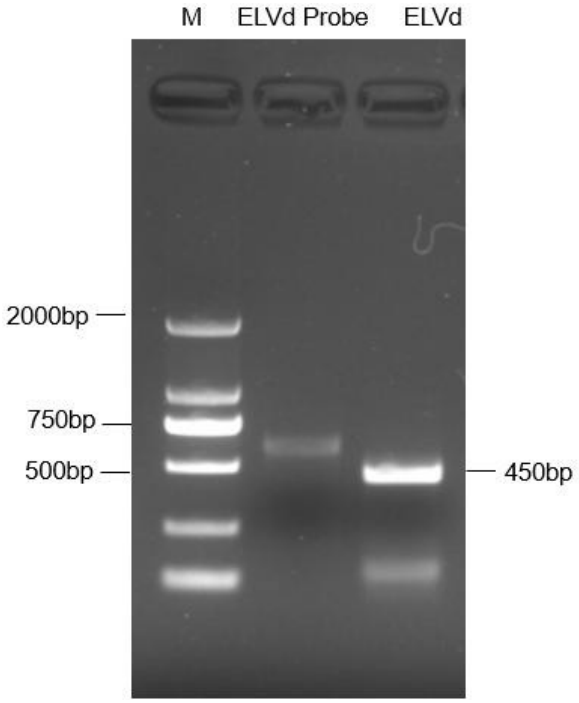

Figure 4.3 Agarose gel electrophoresis showing the syntheses ELVd DNA probe

The ELVd DNA probe was obtained by PCR amplification with dNTPs containing DIG-labelled dUTP. The ELVd and ELVd DNA probe were electrophoresed in 1.0% agarose gel and stained in ethidium bromide. Size of the ELVd and ELVd DNA probe were indicated. M: DNA ladder 2000bp. **(Source: Pengcheng Zhang, 2024)**

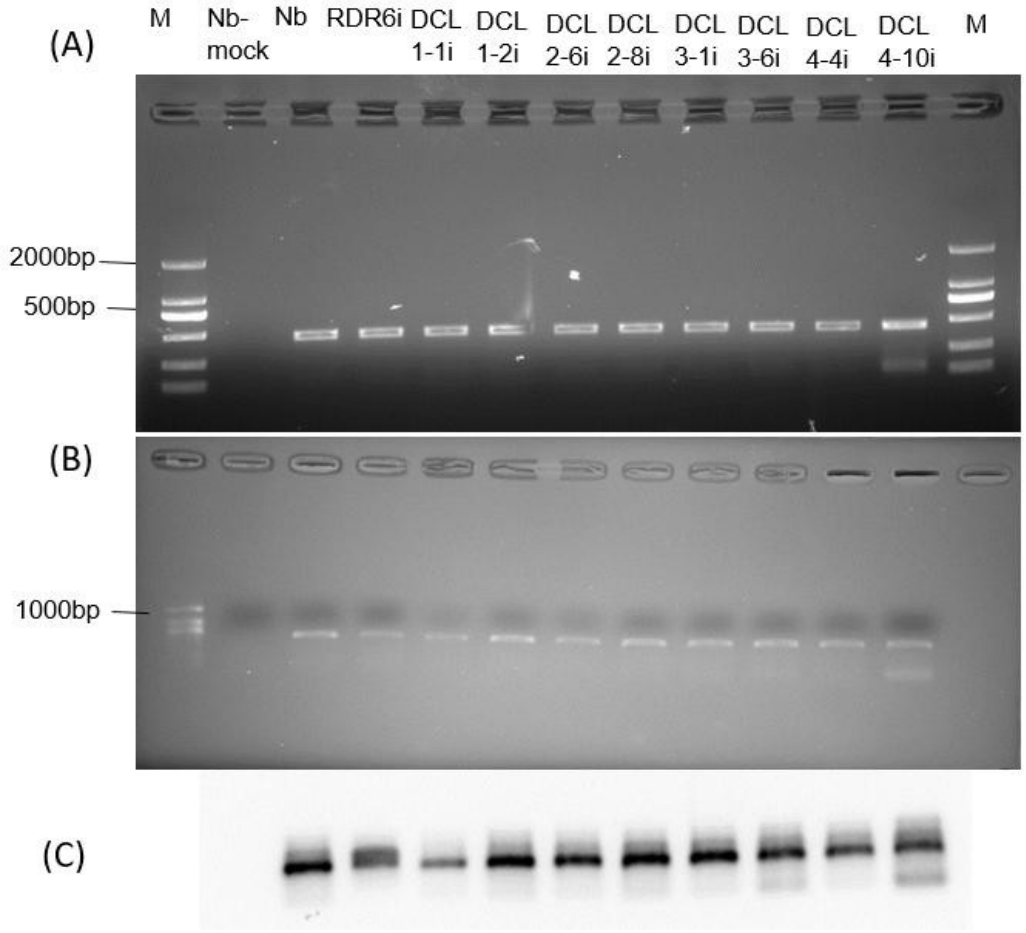

Figure 4.4 Inoculated leaves southern blot at 6dpi

(A) Agarose gel electrophorese of RT-PCR from the inoculated leaves at 6 dpi. (B) 1% denatured agarose gel/TAE- Before transferring. (C) Southern blot using ELVd-specific probe. The products (A and B) were stained in ethidium bromide. The products (C) were indicated as results of hybridisation of ELVd probe to DNA on the transfer membrane. M: DNA ladder 2000bp (A) and DNA ladder 1000bp (B). **(Source: Pengcheng Zhang, 2024)**

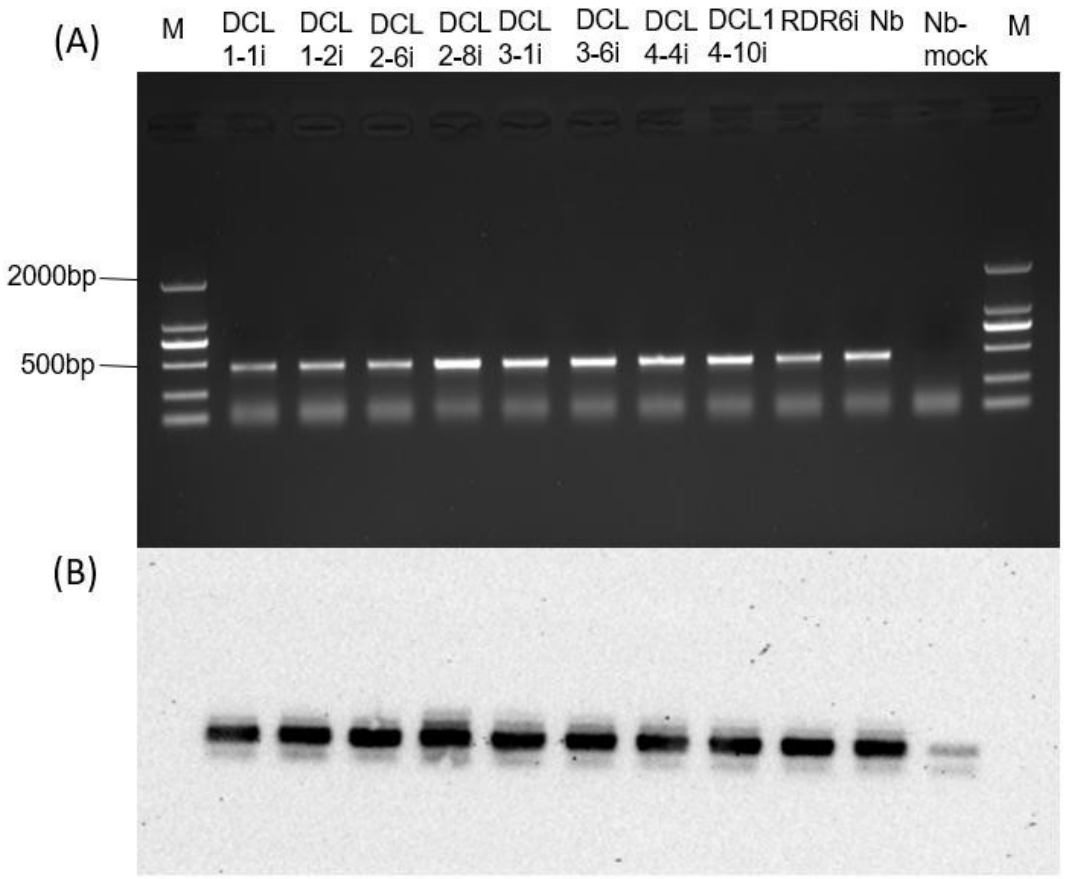

Figure 4.5 Inoculated leaves southern blot at 14dpi

(A) Agarose gel electrophorese of RT-PCR from the inoculated leaves at 14 dpi. The ELVd specific RT-PCR products (A) were stained in ethidium bromide. M: the DNA ladder-2000bp. (B) Southern blot using ELVd-specific probe. The ELVd-specifc RT-PCR products were transferred to member and probed with the ELVd-specific probe (see Figure 4.3). **(Source: Pengcheng Zhang, 2024)**

4.2.4 Effect of DCLi and RDR6i on EVLd RNA accumulation after infection at 6dpi and 14dpi

4.2.4.1 Phenotypic observation of inoculated and new leaves

At 6 dpi, the inoculated leaves showed a slight leaf curl (Figure 4.6) but still maintained a good green growth trend. At 14 dpi (Figure 4.7), most of the curl disappeared and the leaves slowly spread out. After inoculation at 6 dpi and 14 dpi, the newly grown leaf tissue and the inoculated leaves were collected, cooled rapidly in liquid nitrogen, and stored at -80°C in the freezer.

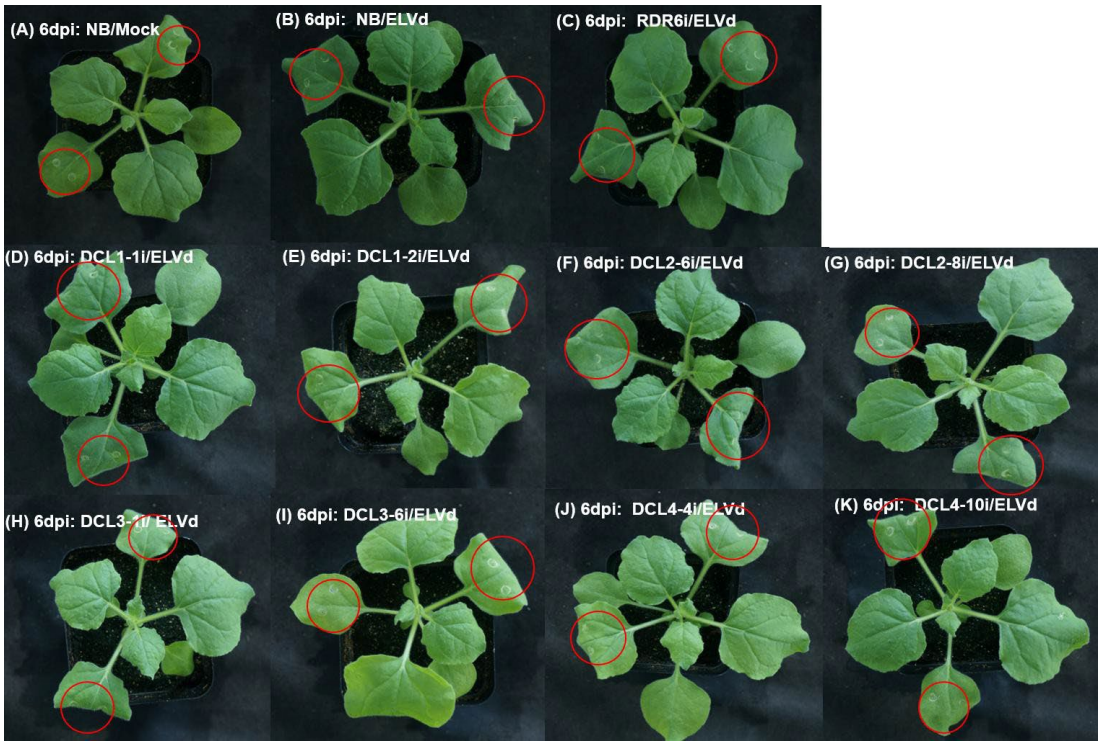

Figure 4.6 Phenotypic observation of inoculated and new leaves at 6dpi

(A) NB/Mock; (B) NB/ELVd; (C) RDR6i/ELVd; (D) DCL1-1i/ELVd; (E) DCL1-2i/ELVd; (F) DCL2-6i/ELVd; (G) DCL2-8i/ELVd; (H) DCL3-1i/ ELVd; (I) DCL3-6i/ELVd; (J) DCL4-4i/ELVd; (K) DCL4-10i/ELVd. Inoculated leaves are indicated by red circles highlighted at 6dpi. Plants were inoculated with ELVd, two leaves were inoculated, and each leaf was inoculated twice. Inoculated leaves were observed to be slightly curled at 6dpi. Photographs were taken at 6 dpi. **(Source: Pengcheng Zhang, 2024)**

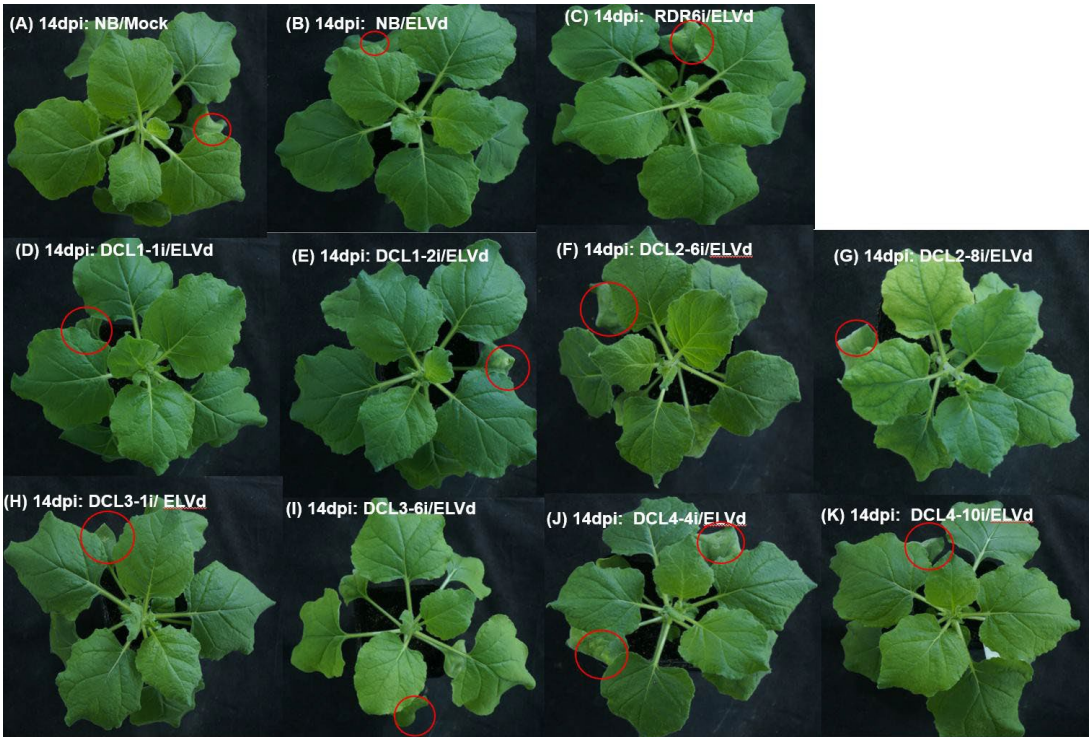

Figure 4.7 Phenotypic observation of inoculated and new leaves at 14dpi

(A) NB/Mock; (B) NB/ELVd; (C) RDR6i/ELVd; (D) DCL1-1i/ELVd; (E) DCL1-2i/ELVd; (F) DCL2-6i/ELVd; (G) DCL2-8i/ELVd; (H) DCL3-1i/ ELVd; (I) DCL3-6i/ELVd; (J) DCL4-4i/ELVd; (K) DCL4-10i/ELVd. Inoculated leaves are indicated by red circles highlighted at 14dpi. Plants were inoculated with ELVd, two leaves were inoculated, and each leaf was inoculated twice. At 14 dpi, inoculated leaves were observed to disappear curling and the leaves slowly unfolded and returned to normal. Photographs were taken at 14 dpi. **(Source: Pengcheng Zhang, 2024)**

4.2.4.2 Inoculated leaf internal reference gene 18s rRNA PCR

To test the consistency of the ELVd infection PCR experiments, we used 18s rRNA as the internal reference gene and primers PP271 and PP272 to amplify 18s rRNA as a control. Inoculated leaves internal reference gene 18s rRNA PCR (Section 2.2.18). PCR of the 18s rRNA gene of the inoculated leaves revealed that 18s rRNA were constantly detected in all inoculated leaves. Agarose gel electrophoresis showed that the width and brightness of the bands of the 18s rDNA internal reference were basically the same, and the results of the analysis of the readings by the ImageJ software were also consistent. As shown in the figure below (Figures 4.8 and 4.9).

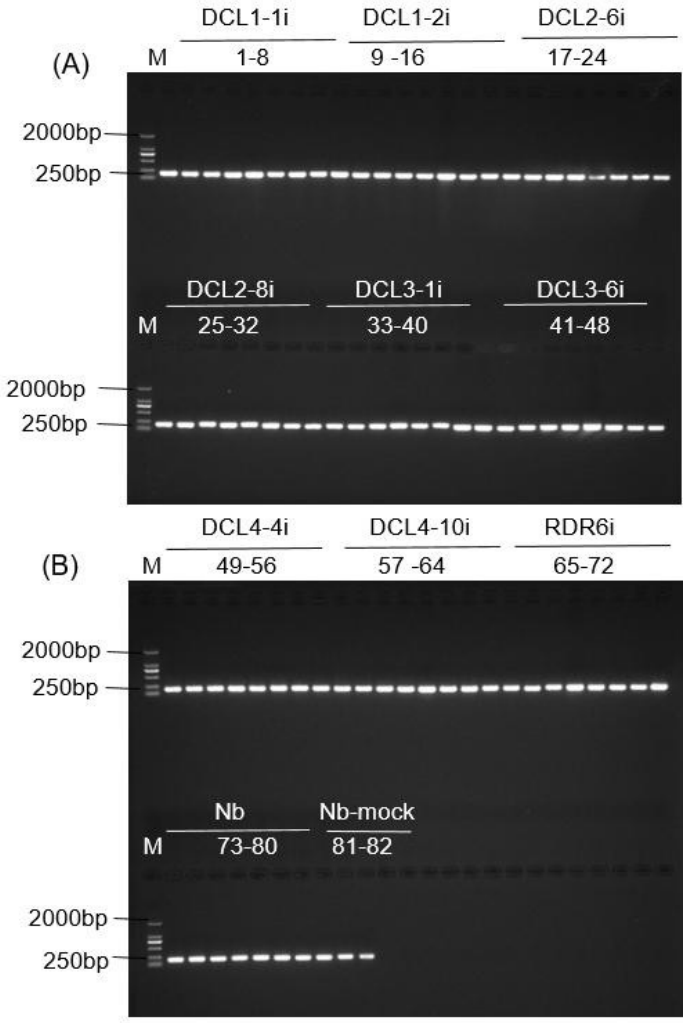

Figure 4.8 18S rRNA RT-PCR at 4dpi (Source: Pengcheng Zhang, 2024)

(A) Agarose electrophoresis showing RT-PCR detection of 18S rRNA in DCL1i, DCL2i, and DCL3i plants at 4dpi. (B) Agarose electrophoresis showing RT-PCR detection of 18S rRNA in DCL4i, RDR6i, Nb and Nb-mock plants at 4dpi. RT-PCR detection of 18S rRNA from Nb-mock were used as a negative control. Lanes 1 to 8 (A) indicated 8 different palnts of the DCL1-1i line. Lanes 9 to 16 (A) indicated 8 different plants of the DCL1-2i line. Lanes 17 to 24 (A) indicated 8 different plants of the DCL2-6i line. Lanes 25 to 32 (A) indicated 8 different plants of the DCL2-8i line. Lanes 33 to 40 (A) indicated 8 different plants of the DCL3-1i line. Lanes 41 to 48 (A) indicated 8 different plants of the DCL3-6i line. Lanes 49 to 56 (B) indicated from 8 different plants of the DCL4-4i line. Lanes 57 to 64 (B) indicated 8 different plants of the DCL4-10i line. Lanes 65 to 72 (B) indicated 8 different plants of the RDR6i line. Lanes 73 to 80 (B) indicated 8 different wild-type *N. benthamiana* (Nb) plants. Lanes 81 to 82 (B) indicated 2 different Nb-mock plants. The 18S rRNA RT-PCR products (A and B) were electrophoresed in 1.0% agarose gel and stained in ethidium bromide. Sizes of the 18S rRNA RT-PCR products (A and B) and the marker DNA ladder 2000bp (M) are indicated.

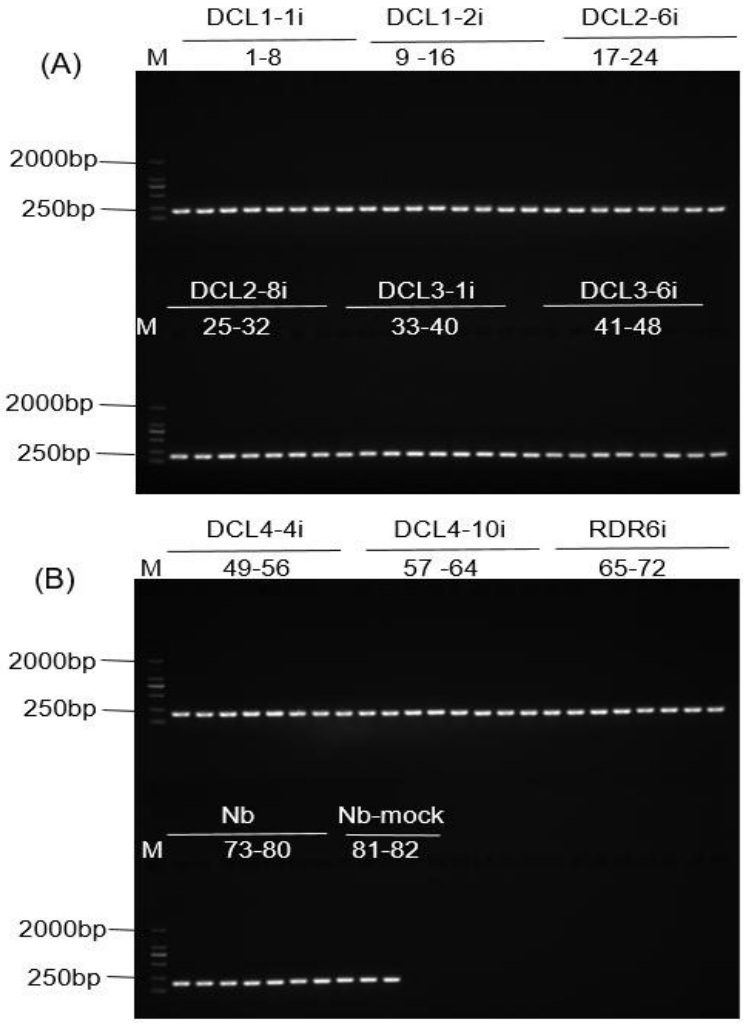

Figure 4.9 18S rRNA RT-PCR at 14dpi

(A) Agarose electrophoresis showing RT-PCR detection of 18S rRNA in DCL1i, DCL2i, and DCL3i plants at 14dpi. (B) Agarose electrophoresis showing RT-PCR detection of 18S rRNA in DCL4i, RDR6i, Nb and Nb-mock plants at 14dpi. RT-PCR detection of 18S rRNA from Nb-mock was used as a negative control. Lanes 1 to 8 (A) indicated 8 different palnts of the DCL1-1i line. Lanes 9 to 16 (A) indicated 8 different plants of the DCL1-2i line. Lanes 17 to 24 (A) indicated 8 different plants of the DCL2-6i line. Lanes 25 to 32 (A) indicated 8 different plants of the DCL2-8i line. Lanes 33 to 40 (A) indicated 8 different plants of the DCL3-1i line. Lanes 41 to 48 (A) indicated 8 different plants of the DCL3-6i line. Lanes 49 to 56 (B) indicated from 8 different plants of the DCL4-4i line. Lanes 57 to 64 (B) indicated 8 different plants of the DCL4-10i line. Lanes 65 to

72 (B) indicated 8 different plants of the RDR6i line. Lanes 73 to 80 (B) indicated 8 different wild-type *N. benthamiana* (Nb) plants. Lanes 81 to 82 (B) indicated 2 different Nb-mock plants. The 18S rRNA RT-PCR products (A and B) were electrophoresed in 1.0% agarose gel and stained in ethidium bromide. Sizes of the 18S rRNA RT-PCR products (A and B) and the marker DNA ladder 2000bp (M) are indicated. **(Source: Pengcheng Zhang, 2024)**

4.2.4.3 Detection of ELVd using Northern blot

As reported in previous studies (Gómez and Pallas, 2010; 2012; Nohales et al., 2012), we found that ELVd was able to establish local infection in *N. benthamiana*. We then utilized transgenic lines in which individual DCLs and RDR6 were knocked out by RNAi (Chen et al, 2018). RNA for ELVd was readily detected by Northern blotting in wild-type *Nb*, *DCLi*, and *RDR6i* leaf tissue infected with ELVd a few days after inoculation (4 dpi and 14 dpi), but not in the mock-inoculated *Nb* control (Figure 4.10 and Figure 4.11).

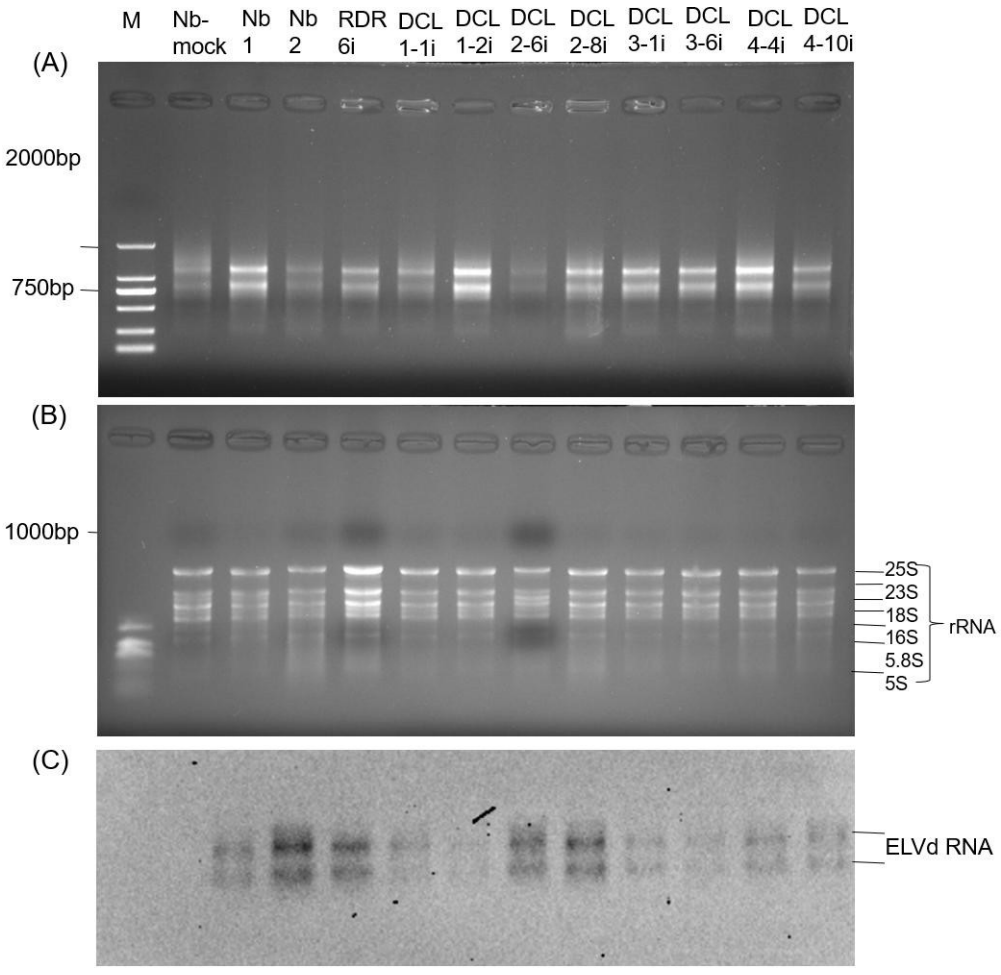

Figure 4.10 Effect of DCLi and RDR6i on ELVd RNA accumulation during

early infection at 4dpi

(A) Agarose gel electrophoresis analysis of total RNA extracted from leaf tissue of wild-type *Nb*, *DCLi,* and *RDR6i* plants at 4 dpi. (B) Total RNA extract analysed in 1% denatured agarose gel in TAE buffer. (C) Northern blot detection of ELVd RNA accumulation in wild-type Nb, DCLi, and RDR6i plants. Total RNA extracted from mock Nb leaf tissue was used as a negative control. The products (A and B) were stained in ethidium bromide. The products (C) were indicated as results of hybridisation of ELVd probe to RNA on the transfer membrane. M: DNA ladder 2000bp (A) and ssRNA ladder 1000bp (B). **(Source: Pengcheng Zhang, 2024)**

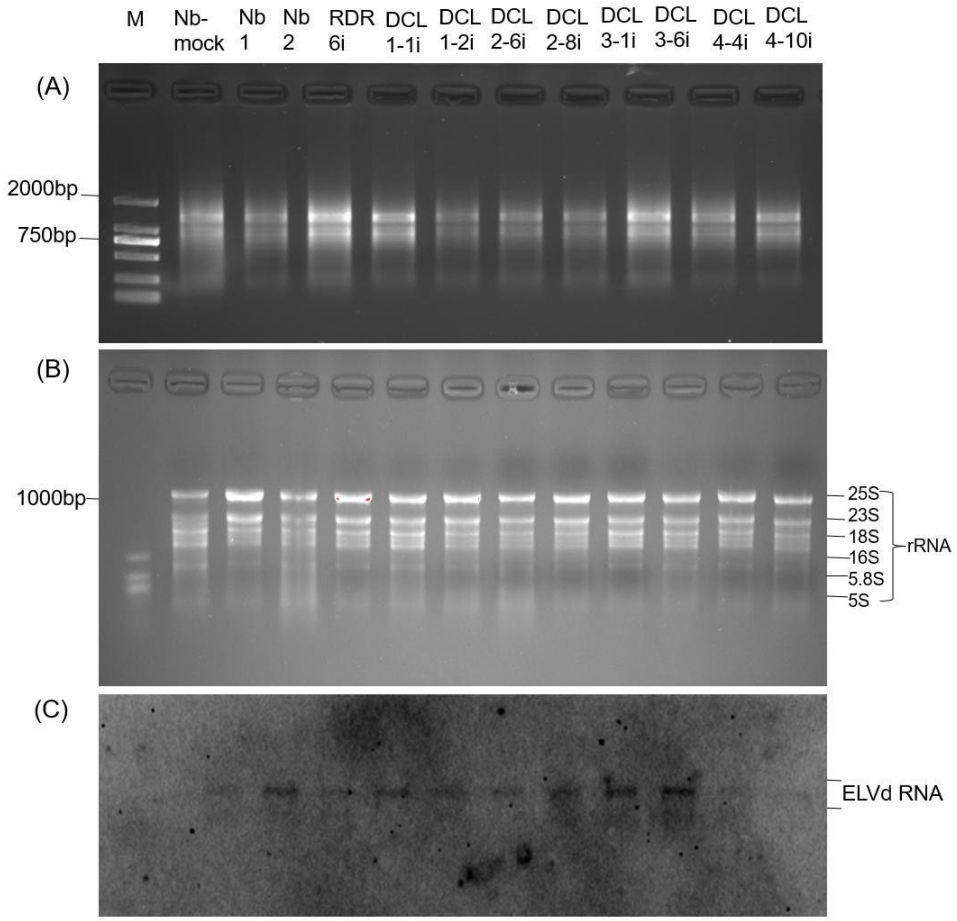

Figure 4.11 Effect of DCLi and RDR6i on ELVd RNA accumulation during later infection at 14dpi

(A) Total RNA extracted from leaf tissue of wild-type *Nb*, *DCLi,* and *RDR6i* plants at 14 dpi. (B) Total RNA extract analysed in 1% denatured agarose gel in TAE buffer. (C) Northern blot detection of ELVd RNA accumulation in wild-type Nb, DCLi, and RDR6i plants. Total RNA extracted from mock Nb leaf tissue was used as a negative control. The products (A and B) were stained in ethidium bromide. The products (C) were indicated as results of hybridisation of ELVd probe to RNA on the transfer membrane.

M: DNA ladder 2000bp (A) and ssRNA ladder 1000bp (B). **(Source: Pengcheng Zhang, 2024)**

4.2.4.4 Semi-quantitative RT-PCR

Due to the limited number of independent samples that could be included in a single gel, we chose to use RT-PCR to quantify the effect of *DCLi* and *RDR6i* on ELVd RNA accumulation (Figure 4.14 and Figure 4.17). The analysis was investigated by designing two batches of Semi-quantitative RT-PCR replicate experiments with a total of 16 biological replicates for individual samples. Analysis was carried out in duplicate to minimise the error. In Figures 4.12 and 4.13; Figures 4.15 and 4.16, DCL1-1i, DCL1-2i, DCL2-6i, DCL2-8i, DCL3-1i, DCL3-6i, DCL4-4i, DCL4-10i, RDR6i, NB, all are successful. Negative control Nb/Mock - no ELVd was detected. The relative intensities of ELVd RNA-specific bands in wild-type Nb, DCLi, and RDR6i plants were quantified using ImageJ software and analyzed by Student's t-test, as in Figure 4.14 and Figure 4.17. ELVd RNA-related gene expression was analyzed by Agarose gel electrophoresis, followed by ImageJ software.

The results showed that the average level of ELVd RNA was significantly increased by 20-60% in *DCLi* leaf tissue compared to wild-type plants. In *RDR6i*, ELVd RNA was also increased by approximately 16%, however, the difference was not statistically significant (Figure 4.14 and Figure 4.17). These data suggest that *DCL1, DCL2, DCL3,* and *DCL4*, but not *RDR6*, are involved in plant defense against ELVd during the early stages of infection.

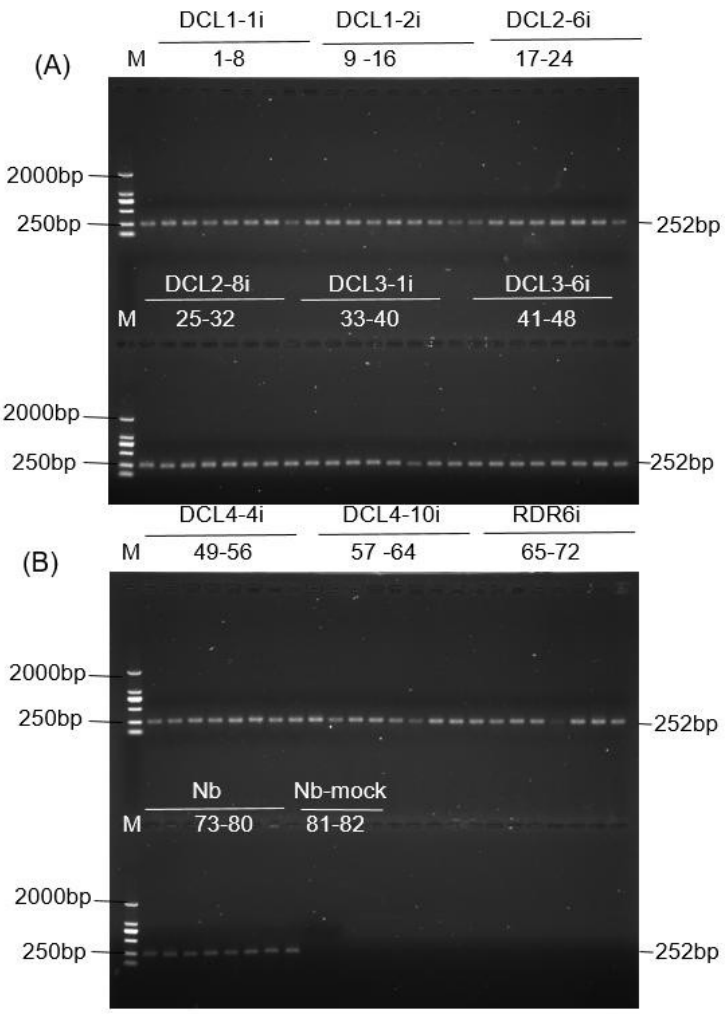

Figure 4.12 Gel analysis of ELVd semi-quantitative RT-PCR at 4dpi

(A) RT-PCR detection of ELVd RNA in DCL1i, DCL2i, and DCL3i plants at 4dpi. (B) RT-PCR detection of ELVd RNA in DCL4i, RDR6i, Nb and Nb-mock plants at 4dpi. Lanes 1 to 8 (A) indicated 8 different palnts of the DCL1-1i line. Lanes 9 to 16 (A) indicated 8 different plants of the DCL1-2i line. Lanes 17 to 24 (A) indicated 8 different plants of the DCL2-6i line. Lanes 25 to 32 (A) indicated 8 different plants of the DCL2-8i line. Lanes 33 to 40 (A) indicated 8 different plants of the DCL3-1i line. Lanes 41 to 48 (A) indicated 8 different plants of the DCL3-6i line. Lanes 49 to 56 (B) indicated from 8 different plants of the DCL4-4i line. Lanes 57 to 64 (B) indicated 8 different plants of the DCL4-10i line. Lanes 65 to 72 (B) indicated 8 different plants of the RDR6i line. Lanes 73 to 80 (B) indicated 8 different wild-type *N. benthamiana* (Nb) plants. Lanes 81 to 82 (B) indicated 2 different Nb-mock plants. The ELVd semi-quantitative RT-PCR products (A and B) were electrophoresed in 1.0% agarose gel and stained in ethidium bromide. Sizes and/or positions of the ELVd semi-quantitative RT-PCR products (A and B) and the marker DNA ladder 2000bp (M) are indicated. **(Source: Pengcheng Zhang, 2024)**

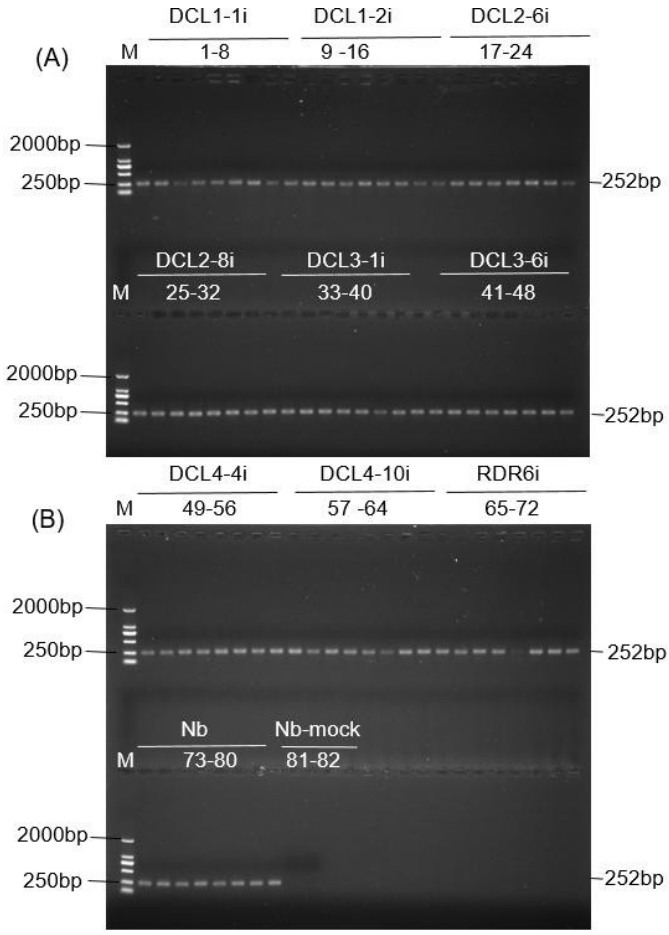

Figure 4.13 Gel analysis of duplicated ELVd semi-quantitative RT-PCR at 4dpi

(A) RT-PCR detection of ELVd RNA in DCL1i, DCL2i, and DCL3i plants at 4dpi. (B) RT-PCR detection of ELVd RNA in DCL4i, RDR6i, Nb and Nb-mock plants at 4dpi. Lanes 1 to 8 (A) indicated 8 different palnts of the DCL1-1i line. Lanes 9 to 16 (A) indicated 8 different plants of the DCL1-2i line. Lanes 17 to 24 (A) indicated 8 different plants of the DCL2-6i line. Lanes 25 to 32 (A) indicated 8 different plants of the DCL2-8i line. Lanes 33 to 40 (A) indicated 8 different plants of the DCL3-1i line. Lanes 41 to 48 (A) indicated 8 different plants of the DCL3-6i line. Lanes 49 to 56 (B) indicated from 8 different plants of the DCL4-4i line. Lanes 57 to 64 (B) indicated 8 different plants of the DCL4-10i line. Lanes 65 to 72 (B) indicated 8 different plants of the RDR6i line. Lanes 73 to 80 (B) indicated 8 different wild-type *N. benthamiana* (Nb) plants. Lanes 81 to 82 (B) indicated 2 different Nb-mock plants. The ELVd semi-quantitative RT-PCR products (A and B) were electrophoresed in 1.0% agarose gel and stained in ethidium bromide. Sizes and/or positions of the ELVd semi-quantitative RT-PCR products (A and B) and the marker DNA ladder 2000bp (M) are indicated. **(Source: Pengcheng Zhang, 2024)**

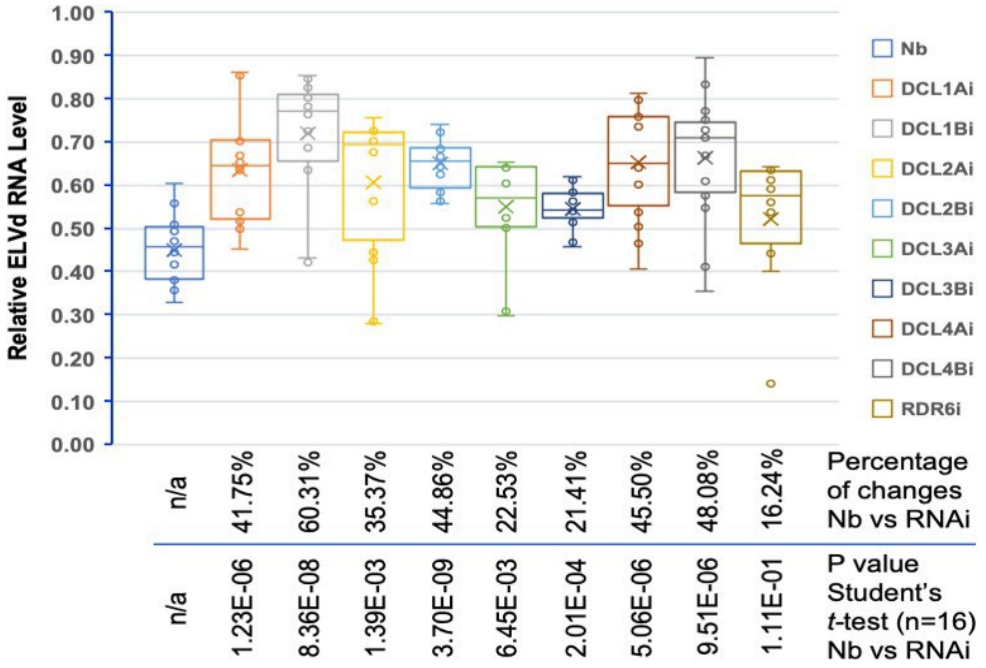

Figure 4.14 Effect of DCLi and RDR6i on ELVd RNA accumulation during early infection at 4 dpi (n=16)

Semi-quantitative analysis of ELVd RNA accumulation in wild-type *Nb*, *DCLi,* and *RDR6i* plants. Percentage of changes in ELVd RNA in Nb versus RNAi (*DCLi* and *RDR6i*) and p-values from Student's t-test of ELVd RNA levels in Nb versus RNAi (*DCLi* and *RDR6i*) are indicated. Total of 16 biological replicates were made for each transgenic line and averaged. After electrophoresis of 10 µl RT-PCR product (From Figure 4.12 and 4.13) in 1.0% agarose gel and stained in ethidium bromide, relative intensity of ELVd specific bands was quantified by ImageJ software and analysed by the Students′t-test. **(Source: Pengcheng Zhang, 2024)**

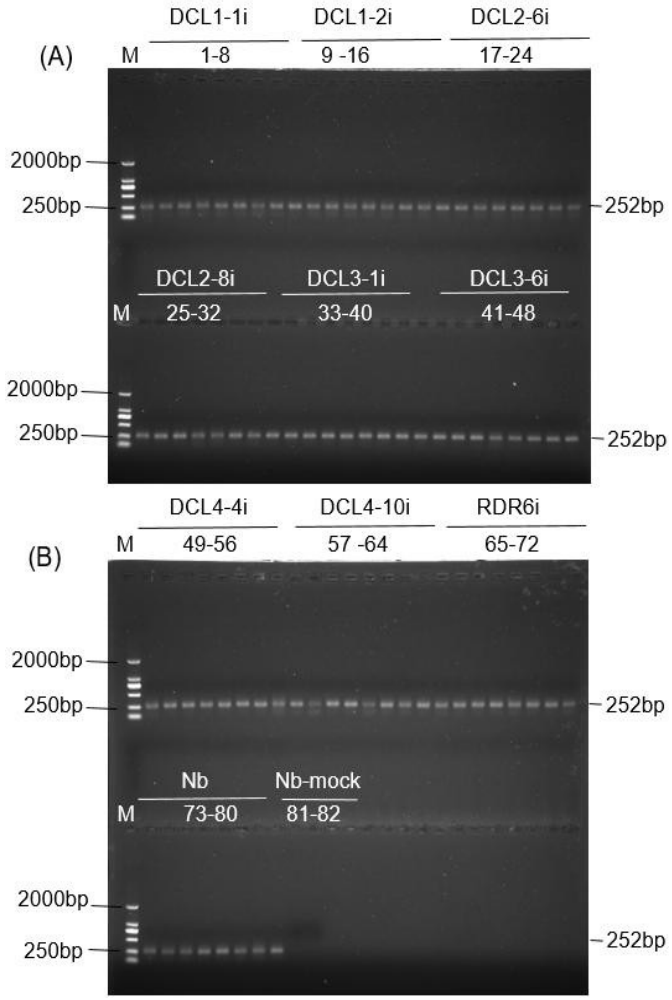

Figure 4.15 Gel analysis of ELVd semi-quantitative RT-PCR at 14 dpi

(Source: Pengcheng Zhang, 2024)

(A) RT-PCR detection of ELVd RNA in DCL1i, DCL2i, and DCL3i plants at 14dpi. (B) RT-PCR detection of ELVd RNA in DCL4i, RDR6i, Nb and Nb-mock plants at 14dpi. Lanes 1 to 8 (A) indicated 8 different palnts of the DCL1-1i line. Lanes 9 to 16 (A) indicated 8 different plants of the DCL1-2i line. Lanes 17 to 24 (A) indicated 8 different plants of the DCL2-6i line. Lanes 25 to 32 (A) indicated 8 different plants of the DCL2-8i line. Lanes 33 to 40 (A) indicated 8 different plants of the DCL3-1i line. Lanes 41 to 48 (A) indicated 8 different plants of the DCL3-6i line. Lanes 49 to 56 (B) indicated from 8 different plants of the DCL4-4i line. Lanes 57 to 64 (B) indicated 8 different plants of the DCL4-10i line. Lanes 65 to 72 (B) indicated 8 different plants of the RDR6i line. Lanes 73 to 80 (B) indicated 8 different wild-type *N. benthamiana* (Nb) plants. Lanes 81 to 82 (B) indicated 2 different Nb-mock plants. The ELVd semi-quantitative RT-PCR products (A and B) were electrophoresed in 1.0% agarose gel and stained in ethidium bromide. Sizes and/or positions of the ELVd semi-quantitative RT-PCR products (A and B) and the marker DNA ladder 2000bp (M) are indicated.

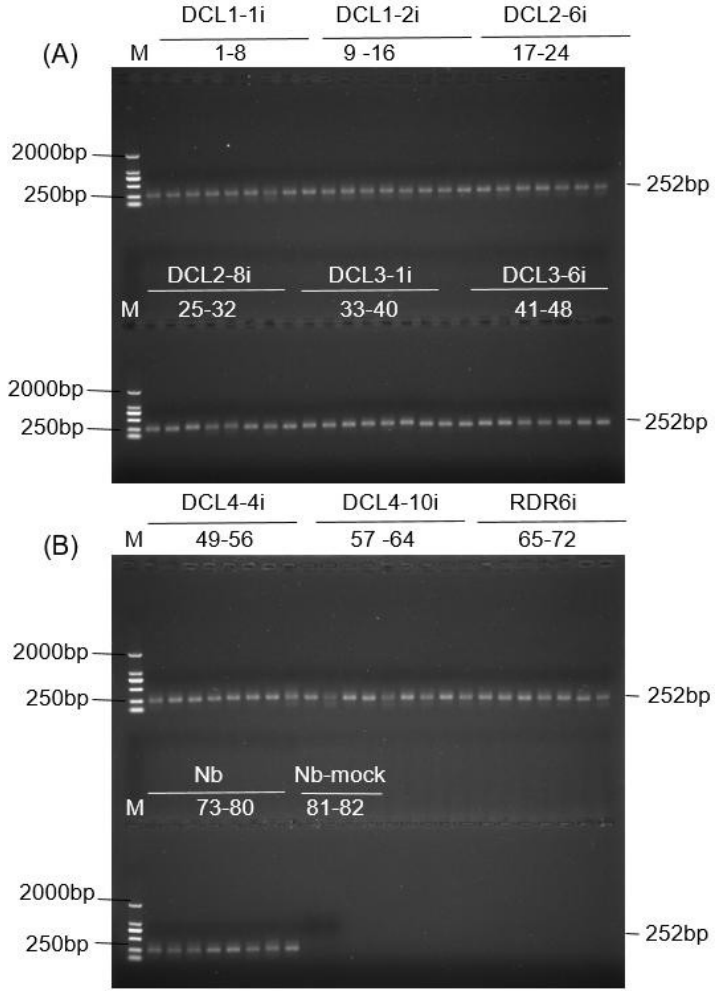

Figure 4.16 Gel analysis of duplicated ELVd semi-quantitative RT-PCR at 14 dpi

(A) RT-PCR detection of ELVd RNA in DCL1i, DCL2i, and DCL3i plants at 14dpi. (B) RT-PCR detection of ELVd RNA in DCL4i, RDR6i, Nb and Nb-mock plants at 14dpi. Lanes 1 to 8 (A) indicated 8 different palnts of the DCL1-1i line. Lanes 9 to 16 (A) indicated 8 different plants of the DCL1-2i line. Lanes 17 to 24 (A) indicated 8 different plants of the DCL2-6i line. Lanes 25 to 32 (A) indicated 8 different plants of the DCL2-8i line. Lanes 33 to 40 (A) indicated 8 different plants of the DCL3-1i line. Lanes 41 to 48 (A) indicated 8 different plants of the DCL3-6i line. Lanes 49 to 56 (B) indicated from 8 different plants of the DCL4-4i line. Lanes 57 to 64 (B) indicated 8 different plants of the DCL4-10i line. Lanes 65 to 72 (B) indicated 8 different plants of the RDR6i line. Lanes 73 to 80 (B) indicated 8 different wild-type *N. benthamiana* (Nb) plants. Lanes 81 to 82 (B) indicated 2 different Nb-mock plants. The ELVd semi-quantitative RT-PCR products (A and B) were electrophoresed in 1.0% agarose gel and stained in ethidium bromide. Sizes and/or positions of the ELVd semi-quantitative RT-PCR

products (A and B) and the marker DNA ladder 2000bp (M) are indicated. **(Source: Pengcheng Zhang, 2024)**

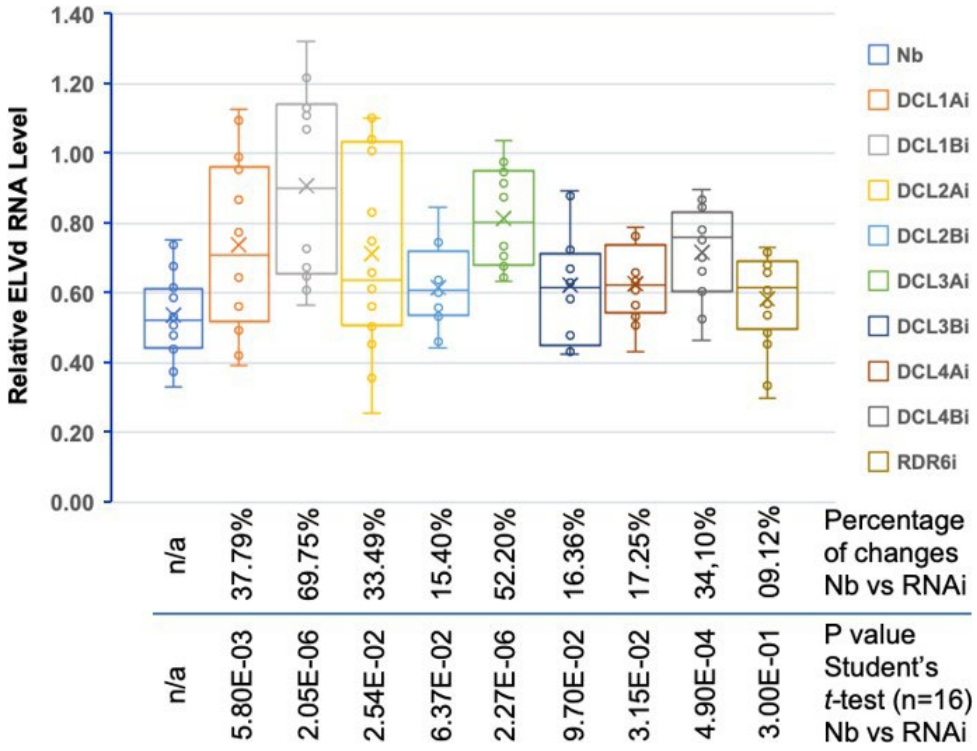

Figure 4.17 Effect of DCLi and RDR6i on ELVd RNA accumulation during later infection at 14 dpi (n=16)

Semi-quantitative analysis of ELVd RNA accumulation in wild-type *Nb*, *DCLi,* and *RDR6i* plants. Percentage of changes in ELVd RNA in Nb versus RNAi (*DCLi* and *RDR6i*) and p-values from Student's t-test of ELVd RNA levels in Nb versus RNAi (*DCLi* and *RDR6i*) are indicated. Total of 16 biological replicates were made for each transgenic line and averaged. After electrophoresis of 10 µl RT-PCR product (From Figure 4.15 and 4.16) in 1.0% agarose gel and stained in ethidium bromide, relative intensity of ELVd specific bands was quantified by ImageJ software and analysed by the Students′t-test. **(Source: Pengcheng Zhang, 2024)**

4.3 Discussion

When viroids infect plant, it will use the chloroplast or nucleus of the plant to replicate. ssRNA is synthesized into dsRNA by base pairing, which is cleaved into 21, 22, and 24 nt vsiRNAs under the action of the Dicer ribonucleic acid endonucleases, DCL4, DCL2, and DCL3. vsiRNAs are then recognized by AGO proteins to form RISC, which specifically recognizes viral mRNAs and targets viral mRNAs for degradation, leading

to gene silencing (Di Serio et al., 2009; Aregger et al., 2012; Csorba et al., 2015; Qin et al., 2017; Chen et al., 2018; Jiang et al., 2019). This mechanism can lead to a decrease in the viral infection, thus enhancing host plant resistance to the viroids. The effects of RNA silencing on viruses are also complex, and we know that both nuclear and chloroplast replicating viruses can be targets for RNA silencing (Bolduc et al., 2010; Dalakouras et al., 2015; Katsarou et al., 2016). Further research has shown that the specific 21-24nt virus siRNA (vd-siRNA) of chloroplast replicating virus are also closely related to RNA silencing (Martinez et al., 2010; Zhang et al., 2014; Chen et al., 2018; Jiang et al., 2019; Navarro, JA., 2021; Bwalya et al., 2023). However, how RNA silencing targeting and combating the chloroplast viroids remains largely unknown.

This section is based on the previously constructed infectious cloning vector pCAMBIA1300-35S-ELVd, which was transformed into the *Agrobacterium* competent state GV3101, and then local infection was established by *Agrobacterium* infiltration inoculation of ELVd virus to infect *N. benthamiana* with different transgenic *DCLi*. The inoculated leaves and new leaves were then analysed by Northern blot assay for ELVd RNA and optionally using semi-quantitative RT-PCR to quantify the effect of DCLi and RDR6i on ELVd RNA accumulation, and finally, the effect of DCLs and RDR6i on ELVd-infected plants was assessed.

The experimental results showed that after a few days of inoculation (4 dpi and 14 dpi) in wild-type Nb, DCLi and RDR6i leaf tissues were always susceptible to the establishment of localised infection and infected leaf phenotypes by ELVd (Figure 4.2, Figure 4.6-4.9), which is similar to the studies that have been reported (Gómez and Pallas., 2010; 2012; Nohales et al., 2012). Further experiments detected ELVd RNA by Northern blotting, whereas it was not detected in the mock-inoculated Nb control (Figures 4.10 and 4.11), and these results are in agreement with previous studies (Qin et al., 2017; Chen et al., 2018; Marquez-Molins et al., 2021).

Alternatively, we chose to use semiquantitative RT-PCR to quantify the effects of DCLi and RDR6i on ELVd RNA accumulation (Figure 4.12-4.17). A total of 16 biological replicates of a single sample were quantified by analyzing the relative intensities of ELVd RNA-specific bands in wild-type Nb, DCLi, and RDR6i plants using ImageJ software and analyzed by Student's t-tests as in Figure 4.14 and Figure 4.17. During early infection at 4 dpi, the average level of ELVd RNA in DCLi leaf tissue was significantly increased by 21-60% compared to wild-type plants. In RDR6i, ELVd RNA

was also increased by about 16%, but the difference was not statistically significant (Figure 4.14). However, during early infection at 4 dpi, the average level of ELVd RNA in DCLi leaf tissue was significantly increased by 15-69% compared to wild-type plants. In RDR6i, ELVd RNA was also increased by about 9% (Figure 4.17). These data suggested that in DCL1, DCL2, DCL3, and DCL4 plants, but not RDR6, ELVd RNA levels were increased in both early and late stages of infection. However, RDR6 had less effect on ELVd RNA accumulation (Figure 4.14 and Figure 4.17). These data results are consistent with those previously reported (Katsarou et al., 2016; Adkar-Purushothama et al., 2020; Marquez-Molins et al., 2021). It also suggested the involvement of plant defense against ELVd in the early stages of infection.

In summary, DCL1, DCL2, DCL3 and DCL4 are all involved in the delivery of transgene-induced RNA silencing. However, it remains unclear how these genes contribute to the transport of virus-induced gene silencing. Further analysis of sRNA distribution and the effect of *DCLi* and *RDR6i* on ELVd sRNA production will be continued in the next section, following high-throughput sequencing by sRNA, from the analysis of sRNA sequencing data in conjunction with bioinformatics.

Chapter 5 Effect of *DCL*i and *RDR6*i on the production of ELVd siRNA in plants

5.1 Introduction

The effects of RNA silencing on viroids are complex and dynamic. It is well known that viroids replicate in the nucleus or chloroplasts of host cells, and both nucleus- and chloroplast-replicating viroids can be targets of RNA silencing, producing siRNAs of 21-24 nt specific to viroid genome sequences (vd-siRNAs). Chloroplast viroids (ELVd) can produce unique chloroplast viral siRNAs (cvd-siRNAs) related to post-transcriptional RNA silencing (Martínez de Alba et al., 2002; Di Serio et al., 2009; St-Pierre et al., 2009; Bolduc et al., 2010). However, this is intriguing due to the physical barrier between chloroplast viroids replication and the subcellular compartment in which the RNA silencing machinery operates. Therefore, it remains unclear how cytoplasmic RNA silencing targets chloroplast viroids for cvd-siRNA biogenesis. It is known that ELVd only locally infects *N. bethamiana* plants when inoculated with infectious RNA transcribed in vitro. To seek answers to the question, infectious RNA clones of ELVd were transformed into binary plasmids and the replication of ELVd in wild-type and transgenic *N. bethamiana* plants knocked down with various DCLs or RDR6 in infiltrated leaves was initiated using the *Agrobacterium* infiltration method. Intracellular RNA translocation between the cytoplasm and chloroplast was investigated and ELVd was examined after replication in chloroplasts. The effect of gene silencing on the biogenesis of virosomal siRNAs derived from ELVd RNAs was examined.

5.2 Experimental Results

5.2.1 Cellular 18-30 nt sRNAs mapped to RNAi pathway genes in healthy control plants

In comparison to these in wild-type *N. benthamiana*, DCLs or RDR6 mRNAs were specifically investigated in each of the independent transgenic lines DCL1i, DCL2Ai, DCL2Bi, DCL3Ai, DCL3Bi, DCL4Ai, DCL4Bi, and RDR6i, degradation of DCLs or RDR6 mRNAs and the mapped gene sequence were analysed by elevated reads of specific 21, 22, and 24 nt siRNAs (Table 5.1). The results showed that RDR6i had no effect on the size of 21, 22, and 24 nt siRNAs, while DCL2i, DCL3i, and DCL4i reduced the production of 22, 24, or 21 nt siRNAs in host cells, respectively (Figure 5.1A and B).

Consistent with our previous reports (Qin et al., 2017; Chen et al., 2018).

Table 5.1 21-24 nt sRNAs mapped to RNAi pathway genes in healthy plants

	Nb	Nb	Nb	RDR6i	DCL1i	DCL2Ai	DCL2Bi	DCL3Ai	DCL3Bi	DCL4Ai	DCL4Bi
RNAigene-DCL1	8	10	177	31	58211	21	17	7	7	12	3
RNAigene-DCL2	612	638	840	263	1092	693496	1026174	871	754	35	136
RNAigene-DCL3	18	16	15	21	26	15	25	269387	124688	29	13
RNAigene-DCL4	62	33	17	15	15	12	23	85	153	200054	237039
RNAigene-Seq5	2	2	2	1	1	1	0	2	0	2	1
RNAigene-Seq6	1	2	8	2	3	0	3	1	3	2	5
RNAigene-Seq7	0	1	4	3	0	0	1	1	0	0	1
RNAigene-Seq8	2	3	1	0	4	1	2	2	7	5	3
RNAigene-Seq9	3	3	1	2	0	5	1	1	3	1	1
RNAigene-Seq10	1	1	0	4	1	1	1	2	5	3	3
RNAigene-Seq11	1	0	2	2	1	0	1	1	1	2	2
RNAigene-Seq12	2	0	0	1	1	2	2	4	2	4	4
RNAigene-Seq13 (RDR6)	10	73	26	253064	14	15	24	12	5	11	7
RNAigene-Seq14	11	12	17	9	9	18	27	19	14	17	16
RNAigene-Seq15	9	8	17	9	8	18	13	14	23	17	10
RNAigene-Seq16	19	16	15	2	19	11	4	41	40	61	58
RNAigene-Seq17	2	3	13	4	6	9	5	7	13	7	10
RNAigene-Seq18	13	12	21	14	7	13	10	22	17	31	8
RNAigene-Seq19	4	2	1	2	2	1	1	3	1	1	3
RNAigene-Seq20	1	1	1	4	2	1	4	2	3	3	1
RNAigene-Seq21	2	2	1	1	3	4	1	3	2	2	2
RNAigene-Seq22	0	0	3	0	3	2	2	4	3	5	0
RNAigene-Seq23	1	5	1	2	2	2	4	0	4	3	4
RNAigene-Seq24	2	2	5	1	0	11	4	6	4	4	1
RNAigene-Seq25	2	3	10	2	8	3	2	6	6	2	6
RNAigene-Seq26	0	0	3	1	0	0	0	0	0	1	3
RNAigene-Seq27	1	1	1	1	3	4	1	4	2	1	0
RNAigene-Seq28	1	4	2	1	3	1	5	6	2	2	4
RNAigene-Seq29	4	3	6	1	1	7	2	1	4	0	3
RNAigene-Seq30	1	3	3	2	6	3	3	5	7	3	6
RNAigene-Seq31	2	3	8	6	8	10	12	1	5	14	5
RNAigene-Seq32	14	6	11	9	16	10	7	15	9	15	10
RNAigene-Seq33	4	1	5	4	2	5	4	1	9	4	0

Note: Sequences for all *Nicotiana benthamiana* RNAi genes can be found in Chen et al., 2018. Besides RNAigene DCL1-4, other RNAigenes from Seq5 to Seq33 in order are dsRNA binding protein 1 (drb1); dsRNA binding protein 2a (drb2a); dsRNA binding protein 2b (drb2b); dsRNA binding protein 3 (drb3); dsRNA binding protein 4 (drb4); dsRNA binding protein 5 (drb5); RNA-dependent RNA-polymerase 1 (rdr1); RNA-dependent RNA-polymerase 2 (rdr2); RNA-dependent RNA-polymerase 6 (rdr6); Argonaute 1a (ago1a); Argonaute 1b (ago1b); Argonaute 2 (ago2); Argonaute 4a (ago4a); Argonaute 4b (ago4b); Argonaute 5 (ago5); Argonaute 6 (ago6); Argonaute 7 (ago7); Argonaute 10 (ago10); Chromomethylase 3a (cmt3a); Chromomethylase 3b (cmt3b); Defective in RNA-Directed DNA Methylation 1 (drd1); Domains Rearranged Methyltransferase 3 (drm3); HUA Enhancer 1 (hen1), Hast1; Methyltransferase 1 (met1); Nuclear RNA Polymerase D 1a (nrpd1a); Nuclear RNA Polymerase D 1b (nrpd1b); Nuclear RNA Polymerase D 2a (nrpd2a) and Suppressor of Gene Silencing 3 (sgs3). **(Source: Pengcheng Zhang, 2024)**

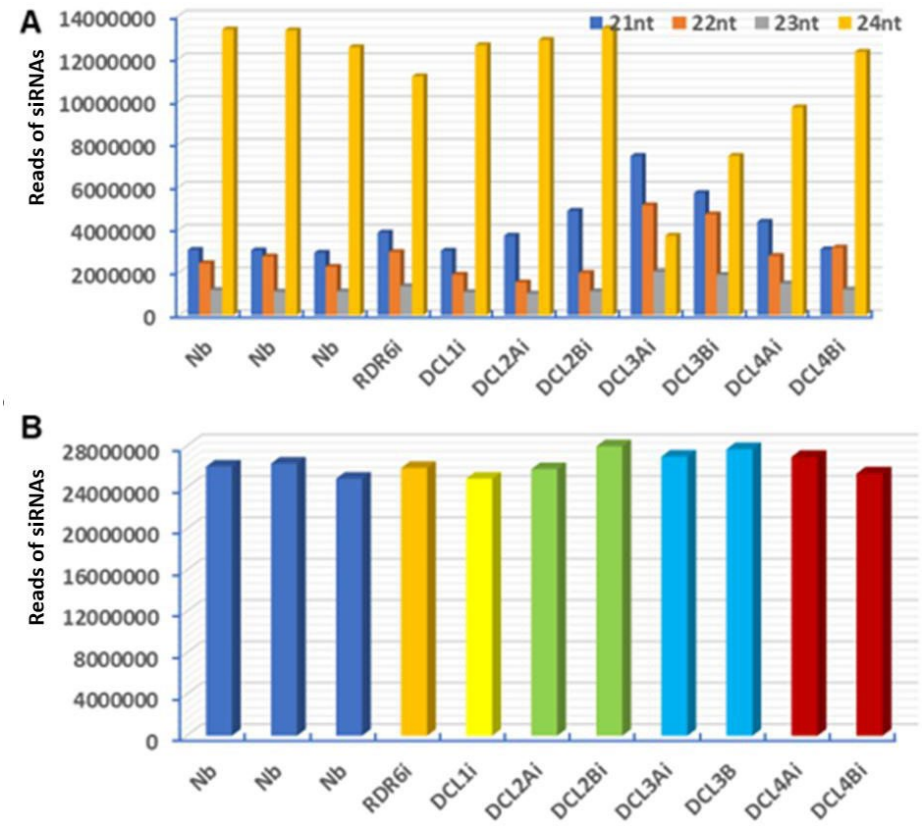

Figure 5.1 Total small RNA reads from healthy control plants

A, Impact of *RDR6i* and *DCLi* on the accumulation of cellular 21-24 nt sRNAs. **B**, Impact of *RDR6i* and *DCLi* on the accumulation of total cellular 18-30 nt sRNAs. Leaf tissues were collected from healthy plants at the growth stage equivalent to those at 6 days post inoculation of ELVd. The 21-24 nucleotide (**A**) and total 18-30 nucleotide (**B**) Accumulations of siRNAs are indicated as colour bars. The reads of siRNAs are indicated in vertical axis in the figure. **(Source: Pengcheng Zhang, 2024)**

5.2.2 Impact of DCLi and RDR6i on cvd-siRNAs at the early stage of ELVd infection

ELVd is able to establish local infection in *N. benthamiana*. We assessed how DCLi and RDR6i affect the biogenesis of ELVd cvd-siRNA. To achieve this, we analyzed sRNA in leaf tissue samples from wild-type Nb, DCLi, and RDR6i plants, which were in early stage of ELVd infection at 6 dpi. In these ELVd-infected Nb and RNAi plants, the 21, 22, and 24 nt siRNAs that were mapped to individual RNA silencing pathway genes (Table 5.2) and the total 18-30 nt sRNA profile (Figure 5.2 A and B) were similar to those found in healthy controls (Figure 5.1 A and B; Table 5.1). These results suggest that ELVd infection per se has no significant effect on transgenic RNAi knockdown of DCLs and RDR6.

Table 5.2 Impact of ELVd early infection on 21-24 nt sRNAs mapped to RNAi pathway genes

	Mock	ELVd								
	Nb	Nb	Nb	RDR6i	DCL1i	DCL2Ai	DCL2Bi	DCL3Ai	ECL3Bi	DCL4Ai	DCL4Bi
RNAigene-DCL1	8	2	130	20	**22494**	5	6	6	9	5	8
RNAigene-DCL2	843	243	381	37	505	**359833**	**373104**	210	284	23	71
RNAigene-DCL3	5	0	0	8	35	0	0	**78432**	**35983**	3	6
RNAigene-DCL4	5	8	23	6	5	6	7	78	5	**70974**	**79745**
RNAigene-Seq5	1	0	2	1	1	1	0	1	0	1	0
RNAigene-Seq6	3	0	4	3	2	5	5	0	4	4	1
RNAigene-Seq7	3	2	2	4	2	4	2	0	1	1	1
RNAigene-Seq8	2	1	2	2	0	2	0	0	1	1	0
RNAigene-Seq9	1	0	0	1	0	1	0	0	0	0	0
RNAigene-Seq10	1	0	1	1	0	0	1	3	0	0	0
RNAigene-Seq11	3	3	1	1	1	0	0	2	1	0	3
RNAigene-Seq12	0	0	2	2	0	2	0	1	0	1	0
RNAigene-Seq13 (RDR6)	83	1	4	**144970**	8	6	9	10	8	10	17
RNAigene-Seq14	10	6	8	13	10	4	6	9	3	9	10
RNAigene-Seq15	10	9	9	17	6	9	7	9	7	12	12
RNAigene-Seq16	32	26	18	1	27	9	9	15	11	273	171
RNAigene-Seq17	3	0	0	0	2	2	2	0	0	1	0
RNAigene-Seq18	3	8	3	12	3	5	5	4	1	3	2
RNAigene-Seq19	1	4	3	4	7	4	5	5	2	7	5
RNAigene-Seq20	1	2	0	1	1	1	2	1	0	0	3
RNAigene-Seq21	2	1	2	0	2	0	0	0	0	0	0
RNAigene-Seq22	3	0	4	1	2	0	0	2	2	4	3
RNAigene-Seq23	3	2	1	0	0	1	0	0	0	0	0
RNAigene-Seq24	0	0	0	4	1	5	4	4	0	2	1
RNAigene-Seq25	2	0	2	0	1	3	1	1	3	0	1
RNAigene-Seq26	0	2	0	1	0	0	2	0	0	0	0
RNAigene-Seq27	2	1	1	1	0	1	0	2	0	1	2
RNAigene-Seq28	3	1	4	6	3	2	1	1	3	0	1
RNAigene-Seq29	0	0	1	1	1	4	0	0	3	3	1
RNAigene-Seq30	1	2	1	2	4	3	0	3	0	4	2
RNAigene-Seq31	7	2	2	3	4	7	2	3	2	1	6
RNAigene-Seq32	14	3	9	1	6	1	2	4	3	8	4
RNAigene-Seq33	0	1	0	3	1	1	1	0	1	1	2

Note: Sequences for all *Nicotiana benthamiana* RNAi genes can be found in Chen et al., 2018. Besides RNAigene DCL1-4, other RNAigenes from Seq5 to Seq33 in order are dsRNA binding protein 1 (drb1); dsRNA binding protein 2a (drb2a); dsRNA binding protein 2b (drb2b); dsRNA binding protein 3 (drb3); dsRNA binding protein 4 (drb4); dsRNA binding protein 5 (drb5); RNA-dependent RNA-polymerase 1 (rdr1); RNA-dependent RNA-polymerase 2 (rdr2); RNA-dependent RNA-polymerase 6 (rdr6); Argonaute 1a (ago1a); Argonaute 1b (ago1b); Argonaute 2 (ago2); Argonaute 4a (ago4a); Argonaute 4b (ago4b); Argonaute 5 (ago5); Argonaute 6 (ago6); Argonaute 7 (ago7); Argonaute 10 (ago10); Chromomethylase 3a (cmt3a); Chromomethylase 3b (cmt3b); Defective in RNA-Directed DNA Methylation 1 (drd1); Domains Rearranged Methyltransferase 3 (drm3); HUA Enhancer 1 (hen1), Hast1; Methyltransferase 1 (met1); Nuclear RNA Polymerase D 1a (nrpd1a); Nuclear RNA Polymerase D 1b (nrpd1b); Nuclear RNA Polymerase D 2a (nrpd2a) and Suppressor of Gene Silencing 3 (sgs3). **(Source: Pengcheng Zhang, 2024)**

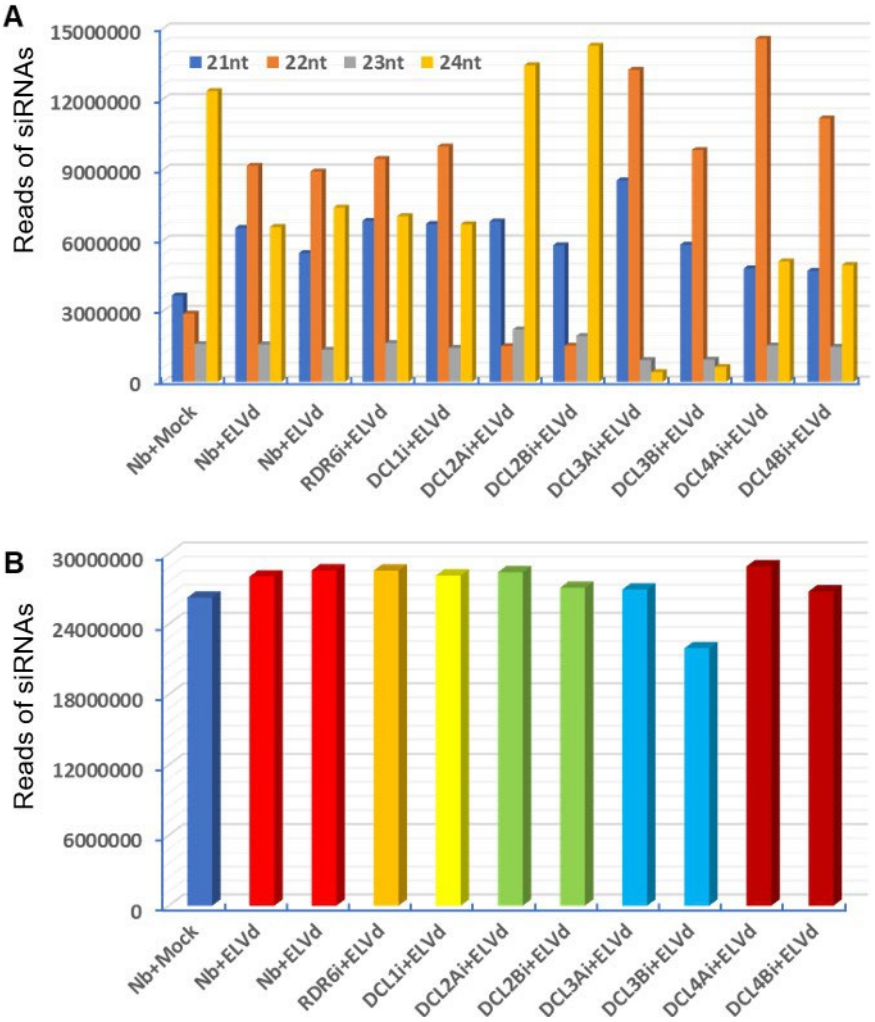

Figure 5.2 Impact of ELVd early infection on cellular small RNA accumulation **A**, Impact of ELVd on the accumulation of cellular 21-24 nt sRNAs in different genetic background *Nb* plants at 6 dpi. **B**, Impact of ELVd on the accumulation of total cellular 18-30 nt sRNAs in different genetic background *Nb* plants at 6 dpi. The 21-24 nucleotide (**A**) and total 18-30 nucleotide (**B**) Accumulations of siRNAs are indicated as colour bars. The reads of siRNAs are indicated in vertical axis in the figure. **(Source: Pengcheng Zhang, 2024)**

We further investigated the effects of DCLi and RDR6i on 21, 22, and 24 nt cvd-siRNAs that were specifically mapped to the ELVd 333 nt RNA genome (NC_039241.1; Figure 5.3 A-L). The size map shows several distinct features of the ELVd cvd-siRNAs. First, the overall numbers of sense (+) and antisense (-) 21, 22, and 24 nt cvd-siRNAs were similar in Nb (Figure 5.3 B, C and L), RDR6i (Figure 5.3 D and L) and all DCLi (Figure 5.3 E-L) plants, although a slight decrease in cvd-siRNAs was seen in DCL2Ai (Figure 5.3 A and L). The number of cvd-siRNAs in healthy Nb controls was almost zero

compared to each ELVd-infected plant (Figure 5.3 A and L), indicating that non-infected plants are unlikely to contain cvd-siRNAs. Second, the most and least abundant cvd-siRNAs in ELVd-infected Nb plants were 22 and 21 nt in length, respectively, with 24 nt cvd- siRNAs were in between (Figure 5.3 B, C and L). The 23 nt sRNA reads were consistently low in all infected plants and were not specifically associated with RDR6 or any DCLs. Third, similar size distributions of 21, 22, and 24 nt cvd-siRNAs and their actual reads were found in Nb, RDR6i, DCL1i, DCL4Ai and DCL4Bi plants (Figure 5.3 B-E and J-K), suggesting that RDR6, DCL1 and DCL4 are not specifically involved in cvd-siRNA biogenesis during the early stages of ELVd infection. Fourth, in DCL2Ai and DCL2Bi, the 22 nt cvd-siRNAs of ELVd were reduced to very low levels, but the 24 nt cvd-siRNAs were significantly increased, while the 21 nt cvd-siRNAs were also reduced less at 6 dpi (Figure 5.3 F, G and L).

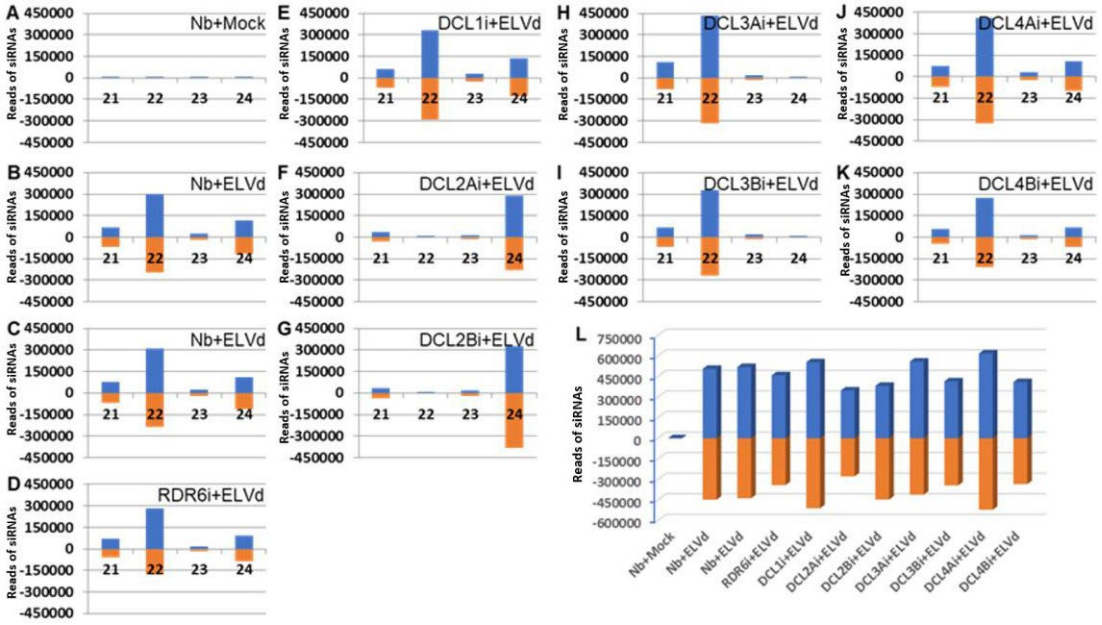

Figure 5.3 Impact of RDR6i or DCLi on accumulation of ELVd 21-24 nt cvd-siRNAs at early stage of infection (Source: Pengcheng Zhang, 2024)

A, Mock inoculation of *N. benthamiana* (*Nb*). **B** and **C**, *Nb* infected with ELVd. **D**, *RDR6i* infected with ELVd. **E** to **K**, *DCLi* infected with ELVd. *DCL1i* (**E**), *DCL2Ai* and *DCL2Bi* (**F** and **G**); *DCL3Ai* and *DCL3Bi* (**H** and **I**); *DCL4Ai* and *DCL4Bi* (**J** and **K**). **L**, Total numbers of 21-24 nt cvd-siRNAs mapped to ELVd. Mock-inoculated or ELVd-infected leaf tissues were collected at 6 days' post inoculation for sRNA analysis. Size profiles are shown for 21-24 nt cvd-siRNAs that were mapped to the ELVd RNA genome of both sense (blue) and complementary-sense (orange) strands. The 21-24 nucleotide (**A-K**) and total 21-24 nucleotide (**L**) Accumulations of siRNAs are indicated as colour bars. The reads of siRNAs are indicated in vertical axis in the figure.

As shown in Figure 5.4 A-K, at 6 days post inoculation, 21-24nt cvd-siRNAs were mapped to the ELVd RNA genome of both sense and complementary-sense strands. DCLi and RDR6i had no significant difference on the distribution of 21, 22, and 24 nt cvd-siRNAs across the two +/- RNA strands of the ELVd RNA genome (Figure 5.4 A-K). Many of the hotspots in Figure 5.4 A-K remained the same or similar across all RNAi systems, implying that hotspots may be intrinsic to RNA structure.

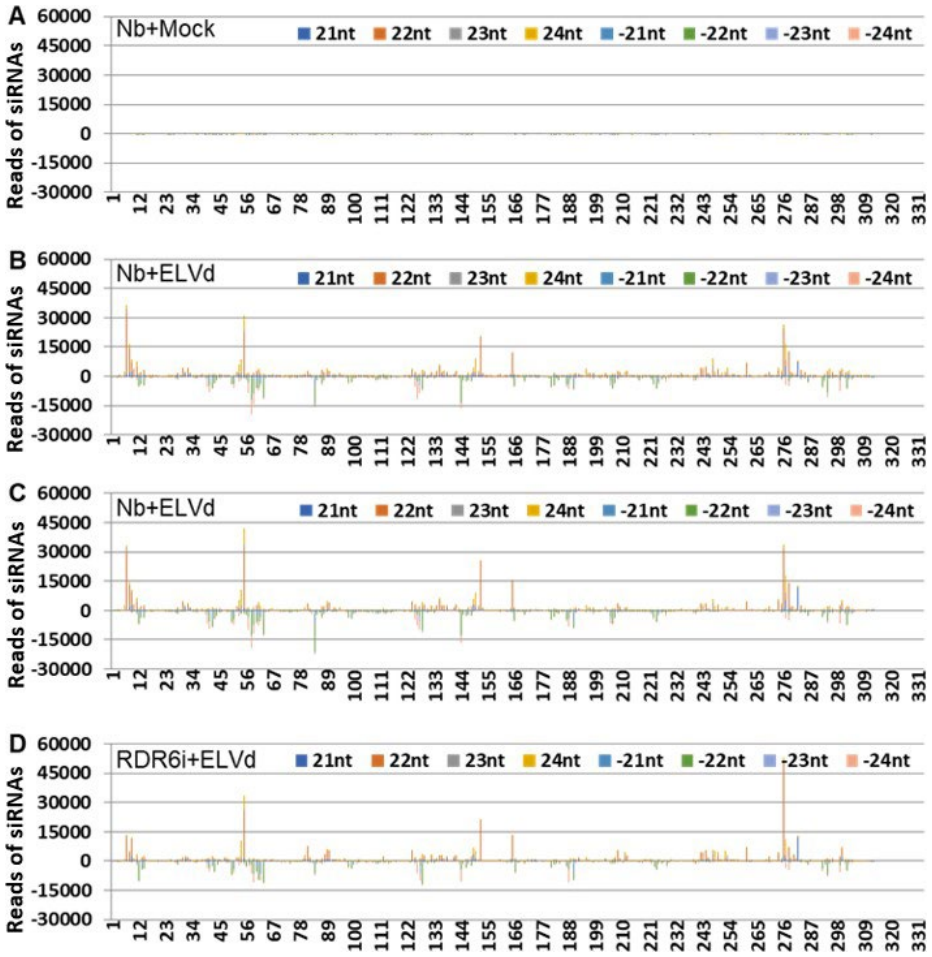

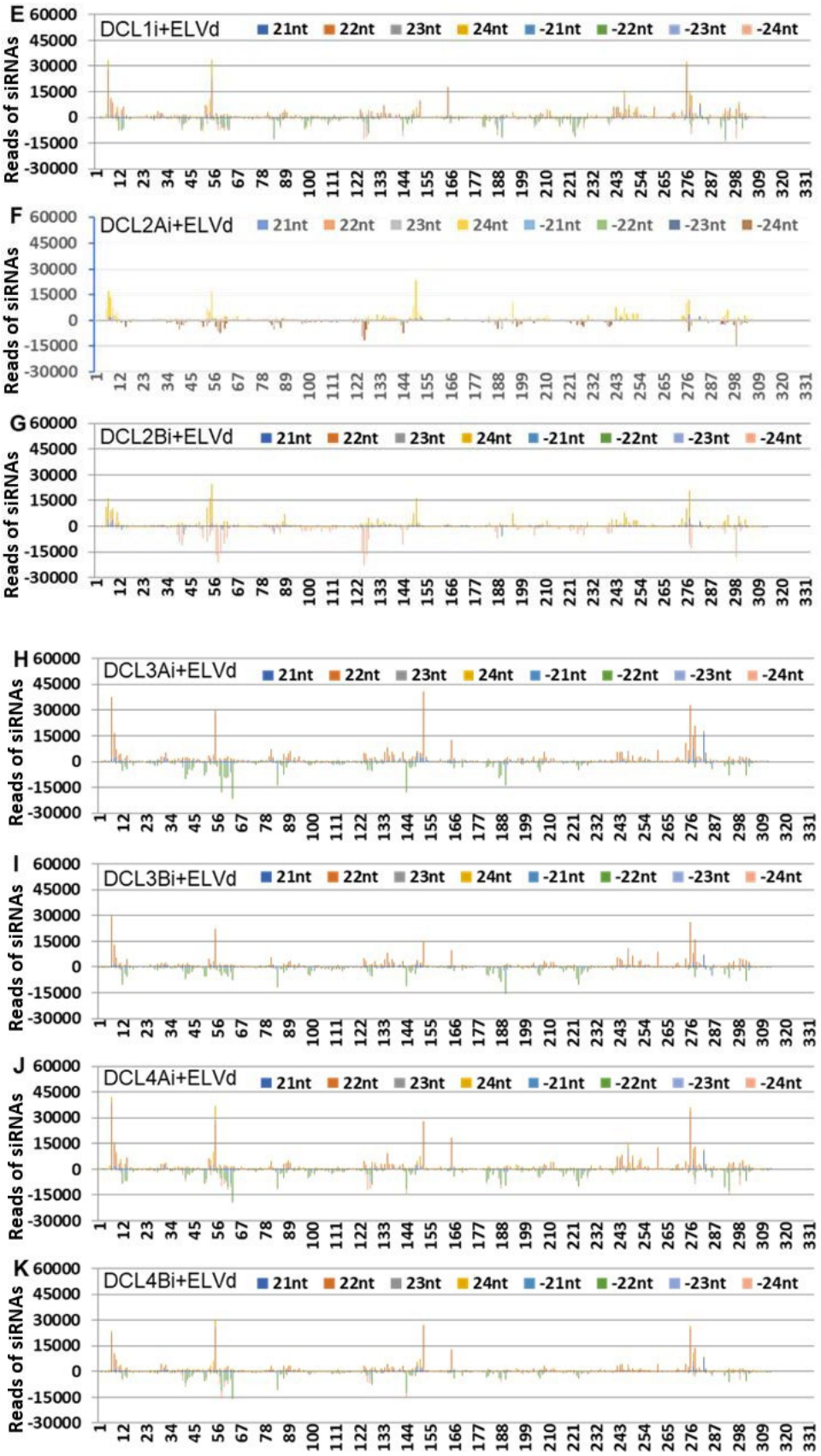

Figure 5.4 Distribution of 21-24 nt cvd-siRNA at early stage of infection across the ELVd RNA genome

A mock inoculation of *N. benthamiana* (*Nb*). **B** and **C**, *Nb* infected with ELVd. **D**, *RDR6i* infected with ELVd. **E** to **K**, *DCLi* infected with ELVd. *DCL1i* (**E**), *DCL2Ai* and *DCL2Bi* (**F** and **G**); *DCL3Ai* and *DCL3Bi* (**H** and **I**); *DCL4Ai* and *DCL4Bi* (**J** and **K**). Mock-inoculated or ELVd-infected leaf tissues were collected at 6 days post-inoculation for sRNA analysis. 21-24nt cvd-siRNAs were mapped to the ELVd RNA genome of both sense and complementary-sense strands. Colour codes for each size of cvd-siRNAs and their polarities are indicated in each panel. The 21-24 nt (**A-K**) Accumulations of siRNAs across ELVd RNA genome are indicated as colour bars. The reads of siRNAs are indicated in vertical axis in the figure. **(Source: Pengcheng Zhang, 2024)**

5.2.3 Impact of *DCL*i and *RDR6*i on cvd-siRNA at the later stage of ELVd infection

In a similar experimental setting, we assayed EVLd RNA and performed sRNA analysis on leaf samples from wild-type Nb and RNAi plants at 14 dpi (the later stage of ELVd infection). The results showed that the impacts of DCLi and RDR6i on cvd-siRNA biogenesis are similar to these in the early infection stage (Figure 5.2 A and B). In these ELVd-infected Nb and transgenic plants, the total sRNA profile (Figure 5.5 A and B) and the 21, 22, and 24 nt siRNAs that were mapped to individual RNA silencing pathway genes (Table 5.3) were similar to those found in healthy controls (Figure 5.1 A and B; Table 5.1).

Table 5.3 Impact of ELVd later infection on 21-24nt sRNAs mapped to RNAi pathway genes

	Mock	ELVd								
	Nb-Mock	Nb1	Nb2	NbRDR6i	NbDCL1i	NbDCL2Ai	NbDCL2Bi	NbDCL3Ai	NbDCL3Bi	NbDCL4Ai	NbDCL4Bi
RNAigene-DCL1	16	7	252	6	9536	17	10	15	7	16	7
RNAigene-DCL2	892	941	1133	434	2342	155765	630439	894	1814	919	212
RNAigene-DCL3	53	5	5	4	10	12	80	66783	24584	118	3
RNAigene-DCL4	5	12	16	48	9	5	11	14	66	12690	33748
RNAigene-Seq5	1	0	0	1	1	0	1	0	0	0	0
RNAigene-Seq6	0	0	4	2	3	0	1	1	6	3	2
RNAigene-Seq7	0	0	1	0	1	0	0	1	4	3	1
RNAigene-Seq8	0	2	3	1	2	0	1	1	1	1	2
RNAigene-Seq9	1	2	2	0	0	1	1	0	1	0	2
RNAigene-Seq10	0	0	1	1	1	0	1	0	1	0	0
RNAigene-Seq11	1	0	3	1	2	3	1	1	4	2	1
RNAigene-Seq12	1	2	6	1	4	0	0	1	2	2	3
RNAigene-Seq13 (RDR6)	56	164	40	124533	11	5	12	13	18	209	15
RNAigene-Seq14	11	10	10	9	13	5	9	4	9	13	3
RNAigene-Seq15	8	6	5	13	17	5	8	3	2	13	9
RNAigene-Seq16	22	58	74	16	94	8	9	72	71	437	296
RNAigene-Seq17	8	0	2	1	0	1	0	0	0	2	5
RNAigene-Seq18	1	5	11	14	9	10	3	2	6	5	10
RNAigene-Seq19	2	3	4	6	5	0	3	2	7	12	3
RNAigene-Seq20	0	0	1	3	0	0	0	0	2	1	0
RNAigene-Seq21	1	0	0	0	1	1	1	0	1	1	1
RNAigene-Seq22	4	4	2	0	4	2	0	2	2	4	3
RNAigene-Seq23	5	0	1	2	0	0	1	1	1	1	0
RNAigene-Seq24	0	2	0	3	0	1	1	1	0	0	3
RNAigene-Seq25	7	2	1	3	2	1	2	1	1	3	2
RNAigene-Seq26	2	0	0	0	0	2	0	1	1	2	0
RNAigene-Seq27	2	1	1	3	1	2	0	0	0	1	2
RNAigene-Seq28	1	0	0	6	1	3	2	3	4	0	1
RNAigene-Seq29	0	1	1	7	0	0	0	1	0	0	2
RNAigene-Seq30	1	1	7	2	3	0	4	4	1	0	4
RNAigene-Seq31	2	4	3	2	4	6	5	3	3	3	5
RNAigene-Seq32	7	11	10	7	5	9	1	6	3	4	8
RNAigene-Seq33	1	0	1	2	2	0	1	3	1	2	0

Note: Sequences for all *Nicotiana benthamiana* RNAi genes can be found in Chen et al., 2018. Besides RNAigene DCL1-4, other RNAigenes from Seq5 to Seq33 in order are dsRNA binding protein 1 (drb1); dsRNA binding protein 2a (drb2a); dsRNA binding protein 2b (drb2b); dsRNA binding protein 3 (drb3); dsRNA binding protein 4 (drb4); dsRNA binding protein 5 (drb5); RNA-dependent RNA-polymerase 1 (rdr1); RNA-dependent RNA-polymerase 2 (rdr2); RNA-dependent RNA-polymerase 6 (rdr6); Argonaute 1a (ago1a); Argonaute 1b (ago1b); Argonaute 2 (ago2); Argonaute 4a (ago4a); Argonaute 4b (ago4b); Argonaute 5 (ago5); Argonaute 6 (ago6); Argonaute 7 (ago7); Argonaute 10 (ago10); Chromomethylase 3a (cmt3a); Chromomethylase 3b (cmt3b); Defective in RNA-Directed DNA Methylation 1 (drd1); Domains Rearranged Methyltransferase 3 (drm3); HUA Enhancer 1 (hen1), Hast1; Methyltransferase 1 (met1); Nuclear RNA Polymerase D 1a (nrpd1a); Nuclear RNA Polymerase D 1b (nrpd1b); Nuclear RNA Polymerase D 2a (nrpd2a) and Suppressor of Gene Silencing 3 (sgs3). **(Source: Pengcheng Zhang, 2024)**

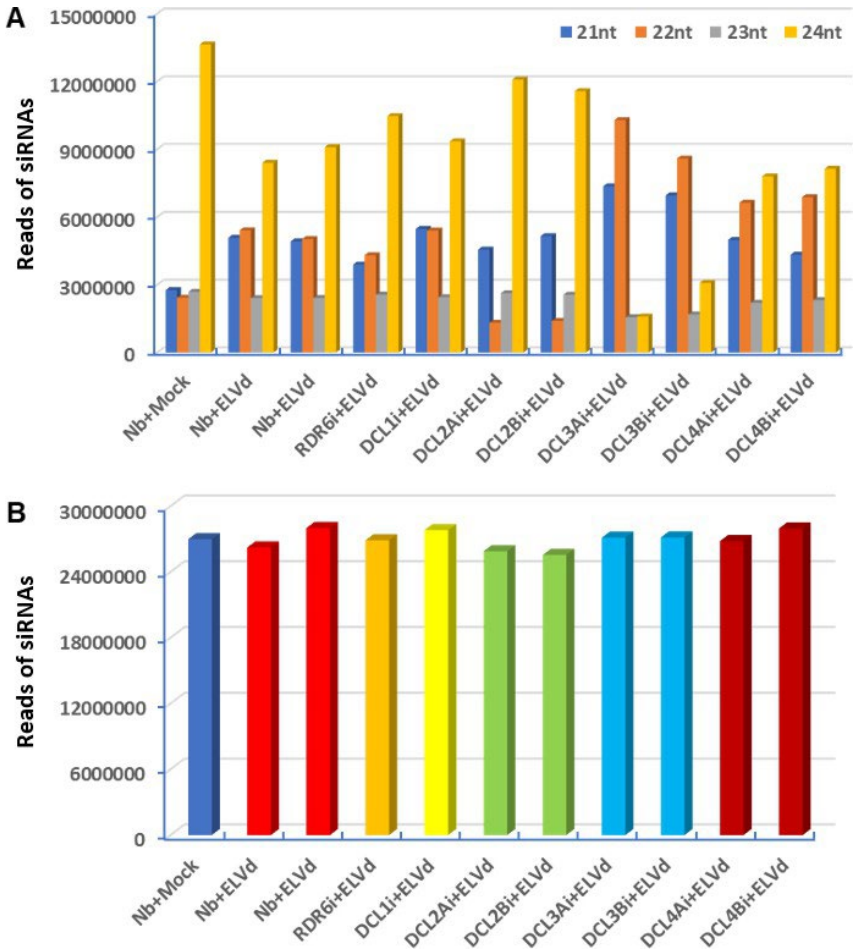

Figure 5.5 Impact of ELVd later infection on cellular small RNA accumulation

A, Impact of ELVd on the accumulation of cellular 21-24 nt sRNAs in different genetic

background *Nb* plants at 14 dpi. **B**, Impact of ELVd on the accumulation of total cellular 18-30 nt sRNAs in different genetic background *Nb* plants at 14 dpi. The 21-24 nucleotide (**A**) and total 18-30 nucleotide (**B**) Accumulations of siRNAs are indicated as colour bars. The reads of siRNAs are indicated in vertical axis in the figure.

(Source: Pengcheng Zhang, 2024)

The size distribution of 21, 22, and 24 nt cvd-siRNAs in Nb or RNAi strains and their distribution in the ELVd genome (Figure 5.6 A-L; Figure 5.7 A-K) was largely similar to that found at 6 dpi (Figure 5.3 A-L, Figure 5.4 A-K). However, we noted some dynamic changes in the total number of 21, 22, and 24 nt cvd-siRNAs in the later stages of ELVd infection. Compared to Nb plants (Figure 5.6 B, C and L), there were significantly fewer ELVd cvd-siRNAs in RDR6i (Fig. 4D and L), whereas production of cvd-siRNAs was increased at 14 dpi in both DCL3i (Figure 5.6 H, I and L) and DCL4i plants (Figure 5.6 J-L).

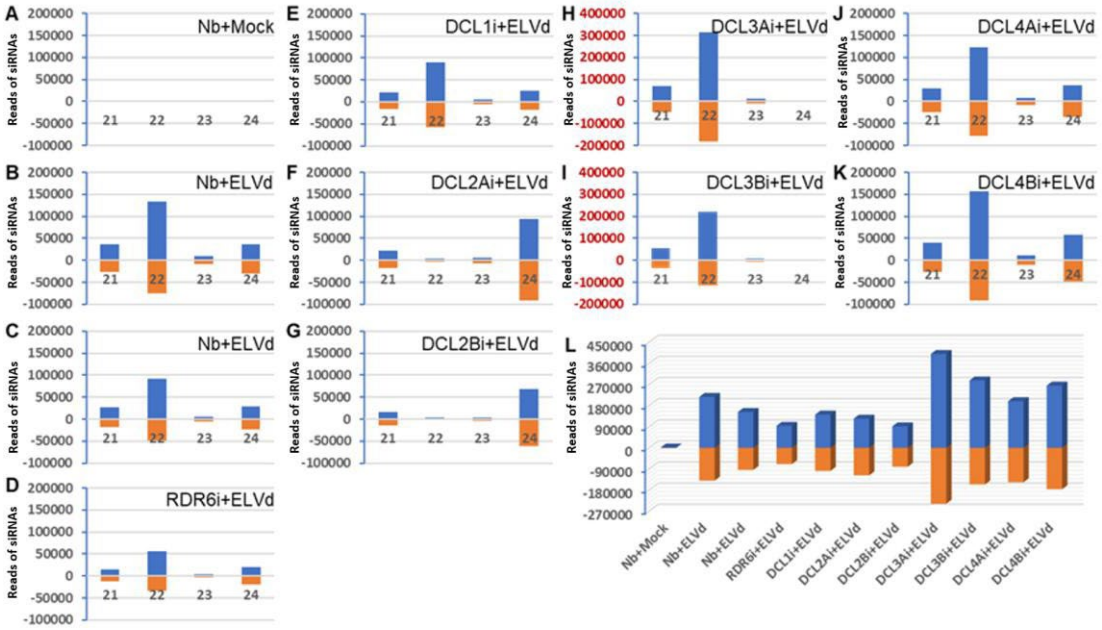

Figure 5.6 Impact of RDR6i or DCLi on accumulation of ELVd 21-24 nt cvd-siRNAs at later stage of infection

A, Mock inoculation of *N. benthamiana* (*Nb*). **B** and **C**, *Nb* infected with ELVd. **D**, *RDR6i* infected with ELVd. **E** to **K**, *DCLi* infected with ELVd. *DCL1i* (**E**), *DCL2Ai* and *DCL2Bi* (**F** and **G**); *DCL3Ai* and *DCL3Bi* (**H** and **I**); *DCL4Ai* and *DCL4Bi* (**J** and **K**). **L**, Total numbers of 21-24 nt cvd-siRNAs mapped to ELVd. Mock-inoculated or ELVd-infected leaf tissues were collected at 14 days' post inoculation for sRNA analysis. Size profiles are shown for 21-24 nt cvd-siRNAs that were mapped to the ELVd RNA genome of both sense (blue) and complementary-sense (orange) strands. The 21-24 nucleotide

(**A-K**) and total 21-24 nucleotide (**L**) Accumulations of siRNAs are indicated as colour bars. The reads of siRNAs are indicated in vertical axis in the figure. **(Source: Pengcheng Zhang, 2024)**

As shown in Figure 5.7 A-K. Mock-inoculated or ELVd-infected leaf tissues were collected at 14 dpi for sRNA analysis. 21-24nt cvd-siRNAs were mapped to the ELVd RNA genome of both sense and complementary-sense strands. DCLi and RDR6i had no significant difference on the distribution of 21, 22, and 24 nt cvd-siRNAs across the two +/- RNA strands of the ELVd RNA genome (Figure 5.7 A-K). Many of the hotspots in Figure 5.7 A-K remained the same or similar across all RNAi systems, implying that hotspots may be intrinsic to RNA structure.

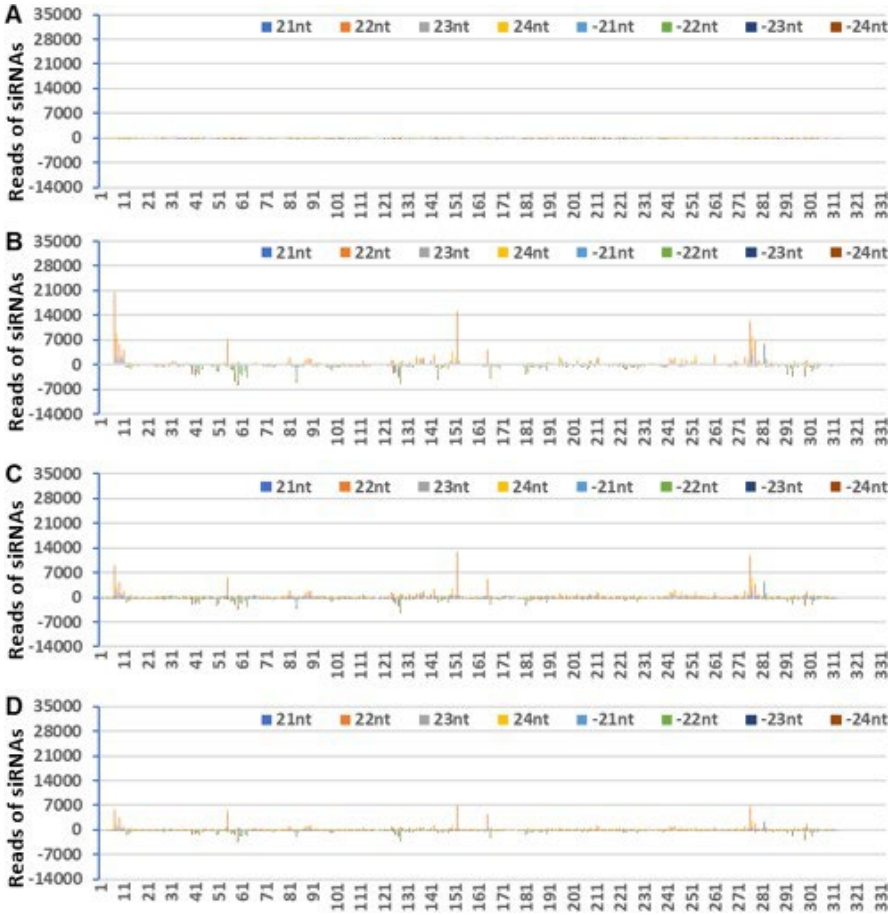

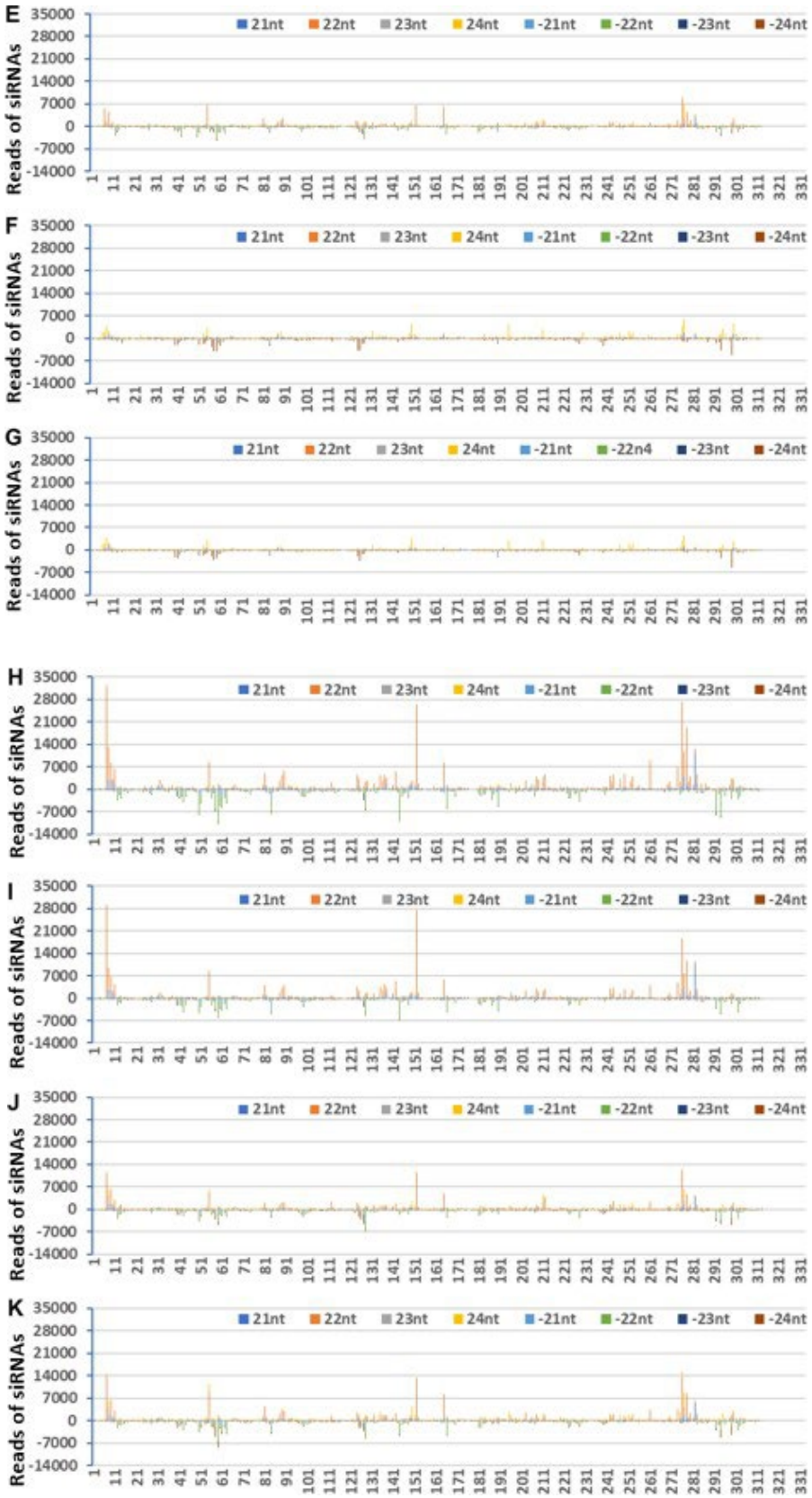

Figure 5.7 Distribution of 21-24 nt cvd-siRNA associated with later infection across ELVd genome

A, Mock inoculation of *Nb*. **B** and **C**, *Nb* infected with ELVd. **D**, *RDR6i* infected with

ELVd. **E** to **K**, *DCLi* infected with ELVd. *DCL1i* (**E**), *DCL2Ai* and *DCL2Bi* (**F** and **G**); *DCL3Ai* and *DCL3Bi* (**H** and **I**); *DCL4Ai* and *DCL4Bi* (**J** and **K**). Mock-inoculated or ELVd-infected leaf tissues were collected at 14 days post-inoculation for sRNA analysis. 21-24 nt cvd-siRNAs were mapped to the ELVd RNA genome of both sense and complementary-sense strands. Color codes for each size of cvd-siRNAs and their polarities are indicated in each panel. The 21-24 nt (**A-K**) Accumulations of siRNAs across ELVd genome are indicated as colour bars. The reads of siRNAs are indicated in vertical axis in the figure. **(Source: Pengcheng Zhang, 2024)**

5.2.4 Effect of ELVd infection on microRNA biogenesis at the early and late stages of ELVd infection

Analysis of the wild-type *N. benthamiana* and the transgenic lines *DCL1i, DCL2Ai, DCL2Bi, DCL3Ai, DCL3Bi, DCL4Ai, DCL4Bi* and *RDR6i* showed that DCLs or RDR6 mRNAs were specifically targeted and the DCLs or RDR6 mRNA degradation with the abundant sRNAs accumulation specific to 21, 22 and 24 nt siRNAs for each gene. Furthermore, RDR6i had no effect on the size of 21, 22 and 24 nt siRNAs, whereas DCL2i, DCL3i, and DCL4i reduced the production of 22, 24 or 21 nt siRNAs in host cells, respectively. Only DCL1i reduced microRNA reads (Table 5.4; Figure 5.8). These results are consistent with our previous reports (Qin et al., 2017; Chen et al., 2018), and further validate the applicability of the DCLi and RDR6i lines suggested in the previous studies. We also examined the effect of ELVd infection on microRNA biogenesis during the early and late stages of ELVd infection.

Table 5.4 Impact of DCLi and RDR6i on microRNA biosynthesis in healthy plants

(Source: Pengcheng Zhang, 2024)

miRNA	Sequence	Nb	Nb	Nb	RDR6i	DCL1i	DCL2Ai	DCL2Bi	DCL3Ai	DCL3Bi	DCL4Ai	DCL4Bi
>miR-157-156-Natt-EU475993	TTGACAGAAGATAGAGAGC	628	247	153	247	171	315	542	589	524	294	524
>miR-157-156-Natt-EU475994	TTGACAGAAGATAGAGAGCAC	582	212	132	220	163	289	493	532	467	269	480
>miR-159-Natt-EU475975	TTTGGATTGAAGGGAGCTCT	162582	231193	152354	119468	31924	211527	155447	268152	232309	161619	209850
>miR-159-Natt-EU475980	TTGGATTGAAGGGAGCTCT	164436	234011	154363	121000	32378	213936	157340	271100	234716	163208	212097
>miR-159-Natt-EU475990	TTTGGATTGAAGGGAGCTC	162907	231675	152656	119759	32002	211899	155739	268610	232652	161905	210171
>miR-159-Natt-EU475991	TTTGGATTGAAGGGAGCTCC	55	49	62	42	3	79	41	56	44	48	46
>miR-159-Natt-EU475995	TTTGGATTGAAGGGAGCTCTT	1291	1396	1230	1102	367	1259	1185	1440	1435	1416	1131
>miR-160-Natt-EU475999	TGCCTGGCTCCCTGTATGCC	22976	27926	29279	29457	16963	27668	24366	33422	15617	22245	40264
>miR-162-Natt-EU475983	TCGATAAACCTCTGCATCC	4274	3831	5228	4670	1664	4361	3655	6857	6068	7581	7378
>miR-164-Natt-EU475970	TGGAGAAGCAGGGCACGTGC	26217	47346	31101	10068	8548	31210	34025	54827	26521	46123	19161
>miR-164-Natt-EU475987	TGGAGAAGCAGGGCACGTG	26271	47455	31184	10105	8568	31307	34099	54940	26592	46239	19207
>miR-166-Natt-EU475978	TCGGACCAGGCTTCATTCCCC	177421	316216	230126	287627	158638	224279	214404	272254	236299	216801	274499
>miR-166-Natt-EU476005	TCGGACCAGGCTTCATTCCT	57136	88246	73554	95938	59519	87244	59635	139810	102087	109461	101029
>miR-167-Natt-EU475969	TGAAGCTGCCAGCATGATCT	22803	25335	33135	20968	20151	19379	24290	52632	23824	22107	27371
>miR-167-Natt-EU475977	TGAAGCTGCCAGCATGATCTGG	2034	1458	1329	1434	798	1328	2448	1729	1588	766	3119
>miR-167-Natt-EU475998	TGAAGCTGCCAGCATGATCTG	2465	1916	1607	1813	1166	1683	2902	2284	2036	1074	3619
>miR-168-Natt-EU475968	TCGCTTGGTGCAGGTCGGG	41096	75295	53622	61002	70993	56325	57401	120898	93896	89059	101494
>miR-168-Natt-EU476004	TCGCTTGGTGCAGGTCGG	41189	75443	53761	61163	71125	56449	57523	121270	94149	89257	101708
>miR-169-Natt-EU475985	CAGCCAAGGATGACTTGCCG	42	54	49	60	29	19	62	158	125	63	120
>miR-169-Natt-EU475997	TAGCCAAGGATGACTTGCCT	103	271	41	205	15	24	121	194	270	39	268
>miR-169-Natt-EU476001	AGCCAAGGATGACTTGCCGG	2	2	3	1	0	4	2	5	1	1	5
>miR-171-Natt-EU475989	TTGAGCCGTGCCAATATCACG	25061	28557	30170	27551	9426	32377	38164	31954	35779	10097	40745
>miR-172-Natt-EU476003	GGAATCTTGATGATGCTGC	8	14	26	2	2	25	4	8	7	4	6
>miR-319-Natt-EU475996	CTTGGACTGAAGGGAGCTCCC	2	60	83	10	4	261	14	16	7	5	34
>miR-396-Natt-EU475972	TTCCACAGCTTTCTTGAACT	39100	29159	18934	35508	28013	19430	47101	44951	37742	27682	52425
>miR-396-Natt-EU475973	TTCCACAGCTTTCTTGAACTG	1388	700	624	1029	1411	1066	1532	1717	980	1833	2168
>miR-396-Natt-EU475974	TTCCACAGCTTTCTTGAACTT	36879	27892	17986	33730	25982	17832	44531	42139	35899	25045	49125
>miR-396-Natt-EU475979	TTCCACAGCTTTCTTG	39300	29285	19035	35726	28243	19552	47345	45255	37916	27888	52710
>miR-396-Natt-EU476002	CCACAGCTTTCTTGAACT	39769	29657	19263	36067	28499	19754	48087	45677	38216	28048	53090
>miR-397-Natt-EU475965	ATTGAGTGCAGCGTTGATG	19230	7110	15298	11638	10005	15120	32732	33009	23412	11876	5817
>miR-397-Natt-EU475992	TCATTGAGTGCAGCGTTGATG	10099	3648	6289	7530	5319	6718	17644	16548	10911	4538	3298
>miR-403-Natt-EU475984	TTAGATTCACGCACAAACTCG	930	669	1068	497	233	1095	1959	991	1042	273	1976
>miR-403-Natt-EU475988	TTAGATTCACGCACAAACTC	1103	823	1278	583	275	1273	2350	1190	1209	318	2272
>miR-408-Natt-EU475986	TGCACTGCCTCTTCCCTGG	6922	3042	8052	8531	7479	9387	10264	19121	9557	19865	3909
>miR-894-Natt-EU475966	CACGTCGGGTTCACC	5681	5338	9783	10336	4834	12131	8743	11172	11501	15117	5114
>miR-894-Natt-EU475967	TCACGTCGGGTTCACC	5673	5327	9767	10314	4828	12111	8739	11168	11489	15107	5110
>miR-894-Natt-EU475971	TTCACGTCGGGTTCACC	5653	5289	9723	10239	4792	12075	8711	11124	11450	15053	5092
>miR-894-Natt-EU475976	TCACGTCGGGTTCAC	5685	5335	9781	10326	4842	12130	8749	11179	11506	15127	5127
>miR-894-Natt-EU475981	TTCACGTCGGGTTCAC	5665	5297	9737	10251	4806	12094	8721	11134	11467	15073	5109
>miR-894-Natt-EU475982	CGTTTCACGTCGGGTTCACC	2969	1827	5252	2506	1693	6235	6364	5536	7539	8290	2552
>miR-894-Natt-EU476000	TTTCACGTCGGGTTCACC	4005	3009	6981	4969	2706	8483	7411	7939	9918	11915	3662

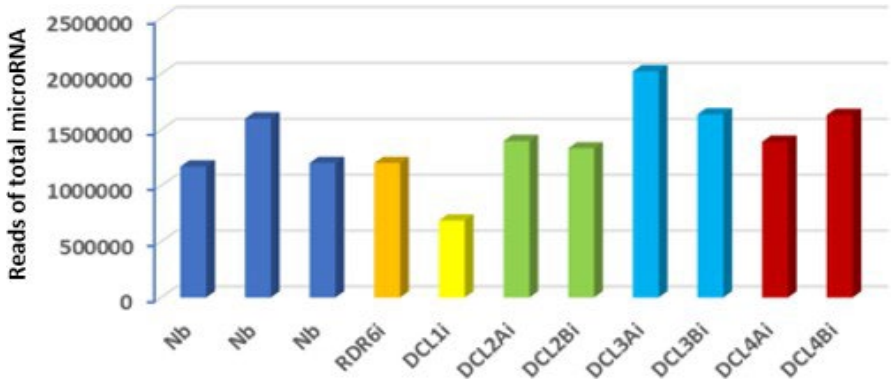

Figure 5.8 Total microRNA reads from healthy control plants. Impact of RDR6i and DCLi on accumulation of cellular microRNAs

Leaf tissues were collected from healthy plants at the growth stage equivalent to those at 6 dpi. The total microRNAs are indicated as colour bars and the reads of total microRNA are indicated in vertical axis in the figure. **(Source: Pengcheng Zhang, 2024)**

In this study, DCL1 was showed not being specifically associated with ELVd cvd-siRNA production and there are no reports of microRNA-mediated antiviral resistance, although it is suggested that cellular microRNAs produced by DCL1 play an important

role in plant defense against pathogens, including plant viroids (Simon-Mateo and Garcia, 2006; Liu et al., 2017). To further verify these suggestions, we analyzed whether ELVd infection affects cellular microRNA biogenesis, and the results are showed in Figure 5.9, Table 5.5 and Table 5.6. In the early stages of infection, ELVd resulted in a 64-90% reduction in total reads of 41 families of microRNAs in ELVd-infected plants compared to healthy wild-type Nb controls, both in wild-type plants and in plants lacking RDR6 and DCLs (Figure 5.9 A; Table 5.5). At late stages of infection, ELVd still resulted in a 21-49% reduction in total reads of 41 microRNAs in ELVd-infected Nb, RDR6i and DCLi plants compared to healthy wild-type Nb controls (Figure 5.9 B; Table 5.6). By investigating the effects produced by ELVd infection of *N. benthamiana* miRNAs, it was found that at 6 dpi of ELVd infection, the abundance of total reads of microRNAs in the examined Nb, RDR6i and DCLi plants was significantly reduced, interestingly, this effect was partially mitigated by the recovery at 14 dpi.

Table 5.5 Impact of ELVd early infection on microRNA biogenesis

(Source: Pengcheng Zhang, 2024)

miRNA	Sequence	mock	ELVd									
		Nb	Nb	Nb	RDR6i	DCLi	DCL2Ai	DCL2Bi	DCL3Ai	DCL3Bi	DCL4Ai	DCL4Bi
>miR-157-156-Natt-EU475993	TTGACAGAAGATAGAGAGC	1567	8680	8192	10480	3640	20052	9552	3166	5307	6567	7366
>miR-157-156-Natt-EU475994	TTGACAGAAGATAGAGAGCAC	1390	8425	7916	10161	3509	6269	9313	3045	5088	6331	7152
>miR-159-Natt-EU475975	TTTGGATTGAAGGGAGCTCT	168884	17447	24328	39920	29643	6261	36038	10137	23227	22835	20997
>miR-159-Natt-EU475980	TTGGATTGAAGGGAGCTCT	171282	17967	24958	41380	30202	32695	36817	10496	24069	23499	21720
>miR-159-Natt-EU475990	TTTGGATTGAAGGGAGCTC	169321	17501	24390	40047	29727	9898	36134	10168	23325	22897	21069
>miR-159-Natt-EU475991	TTTGGATTGAAGGGAGCTCC	69	11	6	35	13	5075	13	5	14	14	16
>miR-159-Natt-EU475995	TTTGGATTGAAGGGAGCTCTT	1000	125	201	276	132	6225	289	84	124	179	162
>miR-160-Natt-EU475999	TGCCTGGCTCCCTGTATGCC	18981	1537	2387	2039	179	11082	1147	1548	385	1420	1501
>miR-162-Natt-EU475983	TCGATAAACCTCTGCATCC	5387	639	739	1745	145	1434	780	354	201	543	810
>miR-164-Natt-EU475970	TGGAGAAGCAGGGCACGTGC	19336	3144	6290	11146	3005	9015	5379	2075	4635	4768	1960
>miR-164-Natt-EU475987	TGGAGAAGCAGGGCACGTG	19381	3148	6316	11171	3011	42341	5394	2075	4647	4773	1969
>miR-166-Natt-EU475978	TCGGACCAGGCTTCATTCCCC	129752	27121	40236	130991	16519	6278	52660	22253	21074	25692	44835
>miR-166-Natt-EU476005	TCGGACCAGGCTTCATTCCT	72904	4760	4689	24234	4155	960	7095	5040	3217	3862	8880
>miR-167-Natt-EU475969	TGAAGCTGCCAGCATGATCT	73615	8096	5877	12348	5036	146398	6439	5474	3615	6568	6104
>miR-167-Natt-EU475977	TGAAGCTGCCAGCATGATCTGG	6356	357	214	759	199	11250	317	208	124	244	291
>miR-167-Natt-EU475998	TGAAGCTGCCAGCATGATCTG	7749	442	277	936	237	43584	416	281	190	313	403
>miR-168-Natt-EU475968	TCGCTTGGTGCAGGTCGGG	111898	16143	24339	27695	10310	6242	27938	12668	7172	12645	24918
>miR-168-Natt-EU476004	TCGCTTGGTGCAGGTCGG	112037	16165	24358	27718	10319	4066	27962	12690	7191	12659	24946
>miR-169-Natt-EU475985	CAGCCAAGGATGACTTGCCG	184	66	49	55	40	927	73	110	75	59	131
>miR-169-Natt-EU475997	TAGCCAAGGATGACTTGCCT	185	179	202	203	36	2863	113	185	102	65	458
>miR-169-Natt-EU476001	AGCCAAGGATGACTTGCCGG	2	28	21	15	18	187	29	50	40	37	47
>miR-171-Natt-EU475989	TTGAGCCGTGCCAATATCACG	89412	5229	10767	28687	4436	4114	9761	5375	3584	6577	8324
>miR-172-Natt-EU476003	GGAATCTTGATGATGCTGC	10	1	1	24	3	5089	0	1	0	4	3
>miR-319-Natt-EU475996	CTTGGACTGAAGGGAGCTCCC	7	5	38	31	5	3452	18	15	5	5	25
>miR-396-Natt-EU475972	TTCCACAGCTTTCTTGAACT	62692	5917	4609	13294	5311	19556	7169	4224	2906	5734	8778
>miR-396-Natt-EU475973	TTCCACAGCTTTCTTGAACTG	4897	585	385	2242	835	42450	621	318	310	736	647
>miR-396-Natt-EU475974	TTCCACAGCTTTCTTGAACTT	55208	4829	3860	9950	4164	17	6168	3479	2317	4382	7410
>miR-396-Natt-EU475979	TTCCACAGCTTTCTTG	63086	5966	4650	13432	5356	11164	7233	4278	2954	5799	8862
>miR-396-Natt-EU476002	CCACAGCTTTCTTGAACT	63805	6037	4686	13519	5400	5232	7284	4295	2988	5832	8968
>miR-397-Natt-EU475965	ATTGAGTGCAGCGTTGATG	9632	8875	15602	18682	6299	4925	9486	9539	10388	14459	8723
>miR-397-Natt-EU475992	TCATTGAGTGCAGCGTTGATG	4430	3388	6081	7381	2461	303	3350	3835	3220	4218	3967
>miR-403-Natt-EU475984	TTAGATTCACGCACAAACTCG	8938	888	1212	2403	1230	77	965	1196	804	1103	1351
>miR-403-Natt-EU475988	TTAGATTCACGCACAAACTC	11136	1173	1563	3138	1457	1277	1224	1558	1049	1450	1746
>miR-408-Natt-EU475986	TGCACTGCCTCTTCCCTGG	2503	1042	1932	3377	907	1042	987	1727	1221	2149	1388
>miR-894-Natt-EU475966	CACGTCGGGTTCACC	4260	3986	2047	2699	1933	6241	3116	2318	2557	1470	7850
>miR-894-Natt-EU475967	TCACGTCGGGTTCACC	4255	3986	2041	2697	1932	4829	3115	2316	2554	1464	7835
>miR-894-Natt-EU475971	TTCACGTCGGGTTCACC	4239	3973	2028	2680	1926	114	3110	2307	2546	1458	7808
>miR-894-Natt-EU475976	TCACGTCGGGTTCAC	4274	3990	2048	2708	1946	11384	3128	2349	2575	1469	7850
>miR-894-Natt-EU475981	TTCACGTCGGGTTCAC	4258	3977	2035	2691	1940	4	3123	2340	2567	1463	7823
>miR-894-Natt-EU475982	CGTTTCACGTCGGGTTCACC	2362	2813	744	1772	1475	32744	2434	1205	1960	866	5810
>miR-894-Natt-EU476000	TTTCACGTCGGGTTCACC	3112	3234	1045	2083	1775	15825	2730	1527	2293	1204	6453

Table 5.6 Impact of ELVd later infection on microRNA biogenesis

(Source: Pengcheng Zhang, 2024)

miRNA	Sequence	Mock	ELVd								
		Nb	Nb1	Nb2	RDR6i	DCL1i	DCL2Ai	DCL2Bi	DCL3Ai	DCL3Bi	DCL4Ai	DCL4Bi
>miR-157-156-Natt-EU475993	TTGACAGAAGATAGAGAGC	2490	10986	11885	8971	6528	14386	7623	7826	3085	10305	15096
>miR-157-156-Natt-EU475994	TTGACAGAAGATAGAGAGCAC	2219	10542	11455	8452	6251	13833	7140	7503	2923	9936	14516
>miR-159-Natt-EU475975	TTTGGATTGAAGGGAGCTCT	127496	58197	64127	77945	116569	102970	126320	71958	83139	79577	69244
>miR-159-Natt-EU475980	TTGGATTGAAGGGAGCTCT	129358	59660	65866	80048	119028	105197	129231	74034	85676	81508	71645
>miR-159-Natt-EU475990	TTTGGATTGAAGGGAGCTC	127727	58295	64232	78082	116746	103136	126514	72080	83285	79747	69373
>miR-159-Natt-EU475991	TTTGGATTGAAGGGAGCTCC	32	21	26	47	49	45	37	34	26	50	33
>miR-159-Natt-EU475995	TTTGGATTGAAGGGAGCTCTT	618	301	280	385	427	306	430	360	355	380	251
>miR-160-Natt-EU475999	TGCCTGGCTCCCTGTATGCC	9020	3722	2618	3118	4138	3780	5530	2627	2275	4486	3346
>miR-162-Natt-EU475983	TCGATAAACCTCTGCATCC	3811	2226	1624	2394	931	3311	3067	2022	1422	2150	2758
>miR-164-Natt-EU475970	TGGAGAAGCAGGGCACGTGC	15020	2864	3581	4720	2529	4831	4408	2328	2035	3004	3777
>miR-164-Natt-EU475987	TGGAGAAGCAGGGCACGTG	15054	2867	3589	4725	2541	4837	4416	2329	2042	3015	3787
>miR-166-Natt-EU475978	TCGGACCAGGCTTCATTCCCC	79303	92553	76598	92276	91701	100770	139499	69200	85953	81090	90423
>miR-166-Natt-EU476005	TCGGACCAGGCTTCATTCCT	33552	13377	10424	14091	19504	14804	27168	7228	2498	12382	14897
>miR-167-Natt-EU475969	TGAAGCTGCCAGCATGATCT	92035	12439	16348	14338	19505	16433	31893	8127	10800	13333	14704
>miR-167-Natt-EU475977	TGAAGCTGCCAGCATGATCTGG	10883	2246	1499	1721	1572	1648	2089	1245	953	1692	1809
>miR-167-Natt-EU475998	TGAAGCTGCCAGCATGATCTG	11949	2431	1644	1870	1690	1766	2266	1333	1047	1768	1932
>miR-168-Natt-EU475968	TCGCTTGGTGCAGGTCGGG	83798	21448	17393	33888	33118	31511	53392	18922	19491	22254	30262
>miR-168-Natt-EU476004	TCGCTTGGTGCAGGTCGG	83907	21473	17424	33924	33162	31551	53449	18969	19529	22293	30307
>miR-169-Natt-EU475985	CAGCCAAGGATGACTTGCCG	162	65	30	67	50	44	159	89	40	51	82
>miR-169-Natt-EU475997	TAGCCAAGGATGACTTGCCT	213	111	93	312	64	173	277	140	172	85	230
>miR-169-Natt-EU476001	AGCCAAGGATGACTTGCCGG	0	20	9	29	19	23	70	50	28	31	50
>miR-171-Natt-EU475989	TTGAGCCGTGCCAATATCACG	41595	21622	25461	25066	25500	28255	22226	16466	23908	23755	17663
>miR-172-Natt-EU476003	GGAATCTTGATGATGCTGC	8	16	1	16	6	13	2	5	3	27	2
>miR-319-Natt-EU475996	CTTGGACTGAAGGGAGCTCCC	6	17	26	39	16	87	41	33	68	151	28
>miR-396-Natt-EU475972	TTCCACAGCTTTCTTGAACT	66294	12329	9339	14818	12316	14702	26251	9467	9165	17830	15138
>miR-396-Natt-EU475973	TTCCACAGCTTTCTTGAACTG	4722	2151	1814	3652	2104	3617	3983	2020	1420	7728	3174
>miR-396-Natt-EU475974	TTCCACAGCTTTCTTGAACTT	59039	9543	7008	10171	9573	10256	21029	6954	7287	8775	11135
>miR-396-Natt-EU475979	TTCCACAGCTTTCTTG	66848	12461	9419	15000	12431	14868	26554	9551	9278	18050	15269
>miR-396-Natt-EU476002	CCACAGCTTTCTTGAACT	67573	12600	9514	15075	12520	14979	26783	9648	9384	18047	15378
>miR-397-Natt-EU475965	ATTGAGTGCAGCGTTGATG	8184	17155	25618	22187	34105	19067	23932	18245	25970	33588	19720
>miR-397-Natt-EU475992	TCATTGAGTGCAGCGTTGATG	3634	6595	9971	9386	10944	4602	7713	5265	10877	10724	4926
>miR-403-Natt-EU475984	TTAGATTCACGCACAAACTCG	3577	2206	3076	2473	2535	3718	3128	2139	2306	2492	3486
>miR-403-Natt-EU475988	TTAGATTCACGCACAAACTC	4172	3179	4208	3279	3295	4798	3996	3048	3074	3374	4622
>miR-408-Natt-EU475986	TGCACTGCCTCTTCCCTGG	1367	6683	6119	6689	11689	11419	9446	5621	7271	37043	10998
>miR-894-Natt-EU475966	CACGTCGGGTTCACC	2822	2048	7026	7216	9221	6112	4514	4569	3640	6837	5858
>miR-894-Natt-EU475967	TCACGTCGGGTTCACC	2819	2039	7018	7212	9206	6111	4509	4567	3633	6827	5852
>miR-894-Natt-EU475971	TTCACGTCGGGTTCACC	2811	2021	6989	7179	9179	6082	4489	4557	3610	6800	5827
>miR-894-Natt-EU475976	TCACGTCGGGTTCAC	2830	2048	7031	7239	9231	6143	4531	4617	3652	6838	5871
>miR-894-Natt-EU475981	TTCACGTCGGGTTCAC	2822	2030	7002	7206	9204	6113	4511	4607	3629	6811	5846
>miR-894-Natt-EU475982	CGTTTCACGTCGGGTTCACC	1715	873	5282	4973	6451	4282	2908	3630	2027	4421	3336
>miR-894-Natt-EU476000	TTTCACGTCGGGTTCACC	2192	1203	5817	5788	7435	5075	3434	4001	2503	5179	4217

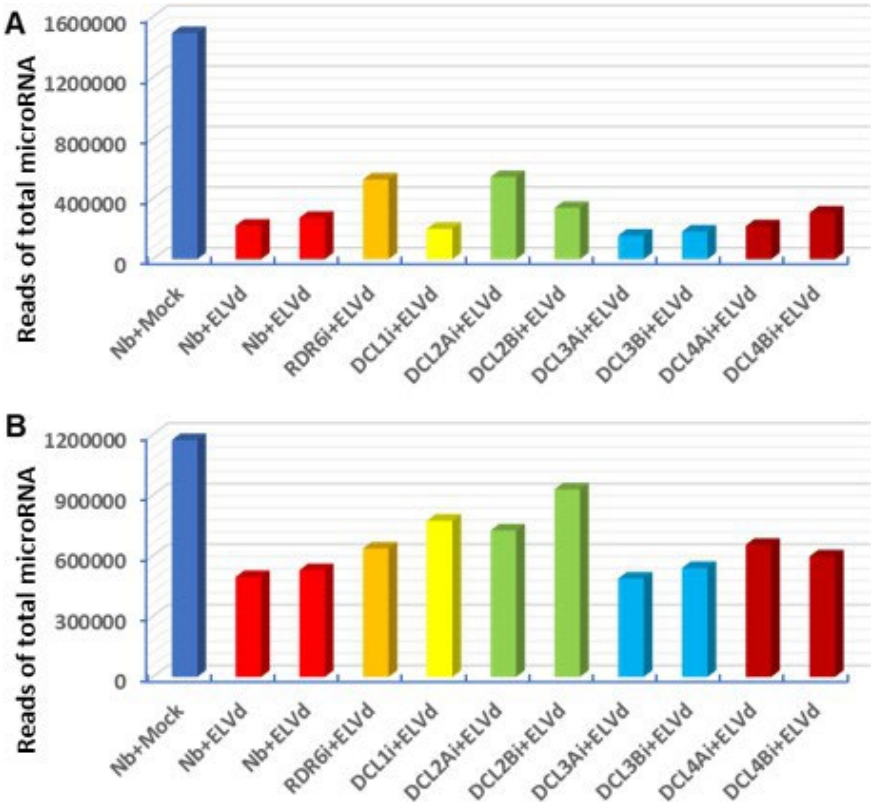

Figure 5.9 Influence of ELVd on accumulation of cellular microRNAs at early and later stages of infection

A, Early infection at 6 dpi. **B**, Later infection at 14 dpi. Mock-inoculated or ELVd-infected leaf tissues were collected at either 6- or 14-dpi for sRNA analysis. Mock inoculation of *N. benthamiana* (Nb+Mock), *Nb* infected with ELVd (Nb+ELVd), *RDR6i* infected with ELVd (RDR6i+ELVd) and *DCLi* infected with ELVd (*DCL1i*+ELVd, *DCL2Ai*+ELVd, *DCL2Bi*+ELVd, *DCL3Ai*+ELVd, *DCL3Bi*+ELVd, *DCL4Ai*+ELVd, *DCL4Bi*+ELVd) are indicated. The total microRNAs are indicated as colour bars and the reads of total microRNA are indicated in vertical axis in the figure. **(Source: Pengcheng Zhang, 2024)**

5.3 Discussion

In plants, chloroplast viruses (ELVd) can produce unique chloroplast virus siRNAs (cvd-siRNAs) associated with post-transcriptional RNA silencing (Di Serio et al. 2009; Bolduc et al. 2010; Navarro et al., 2021a; Wassenegger et al., 2021). However, how cytoplasmic RNA silencing targets chloroplast viruses for cvd-siRNA biogenesis remains unclear. It is known that ELVd only locally infects *N. bethamiana* plants when inoculated with infectious RNA transcribed in vitro. Using *Agrobacterium* - mediated infiltration, the infectious RNA clones of ELVd were trans-infected into the transgenic *N. bethamiana* DCLs or RDR6 knock-out plants. Intracellular RNA translocation between the cytoplasm and chloroplasts was examined at early (6 dpi) and late (14 dpi) stages of infection, and the effect of DCLs and RDR6i mutant plants on ELVd infection and production of vd-siRNAs was analysed.

The results show that, DCL2 is essential for the production of the most abundant 22 nt cvd-siRNAs (Figure 5.3; Figure 5.6). When DCL2 was knocked out in two DCL2-RNAi lines, ELVd was then predominantly targeted by DCL3 for the production of 24 nt cvd-siRNAs, suggesting that DCL2 acts primarily against ELVd RNA silencing, while DCL3 is redundant to DCL2 (Figure 5.3; Figure 5.6). This is in contrast to previous studies reporting synergistic and joint activities of DCL2 and DCL3 in silencing-based defense against nuclear replication viruses such as PSTVd (Dalakouras et al., 2015; Katsarou et al., 2016). The characterization of ELVd 21, 22, and 24 nt cvd-siRNAs (Figure 5.3; Figure 5.4) differs from that of reported cytosolic replication viruses (Martin et al., 2007; Martinez et al., 2010; Jiang et al., 2019), plant RNA and DNA (Blevins et al., 2006; Qin et al., 2017) viruses, transgenic mRNAs and hairpin dsRNAs (Chen et al., 2018), and indeed different from other chloroplast replicating viruses such as *Peach latent leaf virus* (PLMVd) (St-Pierre et al., 2009; Di Serio et al., 2009; Delgado et al., 2019; Di Serio et al., 2023).

In comparison to DCL2, DCL4 is involved in the production of less abundant 21 nt cvd-siRNAs, and the role of DCL4 in anti-ELVd is complex and dynamic (Figure 5.3; Figure 5.6). It is reported that DCL4 is required for efficient nuclear replication of virus infections, leading to a marked increase in vd-siRNA in plants (Dalakouras et al., 2015; Katsarou et al., 2016), however, in this research, DCL4 had little effect on ELVd cvd-siRNA accumulation, especially during the later stages, DCL4 deficiency resulted in escalating levels of EVLd to generate more abundant cvd-siRNA (Figure 5.6). This temporal difference in cvd-siRNA accumulation reflects the fact that RNA silencing during ELVd infection mediated dynamic defense, and/or the active evasion strategy of ELVd to survive this cellular defense, as ELVd (and all other viruses) do not encode silenced suppressors (van Wezel and Hong., 2004; Navarro et al., 2021a).

It is very interesting that RDR6i had no effect on the size of the 21, 22 and 24 nt siRNAs, suggesting no specific association between RDR6i and any DCLs (Figure 5.3; Figure 5.6). Furthermore, considering the marked reduction of cvd-siRNAs in RDR6i plants at 14 dpi (Figure 5.6), any possible involvement of RDR6 in the fight against late ELVd infection seems indirect (Adkar-Purushothama et al., 2020).

It seems that DCL1 and DCL4, RDR6 are not involved in the biogenesis of ELVd-derived siRNAs. Early stages of ELVd infection may not be directly involved in this defence (Figure 5.9). However, microRNAs may be indirectly involved in cellular anti-ELVd defense, e.g., through the microRNA-regulated plant immune genes (Marquez-Molins et al., 2021, 2022; Ortola, B and Daros, JA., 2023).

Although DCL1 was not specifically associated with ELVd cvd-siRNA production (Figure 5.3; Figure 5.6), and no direct involvement of DCL1 in cellular defence against ELVd was observed, but DCL1-processed microRNAs may be indirectly involved in cellular defence against ELVd. Since ELVd infection reduced DCL1-processed microRNAs in both wild-type and RNAi plants. It is plausible that host cells could alleviate the severe ELVd-mediated repression of microRNAs (Marquez-Molins et al., 2021, 2022; Ortola, B and Daros, JA., 2023).

Chapter 6 Effect of ELVd infection on chloroplast-originating csRNA biogenesis

6.1 Introduction

It is reported that small RNAs (sRNAs) can be derived from the mRNA, rRNA, tRNA and intergenic RNAs encoded by the chloroplast genome (St-Pierre et al., 2009; Bolduc et al., 2010; Wang et al., 2011). These sRNAs are the so-called chloroplast sRNAs (csRNAs). csRNAs are how they are generated and whether they are related to the biogenesis of cvd-siRNAs. However, it is unclear whether csRNAs and cvd-siRNAs are produced through the same cellular RNA silencing apparatus or through different sRNA processing/metabolism. To address these questions, we first investigated whether RNAs encoding genes in the source chloroplast genome could be partitioned by DCLs in the cytoplasm (i.e. outside the chloroplast). We constructed a gene-specific hairpin RbCL-RNAi vector, pRNAi-RbCL, which targets the chlorobloss-1,5-bisphosphate carboxylase/oxidase large subunit (RbCL) gene (Kunnimalaiyaan and Nielsen., 1997). RbCL is a gene encoding the Rubisco large subunit (RbCL) of the chloroplast gene that is involved in plant photosynthesis. To produce this construct, a cDNA fragment (250 bp) corresponding to 1182 to 1431 nucleotides of RbCL was amplified with a set of primers and cloned into the RNAi vector pRNAi-LIC (Xu et al., 2010). Sequences of the chloroplast gene RbCL mRNA were shown in appendix 2. Transgenic lines were then utilized in which individual DCLs and RDR6 were knocked out by RNAi and in which ELVd could establish effective local infection in the non-natural host *N. benthamiana*. Two young leaves from each Nb plant (six plants in each experiment were at the six-leaf stage) were inoculated by infiltration with GV3101 carrying pRNAi-RbCL or empty RNAi vectors. Agrobacterium-infiltrated leaf tissue was collected from two to three different plants and pooled on days 6 and 14 after Agrobacterium-infiltrated inoculation. Two pooled samples from different plants were used to extract sRNAs and construct sRNA libraries, which were finally sequenced under the Illumina HisEquation 2000 (Illumina) platform to analyze ELVd infection on chloroplast-derived csRNA data to investigate the effect of ELVd infection on the production of chloroplast-derived small RNAs that sRNAs from chloroplast RbCL mRNA.

6.2 Experimental Results

6.2.1 Production of chloroplast gene sRNA in cytoplasm

Avsunviroids reside and replicate within chloroplasts. This prompted us to investigate whether ELVd infection has an effect on biological processes within the chloroplast, for example, the effect of ELVd infection on csRNA production (Figure 6.1). We first investigated whether RNAs originating from genes encoding the chloroplast genome could be partitioned by DCLs in the cytoplasm (i.e. outside the chloroplast). We constructed an RNAi vector for the generation of hairpin dsRNA (hp-dsRNA), which corresponds to a 250 bp fragment of 1181-1431 nucleotides (Figure 6.1 A) of the chloroplast chlorobulose-1,5-bisphosphate carboxylase/adductase large subunit (*RbCL*) gene (see section appendix 2). Such chloroplast hp-dsRNAs, once expressed in *Nb* leaf tissue in an agricultural filtration assay (Figure 6.1 B). When the hp-dsRNAs were expressed, they were readily targeted by cellular RNA silencing mechanisms for siRNA biogenesis (Figure 6.1 C and D). siRNA size was characterized by the most abundant size of 21 nt together with the large number of 22 and 24 nt, similar to the nuclear (trans)genes mRNAs and the pattern of siRNAs produced by transient nuclear hp-dsRNAs (Chen et al., 2018). Interestingly, in the control *Nb* leaf tissue infiltrated with empty RNAi vectors, the size distribution of csRNAs mapping to the 250 bp region of *RbCL* mRNA was completely different from the siRNAs produced by cellular RNA silencing at 21, 22 and 24 nt, with similar reads for csRNAs of various sizes from 20 to 28 nt (Figure 6.1 E).

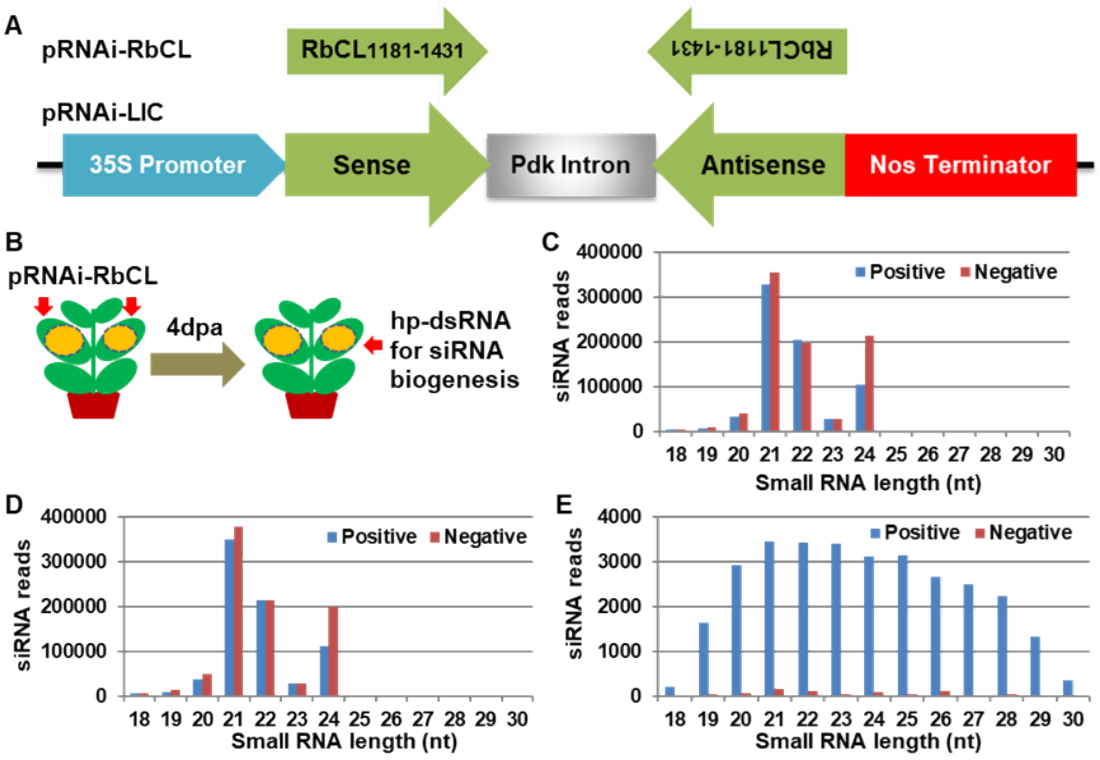

Figure 6.1 Production of chloroplast gene sRNA in cytoplasm

A, Diagrammatic of pRNAi-RbCL construct. A 250-bp fragment corresponding to the nucleotide region 1181-1431 was inverted and cloned into the pRNAi-LIC vector in order to generate hp-dsRNA for siRNA biogenesis in plant cell cytoplasm. **B**, Experimental design. Leaves of *N. benthamiana* plant at the six-leaf stage were infiltrated with agrobacterium carrying either the empty pRNAi-LIC vector or pRNAi-RbCL. At 6 days' post agroinfiltration, leaf tissues were collected, pooled, and used for sRNA analysis. **C** to **E**, Profiles of 18-30 nt siRNAs mapped to the 250nt portion of the *RbCL* mRNA. Leaf tissues expressed *RbCL* hp-dsRNA (**C** and **D**) and controls expressed no *RbCL* hp-dsRNA (**E**). Specific siRNAs were mapped to both mRNA (positive) and complementary (negative) strands of the *RbCL* mRNA fragment (nucleotides 1181-1431). **(Source: Pengcheng Zhang, 2024)**

6.2.2 No silencing transitivity in generation of chloroplastic small RNAs

As shown in Figure 6.2, Specific siRNAs were mapped to both mRNA (positive) and complementary (negative) strands of RbCL mRNA (nucleotides 1-2524). **A** to **D**, Distribution of 21-24 nt chloroplastic small RNAs (csRNAs) across the entire *RbCL* transcript. In *N. benthamiana* leaf tissues expressing the *RbCL* hp-dsRNA (**A** and **C**), abundant 21-24 nt siRNAs generated in the cytoplasm were mapped to the RNAi targeted region (nucleotides 1181-1431). However, only very low levels of 21-24 nt csRNAs were found to be mapped to the 5'- and 3'-UTRs or non-targeted regions of

the *RbCL* mRNA (**B** and **D**). It should be noted that the reads of specific csRNAs mapped to the RNAi target region were left out in order to show the low levels of csRNAs across the rest *RbCL* mRNA portions. **E**, Distribution of background 21-24 nt csRNAs across the *RbCL* mRNA in control plants expressed no *RbCL* hp-dsRNA. In addition, unlike nuclear gene mRNAs, no transgender csRNAs were observed, as evidenced by the similar distribution of csRNAs along other regions of the 2524 nt *RbCL* mRNA in hp-dsRNA-expressing plants and controls without hp-dsRNA expression (Figure 6.2).

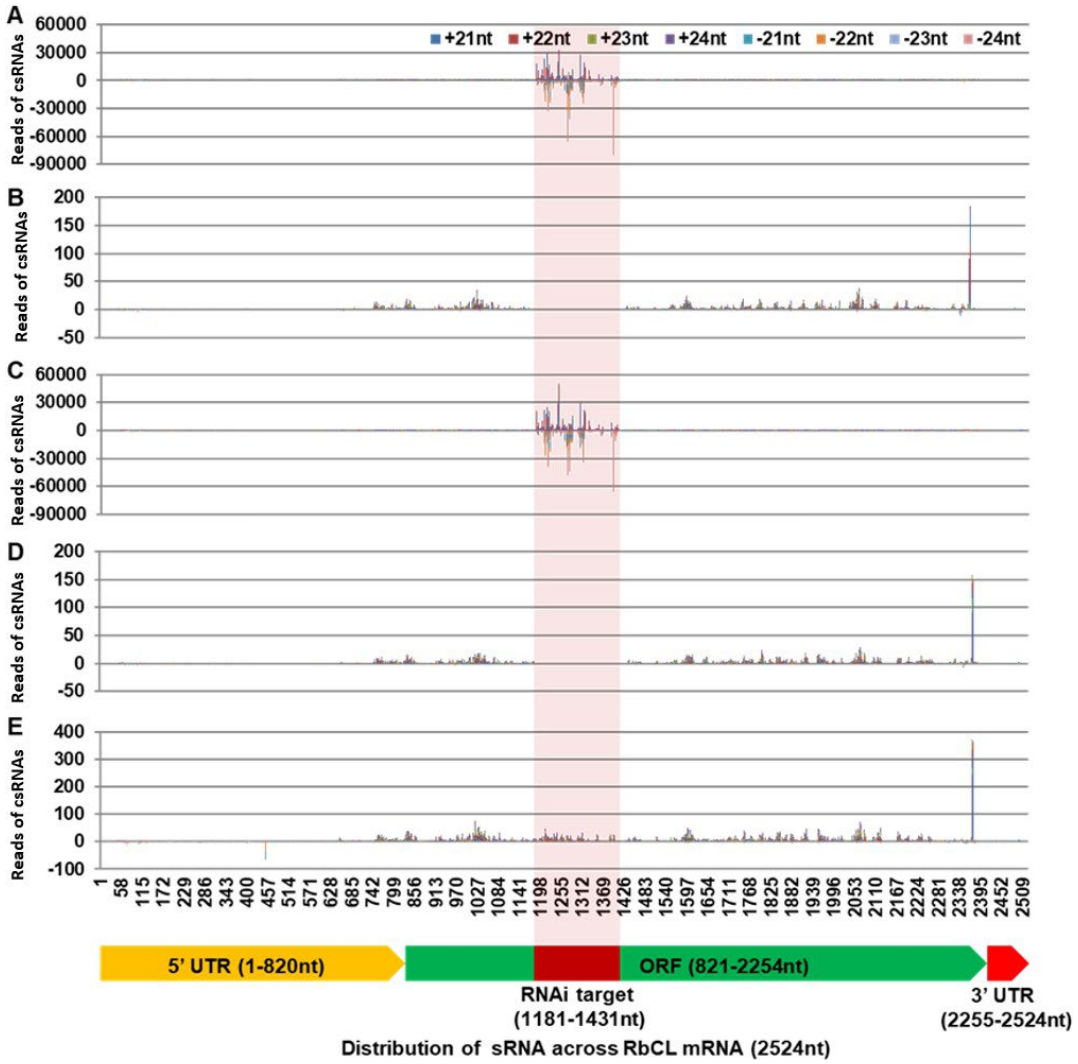

Figure 6.2 No silencing transitivity in generation of chloroplastic small RNAs

A to **D**, Distribution of 21-24 nt chloroplastic small RNAs (csRNAs) across the entire *RbCL* transcript. In *N. benthamiana* leaf tissues expressing the *RbCL* hp-dsRNA (**A** and **C**), abundant 21-24 nt siRNAs generated in the cytoplasm were mapped to the RNAi targeted region (nucleotides 1181-1431). Only very low levels of 21-24 nt csRNAs were found to be mapped to the 5'- and 3'-UTRs or non-targeted regions of

the *RbCL* mRNA (**B** and **D**). It should be noted that the reads of specific csRNAs mapped to the RNAi target region were left out in order to show the low levels of csRNAs across the rest *RbCL* mRNA portions. **E**, Distribution of background 21-24 nt csRNAs across the *RbCL* mRNA in control plants expressed no *RbCL* hp-dsRNA. Specific siRNAs were mapped to both mRNA (positive) and complementary (negative) strands of *RbCL* mRNA (nucleotides 1-2524). Color codes for each size of csRNAs and their polarities are indicated. The 21-24 nt (**A-E**) Accumulations of csRNAs across RbCL mRNA are indicated as colour bars. The reads of csRNAs are indicated in vertical axis in the figure. **(Source: Pengcheng Zhang, 2024)**

6.2.3 Impact of RDR6i or DCLi on accumulation of chloroplastic 18-30 nt csRNAs mapped to RbCL mRNA

Healthy leaf tissues of plants at the equivalent stage to 6 days' post-inoculation were collected for sRNA analysis. Size profiles are shown for 18-30 nt csRNAs that were mapped to the entire RbCL transcript of both mRNA (blue) and complementary (orange) strands. In addition, the size distribution and total reads (Figure 6.3) of csRNAs were similar in healthy wild-type *Nb, RDR6i, DCLi, DCL2i, DCL3i,* and *DCL4i* plants (Figure 6.3 A-J).

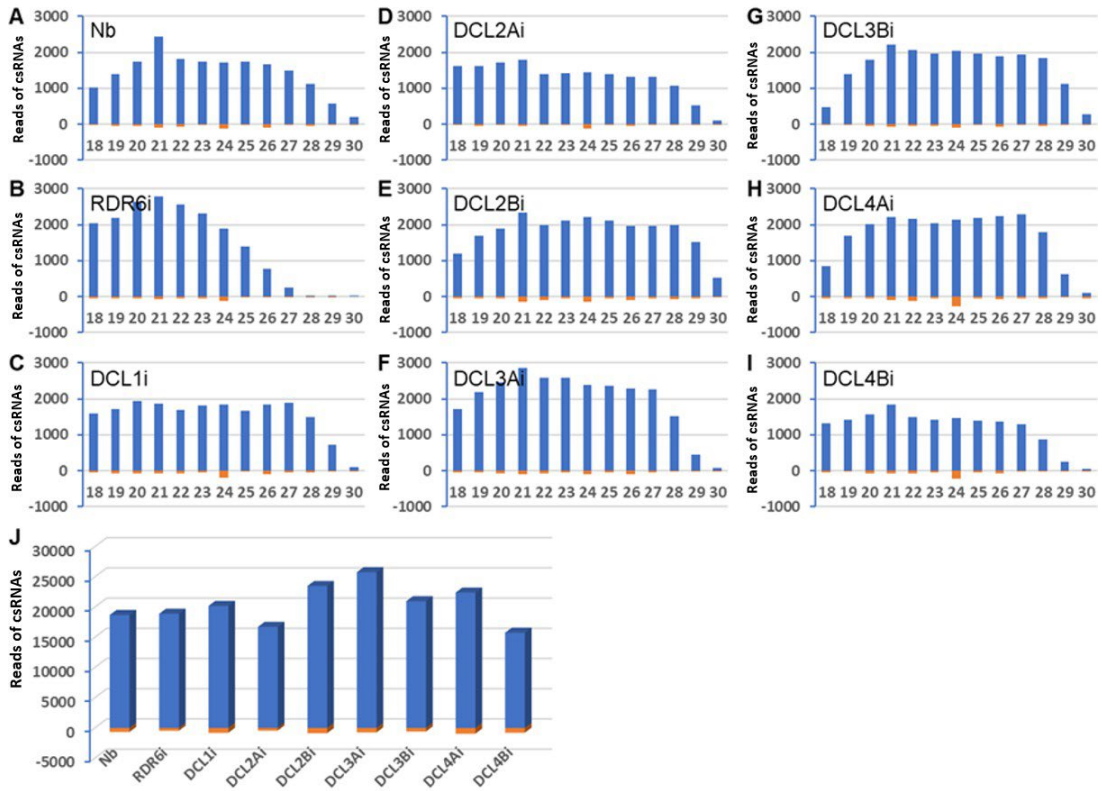

Figure 6.3 Impact of RDR6i or DCLi on accumulation of chloroplastic 18-30 nt

csRNAs mapped to RbCL mRNA

A, *N. benthamiana* (*Nb*). **B**, *RDR6i*. **C** to **I**, *DCLi*. *DCL1i* (**C**), *DCL2Ai* and *DCL2Bi* (**D** and **E**); *DCL3Ai* and *DCL3Bi* (**F** and **G**); *DCL4Ai* and *DCL4Bi* (**H** and **I**). **J**, Total numbers of 18-30 nt csRNAs mapped to *RbCL* mRNA. The 18-30 nucleotide (**A-I**) and total 18-30 nucleotide (**J**) Accumulations of csRNAs are indicated as colour bars. The reads of csRNAs are indicated in vertical axis in the figure. **(Source: Pengcheng Zhang, 2024)**

6.2.4 ELVd reduces accumulation of chloroplastic small RNAs at early infection stage

Mock-inoculated and ELVd-infected leaf tissues were collected at 6 days post inoculation for sRNA analysis. Size profiles are shown for the 18-30nt csRNAs that were mapped to the *RbCL* transcript of both mRNA (blue) and complementary-sense (orange) strands. However, the total number of reads and individual reads of each size (Figure 6.4) was reduced in wild-type *Nb, RDR6i, DCLi, DCL2i, DCL3i,* and *DCL4i* plants infected by ELVd compared to healthy controls (Figure 6.3 A; Figure 6.4 A) for 18-28 csRNAs (Figure 6.4 B-L). However, the size distribution of these reduced csRNAs was similar at 6 dpi in all ELVd-infected *Nb* and *RNAi* plants (Figure 6.4 B-L).

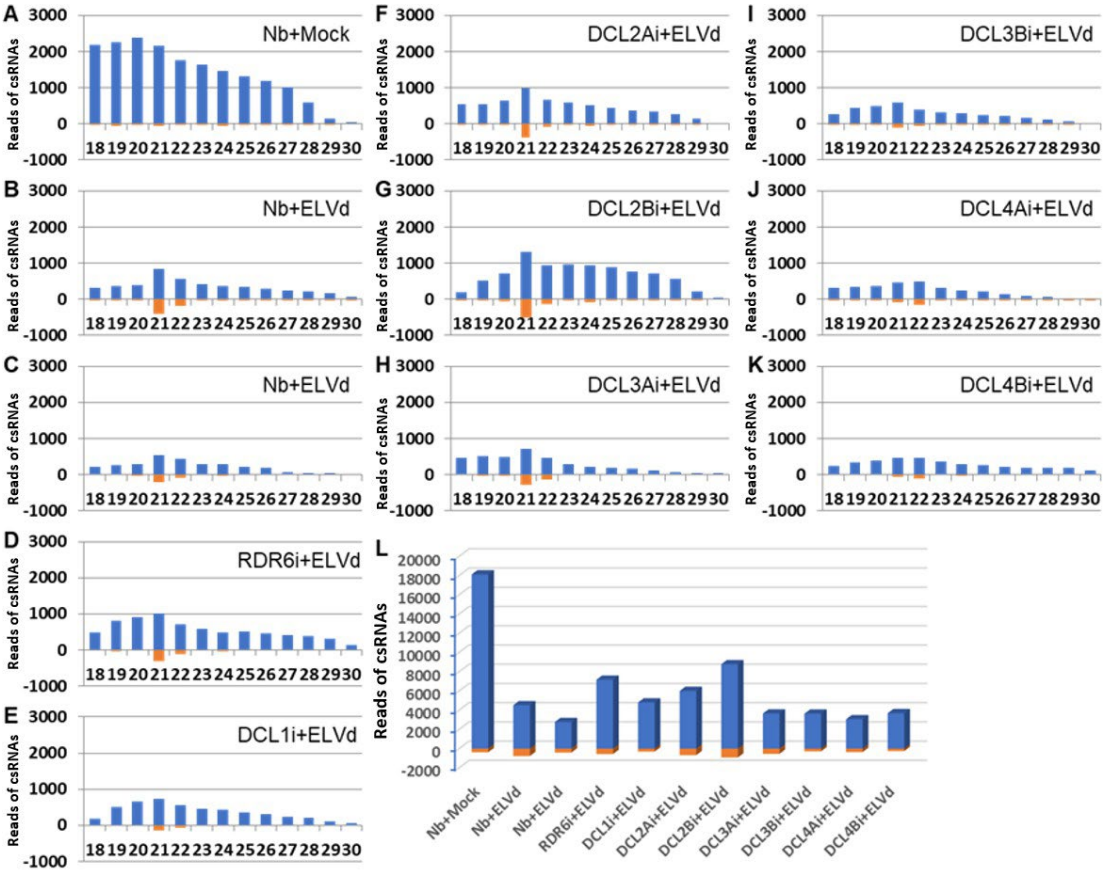

Figure 6.4 ELVd reduces accumulation of chloroplastic small RNAs at early infection stage

A, Mock inoculation of *N. benthamiana* (*Nb*). **B** and **C**, *Nb* infected with ELVd. **D**, *RDR6i* infected with ELVd. **E** to **K**, *DCLi* infected with ELVd. *DCL1i* (**E**), *DCL2Ai* and *DCL2Bi* (**F** and **G**); *DCL3Ai* and *DCL3Bi* (**H** and **I**); *DCL4Ai* and *DCL4Bi* (**J** and **K**). **L**, Total numbers of 18-30 nt csRNAs mapped to the entire *RbCL* mRNA transcript. The 18-30 nucleotide (**A-K**) and total 18-30 nucleotide (**L**) Accumulations of csRNAs are indicated as colour bars. The reads of csRNAs are indicated in vertical axis in the figure. **(Source: Pengcheng Zhang, 2024)**

6.2.5 Reduction of chloroplast csRNAs by ELVd at the later stage of infection

Mock-inoculated or ELVd-infected leaf tissues were collected at 14 days post-inoculation for sRNA analysis. Size profiles are shown for the 18-30 nt csRNAs that were mapped to the *RbCL* transcript of both mRNA (blue) and complementary-sense (orange) strands. As shown in Figure 6.4 and 6.5, the total number of reads and individual reads of each size was reduced in wild-type *Nb, RDR6i, DCLi, DCL2i, DCL3i,* and *DCL4i* plants infected by ELVd compared to healthy controls for 18-28 csRNAs This inhibition of csRNA accumulation persisted until the later stages of ELVd infection, i.e. 14 dpi (Figure 6.5 A-L).

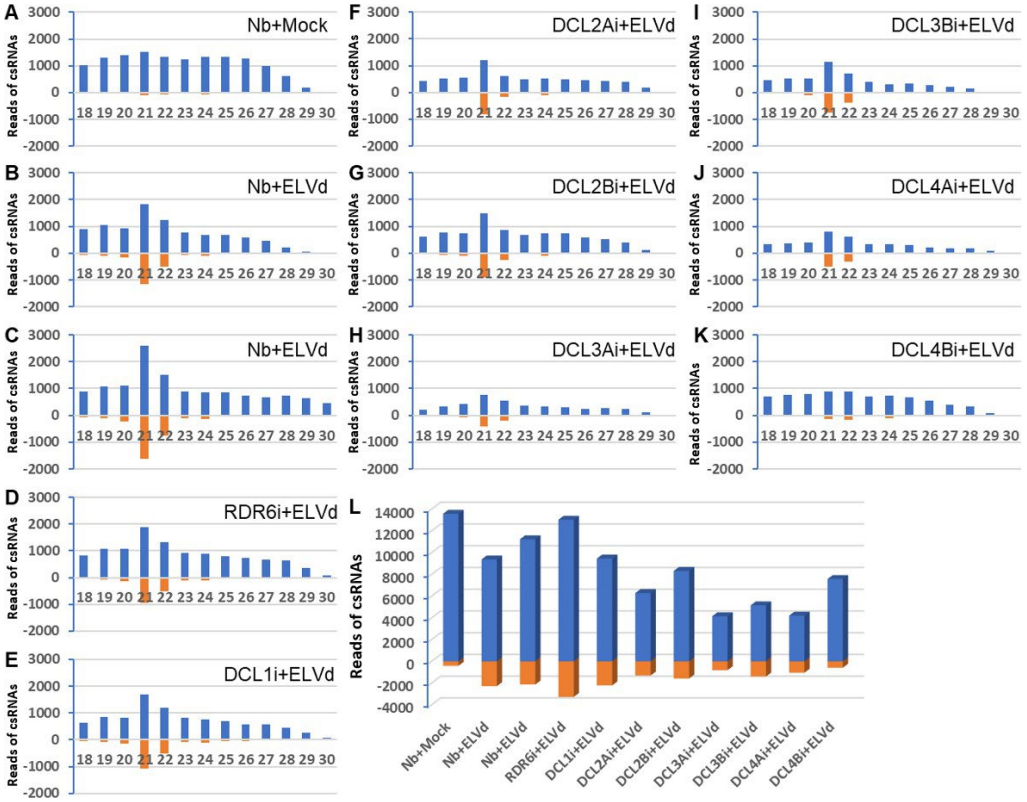

Figure 6.5 Reduction of chloroplast csRNAs by ELVd at the later stage of infection

A, Mock inoculation of *N. benthamiana* (*Nb*). **B** and **C**, *Nb* infected with ELVd. **D**, *RDR6i* infected with ELVd. **E** to **K**, *DCLi* infected with ELVd. *DCL1i* (**E**), *DCL2Ai* and *DCL2Bi* (**F** and **G**); *DCL3Ai* and *DCL3Bi* (**H** and **I**); *DCL4Ai* and *DCL4Bi* (**J** and **K**). **L**, Total numbers of 18-30 nt csRNAs mapped to the entire *RbCL* mRNA transcript. The 18-30 nucleotide (**A-K**) and total 18-30 nucleotide (**L**) Accumulations of csRNAs are indicated as colour bars. The reads of csRNAs are indicated in vertical axis in the figure. **(Source: Pengcheng Zhang, 2024)**

6.3 Discussion

It is still unclear whether csRNAs and cvd-siRNAs are produced through the same cellular RNA silencing apparatus or through different sRNA processing / metabolism (St-Pierre et al., 2009; Bolduc et al., 2010; Wang et al., 2011; Hadidi et al., 2016; Marquez-Molins et al., 2021; Wu et al., 2023). In this section, we investigated whether cytoplasmic RNA silencing targets mRNAs encoded by chloroplast genes. Whether siRNAs produced in the cytoplasm can move to organelles such as chloroplasts to trigger gene silencing and how these related to biogenesis of cvd-siRNA. To seek answers to our questions, we first investigated whether RNAs originating from genes

encoding the chloroplast genome could be compartmentalized by DCLs in the cytoplasm (i.e. outside the chloroplast). We constructed an RNAi vector for the generation of hairpin dsRNA (hp-dsRNA), a fragment corresponding to a 250 bp fragment of 1182-1431 nucleotides of the chloroplast *RbCL* gene (Kunnimalaiyaan and Nielsen., 1997). This chloroplast hp-dsRNAs, once expressed in Nb leaf tissues was used in the Agrobacterium filtration assay.

The results showed that the size of siRNAs was characterized by the most abundant 21 nt siRNAs as well as a large number of 22 and 24 nt siRNAs, consistent with the pattern of siRNAs produced by nuclear gene mRNAs and transient nuclear hp-dsRNAs (Figure 6.1; Figure 6.2) (Chen et al., 2018).

Interestingly, in the control Nb leaf tissue infiltrated with empty RNAi vectors, the csRNAs size distribution was ranged from from 20 to 28 nt (Figure 6.2), completely different from the siRNAs produced by cellular RNA silencing at 21, 22, and 24 nt, with similar reads for csRNAs of various sizes from 20 to 28 nt (Figure 6.2). This is consistent with different csRNA size distributions (Figure 6.1). The roles of these csRNAs in plant, their biogenesis mechanism and any role in ELVd induced gene silencing are still unclear, further investigation is of great interest for both biological research on gene silencing and develop plant virus resistance.

There is no transactivation of csRNAs was observed for chloroplast RbCL mRNA. When a partial chloroplast RbCL mRNA was used as trans-activator in cytoplast, the accumulation profile of the csRNAs targeted to the full-length gene sequence remained similar to these without trans-activator expression (Figure 6.2). Unlike the nuclear gene mRNAs that have the ability to produce the transgender (positive / negative strand) siRNAs, the chloroplast RbCL failed to trans-activate the csRNAs against the full gene sequence, csRNAs is confined in the trans-activator region (1181-1431) but not covered the full length RbCL gene of 2524 nt. This result suggested that the csRNA biogenesis in the chloroplast is different form these in the protoplast, either the involved enzymes or the chloroplast transport, further investigation is required to elucidate the details (Marquez-Molins et al., 2021; Han et al., 2023).

It is showed that the size distribution and total reads of csRNAs were similar in healthy wild-type Nb, RDR6i, DCLi, DCL2i, DCL3i, and DCL4i plants, indicating that none of RDR6i, DCLi, DCL2i, DCL3i, and DCL4i play a critical role in the csRNA biogenesis.

Total reads and individual reads of each size were reduced in 18-28 csRNAs in Nb and RNAi plants infected by ELVd compared to healthy controls, suggesting that csRNAs may be produced by a chloroplast-specific sRNA processing mechanism. The size distribution of these reduced csRNAs was similar at 6 dpi. This inhibition of csRNA accumulation was observed the later stages of ELVd infection (14 dpi) (Figure 6.3; Figure 6.4). The exact nature of this chloroplast-specific sRNA processing mechanism is currently unknown.

The results further indicate that if chloroplast mRNA is transcribed in the nucleus and presented in the cytoplasm, it is readily targeted by cellular RNA silencing mechanisms for 21, 22, and 24 nt siRNA biogenesis (Figure 6.1; Figure 6.2). If chloroplast mRNA is expressed within the chloroplast, it cannot be cleaved by cellular DCLs. Thus, our findings imply that csRNAs may be produced by a chloroplast-specific sRNA processing mechanism. This is consistent with the different csRNA size distribution (Figure 6.1), the lack of transactivation of csRNA observed for chloroplast RbCL mRNA (Figure 6.2), and the marked reduction in csRNA levels in ELVd-infected Nb, RDR6i, and DCLi plants (Figure 6.3; Figure 6.4). The exact nature of this chloroplast-specific sRNA processing mechanism is currently unknown. On the other hand, any role of csRNAs in ELVd plant interactions or/and regulation of chloroplast genes also remains to be elucidated.

Chapter 7 Discussion, conclusion and prospective

7.1 Possible explanations and/or speculations for the findings

Viroids in *Avsunviroidae* family replicate and accumulate in chloroplasts (Navarro et al., 1999; Daròs., 2016), especially in the case of ELVd, the nuclear phase of the life cycle is also shown (Gómez and Pallás., 2012). Subcellular compartmentalisation of chloroplast and nucleus prevents ELVd from being attacked by RNA silencing that operates mainly in the cytoplasm (Figure 7.1). The significant difference between the size characteristics of sRNAs and true csRNAs associated with cellular RNA silencing also suggests that any key components of the cellular RNA silencing machinery, such as DCL2, are not imported into the chloroplast. To explain our results, we envisage a possible cytoplasmic phase during the trafficking of ELVd between the nucleus and chloroplasts within infected cells, as well as during intercellular and long-distance movement in infected plants (Figure 7.1). When ELVd enters the cytoplasm early in infection, cytoplasmic RNA silencing can immediately target and process ELVd genomic RNA into siRNAs at 21, 22, and 24 nt. At a later stage, cytoplasmic ELVd-derived RNA may require cellular RDR6 to produce dsRNA for further cleavage into siRNAs (Figure 7.1). Based on the results of this lab and previous reports, the interesting model proposed is that ELVd RNAs have the potential to shuttle between the nucleus and chloroplasts and that cellular RNAi could potentially attack virosomes in the nucleus or cytoplasm during this trafficking.

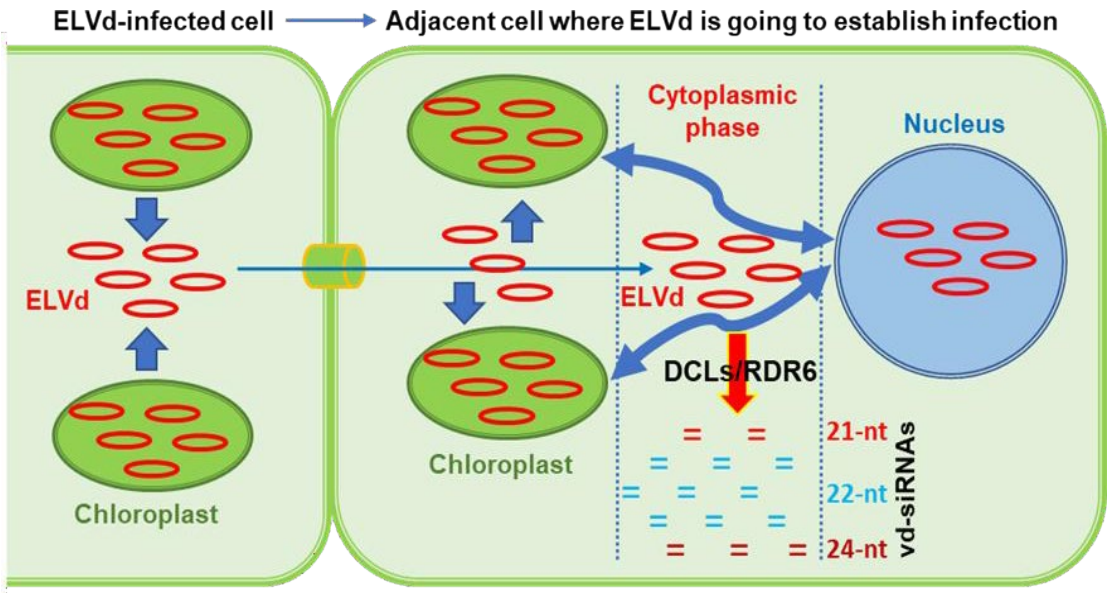

Figure 7.1 Model for biogenesis of cvd-siRNAs derived from chloroplast-replicating viroid

ELVd, a chloroplastic viroid, replicates primarily in chloroplasts and it also endures a nuclear stage during its infection cycle. Subcellular compartments prevent cytoplasmic RNA silencing machinery from targeting and cleaving ELVd RNA. In chloroplasts and nuclei to generate cvd-siRNAs as the size profiles of small RNAs processed by cellular RNA silencing and *bona fide* csRNAs are markedly different. We envisage that a cytoplasmic phase during the shuttling of ELVd from cell to cell via plasmodesmata (represented by a cylinder) or from chloroplast to nucleus and *vice versa* (blue double-arrow line) may exist within infected cells. Thus, when ELVd enters cytoplasm *en route* from chloroplast to the nucleus *or* intercellular movement via plasmodesmata, for example, at the early stage of infection, cytoplasmic RNA silencing machinery can immediately target and process ELVd genomic RNA into cvd-siRNAs by DCLs. DCL2 is the predominant DCL to cleave ELVd RNA for production of 22 nt cvd-siRNA. DCL3 is functionally redundant to DCL2. Only when DCL2 is deficient, DCL3 takes action to dice ELVd RNA for production of 24 nt cvd-siRNA. DCL1, DCL4, and RDR6 may not be directly involved in such defense at the early stage of ELVd infection. However, at a later stage, they may be also required, for example, RDR6 may act to convert ELVd ssRNA into dsRNA for further cleavage into siRNAs in the cytoplasm. ELVd circular ssRNA, chloroplasts, nucleus, and ELVd-siRNAs of various sizes are indicated. **(Source: Pengcheng Zhang, 2024)**

In this PhD thesis, through ELVd infection, sRNA profiling of ELVd cvd-siRNAs and csRNAs producing in *Nb*, *RDR6i*, and *DCLi* plants, we reveal that *DCLs* and *RDR6* on the dynamic RNA silencing-mediated response to ELVd infection. Evidently, ELVd RNA was readily detected by Northern blot. Meanwhile, we used RT-PCR to quantify the impact of *DCLi* and *RDR6i* on ELVd RNA accumulation. Our results suggest that *DCL1i*, *DCL2i*, *DCL3i* and *DCL4i* enhanced ELVd RNA levels, suggesting that all four DCLs are involved in plant defence against ELVd infection, but *RDR6i* had little effect on ELVd RNA accumulation in the early and later infection stages.

In addition, *DCL2* plays an important role in the production of the most abundant 22 nt cvd-siRNAs in RNA silencing-mediated defence against chloroplast-replicating ELVd. *DCL3* is functionally redundant to *DCL2* in terms of targeting ELVd RNA for cvd-siRNA biogenesis. This is in contrast to the synergistic and combined activities of DCL2 and DCL3 in silencing-based defence against nuclear replication viruses such as PSTVd (Dalakouras et al., 2015; Katsarou et al., 2016). The role of *DCL4* in anti-ELVd is complex and dynamic, and/or an active escape strategy for ELVd in this cellular

defence. In contrast, it has been some reported that nucleus-replicating viroids trigger production of a notable population of 24-nt siRNAs in addition to the more abundant 21- and 22-nt size classes of viroid siRNAs (Navarro et al., 2021a; Marquez-Molins et al., 2022). The siRNA size distribution patterns reported in this study are not similar to classes of nucleus-replicating viroids. This is also related to the fact that ELVd is the only species in the genus *Elaviroid* in the family *Avsunviroidae* with a specific secondary structure. The mechanism of transport of this class of viroids is not particularly clear, and it is speculated that it may be related to the intrinsic RNA structure.

Although there is no direct involvement of *DCL1* in cellular defence against ELVd was observed, DCL1-processed microRNAs may be indirectly involved in protecting plants against ELVd. DCL1 is not specifically associated with ELVd cvd-siRNA production, however, there are no reports of microRNA-mediated anti-viroid resistance. Furthermore, ELVd infection reduced DCL1-processed microRNAs in both wild-type and RNAi plants. It is plausible that host cells could alleviate the severe ELVd-mediated repression of microRNAs (Marquez-Molins et al., 2021, 2022; Ortola, B and Daros, JA., 2023). The result suggest that cellular microRNAs produced by DCL1 play an important role in plant defence against pathogens, including plant viruses.

The results showed that the size of siRNAs was characterized by the most abundant 21 nt siRNAs as well as a large number of 22 and 24 nt siRNAs, consistent with the pattern of siRNAs produced by nuclear gene mRNAs and transient nuclear hp-dsRNAs (Chen et al., 2018). Total reads and individual reads of each size were reduced in 18-28 csRNAs in Nb and RNAi plants infected by ELVd, suggesting that csRNAs may be produced by a chloroplast-specific sRNA processing mechanism. Our findings also suggest that sRNAs from nuclear and chloroplast genes may be involved in different silencing mechanisms. It is still unclear that csRNAs and cvd-siRNAs are produced through different sRNA processing/mechanisms (Hadidi et al., 2016; Marquez-Molins et al., 2021; Wu et al., 2023). The changes of csRNAs dynamics during ELVd infection suggest that csRNAs may have biological significance in the interaction between chloroplast viruses and their host plants. These obtained results will provide new clues and theoretical basis to uncovering the molecular mechanism of Intracellular RNA signalling in viral RNAi and its role in antiviral defence.

7.2 Limitations of the study and solutions to those limitations

The effects of RNA silencing on viroids are complex and dynamic. It is well known that viroids replicate in the nucleus or chloroplasts of host cells, and both nucleus- and chloroplast-replicating viroids can be targets of RNA silencing, producing siRNAs of 21-24 nt specific to viroid genome sequences (Dalakouras et al., 2015; Katsarou et al., 2016). In contrast to intercellular and systemic RNA silencing, little is known about spread of RNA silencing among organelles within a cell. However, intracellular RNA silencing can target organelle-specific pathogenic RNAs. There are some hints that non-coding siRNAs have been found to be associated with chloroplast genome. Moreover, certain types of pathogenic RNAs such as the ELVd RNA can specifically move into chloroplasts. These sporadic findings imply that RNA signalling may occur among organelles within plant cells. Nevertheless, how RNA silencing machinery targets and fights against chloroplastic remains largely unknown.

To address this question, we utilized a chloroplast-localized viroid, *Eggplant latent viroid* (ELVd), as a tool, and our newly established series of unique DCL-RNAi *N. benthamiana* transgenic lines in the study. ELVd has a very narrow host range and can be transmitted mechanically and by seed. ELVd systemically and latently infect its natural host eggplant (*Solanum melongena L.*) (Daròs., 2016). However, ELVd can also establish local infection in *N. benthamiana* and it represents an excellent model to investigate intracellular RNA trafficking between cytoplasm and chloroplasts (Gómez and Pallas., 2012). Taking advantage of these discoveries on ELVd and the transgenic lines deficient in cellular RNA silencing generated in our laboratory, we investigated how DCLs and RDR6 influence biogenesis of chloroplastic viroid siRNA.

7.3 Implications of findings

In this project, we used *Eggplant latent viroid* (ELVd), and a suite of transgenic *RDR6*- and *DCL*-RNAi *N. benthamiana* lines as a study to investigate how RNA silencing targets and counteracts a chloroplast-replicating viroid ELVd, by examining the effects of chloroplast-replicating ELVd infection on microRNA and sRNA biogenesis of chloroplast-derived small RNAs in *N. benthamiana* leaves and the role of RNA silencing components on ELVd siRNA production. This was combined with high-throughput sequencing followed by small RNA analysis to reveal dynamic RNA silencing-mediated responses of DCLs and RDR6 to ELVd infection, and extensive experimental data are reported. We investigated how intracellular siRNA propagates from the cytoplasm to the chloroplast and explored how RNA signalling and associated genetic networks on the mechanisms regulating PTGS during intracellular inter-

organelle transport, and its biological relevance to plant antiviral defence. The obtained results established approaches pave the way for investigating the molecular mechanism of Intracellular RNA signalling in other viral RNAi and their roles in antiviral defence.

7.4 Future work

Firstly, our findings suggest that sRNAs from nuclear and chloroplast genes may be involved in different silencing mechanisms. The dynamic course of csRNAs during ELVd infection suggests a possible biological relevance to chloroplast virus-host plant interactions, and roles and molecular details of csRNAs in ELVd plant interactions or/and regulation of chloroplast genes remains to be further investigated.

Secondly, the chloroplast small RNA formation mechanisms will be investigated in the future, this includes searching and identifying the chloroplast-specific RNA enzymes, through RNAi or knock-out related genes, analyzing whether these enzymes affect the effects of nucleus/cytoplasm small RNA movement, etc., and how RNA signaling regulates plant antiviral mechanisms, which is also believed to be of interest to researchers.

8. References list

1. Adkar-Purushothama, CR; Perreault, JP. Suppression of *RNA-dependent RN A polymerase 6* favors the accumulation of potato spindle tuber viroid in *Nic otiana benthamiana*. *Viruses-Basel.* 2019, 11(4), 345. https://doi.org/10.3390/v 11040345.
2. Adkar-Purushothama, CR; Perreault, JP. Current overview on viroid-host inter actions. *Wiley Interdisciplinary Reviews-RNA.* 2020, 11(2): e1570. DOI: 10.10 02/wrna.1570. https://doi.org/10.1002/wrna.1570.
3. Akbergenov, R; Si-Ammour, A; Blevins, T; Amin, I; Kutter, C; Vanderschuren, H; Zhang, P; Gruissem, W; Meins, F; Hohn, T; Pooggin, MM. Molecular ch aracterization of geminivirus-derived small RNAs in different plant species. *N ucleic Acids Ressearch.* 2006, 34(2): 462-471. https://doi.org/10.1093/nar/gkj4 47.
4. Aliyari, R; Ding, SW. RNA-based viral immunity initiated by the Dicer family of host immune receptors. *Immunological Reviews.* 2009 227(1):176-188. htt ps://doi.org/10.1111/j.1600-065X.2008.00722.x.
5. Al Rwahnih, M; Daubert, S; Golino, D; Rowhani, A. Deep sequencing analys is of RNAs from a grapevine showing Syrah decline symptoms reveals a m ultiple virus infection that includes a novel virus. *Virology*. 2009, 387(2):395-401. https://doi.org/10.1016/j.virol.2009.02.028.
6. Andika, IB; Maruyama, K; Sun, L; Kondo, H; Tamada, T; Suzuki, N. Differen tial contributions of plant dicer-like proteins to antiviral defences against pota to virus X in leaves and roots. *Plant Journal*. 2015, 81(5): 781-793. DOI:10. 1111/tpj.12770. https://doi.org/10.1111/tpj.12770.
7. Aregger, M; Borah, BK; Seguin, J; Rajeswaran, R; Gubaeva, EG; Zvereva, AS; Windels, D; Vazquez, F; Blevins, T; Farinelli, L; Pooggin, MM. Primary and secondary siRNAs in Geminivirus-induced gene silencing. PLoS Pathoge ns. 2012, 8: e1002941. https://doi.org/ 10.1371/journal.ppat.1002941.
8. Baek, E; Par, M; Yoon, JY. Chrysanthemum chlorotic mottle viroid-mediated trafficking of foreign mRNA into Chloroplasts. *Research in Plant Disease*. 20 17, 23(3):288-293. https://doi.org/10.5423/RPD.2017.23.3.288.
9. Barba, M; Czosnek, H; Hadidi, A. Historical perspective, development and a pplications of next-generation sequencing in plant virology. *Viruses-Basel.* 20 14,6(1):106-136. https://doi.org/10.3390/v6010106.
10. Barciszewska-Pacak, M; Jarmolowski, A; and Pacak, A. (2016). Virus-Induce d Gene Silencing for Gene Function Studies in Barley. *Methods in molecular*

biology (Clifton, N.J.) 1398, 293-308. https://doi.org/10.1007/978-1-4939-3356-3_22.

11. Baulcombe, D. (2004) RNA silencing in plants. *Nature*. 431(7006):356-363. https://doi.org/10.1038/nature02874.
12. Bélanger, S; Kramer, MC; Payne, HA; Hui, AY; Slotkin, RK; Meyers, BC; Staub, JM. Plastid dsRNA transgenes trigger phased small RNA-based gene silencing of nuclear-encoded genes. *Plant Cell*. 2023, 35(9): 3398-3412. https://doi.org/10.1093/plcell/koad165.
13. Baumberger, N; Tsai, CH; Lie, M; Havecker, E; Baulcombe, DC. The polerovirus silencing suppressor P0 targets Argonaute proteins for degradation. *Current biology*. 2007, 17(18):1609-1614. https://doi.org/10.1016/j.cub.2007.08.039.
14. Bernstein, E; Caudy, AA; Hammond, SM; Hannon GJ. Role for a bidentate ribonuclease in the initiation step of RNA interference. *Nature* 2001, 409(6818), 363-366. https://doi.org/10.1038/35053110.
15. Berg, JM. Retraction. *Science* 2016, 354(6309): 190-190. https://doi.org/ 10.1126/science. aai9397.
16. Blevins T; Rajeswaran, R; Shivaprasad, PV; Beknazariants, D; Si-Ammour, A; Park, HS; Vazquez, F; Robertson, D; Meins, F; Hohn, T; Pooggin, MM. Four plant Dicers mediate viral small RNA biogenesis and DNA virus induced silencing. *Nucleic Acids Research*. 2006, 34(21):6233-6246. https://doi.org/10.1093/nar/gkl886.
17. Bolduc, F; Hoareau, C; St-Pierre, P; Perreault, JP. In-depth sequencing of the siRNAs associated with peach latent mosaic viroid infection. *BMC Molecular Biology*. 2010, 11: 16. https://doi.org/ 10.1186/1471-2199-11-16.
18. Bortolamiol, D; Pazhouhandeh, M; Marrocco, K; Genschik, P; Ziegler-Graff, V. The polerovirus F Box protein P0 targets Argonaute1 to suppress RNA silencing. *Current Biology*. 2007 , 17(18): 1615-1621. https://doi.org/10.1016/j.cub.2007.07.061.
19. Bologna, NG; Voinnet, O. The diversity, biogenesis, and activities of endogenous silencing small RNAs in Arabidopsis. *Annual Review of Plant Biology*. 2014, 65: 473-503. https://doi.org/10.1146/annurev-arplant-050213-035728.
20. Bouche, N; Lauressergues, D (Lauressergues, Dominique); Gasciolli, V; Vaucheret, H. An antagonistic function for Arabidopsis DCL2 in development and a new function for DCL4 in generating viral si RNAs. *The EMBO journal*. 2006, 25(14): 3347-3356. https://doi.org/10.1038/sj.emboj.7601217.

21. Braunstein, TH; Moury, B; Johannessen, M; Albrechtsen, M. Specific degrad ation of 3’ region of GUS mRNA in posttranscriptional silenced tobacco lines may be related to 5’-3’ spreading of silencing. *RNA.* 2002, 8(8): 1034-1044. https://doi.org/10.1017/S1355838202026080.
22. Brosnan, CA; Mitter, N; Christie, M; Smith, NA; Waterhouse, PM; Carroll, BJ. Nuclear gene silencing directs reception of long-distance mRNA silencing in Arabidopsis. *Proceedings of the National Academy of Sciences of the Unite d States of America*. 2007, 104(37),14741-14746. https://doi.org/10.1073/pnas. 0706701104.
23. Brosseau, C and Moffett, P. Functional and genetic analysis identify a role f or Arabidopsis ARGONAUTE5 in antiviral RNA silencing. *Plant Cell.* 2015, 2 7(6): 1742-1754. https://doi.org/10.1105/tpc.15.00264.
24. Brigneti, G; Voinnet, O; Li, WX; Ji, LH; Ding, SW; Baulcombe, DC. Viral pat hogenicity determinants are suppressors of transgene silencing in *Nicotiana benthamiana*. *EMBO Journal*. 1998, 17(22): 6739–6746. https://doi.org/10.109 3/emboj/17.22.6739.
25. Brodersen, P; Voinnet, O. The diversity of RNA silencing pathways in plants. *Trends in Genetics*, 2006, 22(5): 268-280. https://doi.org/10.1016/j.tig.2006.0 3.003.
26. Burgyan, J. and Havelda, Z. Viral suppressors of RNA silencing. *Trends in Plant Science* 2011, 16(5): 265-272. https://doi.org/10.1016/j.tplants.2011.02.0 10.
27. Bwalya, J; Kim, KH. The Crucial Role of Chloroplast-Related Proteins in Vir al Genome Replication and Host Defense against Positive-Sense Single-Stra nded RNA Viruses. *Plant Pathology Journal*. 2023, 39(1): 28-38. https://doi.or g/10.5423/PPJ.RW.10.2022.0139.
28. Chen, XM. Small RNAs and their roles in plant development. *Annual Revie w of Cell and Developmental Biology* 2009, 25:21-44. https://doi.org/10.1146/ annurev.cellbio.042308.113417.
29. Chen, HM; Chen, LT; Patel, K; Li, YH; Baulcombe, DC; Wu, SH. 22-nucleoti de RNAs trigger secondary siRNA biogenesis in plants. *Proceedings of the National Academy of Sciences of the United States of America.* 2010, 107(3 4): 15269-15274. https://doi.org/10.1073/pnas.1001738107.
30. Chen, AYS; Pavitrin, A; Ng, JCK. Agroinoculation of the cloned infectious c DNAs of Lettuce chlorosis virus results in systemic plant infection and produ ction of whitefly transmissible virions. *Virus research*. 2012, 169(1): 310-315.

https://doi.org/10.1016/j.virusres.2012.08.010.

31. Chen, WW; Zhang, X; Fan, YY; Li, B; Ryabov, E; Shi, NN; Zhao, M; Yu, Z M; Qin, C; Zheng, QQ; Zhang, PC; Wang, HZ; Jackson, S; Cheng, Q; Liu, YL; Gallusci, P; Hong, YG. A genetic network for systemic RNA silencing in plants. *Plant Physiology*. 2018 176(4): 2700-2719. https://doi.org/10.1104/pp.17.01828.
32. Chiu, MH; Chen, IH; Baulcombe, DC; Tsai, CH. The silencing suppressor P25 of Potato virus X interacts with Argonaute1 and mediates its degradation through the proteasome pathway. *Molecular Plant Pathology*. 2010, 11(5): 641-649. https://doi.org/10.1111/J.1364-3703.2010.00634.X.
33. Chapman, S.N. Construction of infectious clones for RNA viruses: TMV. *Methods in molecular biology (Clifton, N.J.)*. 2008, 451: 477-490.
34. Cognat, V; Morelle, G; Megel, C; Lalande, S; Molinier, J; Vincent, T; Small, I; Duchêne, AM; Maréchal-Drouard, L. The nuclear and organellar tRNA-derived RNA fragment population in Arabidopsis thaliana is highly dynamic. *Nucleic Acids Research*. 2017, 45(6): 3460-3472. https://doi.org/10.1093/nar/gkw1122.
35. Cordero, T; Cerdán, L; Carbonell, A; Katsarou, K; Kalantidis, K; Daròs, JA. Dicer-Like 4 Is Involved in Restricting the Systemic Movement of *Zucchini yellow mosaic virus* in *Nicotiana benthamiana*. *Molecular Plant-Microbe Interactions*. 2017, 30(1): 63-71. https://doi.org/10.1094/MPMI-11-16-0239-R.
36. Cordero, T; Ortolá, B; Darós, JA. Mutational analysis of Eggplant latent viroid RNA circularization by the eggplant tRNA ligase in Escherichia coli. *Frontiers in Microbiology*, 2018, 9: 635. https://doi.org/10.3389/fmicb.2018.00635.
37. Csorba, T; Lozsa, R; Hutvagner, G; Burgyan, J. Polerovirus protein P0 prevents the assembly of small RNA containing RISC complexes and leads to degradation of Argonaute1. *The Plant Journal*. 2010, 62(3): 463-472. https://doi.org/10.1111/j.1365-313X.2010.04163.x.
38. Csorba, T; Kontra, L. and Burgyán, J. Viral Silencing Suppressors: Tools Forged to Fine-Tune Host-Pathogen Coexistence. *Virology*, 2015, 479:85-103. https://doi.org/10.1016/j.virol.2015.02.028.
39. Cuperus, JT; Carbonell, A; Fahlgren, N; Garcia-Ruiz, H; Burke, RT; Takeda, A; Sullivan, CM; Gilbert, SD; Montgomery, TA; Carrington, JC. Unique functionality of 22-nt miRNAs in triggering RDR6-dependent siRNA biogenesis from target transcripts in Arabidopsis. *Nature Structural Molecular Biology*. 2010, 17(8): 997-1003. https://doi.org/10.1038/nsmb.1866.

40. Dalakouras, A; Dadami, E; Wassenegger, M. Engineering viroid resistance. *Viruses*. 2015, 7: 634-646. https://doi.org/ 10.3390/v7020634.
41. Dadami E; Boutla, A; Vrettos, N; Tzortzakaki, S; Karakasilioti, I; Kalantidis, K. DICER-LIKE 4 but not DICER-LIKE 2 may have a positive effect on pota to spindle tuber viroid accumulation in *Nicotiana benthamiana*. *Molecular Pla nt*. 2013, 6(1): 232-234. https://doi.org/10.1093/mp/sss118.
42. Dadami, E; Dalakouras, A; Wassenegger, M. Viroids and RNA silencing. In Viroids and Satellites, ed. A Hadidi, R Flores, J W Randles, P Palukaitis [M]. Cambridge, UK: Academic, 2017, pp. 115-124.
43. Dalmadi, A; Gyula, P; Balint, J; Szittya, G; Havelda, Z. AGO-unbound cytos olic pool of mature miRNAs in plant cells reveals a novel regulatory step at AGO1 loading. *Nucleic Acids Research*. 2019, 47(18): 9803-9817. https://do i.org/10.1093/nar/gkz690.
44. Dalmay, T; Hamilton, A; Rudd, S; Angell, S; Baulcombe, DC. An RNA-depen dent RNA polymerase gene in Arabidopsis is required for posttranscriptional gene silencing mediated by a transgene but not by a virus. *Cell*. 2000, 101 (5): 543-533. https://doi.org/10.1016/S0092-8674(00)80864-8.
45. Daròs, JA; Marcos, JF; Hernández, C; Flores, R. Replication of avocado su nblotch viroid: evidence for a symmetric pathway with two rolling circles and hammerhead ribozyme processing. *Proceedings of the National Academy of Sciences of the United States of America*. 1994, 91(26): 12813-12817. http s://doi.org/10.1073/pnas.91.26.12813.
46. Daròs, JA; Flores, R. A chloroplast protein binds a viroid RNA in vivo and f acilitates its hammerhead-mediated self-cleavage. *EMBO Journal*. 2002, 21 (4): 749-59. https://doi.org/10.1093/emboj/21.4.749.
47. Daròs, JA. Eggplant latent viroid: a friendly experimental system in the famil y Avsunviroidae. *Molecular Plant Pathology*. 2016, 17(8): 1170-1177. https://d oi.org/10.1111/mpp.12358.
48. Deng, Y; Wang, JB; Tung, J; Liu, D; Zhou, YJ; He, S; Du, YL; Baker, B; Li, F. A role for small RNA in regulating innate immunity during plant growth. *PLoS Pathogens.* 2018, 14, e1006756. https://doi.org/10.1371/journal.ppat.100 6756.
49. Deleris, A., Gallego-Bartolome, J; Bao, J; Kasschau, KD; Carrington, JC; Voi nnet O. Hierarchical action and inhibition of plant Dicer-like proteins in antivi ral defense. *Science*. 2006, 313(5783): 68-71. https://doi.org/10.1126/science. 1128214.

50. Derrien, B; Baumberger, N; Schepetilnikov, M; Viotti, C; De Cillia, J; Ziegler-Graff, V; Isono, E; Schumacher, K; Genschik, P. Degradation of the antiviral component Argonaute1 by the autophagy pathway. *Proceedings of the Natio nal Academy of Sciences*. 2012, 109(39): 15942-15946. https://doi.org/10.107 3/pnas.1908426116.
51. Devanapally, S; Ravikumar, S; Jose, AM. Double-stranded RNA made in C. Elegans neurons can enter the germline and cause transgenerational gene silencing. *Proceedings of the National Academy of Sciences*. 2015, 112(7): 2 133-2138. https://doi.org/10.1073/pnas.1423333112.
52. Devers, EA; Brosnan, CA; Sarazin, A; Albertini, D; Amsler, AC; Brioudes, F; Jullien, PE; Lim, P; Schott, G; Voinnet, O. Movement and differential consu mption of short interfering RNA duplexes underlie mobile RNA interference. *Nature Plants*, 2020, 6(7):789-799. https://doi.org/10.1038/s41477-020-0687-2.
53. Delgado, S; Navarro, B; Serra, P; Gentit, P; Cambra, MA; Chiumenti, M; De Stradis, A; Di Serio, F; Flores, R. How sequence variants of a plastid-repli cating viroid with one single nucleotide change initiate disease in its natural host. *RNA Biology*. 2019, 16(7): 906-917. https://doi.org/10.1080/15476286.20 19.1600396.
54. Diaz-Pendon, JA; Li, F; Li, WX; Ding, SW. Suppression of antiviral silencing by cucumber mosaic virus 2b protein in Arabidopsis is associated with drast ically reduced accumulation of three classes of viral small interfering RNAs. *Plant Cell*. 2007, 19(6): 2053-2063. https://doi.org/10.1105/tpc.106.047449.
55. Ding, B; Kwon, MO; Hammond, R; Owens, R. Cell-to-cell movement of pota to spindle tuber viroid. *The Plant Journal*. 1997, 12(4): 931-936. https://doi.or g/10.1046/j.1365-313X.1997.12040931.x.
56. Ding, B; Wang, Y. Viroids: uniquely simple and tractable models to elucidate regulation of cell-to-cell trafficking of RNA. *DNA and Cell Biology.* 2009, 28 (2): 51-56. https://doi.org/10.1089/dna.2008.0811.
57. Ding, SW. RNA-based antiviral immunity. *Nature Reviews Immunology*. 2010, 10(9): 632-644. https://doi.org/10.1038/nri2824.
58. Di Serio, F; Flores, R. Viroids: molecular implements for dissecting RNA traf ficking in plants. *RNA Biol*. 2008, 5(3): 128-131. https://doi.org/10.4161/rna.5. 3.6638.
59. Di Serio, F; Gisel, A; Navarro, B; Delgado, S; Martinez de Alba, AE; Donvit o, G; Flores, R. Deep sequencing of the small RNAs derived from two sym ptomatic variants of a chloroplastic viroid: implications for their genesis and

for pathogenesis. *PLoS One*, 2009, 4(10): e7539. https://doi.org/10.1371/journal.pone.0007539.

60. Di Serio, F; Martinez de Alba, AE; Navarro, B; Gisel, A; Flores, R. RNA-dependent RNA polymerase 6 delays accumulation and precludes meristem invasion of a viroid that replicates in the nucleus. *Journal of Virology*. 2010a, 84(5): 2477-2489. DOI:10.1128/Jvi.02336-09. https://doi.org/10.1128/JVI.02336-09.
61. Di Serio, F; Martinez de Alba, AE; Navarro, B; Gisel, A; Flores, R. RNA-dependent RNA polymerase 6 delays accumulation and precludes meristem invasion of a viroid that replicates in the nucleus. *Journal of Virology*. 2010b, 84: 5846-5846. https://doi.org/10.1128/Jvi.00695-10.
62. Di Serio, F; Flores, R; Verhoeven, JTJ; Li, SF; Pallas, V; Randles, JW; Sano, T; Vidalakis, G; Owens, RA. Current status of viroid taxonomy. *Archives of Virology*. 2014, 159(12):3467-3478. https://doi.org/10.1007/s00705-014-2200-6.
63. Di Serio, F; Li, S; Matoušek, J; Owens, RA; Pallás, V; Randles, J W; Sano, T; Verhoeven JTJ; Vidalakis, G; Flores, R; ICTV Report Consortium. ICTV Virus Taxonomy Profile: Avsunviroidae. *Journal of General Virology.* 2018, 99(5): 611–612. https://doi.org/10.1099/jgv.0.001045.
64. Di Serio, F; Owens, RA; Li, S; Matousek, J; Pallas, V; Randles, J; Sano, T; Verhoeven, JTJ; Vidalakis, G; Flores, R and ICTV Report Consortium. ICTV Virus Taxonomy Profile: Pospiviroidae. *Journal of General Virology.* 2021, 102(2):001543. https://doi.org/10.1099/jgv.0.001543.
65. Di Serio, F; A. Owens, R; Navarro, B; Serra, P; Martinez de Alba, AE; Delgado, S; Carbonell, A; Gago-Zachert, S. Role of RNA silencing in plant-viroid interactions and in viroid pathogenesis. *Virus Research*. 2023, 323, 198964. https://doi.org/10.1016/j.virusres.2022.198964.
66. Dong, Y; Burch-Smith, TM; Liu, Y; Mamillapalli, P; Dinesh-Kumar, SP. A ligation-independent cloning tobacco rattle virus vector for high-throughput virus-induced gene silencing identifies roles for NbMADS4-1 and -2 in floral development. *Plant Physiol*ogy. 2007, 145(4):1161-1170. https://doi.org/10.1104/pp.107.107391.
67. Donaire, L; Wang, Y; Gonzalez-Ibeas, D; Mayer, KF; Aranda, MA; Llave, C. Deep-sequencing of plant viral small RNAs reveals effective and widespread targeting of viral genomes. *Virology*. 2009, 392(2): 203-214. https://doi.org/ 10.1016/j.virol.2009.07.005.

68. Downward, J. Cell biology: Metabolism meets death. *Nature*. 2003, 424(695 1): 896–897. https://doi.org/ 10.1038/424896a.
69. Duan, CG; Fang, YY; Zhou, BJ; Zhao, JH; Hou, WN; Zhu, H; Ding, SW; G uo, HS. Suppression of Arabidopsis ARGONAUTE1-Mediated Slicing, Transg ene-Induced RNA Silencing, and DNA Methylation by Distinct Domains of th e Cucumber mosaic virus 2b Protein. *The Plant Cell*. 2012, 24(1): 259-274. https://doi.org/10.1105/tpc.111.092718.
70. Dunoyer, P; Himber, C; Voinnet, O. DICER-LIKE 4 is required for RNA interf erence and produces the 21-nucleotide small interfering RNA component of the plant cell-to-cell silencing signal. *Nature Genetics*. 2005, 37(12): 1356-13 60. https://doi.org/10.1038/ng1675.
71. Dunoyer, P; Himber, C; Ruiz- Ferrer, V; Alioua, A; Voinnet, O. Intra- and int ercellular RNA interference in Arabidopsis thaliana requires components of t he microRNA and heterochromatic silencing pathways. *Nature Genetics*. 200 7, 39(7): 848-856. https://doi.org/10.1038/ng2081.
72. Dunoyer, P; Schott, G; Himber, C; Meyer, D; Takeda, A; Carrington, JC; Voi nnet, O. Small RNA duplexes function as mobile silencing signals between plant cells. *Science*. 2010, 328(5980): 912-916. https://doi.org/10.1126/scienc e.1185880.
73. Ekengren, SK; Liu, Y; Schiff, M; Dinesh-Kumar, SP; Martin, GB. Two MAPK cascades, NPR1, and TGA transcription factors play a role in Pto-mediated disease resistance in tomato. *Plant Journal*. 2003, 36(6): 905-917. https://doi. org/10.1046/j.1365-313X.2003.01944.x.
74. Fadda, Z; Daro`s, JA; Fagoaga, C; Flores, R; Duran-Vila, N. Eggplant latent viroid, the candidate type species for a new genus within the family Avsun viroidae (hammerhead viroids). *Journal of Virology*. 2003, 77(11): 6528-6532. https://doi.org/10.1128/JVI.77.11.6528-6532.2003.
75. Fang, XF; Qi, YJ. RNAi in plants: an argonaute-centered view. *Plant Cell*. 2 016, 28(2): 272-285. https://doi.org/10.1105/tpc.15.00920.
76. Feinberg, EH; Hunter, CP. Transport of dsRNA into cells by the transmembr ane protein SID-1. *Science*. 2003, 301, 1545-1547. https://doi.org/10.1126/sci ence.1087117.
77. Fire, A; Xu, S; Montgomery, MK; Kostas, SA; Driver, SE; Mello, CC. Potent and specific genetic interference by double-stranded RNA in *Caenorhabditis Elegans*. *Nature*. 1998, 391(6669): 806-811. https://doi.org/10.1038/35888.
78. Flores, R; Di Serio, F; Hernandez, C. Viroids: the noncoding genomes. *Sem*

inars in Virology. 1997, 8: 65-73. https://doi.org/10.1006/smvy.1997.0107.

79. Flores, R; Randles, JW; Bar-Joseph, M; Diener, TO. A proposed scheme for viroid classification and nomenclature. *Archives of Virology.* 1998, 143(3): 623-629. https://doi.org/10.1007/s007050050318.
80. Flores, R; Delgado, S; Gas, ME; Carbonell, A; Molina, D; Gago, S; De la Pena, M. Viroids: the minimal non-coding RNAs with autonomous replication. *Febs Letters.* 2004, 567(1): 42-48. https://doi.org/10.1016/S0014-5793(04)00493-4.
81. Flores, R; Hernandez, C; de Alba, AEM; et al. Viroids and viroid-host interactions. *Annual Review of Phytopathology*. 2005, 43: 117-139. https://doi.org/10.1146/annurev.phyto.43.040204.140243.
82. Flores, R; Randles, JW; Owens, RA; Bar-Joseph, M; Diener, TO. The subviral agents [M]//Fauquet, CM; Mayo, MA; Maniloff, J; Desselberger, U; Ball, LA. Virus Taxonomy: Eighth report of the International Committe on the Taxonomy of Viruses. Elsevier Academic Press, 2005b: 1147-1161.
83. Flores, R; Gas, ME; Molina, D; Hernandez, C; Daros, JA. Analysis of viroid replication. *Methods in Molecular Biology*, 2008, 451: 167-183. https://doi.org/10.1007/978-1-59745-102-4-12.
84. Flores, R; Gas, ME; Molina-Serrano; D; Nohales; MÁ; Carbonell. A; Gago, S; De la Peña, M; Daròs, JA. Viroid replication: rolling-circles, enzymes and ribozymes. *Viruses-Basel*. 2009, 1(2): 317-34. https://doi.org/10.3390/v1020317.
85. Flores, R; Di Serio, F; Navarro, B; Duran-Vila, N; Owens, RA. Viroids and viroid diseases of plants [M]. Studies in Viral Ecology: Microbial and Botanical Host Systems. Volume 1, 2011, 1:311-346. https://doi.org/10.1002/9781118025666.
86. Flores, R; Minoia, S; Carbonell, A; Gisel, A; Delgado, S; Lopez-Carrasco, A; Navarro, B; Di Serio, F. Viroids, the simplest RNA replicons: how they manipulate their hosts for being propagated and how their hosts react for containing the infection. *Virus Research*. 2015, 209: 136-145. https://doi.org/10.1016/j.virusres.2015.02.027.
87. Fofana, IB; Sangare, A; Collier, R; Taylor, C; Fauquet, CM. A geminivirus induced gene silencing system for gene function validation in *cassava*. *Plant Molecular Biology*. 2004, 56(4): 613–624. https://doi.org/10.1007/s11103-004-0161-y.
88. Fu, DQ; Zhu, BZ; Zhu, HL; Jiang, WB; Luo, YB. Virus-induced gene silencin

g in tomato fruit. T*he Plant Journal*. 2005, 43(2): 299-308. https://doi.org/10.1111/j.1365-313X.2005.02441.x.

89. Fusaro, AF; Matthew, L; Smith, NA; Curtin, SJ; Dedic-Hagan, J; Ellacott, G A; Watson, JM; Wang, MB; Brosnan, C; Carroll, BJ; Waterhouse, PM. RNA interference-inducing hairpin RNAs in plants act through the viral defence pa thway. *EMBO Reports*, 2006, 7(11): 1168-1175. https://doi.org/10.1038/sj.emb or.7400837.
90. Fusaro, AF; Correa, RL; Nakasugi, K; Jackson, C; Kawchuk, L; Vaslin, MFS; Waterhouse, PM. The enamovirus P0 protein is a silencing suppressor whi ch inhibits local and systemic RNA silencing through AGO1 degradation. *Vir ology*. 2012, 426(2): 178-187. https://doi.org/10.1016/j.virol.2012.01.026.
91. Gago, S; Elena, SF; Flores, R; Sanjuán, R. Extremely high mutation rate of a hammerhead viroid. *Science*. 2009, 323(5919): 1308-1308. https://doi.org/1 0.1016/j.virusres.2015.08.018.
92. Gago-Zachert, S. Viroids, infectious long non-coding RNAs with autonomous replication. *Virus Research*. 2016, 212: 12-24. https://doi.org/10.1016/j.virusre s.2015.08.018.
93. Garcia-Perez, RD; Houdt, HV; Depicker, A. Spreading of post-transcriptional gene silencing along the target gene promotes systemic silencing. *Plant Jou rnal*. 2004, 38(4): 594-602. https://doi.org/10.1111/j.1365-313X.2004.02067.x.
94. Garcia-Ruiz, H; Takeda, A; Chapman, EJ; Sullivan, CM; Fahlgren, N; Bremp elis, KJ; Carrington, JC. Arabidopsis RNA-dependent RNA polymerases and dicer-like proteins in antiviral defense and small interfering RNA biogenesis during Turnip Mosaic Virus infection. *The Plant cell*. 2010, 22(2): 481-496. h ttps://doi.org/10.1105/tpc.109.073056.
95. Gasciolli, V; Mallory, AC; Bartel, DP. Vaucheret, H. Partially redundant functi ons of *Arabidopsis* DICER-like enzymes and a role for DCL4 in producing tr ans-acting siRNAs. *Current Biology*. 2005, 15(16): 1494-1500. https://doi.org/ 10.1016/j.cub.2005.07.024.
96. Glick, E; Zrachya, A; Levy, Y; Mett, A; Gidoni, D; Belausov, E; Citovsky, V; Gafni, Y. Interaction with host SGS3 is required for suppression of RNA sile ncing by tomato yellow leaf curl virus V2 protein. *Proceedings of the Nation al Academy of Sciences of the United States of America*. 2008, 105(1):157-161. https://doi.org/10.1073/pnas.0709036105.
97. Gómez, G; Pallás, V. Identification of an in vitro ribonucleoprotein complex b etween a viroid RNA and a phloem protein from cucumber plants. *Molecular Plant-Microbe Interactions*, 2001, 14(7): 910-13. https://doi.org/10.1094/MPM I.2001.14.7.910.

98. Gómez, G; Pallás, V. A long-distance translocatable phloem protein from cucumber forms a ribonucleoprotein complex in vivo with Hop stunt viroid RNA. *Journal of Virology*. 2004, 78(18): 10104-10110. https://doi.org/10.1128/JVI.78.18.10104-10110.2004.
99. Gómez, G; Pallas, V; Noncoding RNA Mediated Traffic of Foreign mRNA into Chloroplasts Reveals a Novel Signaling Mechanism in Plants. *PLoS One*. 2010a, 5(8): e12269. https://doi.org/10.1371/journal.pone.0012269.
100. Gómez, G; Pallas, V. Can the import of mRNA into chloroplasts be mediated by a secondary structure of a small non-coding RNA? *Plant Signal Behavior*. 2010b, 5(11): 1517-1519. https://doi.org/10.1371/journal.pone.0012269.
101. Gómez, G; Pallas, V. A pathogenic non coding RNA that replicates and accumulates in chloroplasts traffics to this organelle through a nuclear-dependent step. *Plant Signal Behavior*. 2012a, 7(7): 882-884. https://doi.org/10.4161/psb.20463.
102. Gómez, G; Pallas, V. Studies on Subcellular Compartmentalization of Plant Pathogenic Noncoding RNAs Give New Insights into the Intracellular RNA-Traffic Mechanisms. *Plant Physiology*. 2012b, 159(2): 558-564. https://doi.org/10.1104/pp.112.195214.
103. Goodin, MM; Zaitlin, D; Naidu, RA; Lommel, SA. *Nicotiana benthamiana*: its history and future as a model for plant-pathogen interactions. *Molecular plant-microbe interactions*. 2008, 21(8): 1015-1026. https://doi.org/10.1094/MPMI-21-8-1015.
104. Guo, S; Kemphues, KJ. Par-1, a Gene Required for Establishing Polarity in C. Elegans Embryo, Encodes a Putative Ser/Thr Kinase That Is Asymmetrically Distributed. *Cell*. 1995, 81(4), 611-620. https://doi.org/10.1016/0092-8674(95)90082-9.
105. Gustavo, G and Pallás, V. A Pathogenic Non Coding RNA That Replicates and Accumulates in Chloroplasts Traffics to This Organelle through a Nuclear-Dependent Step. *Plant Signaling & Behavior*. 2012, 7(7): 882-884. https://doi.org/10.4161/psb.20463.
106. Haas, G; Azevedo, J; Moissiard, G; Geldreich, A; Himber, C; Bureau, M; Fukuhara, T; Keller, M; Voinnet, O. Nuclear import of CaMV P6 is required for infection and suppression of the RNA silencing factor DRB4. *EMBO Journal*. 2008, 27(15): 2102-2112. https://doi.org/10.1038/emboj.2008.129.
107. Hameed, A; Tahir, MN; Asad, S; Bilal, R; Van, EJ; Jander, G; Mansoor, S. RNAi-mediated simultaneous resistance against three RNA viruses in potato,

Molecular Biotechnology. 2017, 59(2-3): 73-78. https://doi.org/10.1007/s12033-017-9995-9.

108. Hamera, S; Yan, YS; Song, XG; Chaudhary, SU; Murtaza, I; Su, L; Tariq, M; Chen XY; Fang, RX. Expression of cucumber mosaic virus suppressor 2b alters FWA methylation and its siRNA accumulation in Arabidopsis thaliana. *Biology Open*. 2016, 5(11): 1727-1734. https://doi.org/10.1242/bio.017244.
109. Hamilton, A; Voinnet, O; Chappell, L; Baulcombe, D. Two classes of short i nterfering RNA in RNA silencing. *EMBO Journal.* 2002, 21(17): 4671-4679. https://doi.org/10.1093/emboj/cdf464.
110. Han, KL; Jia, ZX; Zhang, YH; Zhou, HJ; Bu, S; Chen, JP; Yan, DK, Qi, RD; Yan, F; Wu, J. Chloroplast clustering around the nucleus induced by OMP2 4 overexpression unexpectedly promoted PSTVd infection in *Nicotiana benth amiana*. *Molecular Plant Pathology*. 2023, 24: 1552-1559. https://doi.org/10.11 11/mpp.13385.
111. Haseloff, J; Mohamed, NA; Symons, RH. Viroid RNAs of cadang-cadang dis ease of coconuts. *Nature*. 1982, 299(23): 316-320. https://doi.org/10.1038/29 9316a0.
112. Hashimoto J, Koganezawa H. Nucleotide sequence and secondary structure of apple scar skin viroid. *Nucleic Acids Research*. 1987, 15(17): 7045-7052. https://doi.org/10.1093/nar/15.17.7045.
113. Hadidi, A; Flores, R; Candresse, T; Barba, M. Next-generation sequencing a nd genome editing in plant virology. *Frontiers in Microbiology*. 2016, 7: 1325. https://doi.org/10.3389/fmicb.2016.01325.
114. Heather, JM; Chain, B. The sequence of sequencers: The history of sequen cing DNA. *Genomics*. 2016, 107(1):1-8. https://doi.org/10.1016/j.ygeno.2015.1 1.003.
115. Himber, C; Dunoyer, P; Moissiard, G; Ritzenthaler, C; Voinnet, O. Transitivity -dependent and–independent cell-to-cell movement of RNA silencing. *EMBO Journal*. 2003, 22(17):4523-4533. https://doi.org/10.1093/emboj/cdg431.
116. Hiraguri, A; Itoh, R; Kondo, N; Nomura, Y; Aizawa, D; Murai, Y; Koiwa, H; Seki, M; Shinozaki, K; Fukuhara, T. Specific interactions between Dicer-like proteins and HYL1/DRB-family dsRNA-binding proteins in Arabidopsis thalian a. *Plant Molecular Biology*. 2005, 57(2): 173-188. https://doi.org/10.1007/s111 03-004-6853-5.
117. Hollings, M; Stone, OM. Some properties of chrysanthemum stunt, a virus w ith the characteristics of an uncoated ribonucleic acid. *Annals of Applied Bio*

logy. 1973, 74: 333-348. https://doi.org/10.1111/j.1744-7348.1973.tb07754.x.

118. Holzberg, S; Brosio, P; Gross, C; Pogue, G.P. Barley stripe mosaic virus-induced gene silencing in a monocot plant. *The Plant Journal*. 2002, 30(3): 315-327. https://doi.org/10.1046/j.1365-313X.2002.01291.x.
119. Ho, T; Wang, L; Huang, LF; Li, ZG; Pallett, DW; Dalmay, T; Ohshima, K; Walsh, JA; Wang, H. Nucleotide bias of DCL and AGO in plant anti-virus gene silencing. *Protein & Cell*. 2010, 1(9): 847-858. https://doi.org/10.1007/s13238-010-0100-4.
120. Hu, J; Chen, G; Yin, W; Cui, B; Yu, X; Lu, Y; Hu, Z, Silencing of SlHB2, improves drought, salt stress tolerance, and induces stress-related gene expression in tomato. *Journal Plant Growth Regulation*. 2017, 36(3): 578-589. https://doi.org/10.1007/s00344-017-9664-z.
121. Ito, T; Suzaki, K; Nakano, M; Sato, A. Characterization of a new Apscaviroid from American persimmon. *Archives of Virology*. 2013, 158(12): 2629-2631. https://doi.org/10.1007/s00705-013-1772-x.
122. Kang, M; Seo, JK; Song, D; Choi, HS; Kim, KH. Establishment of an Agrobacterium-mediated Inoculation System for Cucumber Green Mottle Mosaic Virus. *Plant Pathology Journal*. 2015, 31(4): 433-437. https://doi.org/10.5423/PPJ.NT.06.2015.0123.
123. Kim, J. Regulation of short-distance transport of RNA and protein. *Current Opinion in Plant Biology.* 2005, 8(1): 45-52. https://doi.org/10.1016/j.pbi.2004.11.005.
124. Jiang, JH; Zhang, ZX; Hu, B; Hu, GB; Wang, HQ; Faure, C; Marais, A; Candresse, T; Li, SF. Identification of a viroid-like RNA in a lychee transcriptome shotgun assembly. *Virus Research*. 2017, 240:1-7. https://doi.org/10.1016/j.virusres.2017.07.012.
125. Jiang, DM; Wang, M; Li, SF; Zhang, ZX. High-throughput sequencing analysis of small RNAs derived from Coleus blumei viroids. *Viruses*. 2019, 11: 619. https://doi.org/ 10.3390/V11070619.
126. Jones-Rhoades, MW; Bartel, DP; Bartel, B. MicroRNAs and Their Regulatory Roles in Plants. *Annual Review of Plant Biology*. 2006, 57(1): 19-53. https://doi.org/10.1146/annurev.arplant.57.032905.105218.
127. Jones, JDG; Staskawicz, BJ; Dang, JL. The plant immune system: From discovery to deployment. *Cell*. 2024, 187(9): 2095-2116. https://doi.org/10.1016/j.cell.2024.03.045.
128. Jose, AM. Garcia, GA; Hunter, CP. Two classes of silencing RNAs move be

tween *Caenorhabditis Elegans* tissues. *Nature Structural Molecular Biology*. 2011, 18(11): 1184-1188. https://doi.org/10.1038/nsmb.2134.

129. Junqueira, BRT; Nicolini, C; Lucinda, N; Orílio, AF; Nagata, T. A simplified a pproach to construct infectious cDNA clones of a tobamovirus in a binary v ector. *Journal of virological methods*. 2014, 198: 32-36. https://doi.org/10.101 6/j.jviromet.2013.12.024.
130. Daròs, JA; Aragonés, V; Cordero, T. A viroid-derived system to produce larg e amounts of recombinant RNA in *Escherichia coli*. *Scientific Reports*. 2018, 8:1904. https://doi.org/10.1038/s41598-018-20314-3.
131. Kadomura-Ishikawa, Y; Miyawaki, K; Takahashi, A; Noji, S. RNAi-mediated si lencing and overexpression of the FaMYB1, gene and its effect on anthocya nin accumulation in strawberry fruit. *Biologia Plantarum*. 2015, 59(4): 677-68 5. https://doi.org/10.1007/s10535-015-0548-4.
132. Kalantidis, K; Schumacher, HT; Alexiadis, T; Helm, JM. RNA silencing move ment in plants. *Biology of the Cell*. 2008, 100(1): 13-26. https://doi.org/10.10 42/bc20070079.
133. Kamboj, A; Saini, M; Rajan, LS; Patel, CL; Chaturvedi, VK; Gupta, PK. Con struction of infectious cDNA clone derived from a classical swine fever virus field isolate in BAC vector using in vitro overlap extension PCR and recomb ination. *Journal of virological methods*. 2015, 226: 60-66. https://doi.org/10.10 16/j.jviromet.2015.10.006.
134. Katsarou, K; Mavrothalassiti, E; Dermauw, W; Van Leeuwen, T; Kalantidis, K. Combined activity of DCL2 and DCL3 is crucial in the defense against pot ato spindle tuber viroid. *PLoS Pathogens*. 2016, 12(10). https://doi.org/10.137 1/journal.ppat.1005936.
135. Kehr, J; Kragler, F. Long distance RNA movement. New Phytologist, 2018, 2 18(1): 29-40. https://doi.org/10.1111/nph.15025.
136. Klahre, U; Crete, P; Leuenberger, SA; Iglesias, VA; Meins, F. High molecula r weight RNAs and small interfering RNAs induce systemic postreanscription al gene silencing in plants. *Proceedings of the National Academy of Scienc es of the United States of America*. 2002, 99:11981-11986. https://doi.org/10. 1073/pnas.182204199.
137. Kitagawa, M; Fujita, T. A model system for analyzing intercellular communic ation through plasmodesmata using moss protonemata and leaves. *Journal of Plant Research*. 2015, 128(1): 63-72. https://doi.org/10.1007/s10265-014-0 690-7.

138. Klevebring, D; Street, NR; Fahlgren, N; Kasschau, KD; Carrington, JC; Lund eberg, J; Jansson, S. Genome-wide profiling of Populus small RNAs. *BMC Genomics*. 2009, 10: 620. https://doi.org/10.1186/1471-2164-10-620.
139. Kolonko, N; Bannach, O; Aschermann, K; Hu, KH; Moors, M; Schmitz, M; S teger, G; Riesner, D. Transcription of potato spindle tuber viroid by RNA pol ymerase II starts in the left terminal loop. *Virology*. 2006, 347(2): 392-404. h ttps://doi.org/10.1016/j.virol.2005.11.039.
140. Kovalskaya, N; Hammond, RW. Molecular biology of viroid-host interactions and disease control strategies. *Plant Science*. 2014,228:48-60. https://doi.org/ 10.1016/j.plantsci.2014.05.006.
141. Kumagai, MH; Donson, J; Della-Cioppa, G; Harvey, D; Hanley, K; Grill, LK. Cytoplasmic inhibition of carotenoid biosynthesis with virus-derived RNA. *Pro ceedings of the National Academy of Sciences of the United States of Ame rica.* 1995, 92(5): 1679-1683. https://doi.org/10.1073/pnas.92.5.1679.
142. Kumar, V; Mishra, SK; Rahman, J; Taneja, J; Sundaresan, G; Mishra, NS; Mukherjee, SK . Mungbean yellow mosaic Indian virus encoded AC2 protein suppresses RNA silencing by inhibiting Arabidopsis RDR6 and AGO1 activiti es. *Virology*. 2015 , 486: 158-172. https://doi.org/10.1016/j.virol.2015.08.015.
143. Kunnimalaiyaan, M; Nielsen, BL. Fine mapping of replication origins (Ori A a nd Ori B) in Nicotiana tabacum chloroplast DNA. *Nucleic Acids Research* 19 97, 25: 3681-3686. https://doi.org/10.1093/nar/25.18.3681.
144. Kurihara, Y; Watanabe, Y. *Arabidopsis* micro-RNA biogenesis through Dicer-li ke 1 protein functions. *roceedings of the National Academy of Sciences of t he United States of America.* 2004, 101(34): 12753-12758. https://doi.org/10. 1073/pnas.0403115101.
145. Kurihara, Y; Takashi, Y; Watanabe, Y. The interaction between DCL1 and H YL1 is important for efficient and precise processing of pri-miRNA in plant microRNA biogenesis. *RNA*. 2006, 122(2): 206-12. https://doi.org/10.1261/rna. 2146906.
146. Kwon, J; Kasai, A; Maoka, T; Masuta, C; Sano, T; Nakahara, KS. RNA sile ncing-related genes contribute to tolerance of infection with potato virus X a nd Y in a susceptible tomato plant. *Virology Journal*. 2020, 17(1). https://doi. org/10.1186/s12985-020-01414-x.
147. Lakatos, L; Csorba, T; Pantaleo, V; Chapman, EJ; Carrington, JC; Liu, YP; Dolja, VV; Calvino, LF; Lopez-Moya, JJ; Burgyan, J. Small RNA binding is a common strategy to suppress RNA silencing by several viral suppressors.

EMBO Journal. 2006, 25(12): 2768-2780. https://doi.org/10.1038/sj.emboj.7601164.

148. Leastro, MO; Kitajima, EW; Pallas, V; Sanchez-Navarro. Rescue of a Cilevirus from infectious cDNA clones. Virus Research. 2024, 339, 199264. https://doi.org/10.1016/j.virusres.2023.199264.
149. Lee, JY; Cui, WE. Non-cell autonomous RNA trafficking and long-distance signaling. *Journal of Plant Biology*. 2009, 52(1): 10-18. https://doi.org/10.1007/s12374-008-9001-y.
150. Lee, BD; Neri, U; Roux, S; Wolf, YI; Camargo, AP; Krupovic, M; Simmonds, P; Kyrpides, N; Gophna, U; Dolja, VV; Koonin, EV. Mining metatranscriptomes reveals a vast world of viroid-like circular RNAs. *Cell*. 2023, 186 (3): 646-+. https://doi.org/ 10.1016/j.cell.2022.12.039.
151. Lewsey, MG; Hardcastle, TJ; Melnyk, CW; Molnar, A; Valli, A; Urich, MA; Nery, JR; Baulcombe, DC; Ecker, JR. Mobile small RNAs regulate genome-wide DNA methylation. *Proceedings of the National Academy of Sciences of the United States of America*. 2016, 113(6): E801-810. https://doi.org/10.1073/pnas.1515072113.
152. Liang, D; White, RG; Waterhouse, PM. Gene silencing in Arabidopsis spreads from the root to the shoot, through a gating barrier, by template-dependent, nonvascular, cell-to-cell movement. *Plant Physiology*. 2012, 159(3): 984-1000. https://doi.org/10.1104/pp.112.197129.
153. Li, H; Li, WX; Ding, SW. Induction and suppression of RNA silencing by an animal virus. *Science*. 2002, 296(5571): 1319-1321. https://doi.org/10.1126/science.1070948.
154. Li H; Handsaker B; Wysoker A; Fennell T; Ruan J; Homer N; Marth G; Abecasis G; Durbin R; 1000 Genome Project Data Processing Subgroup. The sequence alignment/map format and SAMtools. *Bioinformatics*. 2009, 25: 2078-2079. https://doi.org/ 10.1093/bioinformatics/btp352.
155. Li, J; Xiang, CY; Yang, J; Chen, JP; Zhang, HM . Interaction of HSP20 with a viral RdRp changes its sub-cellular localization and distribution pattern in plants. *Scientific reports* , 2015, 5(1): 14016. https://doi.org/10.1038/srep14016.
156. Li, SJ; Castillo-Gonzalez, C; Yu, B; Zhang, XR. The functions of plant small RNAs in development and in stress responses. *Plant Journal.* 2017, 90(4): 654-670. https://doi.org/10.1111/tpj.13444.
157. Li, XQ; Li, Y; Chen, SY; Wang JG. Construction of stable infectious full-length and eGFP-tagged cDNA clones of Mirabilis crinkle mosaic virus via In-Fu

sion cloning. *Virus Research*. 2020, 286. https://doi.org/10.1016/j.virusres.2020.198039.

158. Li, S; Zhang, ZX; Zhou, CY; Li, SF. RNA-dependent RNA polymerase 1 delays the accumulation of viroids in infected plants. *Molecular Plant Pathology*. 2021, 22(10): 1195-1208. https://doi.org/10.1111/mpp.13104.
159. Li, F; Ge, L; Lozano-Durán, R; Zhou, X. Antiviral RNAi drives host adaptation to viral infection. *Trends in Microbiology*. 2022, 30(10): 915-917. https://doi.org/10.1016/j.tim.2022.07.009.
160. Likhith, RK; Peter, A. Development of Infectious Clones of Tomato Leaf Curl Karnataka Virus (ToLCKV) and Study of Pathogenicity on Tomato (Solanum Lycopersicum L.) through Agroinoculation. *Journal of Advances in Biology & Biotechnology*. 2024, 27 (5):581-594. https://doi.org/10.9734/jabb/2024/v27i5821.
161. Liu, S; Chen, MJ; Li, RD; Li, WX; Gal-On, A; Jia, ZY; Ding, SW. Identification of positive and negative regulators of antiviral RNA interference in Arabidopsis thaliana. *Nature Communications*. 2022, 13(1): 2994. https://doi.org/10.1038/s41467-022-30771-0.
162. Liu, SR; Zhou, JJ; Hu, CG; Wei, CL; Zhang, JZ. MicroRNA-mediated gene silencing in plant defense and viral counter-defense. *Frontiers in Microbiology*. 2017, 8: 1801. https://doi.org/10.3389/fmicb.2017.01801.
163. Llave, C. Virus-derived small interfering RNAs at the core of plant-virus interactions. *Trends in Plant Science*. 2010, 15(2): 701-707. https://doi.org/10.1016/j.tplants.2010.09.001.
164. López-Carrasco, A; Gago-Zachert, S; Mileti, G; Minoia, S; Flores, R; Delgado, S. The transcription initiation sites of eggplant latent viroid strands map within distinct motifs in their in vivo RNA conformations. *RNA Biology*. 2016, 13(1): 83-97. https://doi.org/10.1080/15476286.2015.1119365.
165. López-Carrasco, A; Ballesteros, C; Sentandreu, V; Delgado, S; Gago-Zachert, S; Flores, R; Sanjuán, R. Different rates of spontaneous mutation of chloroplastic and nuclear viroids as determined by high-fidelity ultra-deep sequencing. *PLoS Pathogens*. 2017, 13(9): e1006547. https://doi.org/10.1371/journal.ppat.1006547.
166. Lopez-Gomollon, S; Baulcombe, DC. Roles of RNA silencing in viral and non-viral plant immunity and in the crosstalk between disease resistance systems. *Nature Reviews Molecular Cell Biology*. 2022, 23(10): 645-662. https://doi.org/10.1038/s41580-022-00496-5.

167. Lucifora, J; Delphin, M. Current knowledge on Hepatitis Delta Virus replicatio n. *Antiviral Research*. 2020, 179: 104812. https://doi.org/10.1016/j.antiviral.20 20.104812.
168. Ma, JF; Mudiyanselage, SDD; Park, WJ; Wang, M; Takeda, R; Liu, B; Wan g, Y. A nuclear import pathway exploited by pathogenic noncoding RNAs. *Pl ant Cell*. 2022, 34(10): 3543-3556. https://doi.org/10.1093/plcell/koac210.
169. Ma, JF; Mudiyanselage, S D D; Hao, J; Wang, Y. Cellular roadmaps of viroi d infection. *Trends in Microbiology.* 2023, 31(11): 1179-1191. https://doi.org/10. 1016/j.tim.2023.05.014.
170. Mahajan, A; Bhogale, S; Kang, IH; Hannapel, DJ; Banerjee, AK. The mRNA of a Knotted1-like transcription factor of potato is phloem mobile. *Plant Mol ecular Biology*. 2012, 79(6): 595-608. https://doi.org/10.1007/s11103-012-9931- 0.
171. Mao, YB; Cai, WJ; Wang, JW; Hong, GJ; Tao, XY; Wang, LJ; Huang, YP; Chen, XY. Silencing a cotton bollworm P450 monooxygenase gene by plant- mediated RNAi impairs larval tolerance of gossypol. *Nature Biotechnology*. 2 007, 25(11):1307–1313. https://doi.org/10.1038/nbt1352.
172. Martínez de Alba, AE; Flores, R; Hernandez, C. Two chloroplastic viroids in duce the accumulation of small RNAs associated with posttranscriptional gen e silencing. *Journal of Virology*. 2002, 76: 13094–13096. https://doi.org/ 10.1 128/JVI.76.24.13094-13096.2002.
173. Martínez, F; Marques, J; Salvador, ML; Daros, JA. Mutational analysis of eg gplant latent viroid RNA processing in Chlamydomonas reinhardtii chloroplas t. *Journal General Virology*. 2009, 90: 3057-3065. https://doi.org/10.1099/vir.0. 013425-0.
174. Marquez-Molins, J; Navarro, JA; Seco, LC; Pallas, V; Gomez, G. Might exo genous circular RNAs act as protein-coding transcripts in plants? *RNA Biolo gy*. 2021, 18: 98-107. https://doi.org/10.1080/15476286.2021.1962670.
175. Marquez-Molins, J; Hernandez-Azurdia, AG; Urrutia-Perez, M; Pallas, V; Go mez, G. A circular RNA vector for targeted plant gene silencing based on a n asymptomatic viroid. *The Plant Journal*. 2022, 112: 284-293. https://doi.org/ 10.1111/tpj.15929.
176. Matoušek, J; Trněná, L; Svoboda, P; Oriniakova, P; Lichtenstein, C P. The gradual reduction of viroid levels in hop mericlones following heat therapy: a possible role for a nuclease degrading dsRNA. *Biological Chemistry Hoppe- Seyler*. 1995, 376(12):715-722. https://doi.org/10.1515/bchm3.1995.376.12.715.

177. Matoušek, J; Junker, V; Vrba, L; Schubert, J; Patzak, J; Steger, G. Molecular characterization and genome organization of 7SL RNA genes from hop (Humulus lupulus L.). *Gene*. 1999, 239(1):173-183. https://doi.org/10.1016/S0378-1119(99)00352-2.
178. Matoušek, J; Patzak, J. A low transmissibility of hop latent viroid through a generative phase of Humulus lupulus L. *Biologia Plantarum*. 2000, 43(1):145-148. https://doi.org/10.1023/A:1026531819806.
179. Matoušek J; Orctová, L; Skopek, J; Pesina, K; Steger, G. Elimination of hop latent viroid upon developmental activation of pollen nucleases. *Biological Chemistry*. 2008, 389(7):905-918. https://doi.org/10.1515/BC.2008.096.
180. Maule A J. Plasmodesmata: Structure, function and biogenesis. *Current Opinion in Plant Biology.* 2008, 11(6): 680-686. https://doi.org/10.1016/j.pbi.2008.08.002.
181. Meister, G; Tuschl, T. Mechanisms of gene silencing by double-stranded RNA. *Nature*. 2004, 431(7006): 343-349. https://doi.org/10.1038/nature02873.
182. Melnyk, CW; Molnar, A; Bassett, A; Baulcombe, DC. Mobile 24 nt small RNAs direct transcriptional gene silencing in the root meristems of *Arabidopsis thaliana*. *Current Biology*. 2011, 21(19): 1678-1683. https://doi.org/10.1016/j.cub.2011.08.065.
183. Merai, Z; Kerenyi, Z; Molnar, A; Barta, E; Valoczi, A; Bisztray, G; Havelda, Z; Burgyan, J; Silhavy, D. Aureusvirus P14 is an efficient RNA silencing suppressor that binds double-stranded RNAs without size specificity. *Journal Virology*. 2005, 79(11): 7217-7226. https://doi.org/10.1128/JVI.79.11.7217-7226.2005.
184. Merai, Z; Kerenyi, Z; Kertesz, S; Magna, M; Lakatos, L; Silhavy, D. Double-stranded RNA binding may be a general plant RNA viral strategy to suppress RNA silencing. *Journal Virology*. 2006, 80(12): 5747-5756. https://doi.org/10.1128/JVI.01963-05.
185. Minoia, S; Carbonell, A; Di Serio, F; Gisel, A; Carrington, JC; Navarro, B; Flores, R. Specific argonautes selectively bind small RNAs derived from potato spindle tuber viroid and attenuate viroid accumulation in vivo. *Journal of Virology*. 2014, 88(20): 11933-11945. https://doi.org/10.1128/Jvi.01404-14.
186. Mohamed, A; Jin, Z; Osman, T; Shi, N; Tör, M; Jackson, S; Hong, Y. Hotspot siRNA Confers Plant Resistance against Viral Infection. *Biology-Basel*. 2022, 11(5): 714. https://doi.org/10.3390/biology11050714.
187. Molnar, A; Melnyk, CW; Bassett, A; Hardcastle, TJ; Dunn, R; Baulcombe, D

C. Small silencing RNAs in plants are mobile and direct epigenetic modificat ion in recipient cells. *Science*. 2010, 328(5980): 872-875. https://doi.org/10.11 26/science.1187959.

188. Molina-Serrano, D; Suay, L; Salvador, ML; Flores, R; Daros, JA. () Processi ng of RNAs of the Family Avsunviroidae in Chlamydomonas reinhardtii Chlor oplasts. *Journal of Virology*. 2007, 81(8): 4363-4366. https://doi.org/10.1128/J VI.02556-06.
189. Moreno, M; Vázquez, L; López-Carrasco, A; Martín-Gago, JA; Flores, R; Bri ones, C. Direct visualization of the native structure of viroid RNAs at single-molecule resolution by atomic force microscopy. *RNA Biology*. 2019, 16(3): 295-308. https://doi.org/10.1080/15476286.2019.1572436.
190. Morris, KV; Chan, SW; Jacobsen, SE; Looney, DJ. Small interfering RNA-ind uced transcriptional silencing in human cells. *Science*. 2004, 305(5688): 128 9-1292. https://doi.org/10.1126/science.1101372.
191. Moissiard, G; Voinnet, O. RNA silencing of host transcripts by cauliflower m osaic virus requires coordinated action of the four Arabidopsis Dicer-like prot eins. *Proceedings of the National Academy of Sciences of the United States of America*. 2006, 103(51): 19593-19598. https://doi.org/10.1073/pnas.06046 27103.
192. Moissiard, G; Parizotto, EA; Himber, C; Voinnet, O. Transitivity in arabidopsi s can be primed, requires the redundant action of the antiviral dicer-like 4 a nd dicer-like 2, and is compromised by viral-encoded suppressor proteins. *R NA*. 2007, 13(8): 1268-1278. https://doi.org/10.1261/rna.541307.
193. Mukherjee, K; Campos, H; Kolaczkowski, B. Evolution of animal and plant d icers: early parallel duplications and recurrent adaptation of antiviral RNA bin ding in plants. *Molecular Biology and Evolution*. 2013, 30(30): 627-641. http s://doi.org/10.1093/molbev/mss263.
194. Mudiyanselage, SDD; Wang, Y. Evidence supporting that RNA polymerase II catalyzes de novo transcription using potato spindle tuber viroid circular RN A templates. *Viruses-Basel*. 2020, 12(4): 371. https://doi.org/10.3390/v120403 71.
195. Naoi, T; Kitabayashi, S; Kasai, A; Sugawara, K; Adkar-Purushothama, CR; S enda, M; Hataya, T; Sano, T. Suppression of RNA-dependent RNA polymera se 6 in tomatoes allows potato spindle tuber viroid to invade basal part but not apical part including pluripotent stem cells of shoot apical meristem. *PLo S One.* 2020, 15(7): e0236481. https://doi.org/10.1371/journal.pone.0236481.

196. Napoli, C; Lemieux, C; Jorgensen, R. Introduction of a Chimeric Chalcone S ynthase Gene into Petunia Results in Reversible Co-Suppression of Homolo gous Genes in trans. *Plant Cell*. 1990, 2(4): 279-289. https://doi.org/10.1105/t pc.2.4.279.

197. Navarro, B; Pantaleo, V; Gisel, A; Moxon, S; Dalmay, T; Bisztray, G; Di Seri o, F; Burgyan, J. Deep sequencing of viroid-derived small RNAs from grape vine provides new insights on the role of RNA silencing in plant-viroid intera ction. *PLoS One*. 2009, 4(11): e7686. https://doi.org/10.1371/journal.pone.000 7686.

198. Navarro, JA; Vera, A; Flores, R. A chloroplastic RNA polymerase resistant t o tagetitoxin is involved in replication of avocado sunblotch viroid. *Virology*. 2000, 268(1): 218-225. https://doi.org/10.1006/viro.1999.0161.

199. Navarro, B; Gisel, A; Rodio, ME; Delgado, S; Flores, R; Di Serio, F. Viroids: how to infect a host and cause disease without encoding proteins. *Biochim ie*. 2012b, 94: 1474-1480. https://doi.org/10.1016/j.biochi.2012.02.020.

200. Navarro, B; Flores, R; Di Serio, F. Advances in viroid-host interactions. *Ann ual Review of Virology.* 2021a, 8: 305-325. https://doi.org/10.1146/annurev-vir ology-091919-092331.

201. Navarro, B; Gisel, A; Serra, P; Chiumenti, M; Di Serio, F; Flores, R. Degra dome analysis of tomato and *Nicotiana benthamiana* plants infected with pot ato spindle tuber viroid. *International Journal of Molecular Sciences*. 2021b, 22(7): 3725. https://doi.org/10.3390/ijms22073725.

202. Navarro, JA; Saiz-Bonilla, M; Samchez-Navarro, J; Pallas, V. The mitochondr ial and chloroplast dual targeting of a multifunctional plant viral protein mod ulates chloroplast-to-nucleus communication, RNA silencing suppressor activit y, encapsidation, pathogenesis and tissue tropism. *The Plant Cell*. 2021, 10 8: 197-218. https://doi.org/10.1111/tpj.15435.

203. Nodine, MD; Bartel, DP. MicroRNAs prevent precocious gene expression an d enable pattern formation during plant embryogenesis. *Genes and Develop ment*. 2000, 24(23): 2678-2692. https://doi.org/10.1101/gad.1986710.

204. Nohales, MÁ; Flores, R; Daròs, JA. Viroid RNA redirects host DNA ligase 1 to act as an RNA ligase. *Proceedings of the National Academy of Sciences of the United States of America*. 2012a, 109(34):13805-13810. https://doi.org/ 10.1073/pnas.1206187109.

205. Nohales, MÁ, Molina-Serrano, D; Flores, R; Daròs, JA. Involvement of the c hloroplastic isoform of tRNA ligase in the replication of viroids belonging to t

he family Avsunviroidae. *Journal of Virology*. 2012b, 86(15): 8269-8276. https://doi.org/10.1128/JVI.00629-12.

206. Novina, CD; Murray, MF; Dykxhoorn, DM; Beresford, PJ; Riess, J; Lee, SK; Collman, RG; Lieberman, J; Shankar, P; Sharp, PA. siRNA-directed inhibition of HIV-1 infection. *Nature medicine*. 2022, 8(7): 681-686. https://doi.org/10.1038/nm725.
207. Ocampo, TO; Peralta, SMG; Bacheller, N; Uiterwaal, S; Knapp, A; Hennen, A; Ochoa-Martinez, DL; Garcia-Ruiz, H. Antiviral RNA silencing suppression activity of tomato spotted wilt virus NSs protein. *Genetics and Molecular Research*. 2016, 15(2): 15028625. https://doi.org/10.4238/gmr.15028625.
208. Oparka, KJ. Getting the message across: How do plant cells exchange macromolecular complexes. *Trends in Plant Science*. 2004, 9(1):33-41. https://doi.org/10.1016/j.tplants.2003.11.001.
209. Orilio, AF; Fortes, IM; Navas-Castillo, J. Infectious cDNA clones of the criniv irus Tomato chlorosis virus are competent for systemic plant infection and whitefly-transmission. *Virology*. 2014, 464: 365-374. https://doi.org/10.1016/j.virol.2014.07.032.
210. Ortola, B; Cordero, T; Hu, X; Daròs, JA. Intron-assisted, viroid-based production of insecticidal circular double-stranded RNA in *Escherichia coli*. *RNA Biology*. 2021, 18(11): 1846-1857. https://doi.org/10.1080/15476286.2021.1872962.
211. Ortola, B and Daros, JA. Viroids: Non-Coding Circular RNAs Able to Autonomously Replicate and Infect Higher Plants. *Biology-basel*. 2023, 12(2): 172. https://doi.org/10.3390/biology12020172.
212. Ostendorp, A; Pahlow, S; Krussel, L; Hanhart, P; Garbe, MY; Deke, J; Giavalisco, P; Kehr, J. Functional analysis of Brassica napus phloem protein and ribonucleoprotein complexes. *New Phytologist*. 2017, 214(3): 1188-1197. https://doi.org/10.1111/nph.14405.
213. Otero, S; Helariutta, Y; Benitez-Alfonso, Y. Symplastic communication in organ formation and tissue patterning. *Current Opinion in Plant Biology*. 2016, 29: 21-8. https://doi.org/10.1016/j.pbi.2015.10.007.
214. Oys, RA; Blackburn, M; Ding, B. Possible involvement of the phloem lectin in long-distance viroid movement. *Molecular Plant-Microbe Interactions*. 2001, 14(7): 905-909. https://doi.org/10.1094/MPMI.2001.14.7.905.
215. Palauqui, JC, Elmayan, T, de Borne, FD, Crete, P, Charles, C, Vaucheret, H. Frequencies, timing, and spatial patterns of co-suppression of nitrate red

uctase and nitrite reductase in transgenic tobacco plants. *Plant Physiology.* 1996, 112(4): 1447-1456. https://doi.org/10.1104/pp.112.4.1447.

216. Paluqui, JC; Elmayan, T; Pollien, JM; Vaucheret, H. Systemic acquired silen cing: Transgene specific post-transcriptional silencing is transmitted by graftin g from silenced stocks to non-silenced scions. *The RMBO Journal*. 1997, 16 (15):4738-4745. https://doi.org/10.1093/emboj/16.15.4738.
217. Palauqui, JC, Balzergue, S. Activation of systemic acquired silencing by loca lised introduction of DNA. *Current Biology*. 1999, 9(2): 59-66. https://doi.org/ 10.1016/S0960-9822(99)80016-5.
218. Pantaleo, V; Szittya, G; Burgyan, J. Molecular bases of viral RNA targeting by viral small interfering RNA-programmed RISC. *Journal of Virology*. 2007, 81(8): 3797-3806. https://doi.org/10.1128/JVI.02383-06.
219. Parisi, O; Lepoivre, P; Jijakli, MH. Plant-RNA viroid relationship: a complex host pathogen interaction. *Biotechnologie Agronomie Societe Et Environneme nt*. 2010, 14(3): 461-470. https://doi.org/net/2268/84213.
220. Parizotto, EA, Dunoyer, P; Rahm, N; Himber, C; Voinnet, O. In vivo investig ation of the transcription, processing, endonucleolytic activity, and functional relevance of the spatial distribution of a plant miRNA. *Genes Development*. 2004, 18(18): 2237-2242. https://doi.org/10.1101/gad.307804.
221. Parent, JS; Bouteiller, N; Elmayan, T; Vaucheret, H. Respective contribution of Arabidopsis DCL2 and DCL4 to RNA silencing. *Plant Journal*. 2015, 81(2): 223-232. https://doi.org/10.1111/tpj.12720.
222. Prasad, A; Sharma, A; Sarkar, J. Unraveling the mystery of viroid nuclear i mport. *Trends in Microbiology*. 2023, 31(2): 109-110. https://doi.org/10.1016/j.t im.2022.12.002.
223. Qin, C; Shi, NN; Gu M; Zhang, H; Li, B; Shen, JJ; Mohammed, A; Ryabov, E; Li, CY; Wang, HZ; Liu, YL; Osman, T; Vatish, M; Hong, YG. Involvement of RDR6 in short-range intercellular RNA silencing in *Nicotiana benthamiana*. *Scientific Reports*. 2012, 2: 467. https://doi.org/10.1038/srep00467.
224. Qin, C; Li, B; Fan, YY; Zhang, X; Yu, ZM; Ryabov, E; Zhao, M; Wang, H; Shi, N; Zhang, PC; Jackson, S; Tor, M; Cheng, Q; Liu, YL; Gallusci, P; Ho ng, YG. Roles of Dicer-Like Proteins 2 and 4 in Intra- and Intercellular Anti viral Silencing. *Plant Physiology*. 2017, 174(2): 1067-1081. https://doi.org/10.1 104/pp.17.00475.
225. Qi, Y; Pelissier, T; Itaya, A; Hunt, E; Wassenegger, M; Ding, B. Direct role of a viroid RNA motif in mediating directional RNA trafficking across a specif

ic cellular boundary. *The Plant Cell*. 2004, 16(7): 1741-1752. https://doi.org/10.1105/tpc.021980.

226. Qi, Y; Denli, AM; Hannon, GJ. Biochemical specialization within Arabidopsis RNA silencing pathways. *Molecular cell*. 2005, 19(3): 421-428. https://doi.org/10.1016/j.molcel.2005.06.014.
227. Qi, YJ; He, XY; Wang, XJ; Kohany, O; Jurka, J; Hannon, GJ. Distinct catalytic and non-catalytic roles of ARGONAUTE4 in RNA-directed DNA methylation. *Nature*. 2006, 443(7114): 1008-1012. https://doi.org/10.1038/nature05198.
228. Rajamaki, ML; Streng, J; Valkonen, JPT. Silencing suppressor protein VPg of a potyvirus interacts with the plant silencing-related protein SGS3. *Molecular Plant-Microbe Interactions*. 2014, 27(11): 1199-1210. https://doi.org/10.1094/MPMI-04-14-0109-R.
229. Ramesh, SV; Yogindran, S; Gnanasekaran, P; Chakraborty, S; Winter, S; Pappu, HR. Virus and viroid-derived small RNAs as modulators of host gene expression: molecular insights into pathogenesis. *Frontiers in Microbiology*. 2021, 11: 614231. https://doi.org/10.3389/fmicb.2020.614231.
230. Reagan, BC; Ganusova, EE; Fernandez, JC; McCray, TN; Burch-Smith, TM. RNA on the move: the plasmodesmata perspective. *Plant Science*. 2018, 275: 1-10. https://doi.org/10.1016/j.plantsci.2018.07.001.
231. Rodio, ME; Delgado, S; De Stradis, A; Gomez, MD; Flores, R; Di Serio, F. A viroid RNA with a specific structural motif inhibits chloroplast development. *Plant Cell*. 2007, 19(11): 3610-3626. https://doi.org/10.1105/tpc.106.049775.
232. Romano, N; Macino, G. Quelling: Transient inactivation of gene expression in Neurospora crassa by transformation with homologous sequences. *Molecular Microbiology*. 1992, 6(22): 3343-3353. https://doi.org/10.1111/j.1365-2958.1992.tb02202.x.
233. Rosas-Diaz, T; Zhang, D; Fan, PF; Wang, LP; Ding, X; Jiang, YL; Jimenez-Gongora, T; Medina-Puche, L; Zhao, XY; Feng, ZY; Zhang, GP; Liu, XK; Bejarano, ER; Tan, L; Zhang, H; Zhu, JK; Xing, WM; Faulkner, C; Nagawa, S; Lozano-Duran, R. A virus-targeted plant receptor-like kinase promotes cell-to-cell spread of RNAi. *Proceedings of the National Academy of Sciences of the United States of America*. 2018, 115(6): 1388-1393. https://doi.org/10.1073/pnas.1715556115.
234. Ryabov, EV; van Wezel, R; Walsh, J; Hong, Y. Cell-to-Cell, but not long-distance, spread of RNA silencing that is induced in individual epidermal cells. *Journal of Virology*. 2004, 78, 3149-3154. https://doi.org/10.1128/JVI.78.6.314

9-3154.2004.

235. Ryabov, E.V. Construction of infectious cDNA clones for RNA viruses: Turnip crinkle virus. *Methods in molecular biology (Clifton, N.J.)*. 2008, 451: 491-5 02.

236. SI, Drusin; Suarez, IP; Gauto, DF; Rasia, RM; Moreno, DM. dsRNA-protein interactions studied by molecular dynamics techniques. Unravelling dsRNA re cognition by DCL1. *Archives of biochemistry and biophysics*. 2016, 596: 118 -125. https://doi.org/10.1016/j.abb.2016.03.013.

237. Sano T. Progress in 50 years of viroid research-Molecular structure, pathoge nicity, and host adaptation. *Proceedings of the Japan Academy Series B-Ph ysical and Blological Sciences*. 2021, 97(7): 371-401. https://doi.org/10.2183/ pjab.97.020.

238. Saplaoura, E; Kragler, F. Mobile transcripts and intercellular communication i n plants. *Enzymes*. 2016, 40: 1-29. https://doi.org/10.1016/bs.enz.2016.07.00 1.

239. Sarkies, P; Miska, EA. Small RNAs break out: the molecular cell biology of mobile small RNAs. *Nature Reviews Molecular Cell Biology*. 2014, 15(8): 52 5-535. https://doi.org/10.1038/nrm3840.

240. Savary, S; Willocquet, L; Pethybridge, S.J; Esker, P; McRoberts, N; and Nel son, A. The global burden of pathogens and pests on major food crops. *Na ture Ecology & Evolution*. 2019, 3: 430-439. https://doi.org/ 10.1038/s41559-0 18-0793-y.

241. Schiebel, W; Pelissier, T; Riedel, L; Thalmeir, S; Schiebel, R; Kempe, D; Lot tspeich, F; Sanger, H L; Wassenegger, M. Isolation of an RNA-directed RNA polymerase-specific cDNA clone from tomato. *Plant Cell*. 1998, 10(12): 208 7-2101. https://doi.org/10.1105/tpc.10.12.2087.

242. Schwach, F; Vaistij, FE; Jones, L; Baulcombe, DC. An RNA-dependent RNA polymerase prevents meristem invasion by potato virus X and is required f or the activity but not the production of a systemic silencing signal. *Plant P hysiology*. 2005, 138(4): 1842-1852. https://doi.org/10.1104/pp.105.063537.

243. Schott, G; Mari-Ordonez, A; Himber, C; Alioua, A; Voinnet, O; Dunoyer, P. Differential effects of viral silencing suppressors on siRNA and miRNA loadin g support the existence of two distinct cellular pools of ARGONAUTE1. *EM BO Journal*. 2012, 31(11): 2553-2565. https://doi.org/10.1038/emboj.2012.92.

244. Searle, IR; Pontes, O; Melnyk, CW; Smith, LM; Baulcombe, DC. JMJ14, a J mjC domain protein, is required for RNA silencing and cell-to-cell movement

of an RNA silencing signal in *Arabidopsis*. *Genes Development*. 2010, 24(10): 986-991. https://doi.org/10.1101/gad.579910.

245. Serra, P; Hashemian, SMB; Fagoaga, C; Romero, J; Ruiz-Ruiz, S; Gorris, MT; Bertolini, E; Duran-Vila, N. Virus-viroid interactions: citrus tristeza virus enhances the accumulation of citrus dwarfing viroid in Mexican lime via virus-encoded silencing suppressors. *Journal of Virology*. 2014, 88(2): 1394-1397. https://doi.org/10.1128/JVI.02619-13.
246. Serra, P; Messmer, A; Sanderson, D; James, D; Flores, R. Apple hammerhead viroid-like RNA is a bona fide viroid: autonomous replication and structural features support its inclusion as a new member in the genus Pelamoviroid. *Virus Research*. 2018, 249: 8-15. https://doi.org/10.1016/j.virusres.2018.03.001.
247. Semancik, JS; Weathers, LG. Exocortis disease: Evidence for a new species of "infectious" low molecular weight RNA in plants. *Nature New Biology*. 1972, 237(77): 242-244. https://doi.org/10.1038/newbio237242a0.
248. Semancik, JS; Morris, TJ; Weathers, LG. Structure and conformation of low molecular weight pathogenic RNA from exocortis disease. *Virology*. 1973, 53(2): 448-456. https://doi.org/10.1016/0042-6822(73)90224-9.
249. Shaharuddin, NA; Han, YH; Li, HY; Grierson, D. The mechanism of graft transmission of sense and antisense gene silencing in tomato plants. *FEBS letters*. 2006, 580(28-29): 6579-6586. https://doi.org/10.1016/j.febslet.2006.11.005.
250. Shakir, S; Zaidi, SSA; Hashemi, FSG; Nyirakanani, C; Vanderschuren, H. Harnessing plant viruses in the metagenomics era: from the development of infectious clones to applications. *Trends in Plant Science*. 2023, 28(3): 297-311. https://doi.org/10.1016/j.tplants.2022.10.005.
251. Shi, Y; Gu, M; Fan, Z; Hong, Y. RNA silencing suppressors: how viruses fight back. *Future Virology*. 2008, 3: 125-133. https://doi.org/ 10.2217/17460794.3.2.125
252. Shi, Y; Ryabov, EV; Wezel, R; Li, C; Jin, M; Wang, W; Fan, Z; Hong, Y. Suppression of local RNA silencing is not sufficient to promote cell-to-cell movement of *Turnip crinkle virus* in *Nicotiana benthamiana*. *Plant Signaling Behavior*. 2009, 4(1): 15-22. https://doi.org/10.4161/psb.4.1.7573.
253. Shi, Y; Shi, YJ; Gu, QS; Yan, FM; Sun, XY; Li, HL; Chen, LL; Sun, BJ; Wang, ZY. Infectious clones of the crinivirus cucurbit chlorotic yellows virus are competent for plant systemic infection and vector transmission. J*ournal of General Virology*. 2016, 97: 1458-1461. https://doi.org/10.1099/jgv.0.000453.

254. Simon-Mateo, C; Garcia, JA. MicroRNA-guided processing impairs Plum pox virus replication, but the virus readily evolves to escape this silencing mech anism. *Journal of Virology*. 2006, 80: 2429-2436. https://doi.org/10.1128/JVI.8 0.5.2429-2436.2006.

255. Skopelitis, DS; Benkovics, AH; Husbands, AY; Timmermans, MCP. Boundary formation through a direct threshold-based readout of mobile small RNA gra dients. *Development Cell*. 2017, 43(3): 265-273. https://doi.org/10.1016/j.devc el.2017.10.003.

256. Skopelitis, DS; Hill, K; Klesen, S; Marcos, CF; von Born, P; Chitwood, DH; Timmermans, MCP. Gating of miRNA movement at defined cell-cell interface s governs their impact as positional signals. *Nature Communications*. 2018, 9: 3107. https://doi.org/10.1038/s41467-018-05571-0.

257. Smith, LM; Pontes, O; Searle, L; Yelina, N; Yousafzai, FK; Herr, AJ; Pikaar d, CS; Baulcombe, DC. An SNF2 protein associated with nuclear RNA silen cing and the spread of a silencing signal between cells in Arabidopsis. *Plan t Cell*. 2007, 19(5): 1507-1521. https://doi.org/10.1105/tpc.107.051540.

258. St-Pierre, P; Hassen, IF; Thompson, D; Perreault, JP. Characterization of th e siRNAs associated with peach latent mosaic viroid infection. *Virology*. 200 9, 383: 178-182. https://doi.org/ 10.1016/j.virol.2008.11.008.

259. Suzuki, T; Ikeda, S; Kasai, A; Taneda, A; Fujibayashi, M; Sugawara, K; Oku ta, M; Maeda, H; Sano, T. RNAi-mediated down-regulation of dicer-like 2 an d 4 changes the response of 'Moneymaker' tomato to potato spindle tuber v iroid infection from tolerance to lethal systemic necrosis, accompanied by up -regulation of miR398, 398a-3p and production of excessive amount of react ive oxygen species. *Viruses*. 2019, 11(4): 344. https://doi.org/10.3390/v11040 344.

260. Tang, W; Luo, X; Sanmuels, V. Gene silencing: Double-stranded RNA media ted mRNA degradation and gene inactivation. *Cell Research*. 2001, 11(3): 1 81-186. https://doi.org/10.1038/sj.cr.7290084.

261. Takeda, A; Iwasaki, S; Watanabe, T; Utsumi, M; Watanabe, Y. The mechani sm selecting the guide strand from small RNA duplexes is different among Argonaute proteins. *Plant and Cell Physiology*. 2008, 49(4): 493-500. https:// doi.org/10.1093/pcp/pcn043.

262. Takeda, R; Ding, BA. Viroid intercellular trafficking: RNA motifs, cellular facto rs and broad impacts. *Viruses-Basel*. 2009, 1(2): 210-221. https://doi.org/10.3 390/v1020210.

263. Taochy, C; Gursanscky, NR; Cao, JL; Fletcher, SJ; Dressel, U; Mitter, N; Tu cker, MR; Koltunow, AMG; Bowman, JL; Vaucheret, H; Carroll, BJ. A genetic screen for impaired systemic RNAi highlights the crucial role of DICER-LIK E 2. *Plant Physiology*. 2017, 175(3): 1424-1437. https://doi.org/10.1104/pp.17. 01181.
264. Tenllado, F; Barajas, D; Vargas, M; Atencio, FA; Gonzalez-Jara, P; Diaz-Rui z, JR. Transient expression of homologous hairpin RNA causes interference with plant virus infection and is overcome by a virus encoded suppressor of gene silencing. *Molecular Plant-microbe Interactions: MPMI*. 2003, 16, 149-158. https://doi.org/10.1094/MPMI.2003.16.2.149.
265. Tijsterman, M; May, RF; Okihara, KL; Plasterk, RHA. Genes required for sy stemic RNA interference in *Caenorhabditis Elegans*. *Current Biology*. 2004, 14(2): 111-116. https://doi.org/10.1016/j.cub.2003.12.029.
266. Timmons, L; Tabara, H; Mello, CC; Fire, AZ. Inducible systemic RNA silenci ng in *Caenorhabditis Elegans*. *Molecular Biology of the Cell*. 2003, 14(7): 29 72-2983. https://doi.org/10.1091/mbc.E03-01-0858.
267. Tournier, B; Tabler, M; Kalantidis, K. Phloem flow strongly influences the sys temic spread of silencing in GFP *Nicotiana benthamiana* plants. *Plant Journ al*. 2006, 47(3): 383-394. https://doi.org/10.1111/j.1365-313X.2006.02796.x.
268. Tu, LQ; Wu, SH; Gao, DN; Liu, Y; Zhu, YL; Ji, YH. Synthesis and Characte rization of a Full-Length Infectious cDNA Clone of Tomato Mottle Mosaic Vir us. *Viruses*. 2021, 13(6), 1050. https://doi.org/10.3390/v13061050.
269. Ueki, S; Citovsky, V. Inhibition of systemic onset of post-transcriptional gene silencing by non-toxic concentration of cadmium. *Plant Journal*. 2001, 28(3): 283-291. https://doi.org/10.1046/j.1365-313X.2001.01145.x.
270. Van, Wezel; Hong Y. Virus survival of RNA silencing without deploying protei n-mediated suppression in Nicotiana benthamiana. *FEBS letters*. 2004, 562: 65-70. https://doi.org/10.1016/S0014-5793(04)00184-X.
271. Varallyay, E; Olah, E; Havelda, Z. Independent parallel functions of p19 plan t viral suppressor of RNA silencing required for effective suppressor activity. *Nucleic Acids Research*. 2014, 42(1): 599-608. https://doi.org/10.1093/nar/gkt 846.
272. Valli, AA; Santos, BACM; Hnatova, S; Bassett, AR; Molnar, A; Chung, BY; Baulcombe, D.C. Most microRNAs in the single-cell alga Chlamydomonas re inhardtii are produced by Dicer-like 3-mediated cleavage of introns and untr anslated regions of coding RNAs, *Genome Research*. 2016, 26(4): 519-529.

https://doi.org/10.1101/gr.199703.115.

273. Vogler, H; Kwon, MO; Dang, V; Sambade, A; Fasler, M; Ashby, J; Heinlein, M. Tobacco mosaic virus movement protein enhances the spread of RNA sil encing. *PLoS Pathogens*. 2008, 4(4): e1000038. https://doi.org/10.1371/journa l.ppat.1000038.
274. Voinnet, O; Baulcombe, DC. Systemic signaling in gene silencing. *Nature*. 1 997, 389(6651):553-553. https://doi.org/10.1038/39215.
275. Voinnet, O; Vain, P; Angell, S; Baulcombe, DC. Systemic spread of sequenc e-specific transgene RNA degradation is initiated by localised introduction of ectopic promoterless DNA. *Cell*. 1998, 95(2):177-187. https://doi.org/10.1016/ S0092-8674(00)81749-3.
276. Voinnet, O. Use, tolerance and avoidance of amplified RNA silencing by pla nts. *Trends in plant science*. 2008, 13(7): 317-328. https://doi.org/10.1016/j.tpl ants.2008.05.004.
277. Wagner, SD; Yakovchuk, P; Gilman, B; Ponicsan, SL; Drullinger, LF; Kugel, JF; Goodrich, JA. RNA polymerase II acts as an RNA-dependent RNA poly merase to extend and destabilize a non-coding RNA. *EMBO Journal*. 2013, 32(6): 781-790. https://doi.org/10.1038/emboj.2013.18.
278. Wang, L; Yu, X; Wang, H; Lu, YZ; de Ruiter, M; Prins, M; He, YK. A novel class of heat-responsive small RNAs derived from the chloroplast genome o f Chinese cabbage (Brassica rapa). *BMC Genomics*. 2011, 12: 289. https://d oi.org/10.1186/1471-2164-12-289.
279. Wang, MB; Bian, XY; Wu, LM; Liu, LX; Smith, NA; Isenegger, D; Wu, RM; Masuta, C; Vance, VB; Watson, JM; Rezaian, A; Dennis, ES; Waterhouse, PM. On the role of RNA silencing in the pathogenicity and evolution of viroi ds and viral satellites. *Proc Natl Acad Sci USA*. 2004, 101: 3275-3280. http s://doi.org/10.1073/pnas.0400104101.
280. Wang, Y; Ding, B. Viroids: small probes for exploring the vast universe of R NA trafficking in plants. *Journal of Integrative Plant*. 2010, 52(1):28-39. https: //doi.org/10.1111/j.1744-7909.2010.00900.x.
281. Wang, Y; Cong, QQ; Lan, YF; Geng, C; Li, XD; Liang, YC; Yang, ZY; Zhu, XP; Li, XD. Development of new potato virus X-based vectors for gene over -expression and gene silencing assay. *Virus research*. 2014, 191: 62-69. htt ps://doi.org/10.1016/j.virusres.2014.07.018.
282. Wang, R; Yang, XX; Wang, N; Liu, XD; Nelson, RS; Li, WM; Fan, ZF; Zho u, T. *Plant Journal*. 2016, 86(1): 102-115. https://doi.org/10.1111/tpj.13142.

283. Wang, ZM; Hardcastle, TJ; Pastor, AC; Yip, WH; Tang, SY; Baulcombe, DC. A novel DCL2-dependent miRNA pathway in tomato affects susceptibility to RNA viruses. *Genes & development*. 2018, 32(17-18): 1155-1160. https://doi.org/10.1101/gad.313601.118.

284. Wang, YJ; Gong, Q; Wu, YY; Huang, F; Ismayil, A; Zhang, DF; Li, HA; Gu, HQ; Ludman, M; Fatyol, K; Qi, YJ; Yoshioka, K; Hanley-Bowdoin, L; Hong, YG; Liu, YL. A calmodulin-binding transcription factor links calcium signalin g to antiviral RNAi defense in plants. *Cell Host Microbe*. 2021, 29(9): 1393-1406. https://doi.org/10. 1016/j. chom. 2021. 07. 003.

285. Wang, YJ; Gong, Q; Jin, ZH; Liu, YL; Hong, YG. Linking calcium and RNAi signaling in plants. *Trends in Plant Science*. 2022, 27(4): 328-330. https://doi.org/10.1016/j.tplants.2022.01.002.

286. Warrilow, D; Symons, RH. Citrus exocortis viroid RNA is associated with the largest subunit of RNA polymerase II in tomato in vivo. *Archive of Virology*. 1999, 144(12): 2367-2375. https://doi.org/10.1007/s007050050650.

287. Wassarman, KM; Saecker, RM. Synthesis-mediated release of a small RNA inhibitor of RNA polymerase. *Science*. 2006, 314(5805): 1601-1603. https://doi.org/10.1126/science.1134830.

288. Wassenegger, M; Krczal, G. Nomenclature and functions of RNA-directed R NA polymerases. *Trends in Plant Science*. 2006, 11(3): 142-151. https://doi.org/ 10.1016/j.tplants.2006.01.003.

289. Wassenegger, M; Dalakouras, A. Viroids as a Tool to Study RNA-Directed D NA Methylation in Plants. *Cells*. 2021, 10(5), 1187. https://doi.org/10.3390/cells10051187.

290. Weiberg, A; Wang, M; Lin, FM; Zhao, HW; Zhang, ZH; Kaloshian, I; Huang, HD; Jin, HL. Fungal small RNAs suppress plant immunity by hijacking host RNA interference pathways. *Science*. 2013, 342(6154): 118-123. https://doi.org/10.1126/science.1239705.

291. Wierzbicki, AT; Ream, TS; Haag, JR; Pikaard, CS. RNA polymerase V trans cription guides ARGONAUTE4 to chromatin. *Nature Genetics*. 2009, 41(5): 6 30-634. https://doi.org/10.1038/ng.365.

292. Willmann, MR; Mehalick, AJ; Packer, RL; Jenik, PD. MicroRNAs regulate th e timing of embryo maturation in *Arabidopsis*. *Plant Physiology*. 2011, 155(4): 1871-1884. https://doi.org/10.1104/pp.110.171355.

293. Winston, WM; Molodowitch, C; Hunter CP. Systemic RNAi in *C. Elegans* re quires the putative transmembrane protein SID-1. *Science*. 2002, 295(5564):

2456-2459. https://doi.org/10.1126/science.1068836.

294. Woo YM, Itaya A, Owens RA, Tang L. Characterization of nuclear import of potato spindle tuber viroid RNA in permeabilized protoplasts. *The Plant Journal*. 2010, 17: 627-35. https://doi.org/10.1046/j.1365-313X.1999.00412.x.

295. Wu, HW; Lin, SS; Chen, KC; Yeh, SD; Chua, NH. Discriminating Mutations of HC-Pro of Zucchini yellow mosaic virus with Differential Effects on Small RNA Pathways Involved in Viral Pathogenicity and Symptom Development. *Molecular Plant-microbe Interactions*. 2010, 23(1), 17-28. https://doi.org/10.1094/MPMI-23-1-0017.

296. Wu, QF; Wang, Y; Cao, MJ; Pantaleo, V; Burgyan, J; Li, WX; Ding, SW. Homology-independent discovery of replicating pathogenic circular RNAs by deep sequencing and a new computational algorithm. *Proceedings of the National Academy of Sciences of the United States of America*. 2012, 109(10): 3938-3943. https://doi.org/10.1073/pnas.1117815109.

297. Wu, JG; Zhang, YL; Li, FF; Zhang, XM; Ye, J; Wei, TY; Li, ZH; Tao, XR; Cui, F; Wang, XB; Zhang, LL; Yan, F; Li, SF; Liu, YL; Li, DW; Zhou, XP; Li, Y. Plant Virology in the 21st Century in China: Recent Advances and Future Directions. *Journal of Integrative Plant Biology*. 2023, 11. https://doi.org/10.1111/jipb.13580.

298. Wu, J; Bisaro, DM. Cell-cell communication and initial population composition shape the structure of potato spindle tuber viroid quasispecies. *The Plant Cell*. 2024, 36(4): 1036-1055. https://doi.org/10.1093/plcell/koae012.

299. Xia, CJ; Li, SF; Hou, WY; Fan, ZF; Xiao, H; Lu, MG; Sano, T; Zhang, ZX. Global transcriptomic changes induced by infection of cucumber (Cucumis sativus L.) with mild and severe variants of hop stunt viroid. *Frontiers in Microbiology*. 2017, 8: 2427. https://doi.org/10.3389/fmicb.2017.02427.

300. Xia, C; Zhang, CK. Long-distance movement of mRNAs in plants. *Plants-Basel*. 2020, 9(6): 731. https://doi.org/10.3390/plants9060731.

301. Xie, Z; Johansen, LK; Gustafson, AM; Kasschau, KD; Lellis, AD; Zilberman, D; Jacobsen, SE; Carrington, JC. Genetic and functional diversification of small RNA pathways in plants. *PLoS Biology*. 2004, 2(5): 642-652. https://doi.org/10.1371/journal.pbio.0020104.

302. Xie, Z; Allen, E; Wilken, A; Carrington, JC. DICER-LIKE 4 functions in trans-acting small interfering RNA biogenesis and vegetative phase change in *Arabidopsis thaliana*. *Proceedings of the National Academy of Sciences of America*. 2005, 102(36): 12984-12989. https://doi.org/10.1073/pnas.0506426102.

303. Xu, P; Zhang, YJ; Kang, L; Roossinck, MJ; Mysore, KS. Computational esti mation and experimental verification of off-target silencing during posttranscri ptional gene silencing in plants. *Plant physiology.* 2006, 142(2): 429-440. htt ps://doi.org/10.1104/pp.106.083295.
304. Xu, G; Sui, N; Tang, Y; Xie, K; Lai, Y; Liu, Y. One-step, zero-background lig ation-independent cloning intron-containing hairpin RNA constructs for RNAi i n plants. *New Phytologist*. 2010, 187: 240-250. https://doi.org/ 10.1111/j.1469-8137.2010.03253. x.
305. Yang, L; Huang, WH; Wang, H; Cai, R; Xu, YQ; Huang, H. Characterization s of a hypomorphic Argonaute1 mutant reveal novel AGO1 functions in Ara bidopsis lateral organ development. *Plant Molecular Biology*. 2006, 61(1-2): 63-78. https://doi.org/10.1007/s11103-005-5992-7.
306. Yang, XL; Xie, Y; Raja, P; Li, SZ; Wolf, JN; Shen, QT; Bisaro, DM; Zhou, XP. Suppression of Methylation-Mediated Transcriptional Gene Silencing by beta C1-SAHH Protein Interaction during Geminivirus-Betasatellite Infection. *PLoS Pathogens*. 2011, 7(10): e1002329. https://doi.org/10.1371/journal.ppat. 1002329.
307. Yang, YZ; Mao, LY; Jittayasothorn, Y; Kang, YM; Jiao, C; Fei, ZJ; Zhong, GY. Messenger RNA exchange between scions and rootstocks in grafted gr apevines. *BMC Plant Biology*. 2015, 15: 251. https://doi.org/10.1186/s12870-0 15-0626-y.
308. Yang, ZR; Li, Y. Dissection of RNAi-based antiviral immunity in plants. *Curre nt Opinion in Virology*. 2018, 32: 88-99. https://doi.org/10.1016/j.coviro.2018.0 8.003.
309. Yelina, NE; Smith, LM; Jones, AME; Patel, K; Kelly, KA; Baulcombe, DC. P utative Arabidopsis THO/TREX mRNA export complex is involved in transge ne and endogenous siRNA biosynthesis. *Proceedings of the National Acade my of Sciences of the United States of America*. 2010, 107(31): 13948-1395 3. https://doi.org/10.1073/pnas.0911341107.
310. Yoo, BC; Kragler, F Varkonyi-Gasic, E; Haywood, V; Archer-Evans, S; Lee, YM; Lough, TJ; Lucas, WJ. A systemic small RNA signalling system in plant s. *The Plant Cell*. 2004, 16(8): 1979-2000. https://doi.org/10.1105/tpc.104.023 614.
311. Yoon, JY; Min, BE; Choi, JK; Ryu, KH. Genome Structure and Production of Biologically Active In Vitro Transcripts of Cucurbit-Infecting Zucchini green mottle mosaic virus. *Phytopathology*. 2002, 92(2): 156-163. https://doi.org/ 10.

1094/PHYTO.2002.92.2.156.

312. Yu, Y; Jia, TR; Chen, XM. The “how’ and “where’ of plant microRNAs. *New Phytologist*. 2017, 216(4): 1002-1017. https://doi.org/10.1111/nph.14834.
313. Zhang, XR; Henriques, R; Lin, SS; Niu, QW; Chua, NH. Agrobacterium-mediated transformation of Arabidopsis thaliana using the floral dip method. *Nature Protocols*. 2006, 1(2): 641-646. https://doi.org/10.1038/nprot.2006.97.
314. Zhang, SD; Sun, L; Kragler, F. The phloem-delivered RNA pool contains small noncoding RNAs and interferes with translation. *Plant Physiology*. 2009, 150(1): 378-87. https://doi.org/10.1104/pp.108.134767.
315. Zhang, YY; Li, HX; Shu, WB; Zhang, CJ; Ye, ZB. RNA interference of a mitochondrial APX gene improves vitamin C accumulation in tomato fruit. *Scientia Horticulturae*. 2011, 129(2): 220-226. https://doi.org/10.1016/j.scienta.2011.03.025.
316. Zhang, ZX; Qi, SS; Tang, N; Zhang, XX; Chen, SS; Zhu, PF; Ma, L; Cheng, JP; Xu, Y; Lu, MG; Wang, HQ; Ding, SW; Li, SF; Wu, QF. Discovery of replicating circular RNAs by RNA-seq and computational algorithms. *PLoS Pathogens*. 2014b, 10(12): e1004553. https://doi.org/10.1371/journal.ppat.1004553.
317. Zhang, ZL; Zheng, Y; Ham, BK; Chen, JY; Yoshida, A; Kochian, LV; Fei, ZJ; Lucas, WJ. Vascular-mediated signalling involved in early phosphate stress response in plants. *Nature Plant*. 2016, 2(4): 16033. https://doi.org/10.1038/NPLANTS.2016.33.
318. Zhang, XP; Liu, DS; Yan, T; Fang, XD; Dong, K; Xu, J; Wang, Y; Yu, JL; Wang, XB. Cucumber mosaic virus coat protein modulates the accumulation of 2b protein and antiviral silencing that causes symptom recovery in planta. *PLoS Pathogens*. 2017, 13(7): e1006522. https://doi.org/10.1371/journal.ppat.1006522.
319. Zhang, X; Lai, TF; Zhang, PC; Zhang, XLA; Yuan, C; Jin, ZH; Li, HM; Yu, ZM; Qin, C; Tor, M; Ma, P; Cheng, Q; Hong, YG. Mini review: Revisiting mobile RNA silencing in plants. *Plant science.* 2019, 278: 113-117. https://doi.org/10.1016/j.plantsci.2018.10.025.
320. Zhang, F; Liu, S; Zhang, TY; Ye, ZX; Han, XL; Zhong, KL; Yang, J; Chen, JP; Liu, P. Construction and biological characterization of an infectious full-length cDNA clone of a Chinese isolate of Wheat yellow mosaic virus. *Virology*. 2021, 556: 101-109. https://doi.org/10.1016/j.virol.2021.01.018.
321. Zheng, HY; Xiao, CL; Han, KL; Peng, JJ; Lin, L; Lu, YW; Xie, L; Wu, XH;

Xu, P; Li, GJ; Chen, JP; Yan, F. Development of an agroinoculation system for full-length and GFP-tagged cDNA clones of cucumber green mottle mosaic virus. *Archives of virology*. 2015, 160(11): 2867-2872. https://doi.org/10.1007/s00705-015-2584-y.

322. Zheng, XC; Tong, W; Liu, F; Liang, C; Gao, F; Li, GX; Tong, GZ; Zheng, H. Genetic instability of Japanese encephalitis virus cDNA clones propagated in *Escherichia coli*. *Virus Genes*. 2016, 52(2): 195-203. https://doi.org/10.1007/s11262-016-1289-y.
323. Zheng, Y; Wang, Y; Ding, B; Fei, ZJ. Comprehensive Transcriptome Analyses Reveal that Potato Spindle Tuber Viroid Triggers Genome-Wide Changes in Alternative Splicing, Inducible trans-Acting Activity of Phased Secondary Small Interfering RNAs, and Immune Responses. *Journal of Virology*. 2017, 91(11): e00247-00217. https://doi.org/10.1128/JVI.00247-17.
324. Zhou, Y; Ryabov, E; Zhang, XM; Hong, YG. Influence of viral genes on the cell-to-cell spread of RNA silencing. *Journal of Experimental Botany*. 2008, 59(10): 2803-2813. https://doi.org/10.1093/jxb/ern141.
325. Zhu, Y; Green, L; Woo, Y M; Owens, R; Ding, B. Cellular basis of potato spindle tuber viroid systemic movement. *Virology*. 2001, 279(1): 69-77. https://doi.org/10.1006/viro.2000.0724.
326. Zilberman, Daniel; Cao, Xiaofeng; Jacobsen, Steven E. ARGONAUTE4 control of locus-specific siRNA accumulation and DNA and histone methylation. *Science*. 2003, 299(5607): 716-719. https://doi.org/10.1126/science.1079695.

Appendix 1 p53ELVd

ELVd in bold with a repetition of the hammerhead ribozyme on yellow background. Self-cleavage sites are underlined. **CPMV 5' y 3' UTR** in green. Unique sites **NotI** and **ApaI** on yellow background. **35S promoter** in red with +1 nucleotide underlined. **35S terminator** in fuchsia.

>p53ELVd (Kan^R)

NotI 1300-35S-ELVd F/KpnI

GCGGCCGCGATTCCATTGCCCAGCTATCTGTCACTTTATTGTGAAGATAGTGGAAAA
GGAAGGTGGCTCCTACAAATGCCATCATTGCGATAAAGGAAAGGCCATCGTTGAAGA
TGCCTCTGCCGACAGTGGTCCCAAAGATGGACCCCCACCCACGAGGAGCATCGTGGA
AAAAGAAGACGTTCCAACCACGTCTTCAAAGCAAGTGGATTGATGTGATATCTCCAC
TGACGTAAGGGATGACGCACAATCCCACTATCCTTCGCAAGACCCTTCCTCTATATA
AGGAAGTTCATTTCATTTGGAGAGGTATTAAAATCTTAATAGGTTTTGATAAAAGCG
AACGTGGGGAAACCCGAACCAAACCTTCTTCTAAACTCTCTCTCATCTCTCTTAAAG
CAAACTTCTCTCTTGTCTTTCTTGCGTGAGCGATCTTCAACGTTGTCAGATCGTGCT
TCGGCACCAGTACAACGTTTTCTTTCACTGAAGCGAAATCAAAGATCTCTTTGTGGA
CACGTAGTGCGGCGCCATTAAATAACGTGTACTTGTCCTATTCTTGTCGGTGTGGTC
TTGGGAAAAGAAAGCTTGCTGGAGGCTGCTGTTCAGCCCCATACATTACTTGTTACG
ATTCTGCTGACTTTCGGCGGGTGCAATATCTCTACTTCTGCTTGACGAGGTATTGTT
GCCTGTACTTCTTTCTTCTTCTTCTTGCTGATTGGTTCTATAAGAAATCTAGTATTT
TCTTTGAAACAGAGTTTTCCCGTGGTTTTCGAACTTGGAGAAAGATTGTTAAGCTTC
TGTATATTCTGCCCAAATTTGAACCCCATAGGGTGGTGTGTGCCACCCCTGATGAGA
CCGAAAGGTCGAAATGGGGTTTCGCCATGGGTCGGGACTTTAAATTCGGAGGATTCG
TCCTTTAAACGTTCCTCCAAGAGTCCCTTCCCCAAACCCTTACTTTGTAAGTGTGGT
TCGGCGAATGTACCGTTTCGTCCTTTCGGACTCATCAGGGAAAGTACACACTTTCCG
ACGGTGGGTTCGTCGACACCTCTCCCCCTCCCAGGTACTATCCCCTTTCAAGGATGT
GTTCCCTAGGAGGGTGGGTGTACCTCTTTTGGATTGCTCCGGCCTTCCAGGAGAGAT
AGAGGACGACCTCTCCCCATAGGGTGGTGTGTGCCACCCCTGATGAGACCGAAAGGT
CGAAATGGGGCTCTGGTTTCATTAAATTTTCTTTAGTTTGAATTTACTGTTATTCGG
TGTGCATTTCTATGTTTGGTGAGCGGTTTTCTGTGCTCAGAGTGTGTTTATTTTATG
TAATTTAATTTCTTTGTGAGCTCCTGTTTAGCAGGTCGTCCCTTCAGCAAGGACACA
AAAAGATTTTAATTTTATTCGCTGAAATCACCAGTCTCTCTCTACAAATCTATCTCT
CTCTATTTTCTCCATAAATAATGTGTGAGTAGTTTCCCGATAAGGGAAATTAGGGTT
CTTATAGGGTTTCGCTCATGTGTTGAGCATATAAGAAACCCTTAGTATGTATTTGTA
TTTGTAAAATACTTCTATCAATAAAATTTCTAATTCCTAAAACCAAAATCCAGGGGC
CC 1300-35S-ELVd R/PstI ApaI

CaMV 35S Promoter

CPMV 5'UTR

ELVd

CPMV 3'UTR

CaMV 35S Terminator

ELVd-2F

ELVd-3F

ELVd-3R

ELVd-2R

Appendix 1 Sequence of ELVd infection clone.

Cauliflower mosaic virus (CaMV) 35S promoter and terminator, *Cowpea mosaic virus* (CPMV) 5' and 3' translational enhancing sequences, ELVd, a set of primers and restriction enzymes (RE) for subcloning into the pCAMBIA1300 Vector are indicated/highlighted. **(Source: Pengcheng Zhang, 2024)**

Appendix 2 Sequence of the chloroplast gene RbCL mRNA

Appendix 2 Sequence of the chloroplast gene RbCL mRNA

The protein coding sequence is highlighted yellow. The section used for generating hp-dsRNA by the pRNAi-RbCL vector as well as 5' and 3' UTR is indicated. **(Source: Pengcheng Zhang, 2024)**

Appendix 3 Attended academic meetings

- **Zhang P**, Yu Z, He C, Zhang X, Qin C, Mohamed A, Wang L, Liu S, Jin Z, Zhang Z, Shi N, Tör M, Daròs J-A, Li S, Liu Y, Hong Y*. RNA silencing response to chloroplast-replicating viroid siRNA biogenesis in plants. Association of Applied Biologists (AAB) International Advances in Plant Virology 2022, Ljubljana, Slovenia 5-7 October 2022. (Online)
- **Zhang P**, Yu Z, He C, Zhang X, Qin C, Mohamed A, Wang L, Liu S, Jin Z, Zhang Z, Shi N, Tör M, Daròs J-A, Li S, Liu Y, Hong Y*. RNA silencing response to chloroplast-replicating viroid siRNA biogenesis in plants. Research Seminar Series, School of Science and the Environment 2023-2024, Worcester, UK. 26 September 2023. (Online)

Appendix 4 Participated in research projects during the PhD study

- Scientific Research Fund of the Zhejiang Provincial Education Department. Intracellular RNA signalling in RNAi and its role in antiviral defence. Y202044822. 2020.10-2022.10; 10K RMB; **Project leader**/PI 1/5.
- Zhejiang Provincial Natural Science Foundation of China. Research on the molecular mechanism of SlLHP1 interacted with SlSPL-CNR in regulation tomato fruit ripening. LY22C150009. 2022.01-2024.12; 100K RMB; Participants 4/7.
- National Natural Science Foundation of China. Selective methylation in the control of geminivirus DNA replication – a novel antiviral defence mechanism. 31872636. 2019.01-2022.12; 720K RMB; Participants 3/7.
- Zhejiang Provincial Natural Science Foundation of China. Mechanism research on long-distance movement of Arabopsis Flowering Locus T mRNA. LY19C020002. 2019.01-2021.12; 100K RMB; Participants 3/6.
- Zhejiang Provincial Natural Science Foundation of China. METHYLTRANSFERASE 1-mediated epigenetic inhibition of vivipary during tomato fruit ripening. LY19C150006. 2019.01-2021.12; 90K RMB; Participants 3/5.
- Ministry of Science and Technology of China. China-EU Key S&T Innovation Programme: Virus free Fruit Nurseries. 2018.04-2021.03. 620K/4.04million RMB; Participants.
- National Natural Science Foundation of China.Functional analysis of Arabidopsis FBP gene in regulation flowering initiation. 31770344. 2018.01-2021.12; 650K RMB; Participants 4/7.

✧ Ministry of Agriculture of China. National Key Transgenic Program Subtopics: Virus-based technology for plant genome modification. 2016ZX08009001-004. 2016.01-2020.12 1.54 million/30 million RMB; Participants 9/9.

Appendix 5 Participated in publications during the PhD study

- Ma W[#], **Zhang P**[#], Zhao J*, Hong Y*. Chinese cabbage: an emerging model for functional genomics in leafy vegetable crops. *Trends in Plant Science*. 2023, 28(5): 515-518. (co-first author) https://doi.org/10.1016/j.tplants.2023.02.008.
- **Zhang P**, Yu Q, Liu Y, Wang H, Hu Y, Lai T, Zhou T*. Identification and analysis of miRNA and siRNA in *Botryosphaeria dothidea*. *Journal of Hangzhou Normal University*. 2023. 22(2): 158-166. (In Chinese) https://doi.org/10.19926/j.cnki.issn.1674-232X.2023.02.007.
- **Zhang P**, Yu Q, Li R, Liu Y, Lai T*. Uncovering Small RNAs in Penicillium digitatum by Transcriptome Sequencing. *American Journal of Plant Sciences*. 2022, 13, 1006-1022. https://doi.org/10.4236/ajps.2022.137067.
- Yu Z, Chen W, Wang Y, **Zhang P**, Shi N, Hong Y*. Mobile Flowering Locus T RNA - Biological Relevance and Biotechnological Potential. *Frontiers in Plant Science*. 2022. 12: 792192. https://doi.org/10.3389/fpls.2021.792192.
- Zhang X[#], Lai T[#], **Zhang P**[#], Zhang X, Yuan C, Jin Z, Li H, Yu Z, Qin C, Tör M, Ma P, Cheng Q, Hong Y*. Mini review: Revisiting mobile RNA silencing in plants. *Plant Science*. 2019. 278: 113-117. https://doi.org/10.1016/j.plantsci.2018.10.025.
- Tör M, Hong Y, Telli O, **Zhang P**. Novel sRNA-mediated inhibition of downy mildew pathogen Hyaloperonospora arabidopsidis. Chinese Invention Patent. 2020.6.9. ZL201910114883.1.
- **Zhang P**, Yu Z, He C, Zhang X, Mohamed A, Liu S, Jin Z, Meng Q, Zhang Z, Shi N, Tör M, Daròs J-A, Li S, Liu Y, Hong Y*. RNA silencing response in chloroplast-replicating viroid siRNA biogenesis in plants. 2023. under revision.

Contribution to publication from my work

PC Zhang designed and performed the experiments; participated in the analysis and discussion of the small RNA data while helping to write the paper until its official publication.

For Chinese Invention Patent, PC Zhang was involved in the translation and writing of the application materials, participated in the discussion of the patent application work, and helped to contact the patent company.

Appendix 6 Full paper PDF attached